

TWINLATIN

Twinning European and Latin-American River Basins
for Research Enabling Sustainable Water Resources
Management

Work Package 8 report

Change Effects and Vulnerability Assessment

January 2009



LIST OF CONTENTS

LIST OF CONTENTS.....	II
LIST OF FIGURES.....	V
LIST OF TABLES.....	VIII
LIST OF ANNEXES.....	X
1 INTRODUCTION	1-1
1.1 Changing patterns of Land and Water Use.....	1-2
1.2 Basin developments and the effects of change.....	1-3
1.2.1 Climate change	1-3
1.2.2 Land use change	1-8
1.2.3 Water resources developments and changes in water demand	1-9
1.3 Vulnerability.....	1-11
2 ANALYSING THE EFFECTS OF CHANGE	2-1
2.1 Baker (and Biobío) River Basin (Chile).....	2-1
2.1.1 Introduction	2-1
2.1.2 SWAT model calibration in Biobío and scenario generation for Biobío and Baker.....	2-3
2.1.2.1 Introduction.....	2-3
2.1.2.2 Inputs	2-5
2.1.2.3 Results.....	2-5
2.1.2.4 Baseline.....	2-6
2.1.3 Scenario creation and impact assessment	2-8
2.1.3.1 Separate effects	2-8
2.1.3.2 Combined effects.....	2-13
2.1.4 Vulnerability assessment	2-13
2.1.4.1 Exposure of society in the Chilean case study basins.....	2-13
2.1.4.2 Vulnerability of water stakeholders in the Chilean case study basins.....	2-13
2.1.4.3 Public participation in the Baker Basin and the perception of vulnerability	2-16
2.1.4.4 Adaptation to reduce vulnerability.....	2-17
2.1.5 Summary	2-18
2.2 Catamayo-Chira River Basin (Peru – Ecuador).....	2-20
2.2.1 Introduction	2-20
2.2.1.1 Short description of the basin.....	2-20
2.2.1.2 Special issues and problems.....	2-23
2.2.1.3 Types of changes and effects that are modelled and assessed.....	2-26
2.2.1.4 Limitation of the study area	2-26
2.2.1.5 Models used to analyse the effects of change	2-27
2.2.2 Scenario creation	2-27
2.2.2.1 Climate change	2-27
2.2.2.2 Land use change.....	2-34

2.2.3	Scenario impact assessment	2-40
2.2.3.1	<i>Methods used for impact assessment</i>	2-40
2.2.3.2	<i>Separate effects</i>	2-53
2.2.3.3	<i>Combined effects</i>	2-61
2.2.4	Conclusions	2-61
2.3	Cauca River Basin	2-63
2.3.1	Introduction	2-63
2.3.1.1	<i>General basin characteristics</i>	2-63
2.3.2	Scenario creation	2-64
2.3.2.1	<i>Climate change</i>	2-64
2.3.2.2	<i>Land use change</i>	2-65
2.3.2.3	<i>Changes in water demands</i>	2-67
2.3.3	Scenario impact assessment	2-71
2.3.3.1	<i>Methods used for impact assessment</i>	2-71
2.3.3.2	<i>Separate effects</i>	2-72
2.3.3.3	<i>Combined effects</i>	2-75
2.3.4	Vulnerability assessment	2-76
2.3.5	Summary	2-77
2.4	Cocibolca Lake Basin (Nicaragua – Costa Rica).....	2-79
2.4.1	Introduction	2-79
2.4.2	Water balances and hydrological modelling.....	2-80
2.4.2.1	<i>Introduction</i>	2-80
2.4.2.2	<i>Input data</i>	2-80
2.4.2.3	<i>Results</i>	2-82
2.4.2.4	<i>Baseline</i>	2-84
2.4.3	Scenario creation	2-86
2.4.3.1	<i>Climate change</i>	2-86
2.4.3.2	<i>Land use change</i>	2-91
2.4.3.3	<i>Changes in water demands</i>	2-91
2.4.3.4	<i>Water resources developments</i>	2-91
2.4.4	Scenario impact assessment	2-91
2.4.4.1	<i>Separate effects</i>	2-91
2.4.4.2	<i>Combined effects</i>	2-93
2.4.5	Vulnerability assessment	2-93
2.4.5.1	<i>Exposure of society</i>	2-93
2.4.5.2	<i>Vulnerability of water stakeholder</i>	2-93
2.4.5.3	<i>Public participation and the perception of vulnerability</i>	2-94
2.4.5.4	<i>Adaptation to reduce vulnerability</i>	2-96
2.4.6	Summary	2-98
2.5	Quaraí River Basin (Brazil)	2-101
2.5.1	Introduction	2-101

2.5.2	Scenario creation	2-101
2.5.2.1	Climate change	2-102
2.5.2.2	Land use change.....	2-106
2.5.2.3	Water resources developments.....	2-109
2.5.2.4	Changes in water demands	2-110
2.5.3	Scenario impact assessment	2-110
2.5.3.1	Methods used for impact assessment.....	2-110
2.5.3.2	Separate effects	2-111
2.5.3.3	Combined effects.....	2-121
2.5.4	Vulnerability assessment	2-121
2.5.5	Conclusions	2-121
2.6	Cuareim River Basin (Uruguay).....	2-123
2.6.1	Introduction	2-123
2.6.2	Scenario creation	2-124
2.6.2.1	Climate change	2-124
2.6.2.2	Land use change.....	2-124
2.6.2.3	Changes in water demand.....	2-125
2.6.2.4	Water resources developments.....	2-125
2.6.3	Scenario Impact Assessment	2-129
2.6.3.1	Criteria to determine the area of rice to be planted in the current system.....	2-129
2.6.3.2	Climate change	2-135
2.6.3.3	Rice-grassland production system.....	2-136
2.6.4	Vulnerability assessment	2-137
2.6.4.1	Assessment of water deficit risks for grasslands in the current system	2-137
2.6.4.2	Assessment of water deficit risks in the alternative system.....	2-139
2.6.5	Summary	2-142
2.6.5.1	Current system	2-142
2.6.5.2	Alternative system	2-143
2.7	Water balance in South America.....	2-145
2.7.1	Introduction	2-145
2.7.2	Global Water Availability Assessment (GWAVA) for South America	2-145
2.7.2.1	Introduction.....	2-145
2.7.2.2	Inputs	2-146
2.7.2.3	Results.....	2-146
2.7.2.4	Baseline.....	2-147
2.7.3	Scenario Creation and Impact Assessment.....	2-148
2.7.3.1	Climate change	2-148
2.7.3.2	Land use change.....	2-154
2.7.3.3	Changes in water demands	2-154
2.7.3.4	Combined effects.....	2-156
2.7.4	Vulnerability assessment	2-157

2.7.5	Summary	2-159
3	CONCLUSIONS AND RECOMMENDATIONS	3-1
REFERENCES	R-1

LIST OF FIGURES

Figure 1.1	WP 8 work scheme	1-1
Figure 1.2	Global green house gas emissions from 2000 to 2100 in the absence of additional climate policies	1-4
Figure 1.3	Structure of MAGICC/SCENGEN (Wigley, 2003a).....	1-5
Figure 1.4	Visualization of the 5° x 5° output grid from MAGICC/SCENGEN for the Latin-American Region.....	1-6
Figure 1.5	Overview of SRES scenarios (Nakicenovic and Swart, 2000).....	1-7
Figure 2.1	The Baker River Basin.....	2-1
Figure 2.2	The Biobío Basin, central Chile and the modeled sub-basins, Vergara and Lonquimay	2-2
Figure 2.3	Mean monthly discharge rates for the Vergara and Lonquimay Basins	2-4
Figure 2.4	Observed and simulated discharge time series for the baseline scenario.....	2-6
Figure 2.5	Mean annual temperature [°C] and precipitation [mm yr ⁻¹] for the Baker Basin from the General Water Directorate (DGA, 1987)	2-7
Figure 2.6	Baseline for the Baker River Basin as obtained from the RCM model run (<i>left</i>) mean annual temperature [°C], and (<i>right</i>) mean annual precipitation [mm yr ⁻¹], both for the 1961-1990 reference period.....	2-7
Figure 2.7	Generic framework for change impact assessment through hydrological modelling (Debels et al., 2007)	2-8
Figure 2.8	Change signals obtained from the MAGICC/SCENGEN (v4.1).....	2-9
Figure 2.9	Mean change signals for the Vergara and Lonquimay sub-basins of Biobío obtained from the PRECIS model (RCM) runs	2-10
Figure 2.10	Change signals for all points (cells) of the RCM model mesh for the Baker River Basin.....	2-10
Figure 2.11	Hydrological impacts on mean monthly discharges of change scenarios.....	2-11
Figure 2.12	Relation between % changes in mean annual precipitation (X-axis) and mean annual discharge rates (Y-axis) for the rainfall-fed Vergara and mixed-regime Lonquimay sub-basins.....	2-12
Figure 2.13	Schematic illustration of the Glacial Lake Outburst Flow (GLOF) pathway together with an indication of recent and historic glacier front.....	2-14
Figure 2.14	DGA limnigraph data time series clearly showing the effect of the GLOF on the discharge rates in the Baker River.....	2-15
Figure 2.15	Location of the Cachet-2 periglacial lake and the 2 planned hydropower reservoirs	2-15
Figure 2.16	Stakeholder perception with regard to vulnerability - factors that condition adaptive capacity to climate change	2-16
Figure 2.17	Index for the Evaluation of the Usefulness of Adaptation Practices IUPA	2-18
Figure 2.18	Location of Catamayo Chira river basin	2-20
Figure 2.19	Map from the Catamayo Chira sub basins	2-21
Figure 2.20	Land Use in the Catamayo-Chira basin.....	2-22
Figure 2.21	Yearly sediment entry and accumulated sediment load in the Poechos reservoir (Consorcio ATA – UNP – UNL, 2003)	2-25
Figure 2.22	Study areas for Impact Assessment, Hydrologic Modelling and Change Effects	2-26
Figure 2.23	Tendencies of mean monthly temperature in the study area 1970 and 2000	2-28
Figure 2.24	Tendencies of mean annual precipitation in the study area 1970 and 2000.....	2-29
Figure 2.25	Tendencies of water discharge in the study area 1970 and 2000.....	2-29
Figure 2.26	Simulated monthly temperature change for 2045 – 2055 – B2 scenario	2-31

Figure 2.27 Simulated monthly temperature change for 2045 – 2055 – A1 scenario	2-31
Figure 2.28 Simulated monthly rainfall change for 2045 – 2055 – B2 scenario	2-32
Figure 2.29 Simulated monthly rainfall change for 2045 – 2055 – A1 scenario	2-33
Figure 2.30 Meteorological stations to apply patterns of climate change	2-33
Figure 2.31 Actual land use map (left) and modified land use map – Development based on actual trends	2-35
Figure 2.32 Categorized land use changes – Development based on actual trends	2-37
Figure 2.33 Actual land use map (left) and Sustainable Development Scenario (right)	2-39
Figure 2.34 Categorized land use changes – Sustainable Development Scenario	2-39
Figure 2.35 Meteorological stations used for SWAT application in the Catamayo-Chira basin	2-42
Figure 2.36 Visualization of precipitation regimens – Stations used for SWAT	2-43
Figure 2.37 Soil types used in SWAT	2-44
Figure 2.38 Microbasins with largest predicted soil losses	2-47
Figure 2.39 Predicted sediment production in different hydrological years	2-47
Figure 2.40 Water production in different hydrological years	2-48
Figure 2.41 Most water producing microbasins	2-50
Figure 2.42 Water production [$10^6 \text{ m}^3 \text{ yr}^{-1}$]	2-50
Figure 2.43 Mean annual soil loss predicted by WaTEM/SEDEM - baseline situation	2-52
Figure 2.44 Mean annual sediment river export predicted by WaTEM/SEDEM – baseline situation	2-52
Figure 2.45 Microbasins with highest soil erosion (left) and sediment export (right) – baseline situation	2-53
Figure 2.46 Climate stations where climate changes estimated with MAGICC/SCENGEN were applied	2-54
Figure 2.47 Predicted water yield in different climate change scenarios (SWAT)	2-55
Figure 2.48 Predicted sediment yield in different climate change scenarios (SWAT)	2-55
Figure 2.49 Predicted runoff for baseline situation (left), scenario 1 (centre) and scenario 2 (right)	2-57
Figure 2.50 Predicted evapotranspiration for baseline situation (left), scenario 1 (centre) and scenario 2 (right)	2-57
Figure 2.51 Simulated water discharge at Ardilla station for the baseline situation and two land use change scenarios – 1987-1988(SWAT)	2-58
Figure 2.52 Simulated soil losses [t ha^{-1}] for the baseline situation and two land use change scenarios – 1987-1988 (SWAT)	2-58
Figure 2.53 Predicted soil losses [$\text{t ha}^{-1} \text{ yr}^{-1}$] for baseline situation (left), scenario 1 (centre) and scenario 2 (right)	2-59
Figure 2.54 Mean annual soil loss for baseline situation (left), scenario 1 (centre) and scenario 2 (right) (WaTEM/SEDEM) 2-60	
Figure 2.55 Mean annual sediment river export for baseline situation (left), scenario 1 (centre) and scenario 2 (right) (WaTEM/SEDEM)	2-60
Figure 2.56 Most affected microbasins by water erosion – baseline condition compared to scenario 1 (left), baseline condition compared to scenario 2 (right) (WaTEM/SEDEM)	2-61
Figure 2.57 Location of the Tuluá river basin, pilot basin for WP 8	2-63
Figure 2.58 Results of MAGICC/SCENGEN: (a) 2020 and (b) 2050	2-65
Figure 2.59 Identification of maximum areas for land use change scenario creation	2-66
Figure 2.60 Productive systems and maximum productive areas according to limiting factors (2006 and 2020)	2-67
Figure 2.61 Production and consumption and hydrologic stations in the Tuluá river basin	2-68
Figure 2.62 Projected agricultural water demands in the Tuluá river basin (2020)	2-71
Figure 2.63 Predicted effects of climate change on discharge	2-73
Figure 2.64 Predicted effects of de/afforestation in the Tuluá river basin	2-73
Figure 2.65 Water balance in 2006 and 2020 considering agricultural demands in the Tuluá river basin	2-74
Figure 2.66 Actual and predicted water balance in the Tuluá river basin	2-76

Figure 2.67 The Cocibolca Lake Basin	2-79
Figure 2.68 Availability of time series of monthly precipitation data for the Cocibolca Basin and immediate surroundings	2-81
Figure 2.69 Availability of time series of mean daily temperature data for the Cocibolca Basin and immediate surroundings	2-81
Figure 2.70 Number of stations per year with available time series of precipitation data	2-82
Figure 2.71 Availability of discharge data for the Nicaraguan part of the Cocibolca Lake Basin	2-82
Figure 2.72 Limits of acceptability around the observed monthly discharge [mm] in the Mayales catchment	2-83
Figure 2.73 Discharge [mm] from the WASMOD validation (1970-1990).....	2-83
Figure 2.74 Mean annual precipitation [mm yr ⁻¹] for the Cocibolca Basin (1975-1994)	2-84
Figure 2.75 Mean annual precipitation [mm yr ⁻¹] as interpolated from the INETER isolines	2-85
Figure 2.76 PRECIS/Hadley: simulated mean annual precipitation patterns over the Cocibolca Basin for the reference period 1961-1989	2-85
Figure 2.77 PRECIS/Echam: simulated mean annual precipitation patterns over the Cocibolca Basin for the reference period 1961-1989	2-86
Figure 2.78 Generic framework for change impact assessment for basin hydrology (Debels et al., 2007)	2-87
Figure 2.79 Results from MAGICC/SCENGEN for 6 SRES marker scenarios and 9 different GCMs	2-88
Figure 2.80 Results from MAGICC/SCENGEN for 6 SRES marker scenarios and 9 different GCMs	2-88
Figure 2.81 PRECIS/Hadley SRES A2 emission scenario	2-89
Figure 2.82 PRECIS/Hadley SRES B2 emission scenario	2-90
Figure 2.83 PRECIS/Echam SRES A2 emission scenario	2-90
Figure 2.84 PRECIS/Echam SRES B2 emission scenario.....	2-91
Figure 2.85 Cocibolca Lake Basin's stakeholder perception with regard to vulnerability - factors that condition adaptive capacity to climate change	2-94
Figure 2.86 Cocibolca Lake Basin's stakeholder perception with regard to vulnerability - factors that condition adaptive capacity to climate change	2-95
Figure 2.87 Cocibolca Lake Basin's stakeholder perception with regard to vulnerability - factors that condition adaptive capacity to climate change	2-95
Figure 2.88 Cocibolca Lake Basin's stakeholder perception with regard to vulnerability - factors that condition adaptive capacity to climate change	2-95
Figure 2.89 The Index for the Evaluation of the Usefulness of Adaptation Practices (IUPA)	2-98
Figure 2.90 Changes in mean temperature and precipitation in the region of Quaraí watershed for 2020	2-104
Figure 2.91 Changes in mean temperature and precipitation in the region of Quaraí watershed for 2050	2-105
Figure 2.92 Changes in mean temperature and precipitation in the region of Quaraí watershed for 2085	2-105
Figure 2.93 Cumulative distribution of reservoir area for 402 reservoirs (surface > 3 ha) in the Quaraí river basin	2-110
Figure 2.94 Relative changes in stream flow of the Quaraí River related to changes in rainfall	2-112
Figure 2.95 Relative changes in stream flow of the Quaraí River related to changes in temperature.....	2-112
Figure 2.96 Climate change effects on the flow duration curve of the Quaraí River.....	2-113
Figure 2.97 Changes in low flows (Q95) for each month using climate change prediction for 2050	2-114
Figure 2.98 Flow duration curves of the Quaraí River at Barra do Quaraí	2-116
Figure 2.99 Flow duration curves of the Quaraí River at Quaraí/Artigas.....	2-117
Figure 2.100 Flow duration curves of the Quaraí River at Barra do Quaraí (river outlet).....	2-118
Figure 2.101 Flow duration curves of the Quaraí river at Barra do Quaraí (river outlet)	2-119
Figure 2.102 Flow duration curves of the Quaraí River at Barra do Quaraí (river outlet).....	2-119
Figure 2.103 Flow duration curves of the Quaraí River at Barra do Quaraí (river outlet).....	2-120
Figure 2.104 Current rice crops (dark green) and potential expansion in the Tres Cruces basin.....	2-125

Figure 2.105 satellite image showing a large number of small reservoirs in the Cuareim river basin.....	2-127
Figure 2.106 Location of the reservoirs and direct intakes in the Tres Cruces basin.....	2-127
Figure 2.107 Location of the reservoirs and its contributing areas of the alternative system.....	2-128
Figure 2.108 Frequency of the normalized net return during the study period for the (iii) planting criterion.....	2-133
Figure 2.109 Precipitation in Nov-Feb as a function of the average N3.4 index in Sep-Oct In red, the lineal fit of the forecast used in the criteria (v) and (vi).....	2-134
Figure 2.110 Evolution of the mean IBH for Oct-Mar and for the dominant soils in the Tres Cruces basin (1931-2002) ..	2-137
Figure 2.111 Histogram of the mean IBH (Oct-Mar) for dominant soils in the Tres Cruces basin (1931-2002).....	2-137
Figure 2.112 Ad hoc function relating IBH with meat production in a rain fed grassland.....	2-138
Figure 2.113 Histogram of the normalized meat production in the Tres Cruces basin (1931-2002).....	2-139
Figure 2.114 Percentage of irrigated grassland in the alternative system (2 large reservoirs) during simulation period.....	2-140
Figure 2.115 Evolution of mean IBH for Oct-Mar for the grasslands of the alternative system (1931-2002).....	2-141
Figure 2.116 Histogram of the average IBH for Oct-Mar and for the 3 dominant soils in the Tres Cruces basin for the grassland of the alternative system.....	2-141
Figure 2.117 Histogram of the normalized meat production in the grasslands under irrigation for the alternative system.	2-142
Figure 2.118 Maps illustrating a) WAI Type 1 b) WAI Type 3 and c) WAI Type 4 for South America computed for the baseline period 1961-1990.....	2-148
Figure 2.119 Summary plot of the global rise in surface temperatures for the three SRES scenarios. Source: Meehl et al. (2007).....	2-148
Figure 2.120 Absolute change in annual air temperature for eight GCMs (A1B scenario) and mean change of the eight models (bottom left).....	2-149
Figure 2.121 Patterns of change in annual precipitation by 2080 for eight GCMs. Blue colours indicate an increase in precipitation, the bottom left figure represents the mean change of the eight models.....	2-150
Figure 2.122 Changes in the low flow index (above) and WAI 4 (below) for 2020, 2050 and 2080.....	2-152
Figure 2.123 Summary plot of the number of cells experiencing water stress under one GCM (HADCM3) for three timeslices: 2020, 2050 and 2080.....	2-153
Figure 2.124 Summary plots comparing the number of cells in a water stressed state for eight GCMS (left) and the three SRES scenarios (right).....	2-154
Figure 2.125 Population projections (medium variant) for South American nations to the year 2050.....	2-154
Figure 2.126 Mapping the Type 4 Water availability index for South America for two water demand scenarios of population growth for the years a) 2020 and b) 2050.....	2-156
Figure 2.127 Plots of the Type 4 index for South America for the three combined scenarios.....	2-157
Figure 2.128 Summary plot comparing the number of cells experiencing deficits for single and combined scenarios	2-158

LIST OF TABLES

Table 1-1 GCMs for which the global ΔT simulations from MAGICC were used to produce regionalized change patterns for the TWINLATIN study sites.....	1-6
Table 1-2 Future climate change scenarios in TWINLATIN basins.....	1-7
Table 1-3 Future land use change scenarios in TWINLATIN basins.....	1-9
Table 1-4 Future water resources development and changes in water demand scenarios in TWINLATIN basins.....	1-10
Table 2-1 Calibration and validation results for the reference SWAT hydrological component model runs for the Vergara and Lonquimay sub-basins.....	2-5
Table 2-2 Climatic zones in Catamayo Chira river basin.....	2-21
Table 2-3 Changes applied to land use classes – Development based on actual trends.....	2-36
Table 2-4 Changes applied to land use classes – Sustainable Development Scenario.....	2-38

Table 2-5 Classification of hydrological years.....	2-45
Table 2-6 Sediment contribution in 5 measurement stations in the basin.....	2-45
Table 2-7 Largest sediment contributing microbasins in different hydrological conditions.....	2-46
Table 2-8 Water production in microbasins	2-49
Table 2-9 Predicted effects of climate change on water balance (SWAT)	2-54
Table 2-10 Predicted effects of land use change on the water balance (SWAT).....	2-56
Table 2-11 Predicted effects of land use change on soil loss and sediment river export (WaTEM/SEDEM).....	2-59
Table 2-12 Use of land for agriculture in 2006 and 2020.....	2-66
Table 2-13 Actual and projected rural population in the Tuluá river basin	2-69
Table 2-14 Projected rural and urban domestic water demands in the Tuluá river basin (2020).....	2-69
Table 2-15 Inventory and 2020 estimate of bovine water demand in the Tuluá river basin	2-70
Table 2-16 Projected industrial water demands in the Tuluá river basin (2020)	2-71
Table 2-17 Water balance in 2006 and 2020 considering agricultural demands in the Tuluá river basin.....	2-74
Table 2-18 Actual and predicted water demand associated to socio-economic factors	2-75
Table 2-19 Actual and predicted water balance in the Tuluá river basin.....	2-76
Table 2-20 Mean annual precipitation over the Cocibolca Lake Basin [mm yr^{-1}] for the reference climate and a simulated change scenario (2071-2099)	2-92
Table 2-21 Changes in mean annual precipitation over the Cocibolca Lake Basin [%] for the reference climate and a simulated change scenario (2071-2099).....	2-93
Table 2-22 Some important tasks for ongoing research in the Cocibolca Lake Basin.....	2-99
Table 2-23 Scenarios to be analyzed in the Quaraí river basin.....	2-102
Table 2-24 Parameter values related to vegetation types adopted in the MGB-IPH model.....	2-109
Table 2-25 Summary of land use change scenario impact assessment at Quaraí (gauging station) values are in $\text{m}^3 \text{s}^{-1}$	2-115
Table 2-26 Summary of land use change scenario impact assessment at Quaraí (gauging station) values are in % of change compared to the natural scenario.....	2-115
Table 2-27 Summary of land use change scenario impact assessment at Barra do Quaraí (outlet of the Quaraí river basin) values are in $\text{m}^3 \text{s}^{-1}$	2-116
Table 2-28 Summary of land use change scenario impact assessment at Barra do Quaraí (outlet of the Quaraí river basin) values are in % change compared to the natural scenario.....	2-116
Table 2-29 Parameters of the registered reservoirs in the Tres Cruces basin	2-126
Table 2-30 Parameters of the projected reservoirs in the Tres Cruces basin	2-128
Table 2-31 Average planted and harvested area for each reservoir using the (i) planting criterion.....	2-130
Table 2-32 Average planted and harvested area for each reservoir using the (ii) planting criterion.....	2-130
Table 2-33 Average planted and harvested areas for each reservoir using the (iii) planting criterion.....	2-131
Table 2-34 Average planted and harvested areas for each reservoir using the (iv) planting criterion	2-132
Table 2-35 Average planted and harvested areas for each reservoir using the (v) planting criterion	2-134
Table 2-36 Average planted and harvested areas for each reservoir using the (vi) planting criterion	2-135
Table 2-37 Effect of climate change on average planted and harvested areas for each reservoir using the (iii) planting criterion.....	2-136
Table 2-38 Parameter λ , percentage harvested area and percentage maximum net return for the different planting criteria under the current irrigation system.....	2-142
Table 2-39 Parameter λ , percentage harvested area and percentage maximum net return for the different planting criteria (reservoir TCch1).....	2-143
Table 2-40 Parameter λ , percentage harvested area and percentage maximum net return for the different planting criteria (reservoir TCp4).....	2-143

Table 2-41 Summary of water availability indices for surface water, groundwater and combined sources as computed in GWAVA	2-147
Table 2-42 Summary of GCM modelling group/model name and resolution for the eight models examined	2-151
Table 2-43 Comparison of flow statistics and water availability indices for eight climate scenarios in 2080	2-153
Table 2-44 Projected urban and rural populations (thousands) and percentage urban population for South America by country for 2020 and 2030	2-155
Table 2-45 Values of per capita water use estimated for baseline and two future scenarios	2-156
Table 2-46 Summary of the three combined scenarios performed and the driving data for each	2-157
Table 2-47 Comparison of the WAI4 Index and the total population at risk of water deficits	2-158
Table 3-1 Summary impact assessment climate change scenarios	3-2
Table 3-2 Summary impact assessment of land use change scenarios	3-3
Table 3-3 Summary impact assessment of water resources development and changes in water demand scenarios	3-3

LIST OF ANNEXES

ANNEX 1 – ANÁLISIS DE LA (VARIABILIDAD EN LA) DIRECCIÓN Y MAGNITUD DE SEÑALES DE CAMBIO CLIMÁTICO PARA LAS ÁREAS DE ESTUDIO DEL PROYECTO TWINLATIN..... A-1

ANNEX 2 – QUESTIONNAIRES: LAND USE CHANGE SCENARIO CREATION/MODELLING A-43

1 INTRODUCTION

Work Package 8 “Change effects and Vulnerability assessment” was formulated to estimate water body’s vulnerability to pressure, based on monitoring data and model calculations. Main interests are the effects of future climate change, land use change and water resources developments on the hydrological regime, on water availability and water quality, and its ecological, societal and economical consequences. The hydrological, chemical and biological/ecological effects of changed conditions are estimated using GIS and physically-based models.

The objectives of WP 8 are: i) to assess the effect of climate change scenarios regarding frequency and magnitude of flooding events, water availability and water quality using scenario modelling for the Latin American river basins, and to analyse the ecological, societal and economical consequences; ii) to identify planned or foreseen rural and urban development, to model future pollution pressure and changed water abstraction, and to estimate the hydrological, chemical and biological/ecological effects of these changed conditions using GIS and physically-based scenario modelling; and iii) to assess water body vulnerability based on the modelled changes caused by climate and human development.

In this WP 8 Report, the analysis of the effects of climate change, land use change and human development in the TWINLATIN basins is described. The composition of scenarios and results of scenario analyses, i.e. the modelled change compared to the baseline scenario (assuming no change in climate or human development) are explained. Furthermore, levels of water body vulnerability are assessed.

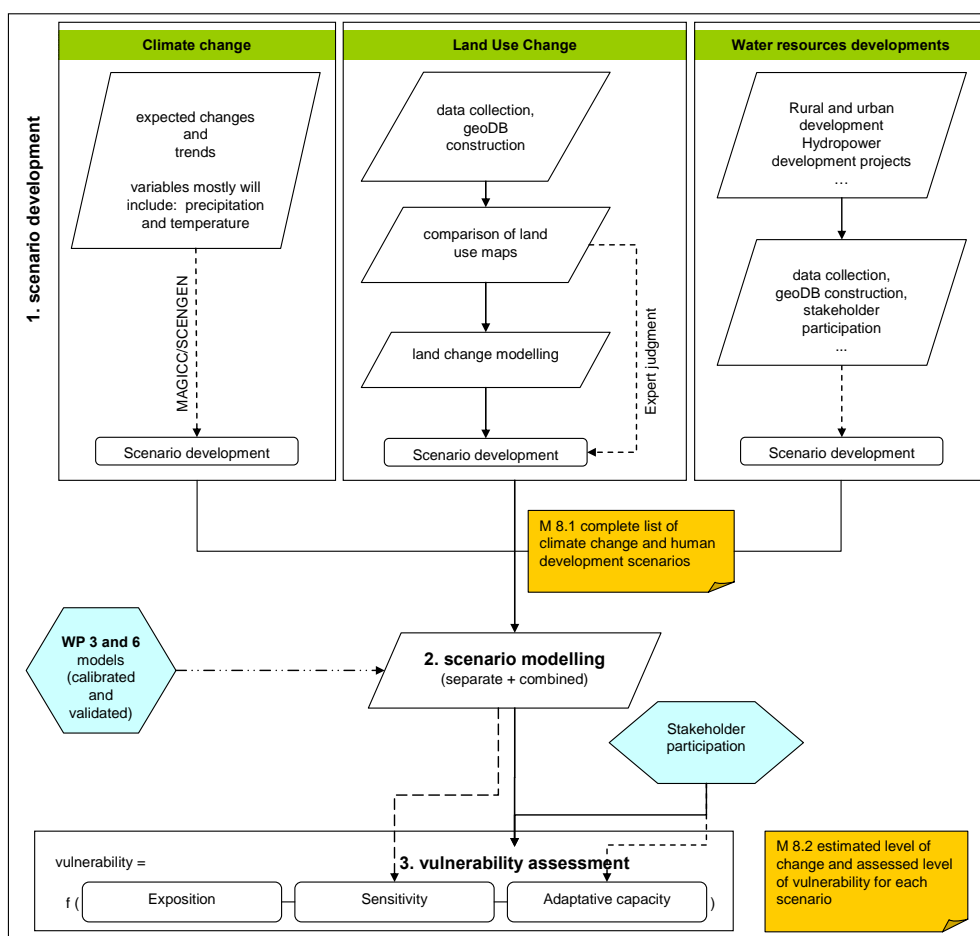


Figure 1.1 WP 8 work scheme

The work scheme shows how work has been planned in WP 8 (Figure 1.1). In the first phase, future scenarios were created. The scenarios concern climate change, land use change and water resources development (rural and urban development, hydropower projects, etc.). After change scenarios were

created, the impact of these scenarios was estimated using calibrated and validated models. For that reason, input from Work Packages 3 (“Hydrological modelling, flooding, erosion, water scarcity and water abstraction”) and 6 (“Pollution pressure and impact analysis”) was needed. In a third phase, vulnerability of water bodies was assessed based on the modelled impacts of future scenarios.

1.1 CHANGING PATTERNS OF LAND AND WATER USE

Growth in population, increased economic activity and improved standards of living lead to increased competition for and conflicts over the limited freshwater resource. A combination of social inequity and economic marginalisation forces people living in extreme poverty to overexploit soil and forestry resources, with damaging impacts on water resources. Here are a few reasons why many people argue that the world faces an impending water crisis:

- Water resources are increasingly under pressure from population growth, economic activity and intensifying competition for the water among users;
- Water withdrawals have increased more than twice as fast as population growth and currently one third of the world's population live in countries that experience medium to high water stress;
- Pollution is further enhancing water scarcity by reducing water usability downstream;
- Shortcomings in the management of water, a focus on developing new sources rather than managing existing ones better, and top-down sector approaches to water management result in uncoordinated development and management of the resource;
- More and more development means greater impacts on the environment;
- Current concerns about climate variability and climate change demand improved management of water resources to cope with more intense floods and droughts.

Human beings can clearly affect the productivity of the water resource. They can reduce the availability and quality of water by actions, such as mining of groundwater, polluting surface- and groundwater and changing land use (afforestation, deforestation, urbanization) which alter flow regimes within surface water systems.

Latin America's development will be characterised by further expansion of megacities, in which 85% of the population will live by 2025. The large metropolitan centres will not likely be able to cope with the resource needs and waste production of households and industries. Currently only 2% of the sewage from urban centres is treated. Untreated effluents will cause major problems with water supply downstream, and proliferation of pathogenic diseases from pollution and vector-borne diseases from expanded reservoir construction is likely. Conflicts will arise at many levels, ranging from small upper catchments to large international river basins. Based on an average South American deforestation rate of 3% (1990-1995), it is estimated that, by 2025, more than 50% of the current forest cover will be lost. Increasing evidence shows that deforestation and land conversion in Central America has severe impacts on the water supply, and aggravates the threat of landslides and mudflows posed by hurricanes and extreme precipitation. The effects of El Niño are also expected to become more extreme, leading to more frequent flooding during wet cycles and water shortages during dry cycles. In Central America, the construction of small- to medium-size dams, which is projected to increase sharply during coming decades, is likely to affect freshwater biological diversity dramatically. Already 103 fish, 27 amphibian, 76 reptile, 353 bird and 263 mammal species are threatened. Mining is another major threat to water resources throughout Latin America. Past mercury emissions from gold mining, for example, were estimated at 5,000 tonnes for the period 1970-1995 (Shiklomanov, 1999; UNEP, 1999; WRI, 1998).

Latin America's water resources prospects for 2025, without intervention (IUCN, 2000)

South America is a highly heterogeneous region, in terms of climate zones, its hydroecology and natural resources as well as the socio-political systems, economic development, cultures and traditions. Economy and society are dynamic and the natural environment is also subject to change,

IWRM systems will, therefore, need to be responsive to change and be capable of adapting to new economic, social and environmental conditions.

1.2 BASIN DEVELOPMENTS AND THE EFFECTS OF CHANGE

The vulnerability of water bodies to environmental changes and external pressures can be assessed by means of expert judgement, monitoring, and the analysis of historical data sets and modelling approximations. The approach followed in the TWINLATIN project builds mainly on the use of the mathematical models developed in Work Package 3 and Work Package 6. Future anthropogenic pressure and changes in water demand are forecasted/predicted, and the hydrological, chemical and biological/ecological effects of these changed conditions are estimated using GIS and modelling techniques. Examples of large-scale changes that are analysed are climate change, land use change, changes in agricultural and forestry practices, urbanisation, hydropower development projects etc.

Existing results from *General Circulation Models (GCMs)* are used to estimate the impact of global climate change on the regional climate and meteorology of the study areas (downscaling). Hypothetical future meteorological time series are synthesised based on historical and actual local observations, and the corresponding output from the GCMs. In the TWINLATIN project, a harmonized approach was used to generate climate change scenarios for the different basins: MAGICC/SCENGEN. The functionality of the model is described more in detail in paragraph 1.2.1, page 1-3.

Starting from the historical and current anthropogenic pressure described for each basin in Work Package 1, and from the more detailed analysis realised in Work Package 3 and Work Package 6, the spatial and temporal dimensions of rural and urban development scenarios, as planned and foreseen by local experts and authorities, or as derived from scientific analyses, as well as future land use change scenarios are defined. The method to create these scenarios was different for each basin.

Based on these predictions, both a separate and a combined analysis of the effects of (i) climate change and (ii) changes in pressure due to human activities are performed. The latter can be divided into land use change and water resources developments and changes in water demands. Effects on the hydrological regime, on erosion and sediment transport, water availability and/or water quality are modelled, and the ecological, societal and economical consequences are analysed and used as the first approach to the problem.

Change effects and vulnerability assessments have been made for the mainland South American continent, in addition to those for the TWINLATIN basins, using a grid-based modelling approach (GWAVA; Meigh et al., 1998) which enables a consistent methodology to be applied across the whole continent. The incorporation of water resource components such as abstractions, reservoirs, lakes, interbasin transfers, etc facilitates a more realistic representation of basin water resources and water availability (i.e. supply minus demand), capturing variations which might otherwise be masked by analysis of national statistics. The need for coherent river basin management plans has become a driving force behind the use of models, in conjunction with future climate change and water demand scenarios, in understanding how basin hydrology will be affected by change.

1.2.1 Climate change

Climate change refers to a change in the state of the climate that can be identified (e.g. using statistical tests) by changes in the mean and/or the variability of its properties, and that persists for an extended period. It refers to any change in climate over time, whether due to natural variability of as a result of human activity (IPCC, 2007).

Warming of the climate system is unequivocal, as is now evident from observations of increases in global average air and ocean temperatures, widespread melting of snow and ice and rising global average sea level. Precipitation is significantly increasing in eastern parts of North and South America, northern Europe and northern and central Asia, whereas precipitation declined in the Sahel, the

Mediterranean, southern Africa and parts of southern Asia. Additionally, some extreme weather events have changed in frequency and/or intensity over the last 50 years.

The radiative forcing of the climate system is dominated by the long-lived green house gasses (carbon dioxide, methane, nitrous oxide and halocarbons): changes in the atmospheric concentrations of green house gasses and aerosols, land cover and solar radiation alter the energy balance of the climate system and are drivers of climate change. Global green house gas emissions due to human activities have grown since pre-industrial times, with an increase of 70 % between 1970 and 2004.

There is much evidence that with current climate change mitigation policies and related sustainable development practices, global green house gas emissions will continue to grow over the next few decades. The SRES scenarios (Special Report on Emissions Scenarios) project and increase of baseline global green house gas emissions by 25 to 90 % between 2000 and 2030 (Nakicenovic and Swart, 2000). The SRES scenarios are grouped into four scenario families (A1, A2, B1 and B2) that explore alternative development pathways, covering a wide range of demographic, economic and technological driving forces and resulting green house gas emissions.

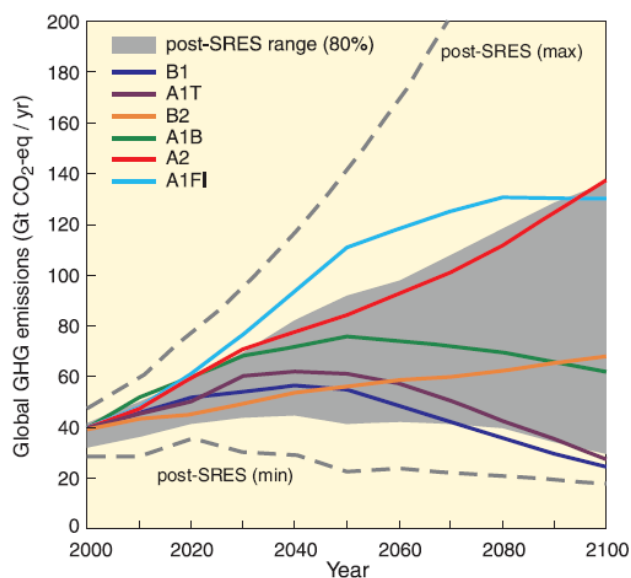


Figure 1.2 Global green house gas emissions from 2000 to 2100 in the absence of additional climate policies

Six illustrative SRES marker scenarios (coloured lines) and 80th percentile range of recent scenarios published since SRES (gray shaded area), dashed lines show the full range of post-SRES scenarios (IPCC, 2007)

Climate change is expected to exacerbate current stresses on water resources (IPCC, 2007). Changes in precipitation and temperature lead to changes in runoff and water availability. Runoff will increase by 10 to 40% by mid-century at higher latitudes and in some wet tropical areas, and decrease by 10 to 30% over some dry regions at mid-latitudes and dry tropics, due to decreases in rainfall and higher rates of evapotranspiration. Drought-affected areas are projected to increase in extent, with the potential for adverse impacts on multiple sectors, e.g. agriculture, water supply, energy production and health. Available research also suggests a significant future increase in heavy rainfall events in many regions, including some in which the mean rainfall is projected to decrease. The resulting increased flood risk poses challenges to society, physical infrastructure and water quality.

In the TWINLATIN project, all partners agreed to use a harmonized approach in the context of the analysis of climate change effects. Therefore, in all Latin American basins future scenario projections were created with MAGICC/SCENGEN version 4.1 (Wigley, 2003a), that then could be used for perturbation of baseline scenarios. An adapted manual for the use of MAGICC/SCENGEN was prepared (see Annex 1, in Spanish). Furthermore, the use of MAGICC/SCENGEN in all Latin American basins allowed for sharing experiences and comparison of results.

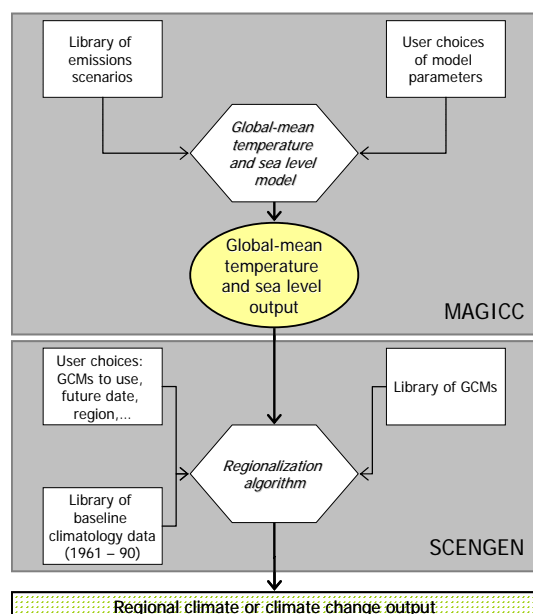


Figure 1.3 Structure of MAGICC/SCENGEN (Wigley, 2003a)

change in different regions (e.g. SCENGEN) (Hulme et al., 1995). SCENGEN uses a pattern scaling method to produce regional climate and climate change information. The regional results are based on the output of 17 AOGCMs interpolated to a 5° by 5° grid.

MAGICC/SCENGEN is a coupled gas-cycle/climate model (MAGICC) that drives a spatial climate change scenario generator (SCENGEN). MAGICC (Model for the Assessment of Greenhouse gas Induced Climate Change) provides internally consistent estimates of global-mean temperature and sea level change between 1990 and 2100, resulting from scenarios of anthropogenic emissions, i.e. CO₂, CH₄, N₂O, the halocarbons, and SO₂ (Hulme et al., 1995). MAGICC has been used in all IPCC reports to produce projections of future global mean temperature and sea level change, and version 4.1 reproduces the results given in the IPCC Third Assessment Report (TAR). The projections of global-mean climate indicators may then be used to scale general circulation model (GCM) results in order to produce regional scenarios of climate

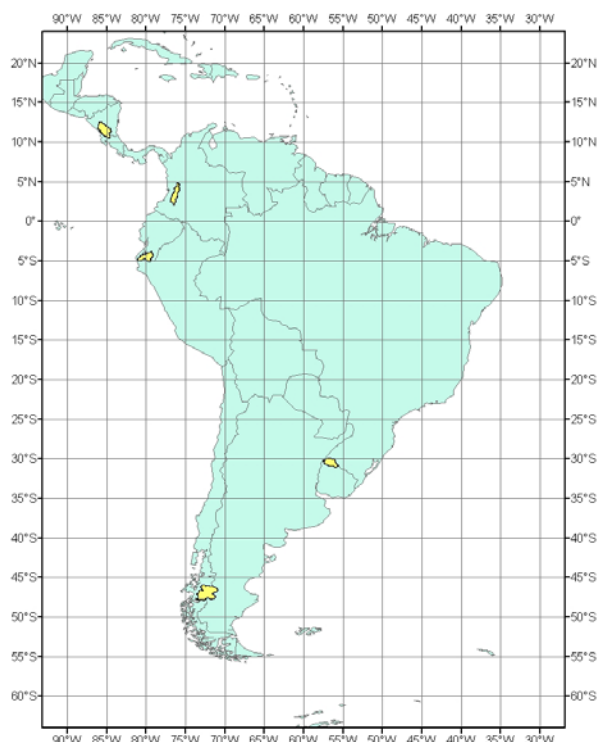


Figure 1.4 Visualization of the 5° x 5° output grid from MAGICC/SCENGEN for the Latin-American Region (the TWINLATIN case study basins are marked in yellow)

The combined use of MAGICC and SCENGEN offers the user complete flexibility about the choice of emissions scenario, a range of global-mean temperature projections and then a choice about the origin of the global or regional climate change scenario generated (Hulme et al., 1995).

In the present study – in order to incorporate in our evaluation the impact of uncertainty associated with the conceptualization/simplification of the global and regional climatological processes in the different models, as well as with the existence of different scenarios for the future emissions of greenhouse gases – we analyzed the change signals obtained from MAGICC-SCENGEN for 9 different GCMs (Table 1-1).

Table 1-1 GCMs for which the global ΔT simulations from MAGICC were used to produce regionalized change patterns for the TWINLATIN study sites

GCM	CCCMa	CCSR/NIES	CSIRO	ECHAM4.5	GFDL	HADCM2	HADCM3	NCAR/PCM	CSM
SCENGEN name	CCC199	CCSR96	CSI296	ECH498	GFDL90	HAD295	HAD300	PCM	CSM98
Country	Canada	Japan	Australia	Germany	USA	UK	UK	USA	USA

The following SRES (Special Report on Emission Scenarios) marker scenarios were used to create global-mean climate indicators:

- A1FI: very rapid economic growth, global population that peaks in mid-century and declines thereafter, and rapid introduction of new and more efficient technologies; fossil intensive
- A1T: very rapid economic growth, global population that peaks in mid-century and declines thereafter, and rapid introduction of new and more efficient technologies; predominantly non-fossil
- A1B: very rapid economic growth, global population that peaks in mid-century and declines thereafter, and rapid introduction of new and more efficient technologies; balanced across energy sources
- A2: a very heterogeneous world with continuously increasing global population and regionally oriented economic growth that is more fragmented and slower than in other scenarios
- B2: a world in which the emphasis is on local solutions to economic, social, and environmental sustainability, with continuously increasing population (lower than A2) and intermediate economic development
- B1: a convergent world with the same global population as in the A1 storyline but with rapid changes in economic structures toward a service and information economy, with reductions in material intensity, and the introduction of clean and resource-efficient technologies

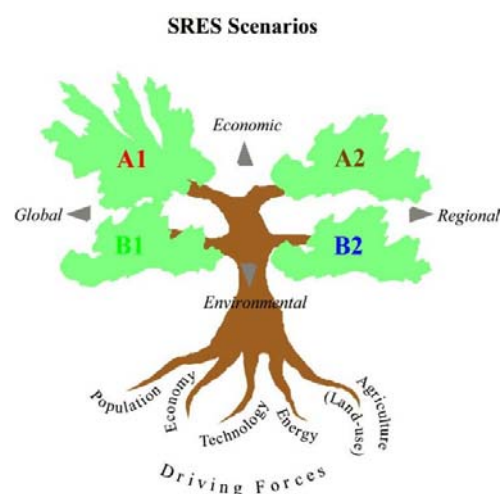


Figure 1.5 Overview of SRES scenarios (Nakicenovic and Swart, 2000)

In the following chapters, the analysis of the effects of change in different Latin American basins is described in detail per basin, and for the South America continent. The following table summarizes which climate change scenarios were developed, the methods used to create the scenarios, and what methods were used to assess the impact of future climate change scenarios (Table 1-2).

Table 1-2 Future climate change scenarios in TWINLATIN basins

Basin	Climate change scenarios	Method of scenario creation	Method of impact assessment
Baker	Perturbations of time series with change signals for temperature and precipitation	MAGICC/SCENGEN Regional Climate Model	SWAT
Catamayo-Chira	2 climate change scenarios based on A1 and B2 and 4 Global Climate Models	MAGICC/SCENGEN	SWAT
Cauca	Perturbations of time series with change signals for temperature and precipitation	MAGICC/SCENGEN	HBV
Lake Nicaragua	Perturbations of time series with change signals for temperature and precipitation	MAGICC/SCENGEN Regional Climate Model	Analysis of change values, expert judgement

Basin	Climate change scenarios	Method of scenario creation	Method of impact assessment
Quaraí/ Cuareim	Hypothetical changes in annual mean precipitation and temperature for sensitivity analysis (precipitation: -20%, -10%, -5%, -1%, +1%, +5%, +10%, +20%; temperature: from -3 °C to +3 °C in steps of 1 °C)	Expert judgement	MGB-IPH
	Monthly changes in temperature and precipitation	MAGICC/SCENGEN	
	Extrapolation of frequency of ENSO events an non-linear tendency	Analysis time series 1931-2002	Assessment of irrigated/harvested area and net returns
South America	8 Global Climate Models with one SRES scenario A1B, and HADCM3 with three SRES scenarios A1B, A2 and B1, for time horizons 2020, 2050 and 2080.	IPCC website www.ipcc-ddc.org	GWAVA

1.2.2 Land use change

Land use is defined by the purposes for which humans exploit the land cover (Lambin et al., 2003). Human use of land alters the structure and functioning of ecosystems, and it alters how ecosystems interact with the atmosphere, with aquatic systems, and with surrounding land (Vitousek et al., 2007). Understanding land transformation is a difficult challenge; it requires integrating the social, economic, and cultural causes of land transformation with evaluations of its biophysical nature and consequences.

Land use change modelling, especially if done in a spatially-explicit, integrated manner, is an important technique for the projection of alternative pathways into the future (Lambin et al., 2000).

The methodology that was proposed in WP 8 was based on 3 important steps:

- I. The identification of historical land use changes within the study area, data collection and geo-database construction

In this step historical land use maps are collected in the basins. Also agricultural census data and national statistics can be useful for larger scale application. Different maps can than be compared to identify the location and time periods of the main land use changes that have occurred in the past. Also main driving factors of land use changes can be identified.

- II. The generation of plausible future land use scenarios

Future land use change scenarios can in some cases be generated using land use/land cover change models. These can be (i) empirical-statistical models, (ii) stochastic models, (iii) optimisation models, and (iv) dynamic or process-based simulation models. The different kinds of models can be used to address different questions; different models may also require a different set of input data (preliminary information). Nevertheless, land use change model performance is highly dependent on the quality of the input maps (Van Dessel et al., in prep.). In none of the TWINLATIN basins land use change was modelled using land use/land cover change models. The main reason was limited data availability and quality. In stead, land use change scenarios were created using expert judgement.

- III. The modelling of the potential impact of these plausible scenarios on availability & quality of natural resources (e.g. water, soil), as well as the associated societal impacts (*integration of results from WP 8 in activities of for example WP 3, WP 9 and WP 6*)

In this step, the effects of land use change on surface runoff, soil erosion, sediment delivery, water availability, water quality... are assessed using models. Results from this analysis can then be used in the evaluation of management options and their socio-economic impacts (Work Packages 5 and 9).

A questionnaire was held in order to plan Work Package 8 activities. The results of the questionnaire are summarized in ANNEX 2 page A-43 (in Spanish).

In the following chapters, the analysis of the effects of change in different Latin American basins is described in detail per basin, and for the South America continent. The following table summarizes which land use change scenarios were developed, the methods used to create the scenarios, and what methods were used to assess the impact of future land use change scenarios (Table 1-3).

Table 1-3 Future land use change scenarios in TWINLATIN basins

Basin	Land use change scenarios	Method of scenario creation	Method of impact assessment
Baker	none		
Catamayo-Chira	1. Development based on actual trends	Expert judgement	SWAT and WaTEM/SEDEM
	2. Sustainable development scenario	Expert judgement based on ecologic/economic landscape study	
Cauca	Changes of cropland area	Modelling of change patterns and maximum areas	HBV
	De/afforestation (25 – 35 – 40 % of the basin covered by forest)	Expert judgement	
Lake Nicaragua	none		
Quaraí	10% of the land covered with pasture changes into forest plantations (Eucalyptus) <ol style="list-style-type: none"> 1. without contact to groundwater 2. with moderate access to groundwater 3. with facilitated access to groundwater 	Expert judgement	MGB-IPH
Cuareim	Soils suitable for summer crops will change from pasture into rice	Expert judgement	Assessment of irrigated/harvested area and net returns
South America	none		

1.2.3 Water resources developments and changes in water demand

The world's freshwater resources are under increasing pressure. Growth in population, increased economic activity and improved standards of living lead to increased competition for and conflicts over the limited freshwater resource. A combination of social inequity, economic marginalization and lack of poverty alleviation programmes also force people living in extreme poverty to overexploit soil and forestry resources, which often results in negative impacts on water resources. Lack of pollution control measures further degrades water resources.

Human beings can clearly affect the productivity of the water resource. They can reduce the availability and quality of water by actions, such as mining of groundwater, polluting surface- and groundwater and changing land use (afforestation, deforestation, urbanization) which alter flow regimes within surface water systems.

Water resources measures generally are designed to store and redistribute water in a river basin. The main purpose can be the storage of irrigation water to be used during the dry season or (combined with) hydropower generation.

The concept of Integrated Water Resources Management at its most fundamental level is as concerned with the management of water demand as with its supply. Thus, integration can be considered under two basic categories: (i) the natural system, with its critical importance for resource availability and quality, and (ii) the human system, which fundamentally determines the resource use, waste production and pollution of the resource, and which must also set the development priorities. Integration has to occur both within and between these categories, taking into account variability in time and space.

For example the decisions of economic sector actors (from trans-national or large state-owned companies to individual farmers or households) will in most countries have significant impact on water demands, water-related risks and the availability and quality of the resource.

It is important to stress that the water knowledge base must include data on the variables which influence demand; only with such data can a flexible and realistic approach to assessing water demands be taken. The use of scenario building for water demand projections may be advantageous and serve to identify possible ranges for various categories of future water demands. In addition, assessing effective demand by analysing the behaviour of users as they react to water scarce situations provides key information that is vital to determining appropriate pricing policies.

In the following chapters, the analysis of the effects of change in different Latin American basins is described in detail per basin, and for the South America continent. The following table summarizes which water resources development scenarios were developed, the methods used to create the scenarios, and what methods were used to assess the impact of future water resources development scenarios (Table 1-4).

Table 1-4 Future water resources development and changes in water demand scenarios in TWINLATIN basins

Basin	Water resources development and changes in water demand scenarios	Method of scenario creation	Method of impact assessment
Baker	Hydropower development		Refer to WP 9
Catamayo-Chira	none		
Cauca	Changes in water demand related to population growth, bovine industry, agriculture and industry	Population growth projection Expert judgement	HBV
Lake Nicaragua	none		
Quaraí	Five scenarios related to the presence or absence of water resources structures related to irrigation: <ol style="list-style-type: none"> 1. Actual situation: widespread use of water for irrigation and large number of small reservoirs 2. No reservoirs, no water abstractions (baseline for comparison) 3. Reservoirs, but no water abstractions (analyse the effect of reservoirs on main river stream flow) 4. Reservoirs and water abstractions only from reservoirs 5. Reservoirs and water abstraction from rivers 	Expert judgement	MGB-IPH

Basin	Water resources development and changes in water demand scenarios	Method of scenario creation	Method of impact assessment
	and reservoirs, but no return flow from the irrigated rice fields		
Cuareim	Changes in water demand related to the conversion from pasture into rice, and because of irrigation of grasslands Two large reservoirs in the upper basin	Expert judgement	Assessment of irrigated/harvested area and net returns
South America	Changes in water demand related to population growth for time horizons 2020 and 2050	Population growth projection Expert judgement	GWAVA

1.3 VULNERABILITY

Vulnerability is defined as the extent to which a natural or social system is susceptible to sustaining damage from for example climate change. Vulnerability is a function of the sensitivity of a system to changes (the degree to which a system will respond to a given change, including both beneficial and harmful effects) and the ability to adapt the system to changes (the degree to which adjustments in practices, processes or structures can moderate or offset the potential for damage or take advantage of opportunities created, due to a given change). Under this framework, a highly vulnerable system would be one that is highly sensitive to modest changes, where the sensitivity includes the potential for substantial harmful effects, and one for which the ability to adapt is severely constrained.

The availability of water is an essential component of welfare and productivity. Climate change, land use changes and water resources developments could exacerbate periodic and chronic shortfalls of water, particularly in arid and semi-arid areas of the world. Developing countries are highly vulnerable to change, because many are located in arid and semi-arid regions, and most derive their water resources from single-point systems such as boreholes or isolated reservoirs. These systems, by their nature, are vulnerable because there is no redundancy in the system to provide resources, should the primary supply fail. Also, given the limited technical, financial and management resources possessed by developing countries, adjusting to shortages and/or implementing adaptation measures will impose a heavy burden on their national economies. The impacts of change will depend on the baseline condition of the water supply system and the ability of water resources managers to respond not only to climate and land use change but also to population growth and changes in demands, technology and economic, social and legislative conditions.

From a social perspective, vulnerability can be defined as a function of exposure, sensitivity and adaptive capacity:

$$\text{vulnerability} = f(\text{exposure, sensitivity, adaptive capacity})$$

Exposure is the changed environmental conditions a stakeholder will need to deal with. Vulnerability in the context of climate change is a consequence of changing exposure, in combination with the sensitivity of society or the stakeholder's productive system towards these new conditions, and his adaptive capacity; adaptive capacity refers to the means over which society or a given stakeholder (or stakeholder group) disposes in order to positively adapt to these new conditions, and as such, reduce its vulnerability.

2 ANALYSING THE EFFECTS OF CHANGE

2.1 BAKER (AND BIOBÍO) RIVER BASIN (CHILE)

2.1.1 Introduction

The Baker River Basin, located in Patagonia, is Chile's second biggest river basin. Climatic and morphologic conditions in the Basin vary widely in space (*these are described in more detail in the Work Package 1 and 2 reports*), but 2 very important characteristics of the Basin deserve to be mentioned here again: (i) many of the rivers in the Basin are fed by snow- and glacier melt (an important part of the Northern Patagonian Ice Field is located within the Basin limits); (ii) many rivers in the Basin first drain into the General Carrera Lake – the second biggest lake in South-America - before their waters continue to the Pacific Ocean through the Baker river itself; the lake has an important buffering effect on the discharge rates in the upper reaches of the Baker river (Figure 2.1).

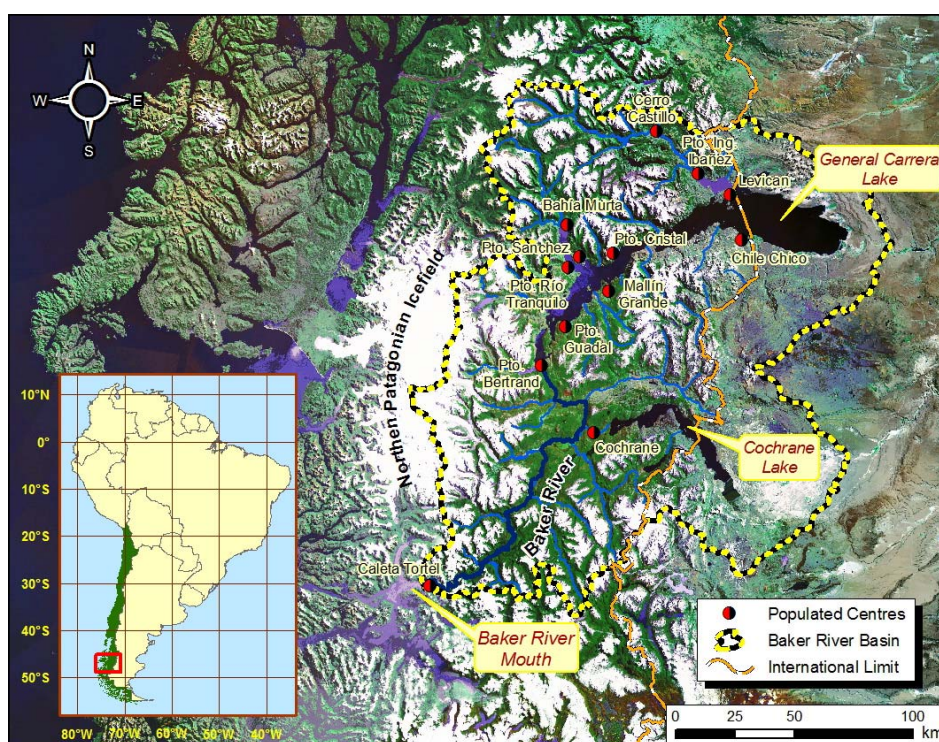


Figure 2.1 The Baker River Basin

Due to its particular climatic and geomorphological characteristics, and its resulting difficult accessibility, disclosure of the basin for human development and tourism has been very slow. As a consequence of this, also the development of environmental or hydrometeorological monitoring networks has been very limited (*see also the Work Package 2 report*). Therefore, considering the very limited amount of observed hydrometeorological time series data for the Baker River Basin (and especially, considering the nearly-complete absence of measurements from the higher parts of the Basin where it is assumed that most of the input into the basin water balance takes place), for the analysis of the potential impacts of change scenarios on the water resources in the Basin the following indirect approach was proposed and used under TWINLATIN:

- Under a previous twinning project TWINBAS (EC 6FP Contract N° 505287) hydrological modeling using the **SWAT** tool was conducted for a selected sub-basin (**Vergara**) of the Biobío Basin, which itself is located in Central Chile. The selected sub-basin is located in the Chilean Central Valley between the Andean and Coastal Mountain ranges and it therefore presents a hydrological regime

which is mainly rain-fed. The Vergara Basin represented a first, relatively simple case study for testing the applicability and usefulness of the hydrological component of SWAT in Chile, under the conditions of limited data availability which typically exist in many parts of the country (but which, even so, are much better than those for the Baker river basin); the results from this research conducted under TWINBAS are described in Stehr et al. (2008), and also in the SWAT textbook for the developing world, published in January 2009 (Arnold et al., 2009).

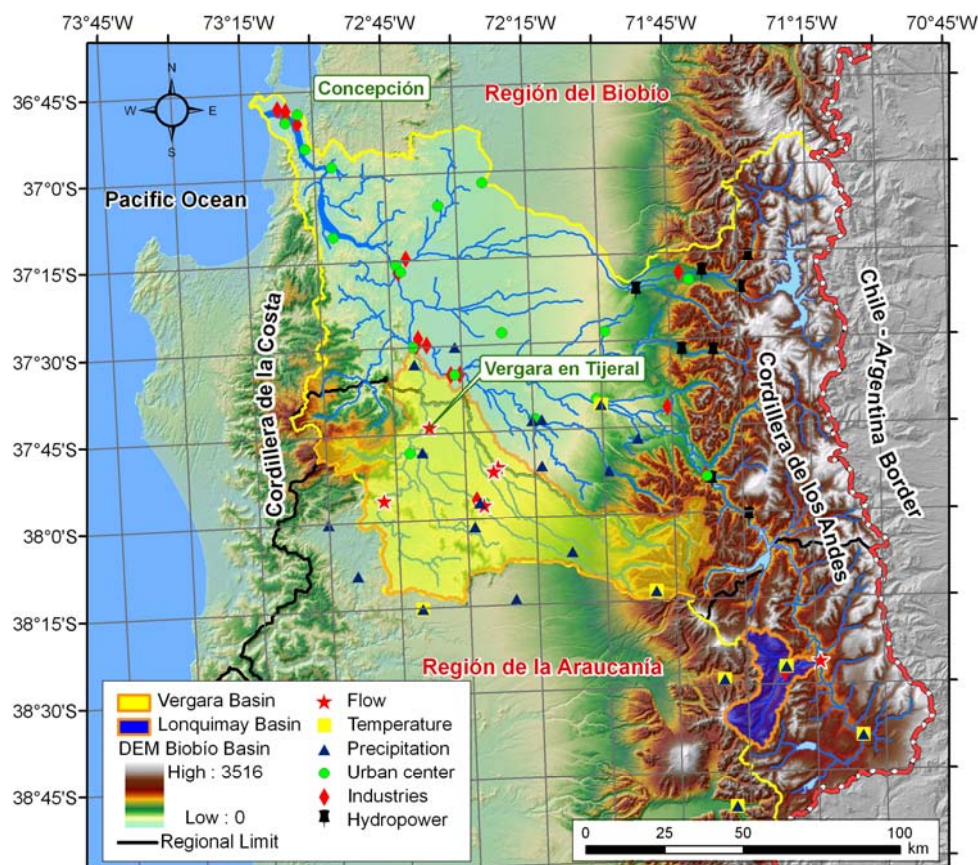


Figure 2.2 The Biobío Basin, central Chile and the modeled sub-basins, Vergara and Lonquimay

- Building further upon the experiences acquired under TWINBAS, in TWINLATIN a more complex SWAT model application was attempted in the **Lonquimay** sub-basin, another sub-basin of Biobío which is located in the Andean Mountain Range (Figure 2.2) and in which **snowmelt** contributions are important (see also the Work Package 3 report). Minimum data availability exists for this sub-basin, and it was considered that an attempt to model this sub-basin may provide highly useful information that throws a light on the possibilities and additional monitoring needs which would enable future similar efforts on the Baker River Basin. Additionally, after calibration and validation of the model application for the Lonquimay Basin, the differential impact of climate change – through mathematical simulation of different change scenarios – on a snow-fed or mixed versus a rainfall-fed river basin was clearly demonstrated. Unfortunately, current availability of input data for the Baker Basin itself does not allow for meaningful applications of such an approach on any of its sub-basins. Even so, results from the application on Lonquimay already allow for a first – qualitative – extrapolation of the potential impacts of climate change in the Baker River Basin.
- Change scenarios for the impact modeling exercise on the Lonquimay sub-basin were obtained from 2 important sources: (i) the **MAGICC/SCENGEN** tool (Hulme et al., 2000; Wigley, 2003a; Wigley, 2003b; Wigley et al., 2000); and (ii) the results from a **Regional Climate Model (RCM)** run for Chile recently conducted for the Chilean Environmental Administration CONAMA by the Department of Geophysics of the University of Chile (CONAMA-DGF, 2006). These scenarios were used to drive the change analysis of the hydrology of the Lonquimay Basin. For this purpose, a

step-by-step manual (*in Spanish*) on the use of the MAGICC/SCENGEN tool v4.1 for the generation of change signals was developed at EULA (Chile) and CIEMA (Nicaragua), applied to the Biobío (and also Cocibolca) Basin, and made available as a “twinning contribution” to the other Latin-American project partners (see Annex 1, in Spanish).

- In addition to the former, the same approach based on MAGICC/SCENGEN and the RCM runs was also used to generate change scenarios for the Baker River Basin itself. Even without conducting the hydrological modeling for the Baker Basin, this change signal information already provides very useful information which allows making a first estimation of the potential local and regional impacts of climate change.
- The information obtained from the RCM run for the Baker River Basin was incorporated in the Georeferenced Environmental Database for the Baker Basin **SIGACB** using for this purpose the ArcHydro data model, and is available for future reference.
- The topic of **Glacial Lake Outburst Flows (GLOFs)** – which had been registered in the past in the Baker River Basin during the decade of the 1950s, and which have now occurred again on several occasions during 2008 – is briefly touched, as this may be relevant from the perspective of (hydropower) development versus climate change impacts.
- A basic **vulnerability** assessment exercise was conducted with the stakeholders during the twinning workshops which were held in the Basin.
- An index for the evaluation of **adaptation** practices is proposed.

2.1.2 SWAT model calibration in Biobío and scenario generation for Biobío and Baker

2.1.2.1 Introduction

In what follows, we give a short description of the Biobío study site on which the hydrological modeling with snowmelt contributions exercise was conducted. Details on the characteristics of the Baker River Basin itself are not repeated here, but can be found in the Work Package 1, 2 and 3 reports.

The Biobío River Basin (24.371 km²; Figure 2.2) is the third biggest river basin in Chile. It is located in the South-Central part of the country (36°45' - 38°49' S; 71°00' - 73°20' O) and covers approximately 3 % of the national territory. It extends from the Andean Mountain Range in the East to the Pacific Ocean in the West. It is influenced by the temperate climate of southern Chile and by the Mediterranean climate of the central part of the country. The basin constitutes the centre for the forestry activities in the country, contains a substantial portion of all agricultural soils and plays a very important role in the national production of hydropower.

The modeling work described in what follows focuses on 2 sub-basins of Biobío: the first one (Lonquimay) is located in the Andes, whereas the second one (Vergara) is located in the Central Valley (see also Figure 2.2). The Lonquimay sub-basin (38°20' – 38°41' S; 71°13' - 71°35' O) has a surface area of 455 km². The lowest point in the basin is located at 880 m a.s.l., the highest at 2533 m a.s.l. The basin presents a mixed snow/rain-fed hydrological regime, and has maximum and minimum discharge rates during the months of June and March respectively, with a second peak in discharge rates – the snowmelt maximum – during October (Figure 2.3).

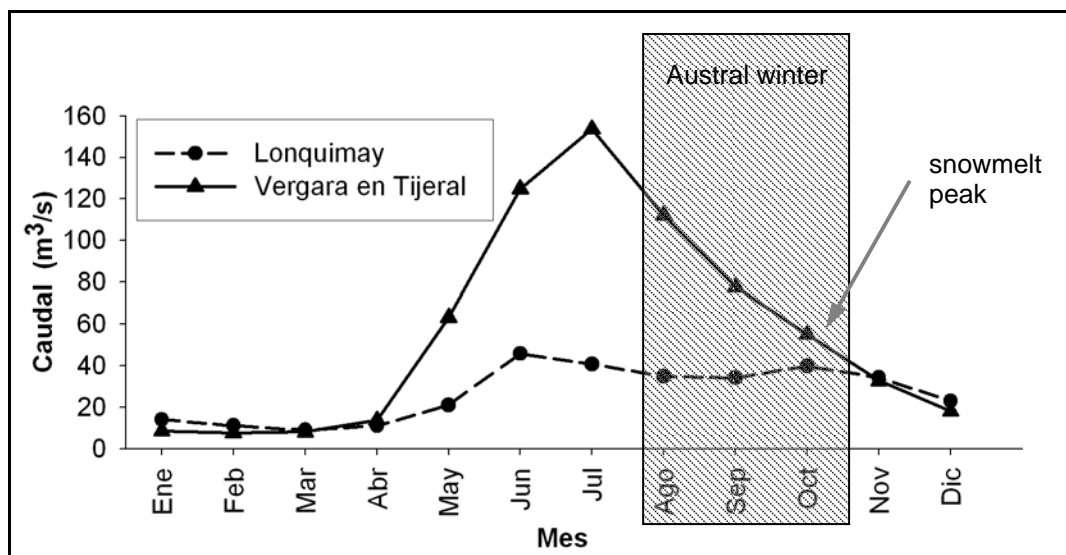


Figure 2.3 Mean monthly discharge rates for the Vergara and Lonquimay Basins for the Lonquimay basin, the presence of 2 peaks can clearly be observed

The Vergara sub-basin (37°29' - 38°14' S; 71°36' - 73°20' O) covers an area of 4.265 km² (approximately 17% of the whole Biobío Basin). The lowest point is located at 53 m a.s.l. and the highest at 1923 m a.s.l. Its hydrological regime is predominantly rain-fed, with maximum and minimum discharge rates in July and February, respectively (Figure 2.3).

For the hydrological modeling of the potential impacts of climate change in the 2 selected sub-basins of Biobío (Vergara under TWINBAS, and Lonquimay under TWINLATIN), the SWAT model (Arnold et al., 1998; Di Luzio et al., 2002) was used. SWAT or “Soil & Water Assessment Tool” is a spatially (semi-) distributed hydrological and water quality model, designed to calculate the generation and transport of runoff, sediments and contaminants from individual drainage units (sub-basins) towards the outlet of a river basin. The model was developed in the 1990s at the Department of Agriculture of the United States of America (USDA). Due to the flexibility that the model offers, as far as the requirements for input data is concerned, SWAT has been widely applied in different parts of the world, and under different conditions of (input) data availability (e.g., applications exists from the USA, Europe, India, New Zealand, etc; (Abu El-Nasr et al., 2005; Cao et al., 2006; Eckhardt et al., 2005; Gosain et al., 2005; Govender and Everson, 2005; Tripathi et al., 2006)). In SWAT, the hydrology of a river basin is conceptually divided in two big components, (i) the terrestrial phase of the hydrological cycle and (ii) the propagation phase in the river network: the contributions of the total surface area of a sub-basin to its principal river are controlled by the terrestrial component of the model, whereas in the propagation component, the movement of water through the river network towards the outlet of the basin and/or towards the internal control points (i.e. points within the basin for which limnigraph station data is available for calibration and validation purposes). A more complete description of the SWAT model and its different components can be found in Neitsch et al. (2002).

An interesting aspect of the SWAT model that facilitates its use in the analysis of impacts consists in the option to apply change factors to the input time series of precipitation and temperature. This allows for the simulation of the hydrological impact of future climatic scenarios. For this purpose, a rather simple methodology – useful as a first approximation – was implemented in the model: the whole time series used for the modeling exercise is adapted by means of the following equation

$$P_{\text{day, scenario}} = P_{\text{day, baseline}} * \left(1 + \frac{\text{change}_{\text{pcp}}}{100} \right)$$

where P_{day} is the precipitation that falls on a sub-basin for a given day and $\text{change}_{\text{pcp}}$ is the percentage of estimated change for the rainfall

$$T_{\text{max, scenario}} = T_{\text{max, baseline}} + \text{change}_{\text{tmp}}$$

$$T_{\max, \text{scenario}} = T_{\max, \text{baseline}} + \text{change}_{\text{tmp}}$$

where T_{\max} is the daily maximum temperature, T_{\min} is the minimum daily temperature and $\text{change}_{\text{tmp}}$ is the estimated change for temperature.

The change terms can vary from month to month, so as to simulate seasonal variations in the change of climatic conditions.

2.1.2.2 Inputs

The meteorological datasets (available time series of precipitation and temperature, with a daily time step; for station locations see Figure 2.2) used for the reference period runs of the SWAT model application for both sub-basins (this includes the calibration and validation) were obtained from the National Water Database or “*Banco Nacional de Aguas*”, which belongs to the Chilean General Water Directorate (“*Dirección General de Aguas*”, DGA). In order to model the spatial patterns of runoff, the hydrological component of the SWAT model was provided with a Digital Elevation Model based on the SRTM 90-m resolution data set for the study area. The description of land use/cover and soil types in the Basin was made based on the nationally available datasets. A more detailed description of these data sets and the processes used in their preparation for the model application can be found in Stehr et al. (2008). Additional information on input data sets for the hydrological model application can also be found in the Work Package 3 report.

For both sub-basins, with the aim of selecting the most relevant parameters for the calibration process, a sensitivity analysis was conducted (van Griensven et al., 2006). For calibration purposes, the automated PARASOL procedure (*Parameter Solution Method*; (van Griensven and Bauwens, 2003)) which comes implemented in SWAT2005 was applied.

2.1.2.3 Results

The calibration and validation for the reference period was conducted using the monthly output data from the SWAT model. Three statistical indicators were used: Nash-Sutcliffe efficiency (EF), percentual bias PBIAS and R^2 . In addition to this, a visual inspection was made of the correspondence between modeled and observed discharge data sets. It is considered that a model performs better WHEN EF and R^2 approach unity (1), PBIAS approaches 0 and when a general good correspondence between observed and modeled time series exists.

In the case of the application of the model to the sub-basins of the Vergara and Lonquimay rivers, the obtained results indicate a good performance of the model in both sub-basins (Table 2-1) during the calibration phase; for the validation phase, the performance is satisfactory for Lonquimay and good for Vergara. From Figure 2.4 it can be observed that in general a good correspondence was obtained between the observed and modeled discharge rates, with the notable exception of the highest discharge values.

Table 2-1 Calibration and validation results for the reference SWAT hydrological component model runs for the Vergara and Lonquimay sub-basins

	Vergara*		Lonquimay	
	Calibration	Validation	Calibration	Validation
EF	0.93	0.93	0.81	0.56
PBIAS	11.78	2.77	4.88	7.86
R^2	0.96	0.93	0.87	0.57

2.1.2.4 Baseline

The observed and modelled discharge time series for the period 1994-2002 for both sub-basins of the Biobío are given in Figure 2.4.

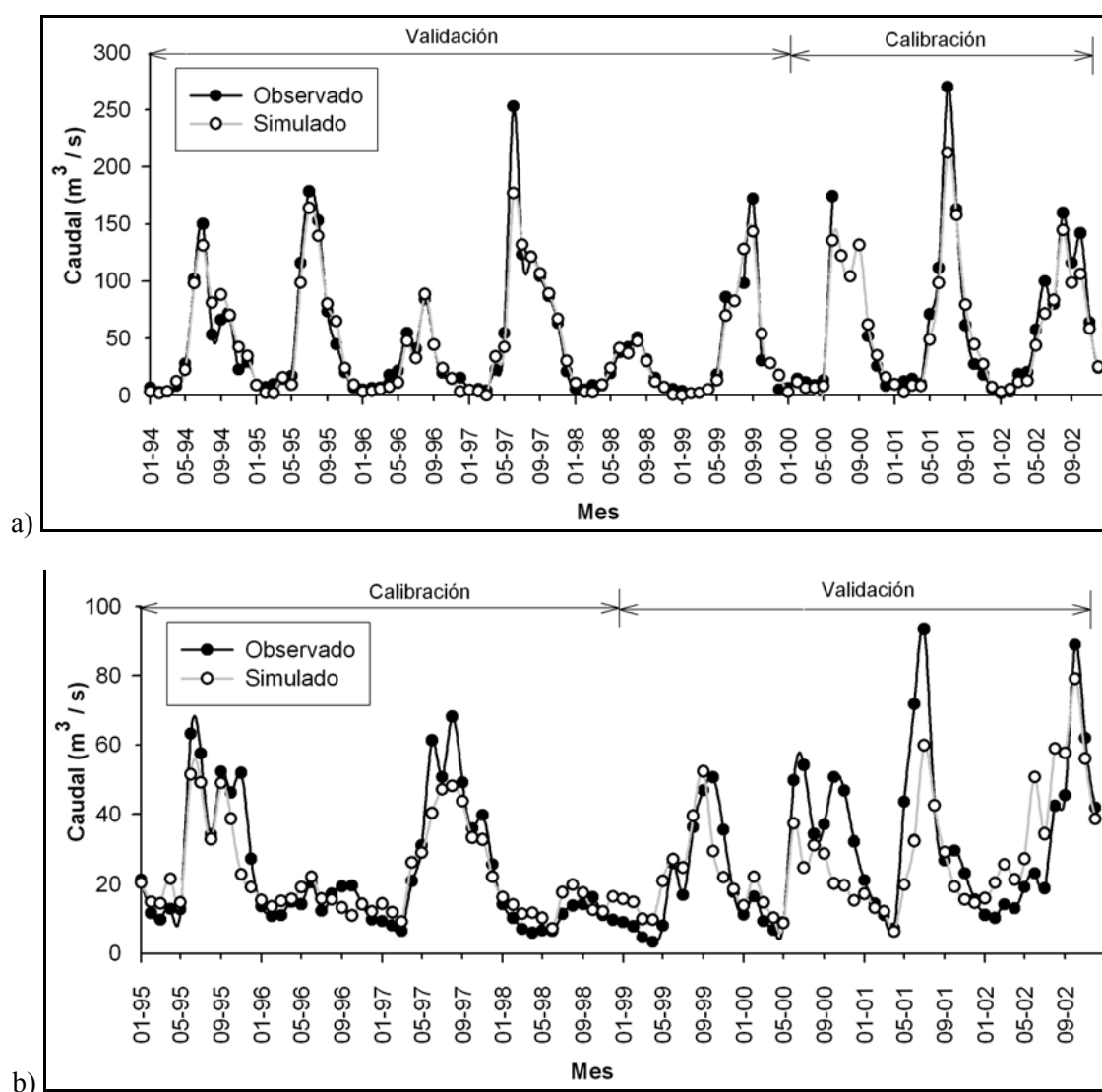


Figure 2.4 Observed and simulated discharge time series for the baseline scenario calibration and validation results for the Vergara (a) and Lonquimay (b) sub-basins

For the scenario modelling, in the work under TWINLATIN however the RCM simulated baseline has been used for further impact assessment rather than the observed baseline. Impact assessment made by applying change factors to observed rather than simulated baseline data presents advantages – especially when interpreting future values in absolute terms – but the application of change factors directly to the RCM simulated baseline offers a fast and easy means to compare relative impacts from change factors obtained from the RCM runs with those obtained from the application of MAGICC/SCENGEN. The last approach has been used here.

For the Baker River Basin itself, we proceed here to depict the “official” (DGA, 1987) and RCM-simulated baseline, respectively, in Figure 2.5 and Figure 2.6.

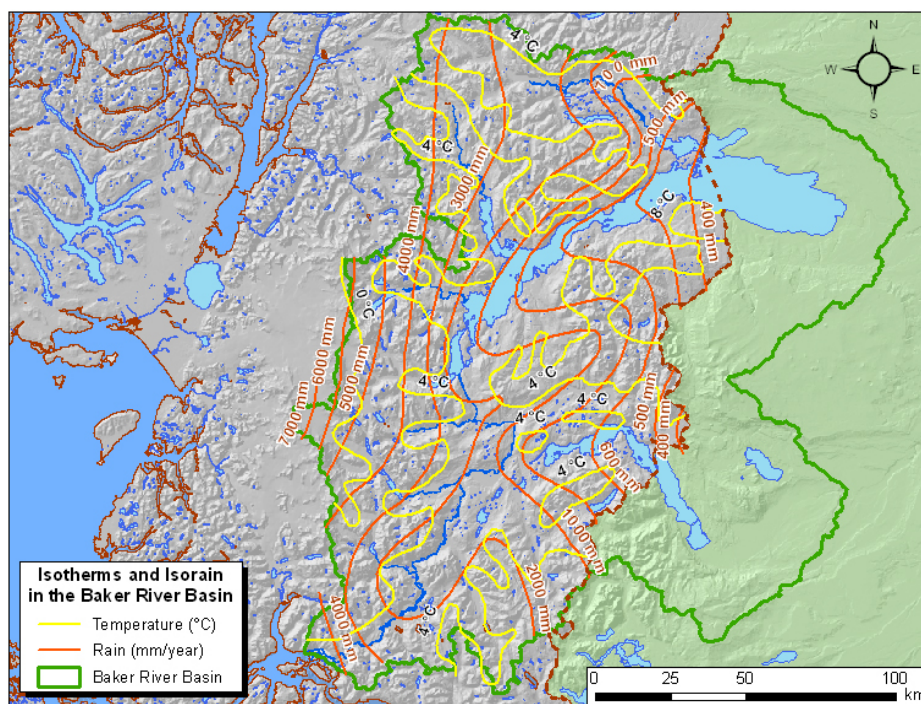


Figure 2.5 Mean annual temperature [$^{\circ}\text{C}$] and precipitation [mm yr^{-1}] for the Baker Basin from the General Water Directorate (DGA, 1987)

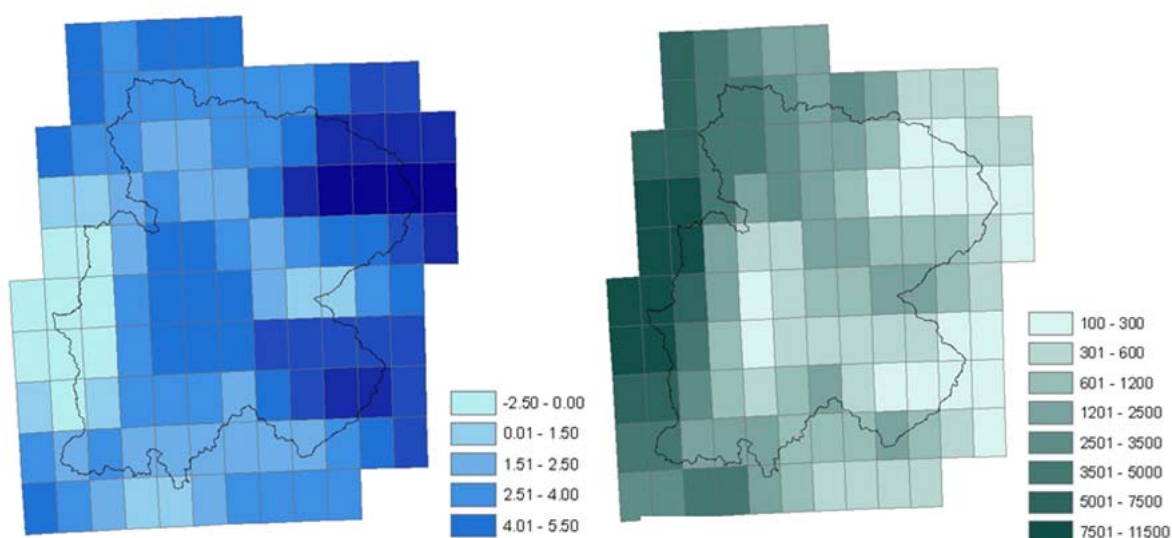


Figure 2.6 Baseline for the Baker River Basin as obtained from the RCM model run (left) mean annual temperature [$^{\circ}\text{C}$], and (right) mean annual precipitation [mm yr^{-1}], both for the 1961-1990 reference period

When making a coarse comparison of Figure 2.5 and Figure 2.6, the RCM model run for the reference period seems to provide a relatively good first approximation of the “real” magnitude and spatial patterns of precipitation and temperature over the Baker Basin. This seems to indicate that the simulation of future climatic conditions over the Baker Basin by means of the RCM driven by the HADCM3 may provide interesting information for stakeholders, with regard to potential future climatic conditions in the Basin.

2.1.3 Scenario creation and impact assessment

2.1.3.1 Separate effects

A Climate change

The scenario modelling exercise for the Biobío sub-basins was inspired on a generic methodological framework initially developed under TWINBAS and further implemented under TWINLATIN. The framework is shown in Figure 2.7. The implementation of the components in the left part of the framework has already been described in the previous chapter.

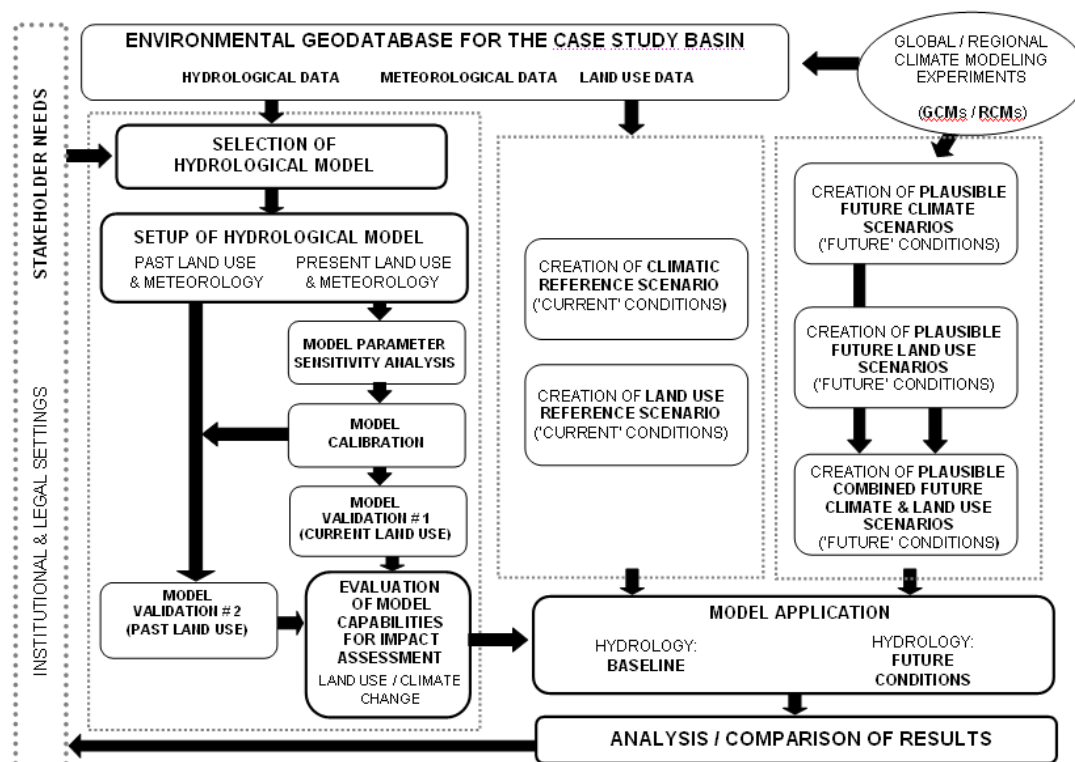


Figure 2.7 Generic framework for change impact assessment through hydrological modelling (Debels et al., 2007)

For the Chilean case study basins, attention under TWINLATIN was focused on the climate change component (model validation for Lonquimay has currently been conducted for 1 land use condition only).

- **Creation of scenarios with MAGICC/SCENGEN**

The MAGICC/SCENGEN tool v4.1. (“*Model for the Assessment of Greenhouse-gas Induced Climate Change/Scenario Generator*”) (Wigley, 2003b; Wigley, 2003a) is a simple climate scenario generator, useful for conducting impact studies in which the effect of uncertainties associated with the existence of different Global Circulation Models (GCM) and greenhouse gases emission scenarios can be taken into account. The user-friendly software tool consists of 2 main components: MAGICC is a simple climatic model (coupled gas-cycle model for mean global temperature and sea level changes) which allows the user to make both independent simulations as well as to emulate the global results of the more complex, fully 3-D GCMs (IPCC, 1997). MAGICC allows the user to select from different emission scenarios for greenhouse gases, aerosols and sulphur dioxide; these selections are then taken by the model as input for the calculation of future conditions of the mean global temperature. The 4.1 version of the tool – which is the version used in TWINLATIN – has been applied by the IPCC in its Third Assessment Report (IPCC TAR); it includes the option to simulate global climatic change for many of the emission scenarios contained in the Special Report on Emission Scenarios (SRES) from

the IPCC. The second component of the tool, SCENGEN, consists fundamentally of a database which contains the “normalized” spatial patterns (i.e., patterns of regional changes per unitary change in the mean global temperature) which were generated from a large number of 3-D model runs of the more complex GCMs, and a regionalization algorithm: starting with the change in mean global temperature provided by the MAGICC run, and by means of a scaling algorithm, SCENGEN allows, among other options, “simulating” the spatial patterns of regional changes in temperature and precipitation produced by each one of a total of 17 GCMs (for more details on the scaling process we refer to the literature on the tool which has been cited above). SCENGEN produces output for a raster with global coverage, consisting of 5° x 5° cells.

In the present study – in order to incorporate in our evaluation the impact of uncertainty associated with the conceptualization/simplification of the global and regional climate processes in the different models, as well as with the existence of different scenarios for the future emissions of greenhouse gases – we analyzed the change signals obtained from MAGICC/SCENGEN for 7 different GCMs: HADCM3, ECHAM4.5, GFDL, CCSR/NIES, CCCMa, NCAR/PCM and CSIRO. We considered the combined effects of greenhouse gases and aerosols, and for each GCM we simulated change for the 6 SRES “marker” emission scenarios: A1FI, A1T, A1B, A2, B2, B1 (IPCC, 2001). As such, a total of 42 scenarios were obtained from the tool. Changes for precipitation and temperature were simulated for a future time window of 30 years centered on 2085 and 2050; the mean annual results were used for the impact assessment modeling, and are shown in Figure 2.8. The exercise was conducted for both the Biobío Basin (these results were used for the impacts assessments with the hydrological model application) as well as for the Baker River Basin (these results were used to obtain a first impression of potential future conditions in the area of the Baker Basin).

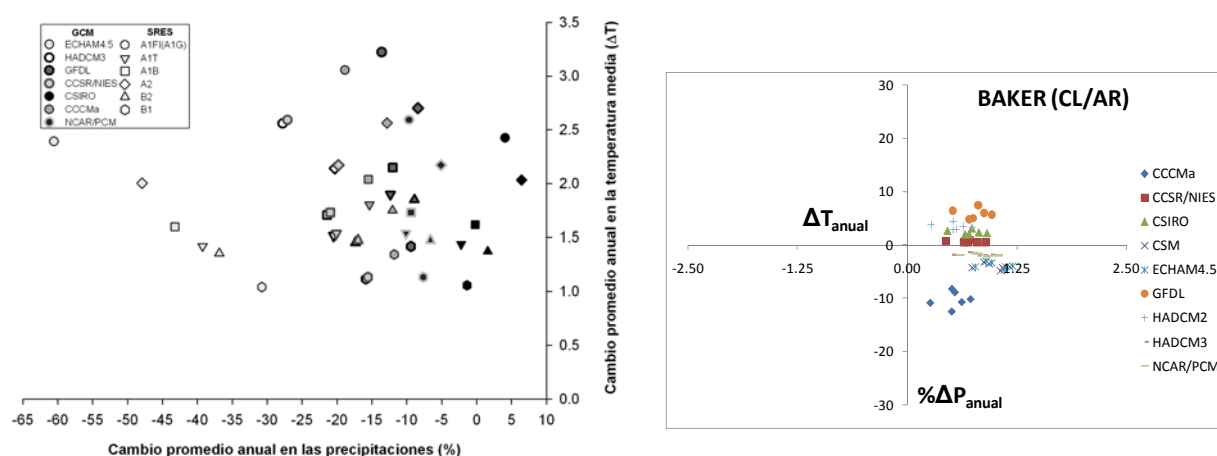


Figure 2.8 Change signals obtained from the MAGICC/SCENGEN (v4.1) 5°x5° pixel corresponds to the (left) Biobío Basin and (right) Baker Basin; change is for a 30-year time window centered around 2085 (Biobío) and 2050 (Baker) with regard to the modeled reference period 1961-1990, for 7 different GCMs and 6 SRES marker scenarios

- **Creation of regional scenarios based on the output from an RCM**

In the “Study on Climatic Variability in Chile for the XXIst Century” (CONAMA-DGF, 2006), a large-scale model (HadCM3, mean resolution = 300 x 300 km) was used to indirectly force the regional-scale simulations. The atmospheric model which is forced at the surface with the output from the previously mentioned GCM is HadAM3, which is very similar but has a higher resolution. Regional simulations with a spatial resolution of 25 km are then finally generated by means of the PRECIS tool. The different output variables of this model (e.g. mean, minimum and maximum temperature and precipitation) are available for each point of a grid with a spatial extension of 18°–57°S, 62°–85°O, area which includes both the Biobío and Baker River Basins. In this way, for each variable, at each point of the grid, 3 daily time series can be obtained, each one of these covering a 30-years modeling period: a first series corresponds to the simulated reference or control climate (“current” climate, which corresponds to the 1961-1990 period), whereas the other 2 series correspond to “future climates” for the period 2070-2100, one for the SRES A2 emission scenario and another one

for the SRES B2 emission scenario. From the results of these RCM runs conducted at the DGF-UChile, the time series at the data points that correspond to the Biobío and Baker study areas were extracted. A change factor for mean annual values has been calculated at the different points in the Baker River Basin (Figure 2.10), and the full time series have been incorporated in the ArcHydro-based Environmental Database for the Basin. In the case of the Biobío Basin, the change factors were also further used for the impact assessment modeling by means of the SWAT model.

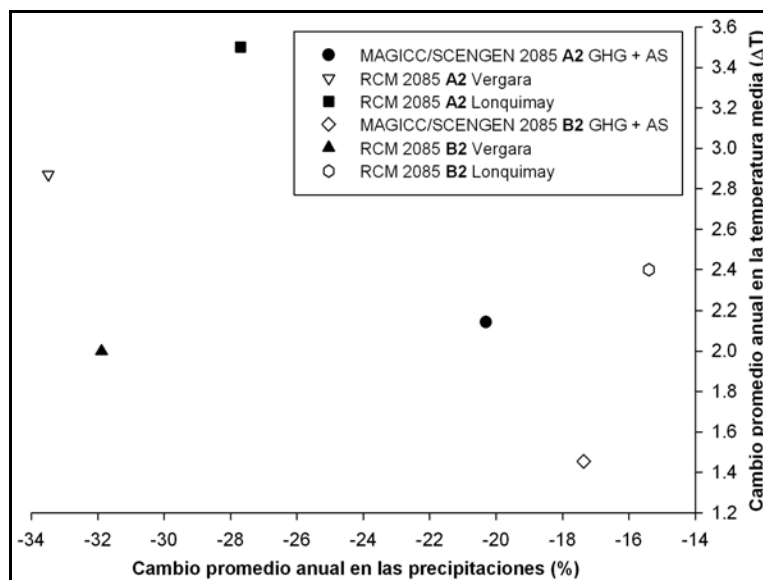


Figure 2.9 Mean change signals for the Vergara and Lonquimay sub-basins of Biobío obtained from the PRECIS model (RCM) runs
% change in annual precipitation in the X-axis and absolute change in mean annual temperature in the Y-axis; the corresponding results from MAGICC/SCENGEN are also given for comparison purposes

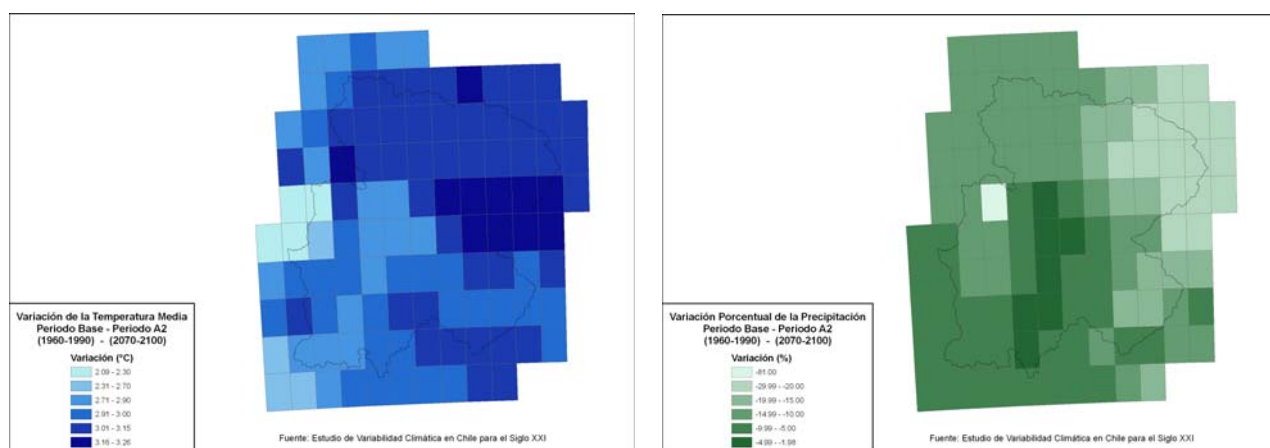


Figure 2.10 Change signals for all points (cells) of the RCM model mesh for the Baker River Basin 2070-2100 versus the 1960-1990 reference period; changes for both mean annual temperature (absolute change) and precipitation (% change)

- **Scenario simulation and analysis under TWINLATIN**

In order to evaluate the sensitivity of the hydrology of the two sub-basins of Biobío to climate change, the impacts of the different plausible future climatic scenarios developed and described under the previous point were simulated. First, the meteorological series for the Basin for the 1961-1990 reference period generated by means of the RCM model (CONAMA-DGF, 2006) was used to establish a “simulated” baseline (in future efforts, the real observed baseline can also be used for studying change impacts, in combination with change factors). The RCM reference period also

corresponds to the baseline period modeled by the MAGICC/SCENGEN tool, so this allows for an easy first comparison of the hydrological results obtained by perturbing the “baseline” input time series for the SWAT model with the change signals obtained from both the GCMs (MAGICC/SCENGEN) as well as those from the finer-scale RCM runs. As such, the used methodology allows for both an evaluation of the impacts of uncertainty associated with the existence of different GCMs and emission scenarios, as well as of the effects of scale on change signals (Figure 2.9) and their associated impacts.

As a first approximation to the analysis of the hydrological sensitivity of the Lonquimay system to climate change, and in order to allow for a more direct comparison of change factors obtained from MAGICC/SCENGEN and the RCM, the perturbations of the control time series in both cases were assumed to be uniform in space and time; as such only the magnitude of the variables temperature and precipitation was affected and not their spatial and temporal distribution. The results obtained for the Vergara sub-basin are also given here, as they allow for an evaluation of the differential impacts of climate change in a rainfall-fed versus a mixed snow/rain-fed river basin.

The vast majority of the 42+2 climate change scenarios (2071-2100 versus 1961-1990) developed for each sub-basin under TWINLATIN from the Regional and Global Circulation Models indicate a reduction in annual precipitation rates for the Biobío Basin (values range from + 7 % to – 60 %). This change in precipitation rates is accompanied by a rise in the mean annual temperature (all scenarios, without exception), which varies between + 1 °C and + 3.5 °C (Figure 2.8). Whereas due to scale, the MAGICC/SCENGEN tool only provides a single change value for both Biobío sub-basins, with the RCM application a more sub-basin specific change factor could be obtained. From these RCM results, it can be seen how the increase in temperature tends to be higher in the Andean sub-basin; however the decrease in precipitation tends to be less drastic (Figure 2.9).

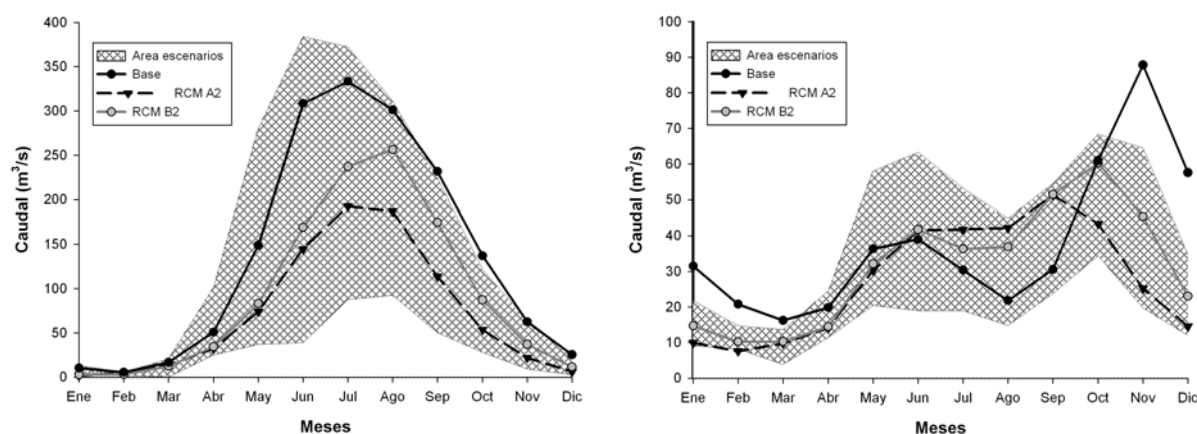


Figure 2.11 Hydrological impacts on mean monthly discharges of change scenarios the rainfall-fed Vergara and (b) mixed snow/rain-fed Lonquimay sub-basins (the pattern-filled areas indicate the total range of outcomes from the 42 MAGICC/SCENGEN scenarios)

From the modeling of the hydrological response in the Vergara and Lonquimay basins to the 42+2 climate change scenarios – which was conducted using the previously calibrated and validated SWAT model tool- a wide range of variations in possible future mean annual and monthly discharge rates was obtained (Figure 2.11 and Figure 2.12). Even when differences in the results can be observed depending on the modeled scenario, it is possible to conclude that in both basins the hydrology – according to the results of SWAT – appears to be highly sensitive to changes in the modeled climatic variables.

In the case of the Vergara Basin, the percentage reduction in discharge rates is considerably higher than the corresponding percent change in annual precipitation (Figure 2.12). This indicates a major impact from climate change in the basin hydrology than what might be initially expected by just considering the value of the change in annual precipitation. Even so, a clear linear relationship between both changes can be observed from Figure 2.12, which would allow for making a first

assessment of potential impacts in water resources for this and other nearby basins directly from change signals for annual precipitation.

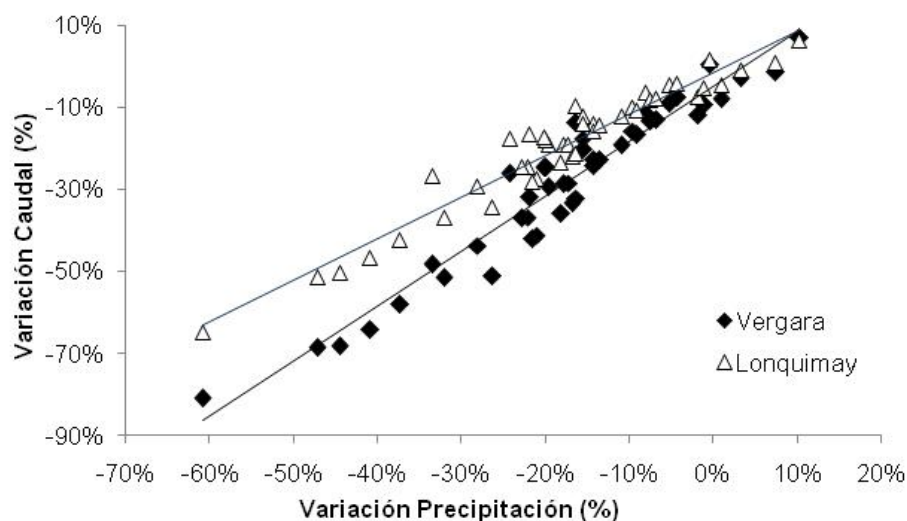


Figure 2.12 Relation between % changes in mean annual precipitation (X-axis) and mean annual discharge rates (Y-axis) for the rainfall-fed Vergara and mixed-regime Lonquimay sub-basins (Biobío Basin, Chile)

A similar phenomenon can be observed in the case of the Lonquimay Basin. It should be mentioned, however, that for this sub-basin the proportional increase in the changes in discharge (with regard to changes in precipitation) is much less pronounced. On the other hand, in the case of this sub-basin of mixed (rainfall-snowmelt) hydrological regime, the combined effect of changes in precipitation and temperatures leads to significant modifications in the form of the annual hydrograph (Figure 2.11). The simulations clearly illustrate what has been expressed by Gleick (1986), Chalecki and Gleick (1999) and Lopez-Moreno and Nogues-Bravo (2005), i.e. a rise in the rate of rainfall versus snowfall during the winter months, a shorter snow season, and an earlier snowmelt discharge maximum due to global warming.

Even if only 2 sub-basins of Biobío have been modeled (approximately 20% of the total Biobío Basin area), the results already allow for a first qualitative, or even semi-quantitative interpretation of what may occur in the Biobío Basin – and other similar basins – as a consequence of climate change. The results of this work clearly indicate how climate change can and most probably will constitute an additional stress factor to ecosystems and human society in many river basins, clearly indicating the importance and usefulness of anticipated mitigation and adaptation actions, such as a major awareness building among stakeholders on the needs for rational water use, and a further promotion of the concepts of integrated and adaptive water resources management practicing.

For the Baker River Basin, it can be seen from Figure 2.6 that different GCMs produce different change signals for precipitation, whereas all GCMs produce a rise in temperature. The HADCM3 produces a slight decrease in precipitation (2050), the results from the RCM runs – which have been driven by the HADCM3 – indeed also show a decrease in precipitation for the time window centered on 2085. However, in certain sectors of the basin the simulated decrease is considerably higher than the mean value obtained for 2050 from MAGICC/SCENGEN. In the Baker Basin, the divergence in the results obtained for mean annual precipitation from MAGICC/SCENGEN for the different GCMs thus complicates an unambiguous evaluation of the potential impacts of climate change on water resources; however, increased snowmelt and associated hydrological changes due to increased temperatures (all models) can certainly be foreseen. In addition to this, we remember the relative good representation of the baseline in the Basin by means of the HADCM3-driven RCM model run.

B Land use changes

Due to the specific characteristics of the Baker river basin (see also WP 2 report), no hydrological impact modelling due to land use changes was conducted under TWINLATIN.

C Changes in water demands

Due to the specific characteristics of the Baker river basin (see also WP 2 report), no such hydrological impact modelling was conducted under TWINLATIN. A simple projection of potential additional water demands in the immediate future however was given under WP 7, by means of an indication of requests for “water use rights” which are currently being revised by the competent authorities.

D Water resources developments

The most important human-induced, potential change for the near future in the Baker river basin (i.e. this decade) is the highly controversial planned hydropower (2 dams) development. The combined Environmental Impacts Assessment for these projects has been recently delivered to the corresponding authorities, and a considerable amount of observations has been formulated. As this development project is mainly focused on a sub-sector of the Basin (the Baker river itself), and as it has been/should have been extensively addressed by the project’s EIA, no specific work on this topic has been conducted in TWINLATIN under this work package. Rather, TWINLATIN aimed at filling in other relevant and important knowledge gaps, which currently cannot and are not being (completely) addressed by other means (*~complementarity of research efforts*). For this reason, work related to the hydropower development in the Basin was mainly limited to the work conducted under WP 9 (economics), as an important knowledge gap with respect to certain of its economic impacts did exist, which were not being addressed by other means.

2.1.3.2 Combined effects

No such modelling was conducted in the Baker or Biobío river basin under TWINLATIN.

2.1.4 Vulnerability assessment

2.1.4.1 Exposure of society in the Chilean case study basins

Results obtained from the scenario modelling and documented in the previous chapter relate to the “exposure” component of vulnerability, in the specific field of climate change impacts on water resources (basin hydrology). Both the results from the SWAT hydrological scenario modelling work on the 2 sub-basins from Biobío as well as the generation of climate change scenarios for the Baker Basin show high probabilities for an exposure of society to considerably different future conditions of availability (*which will also impact quality*) in the water resources in both Basins.

2.1.4.2 Vulnerability of water stakeholders in the Chilean case study basins

Without having conducted major, quantitative analyses on the “sensitivity” component of vulnerability, the magnitude of the “*plausible*” impacts obtained from the scenario modeling in Vergara and Lonquimay (which indicate a high probability of exposure of water users to considerable changes in the total availability and temporal distribution of water resources in the modeled sub-basins) in combination with the type of water uses that exist in the basin (irrigation, industry, drinking water, ...) allow us to assume that a considerable vulnerability potential exists in these Chilean case study basins.

From these results, it can thus be assumed that a considerable amount of adaptive capacity will be required from stakeholders in the basin if their vulnerability towards the impacts from climate change on water resources is to be reduced/brought down or maintained at levels which are acceptable for society. Even if only 2 sub-basins have been modeled (approx. 20 % of the total Biobío Basin), the

model results illustrate clearly enough how the water resources sector could be impacted basin-wide. Extrapolation of the obtained results – in particular those obtained for the mixed-regime Lonquimay Basin – to the Baker River Basin also enable us to foresee certain vulnerabilities of society in the Baker River Basin as well.

Indications of existing and potential future vulnerability of society in the Baker River Basin to the effects of climate change already exist indeed: as an illustration of this, we mention here the repeated occurrence during 2008 (3 different events) of a phenomenon which leads to extreme hydrological events, and which is known as “Glacial Lake Outburst Flow” (GLOF).

A GLOF can occur when the contention of a lake by a glacier or a terminal moraine dam suddenly fails. This can happen due to erosion, a buildup of water pressure upstream of the glacier or dam, an avalanche of rock or heavy snow, an earthquake or cryoseism, volcanic eruptions under the ice, or if a large enough portion of a glacier breaks off and massively displaces the waters in a glacial lake at its base.

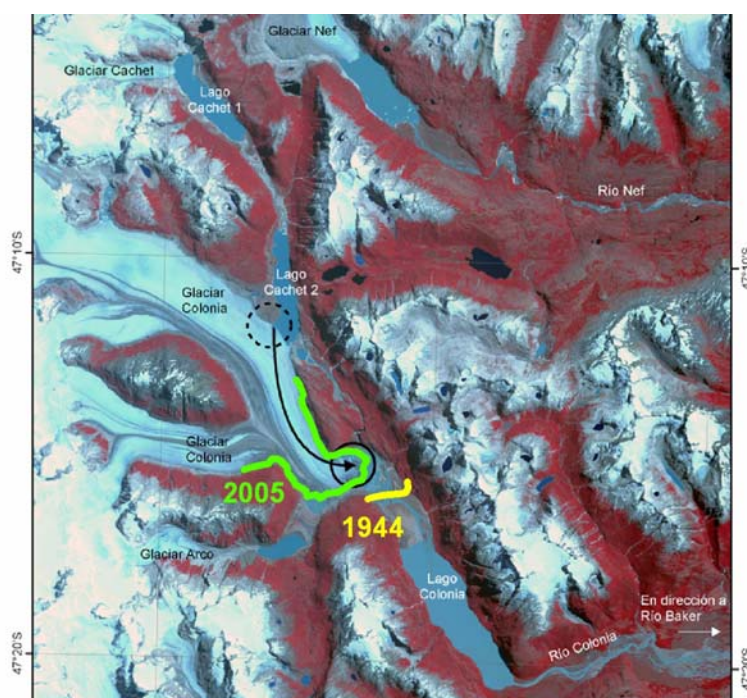


Figure 2.13 Schematic illustration of the Glacial Lake Outburst Flow (GLOF) pathway together with an indication of recent and historic glacier front
 the above figure is based on a combination of information sources available from <http://www.glaciologia.cl/>

In the case of the 2008 Cachet-2 lake GLOFs in the Baker River Basin, increased pressure on the glacier wall due to increased melt water accumulation in the periglacial lake, caused by unusually high summer temperatures in the area would be at the basis of the occurrence of the phenomenon: a tunnel was generated by the water through the glacier wall (Figure 2.13), leading to a sudden emptying of the lake; the tunnel then collapsed after the occurrence of the GLOF, causing the lake to fill up again and leaving the possibility for a new occurrence of the same phenomenon later on during the same year.

The sudden release of the tremendous volume of water, originally contained in the lake, led to unusual peak discharges and flash floods in the downstream river network, with damages to local human society as a consequence (Figure 2.14).

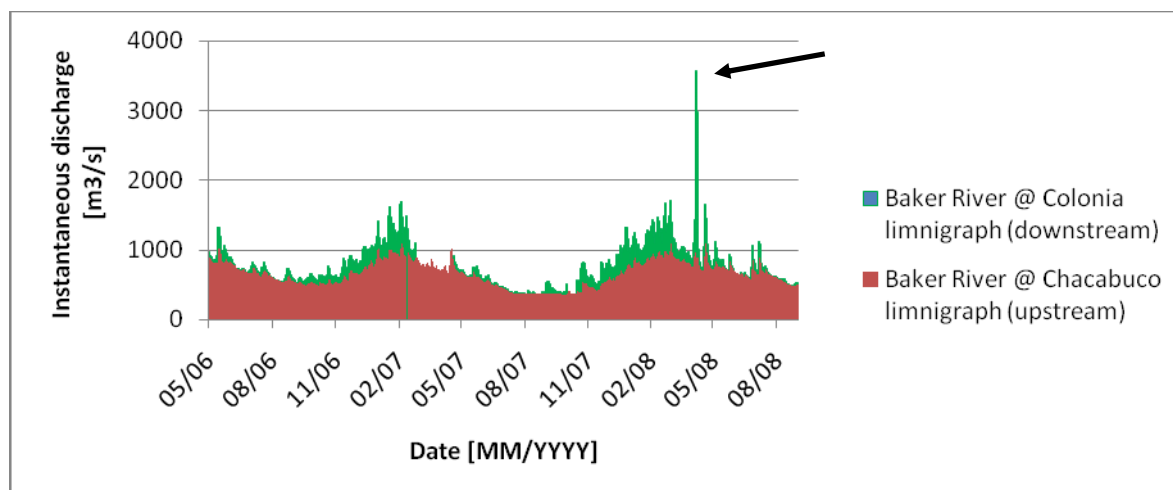


Figure 2.14 DGA limnigraph data time series clearly showing the effect of the GLOF on the discharge rates in the Baker River

Chacabuco and Colonia limnigraph stations are located up- and downstream of the confluence between the Baker River and the tributary (Colonia river) on which the GLOF occurred

In April of 2008 – after the occurrence of the Baker Basins’ first Cachet-2 Lake GLOF that year – researchers from the *Centro de Estudios Científicos* (CECS), Valdivia, Chile – which have conducted a lot of work on glaciology in the Patagonian Ice Fields – made public their concern over the increasing frequency with which glacial lakes were emptying, attributing this phenomenon as a “probable consequence of climate change”. Earlier registers of GLOFs in the Baker River Basin date from the 1950’s. A more detailed inventory of the presence of periglacial lakes, or the potential future formation of periglacial lakes in the Basin, acquire relevance in this context and should be set forward as a task for future work, especially in the context of (hydropower) development plans on and around the Baker River.

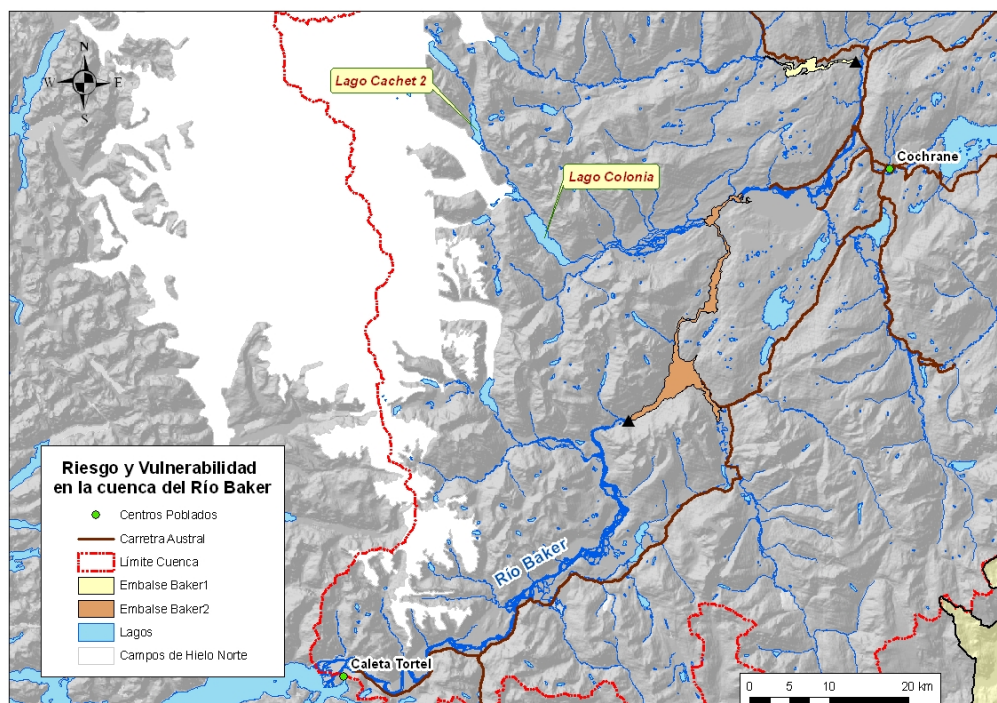


Figure 2.15 Location of the Cachet-2 periglacial lake and the 2 planned hydropower reservoirs “Embalse Baker 1 and 2” are indicated by the yellow and brown polygons on the Baker River, respectively

2.1.4.3 Public participation in the Baker Basin and the perception of vulnerability

During the public participation workshops held in the second half of 2008 in the different municipalities of the Baker River Basin, a small exercise was conducted as to evaluate the existing perception of vulnerability towards the effects of climate change among stakeholders in the basin. For this purpose, through a questionnaire, stakeholders were allowed to express their perceptions with regard to the factors that in their opinion most influence their vulnerability towards the (water resources-related) effects of climate change (Figure 2.16). Previous to the application of the enquiry, a powerpoint presentation was given in which the concepts of vulnerability, exposure, sensitivity and adaptive capacity were explained in simplified terms. The enquiry was applied twice, once before and once after results from the work on the exposure component in TWINLATIN (described in previous chapters of this report) were shown (also in a simplified manner). The aim here was to see if the provision of information from site- or region-specific research influenced the stakeholder's perception of vulnerability.

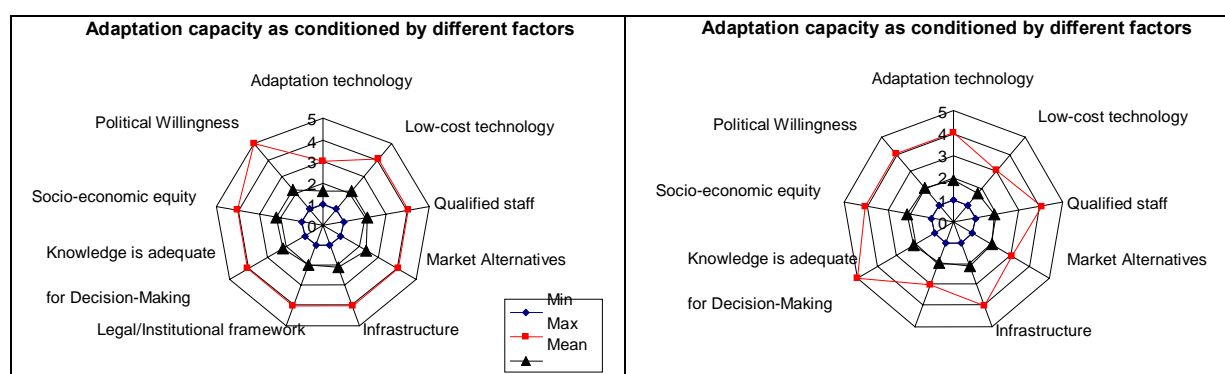


Figure 2.16 Stakeholder perception with regard to vulnerability - factors that condition adaptive capacity to climate change perception before (left) and after (right) the results from TWINLATIN research

Figure 2.16 shows outcome from this public participation process. Each axis in the graph represents a factor which is considered to influence the adaptive capacity of stakeholders. Participants were asked to assign a high value to those factors whose current conditions in the Basin or country positively contribute to their adaptive capacity, whereas a low score needed to be assigned to those factors whose current condition is seen as a cause of low adaptive capacity, and which thus contribute to higher vulnerability.

Factors were: (i) the existence of technology which would enable adaptation; (ii) the availability of this technology at accessible costs; (iii) the existence of qualified personnel to make use of such technology; (iv) the existence of market alternatives (*this could be eg. good market prices for more drought-resistant crop alternatives in case of predictions of a drier climate*); (v) the availability of adequate public infrastructure (*this could be eg. flood protection dams; early warning systems, etc.*); (vi) and adequate legal/institutional framework; (vii) adequate knowledge for decision-making (*eg. results from research on climate change impacts; adequate monitoring networks*); (viii) socio-economic equity (*inequity is a negative factor as the poor tend to have less adaptive capacity*); (ix) political willingness to act.

From the results (minimum versus maximum scores) it can be seen how different stakeholders had different opinions with regard to the impact of the different factors; however, mostly a low adaptive capacity was indicated in the results. After information from the TWINLATIN assessments on the potential impacts of climate change was presented to the stakeholders, only for 2 factors a higher maximum score was obtained (one of them being the availability of knowledge for decision-making). For several other factors, a lower maximum score was obtained. It is important to indicate here that the current results are based on a small amount of questionnaires only (participation of stakeholders in public events in the Baker Basin was typically very low). For this reason, we do not conduct a more in-depth analysis of the obtained results here. We do believe however that larger-scale applications of

the conducted approach can provide highly valuable information on the fields/those aspects from society where efforts need to be focused, if vulnerability levels are to be lowered.

2.1.4.4 Adaptation to reduce vulnerability

In order to reduce vulnerability, a timely adaptation to probable new environmental conditions under climate change becomes imperative. Adaptation in the context of human society can be defined as: ‘adjustments in human systems in response to actual or expected climatic stimuli (*~exposures*) or their effects (*~exposures + sensitivity*), in order to moderate harm or exploit beneficial opportunities’ (IPCC 2001). It is an integral part of the implementation of the United Nations Framework Convention on Climate Change (UN, 1992), and ‘requires urgent attention and action on the part of all countries’ (UNFCCC, 2002).

After the evaluation of vulnerability, a next logical step in the preparation of society for the potential impacts of climate change thus consists of the definition of adaptation practices for stakeholders in the water resources sector. Through the implementation of such adaptation practices, vulnerability can be addressed and reduced.

In this context, at EULA-Chile/CIEMA-UNI under TWINLATIN and through a collaborative research effort with a group of non-TWINLATIN researchers from the Latin-American and Caribbean Region brought together by the Inter-American Institute on Global Change Research (IAI), starting from a common interest in impacts in the water resources sector a prototype multi-purpose index was developed and proposed for use in the evaluation of practices for adaptation to climate variability and change. The Index of Usefulness of Practices for Adaptation (IUPA) allows the user to assign weights and scores to a set of user-defined criteria for evaluating the general usefulness of adaptation practices. Individual criterion scores are then aggregated into a final index value. Both the final value and the individual parameter scores provide useful information for improved decision making in the context of the definition of adaptation measures for climate change. An innovative aspect of this IUPA index is that guidance is given to the user through the inclusion of recommendations on evaluation criteria and criterion-specific weight factors. This guidance is provided by the aforementioned expert panel from the Latin-American and Caribbean Region (LAC). Although the index has not been applied yet in any of the TWINLATIN case study basins (no major adaptation practices are known), its usefulness for both TWINLATIN and other basins in the world was demonstrated through a practical application for an existing adaptation practice well-known to one of the research group members. The proposed index is particularly practical for a quick first assessment or when limited financial resources are available, making the tool especially useful for practitioners in the developing world. The index is flexible both from the perspective of its construction and use, and additional expert opinions can easily be included in future versions of the tool. The excel worksheet used for calculating the index value is shown in Figure 2.17. The index and its application are described in detail in Debels et al. (2008).

Index for the evaluation of the Usefulness of Practices for Adaptation - IUPA v1.0													
Case Study: Improving Disaster Management, Chile													
I VARIABLES			II SUGGESTIONS OF THE PANEL					III EVALUATION BY THE USER					
NAME OF THE VARIABLE			SUGGESTED WEIGHT (0-10)	SUGGESTED RELEVANCE	n	σ	level of agreement	ASSIGNED WEIGHT	ASSIGNED RELEVANCE	SCORE (design phase)	WEIGHTED SCORE (design)	SCORE (post-implementation)	WEIGHTED SCORE (post-)
A	B	C	D	E	F	G	H	I	J	K	L	M	N
A SUGGESTED "CORE" VARIABLES	1	ACCOMPLISHMENT OF THE OBJECTIVES	8.3	HIGH	8	1.0	M	9	HIGH		-	8	72
	2	REQUIRED IMPLEMENTATION TIME	6.8	MEDIUM	8	0.7	H	7	HIGH		-	8	56
	3	TOTAL COST	6.6	MEDIUM	8	1.3	M	7	HIGH		-	9	63
	4	ROBUSTNESS AND/OR FLEXIBILITY OF THE SOLUTION	8.9	HIGH	8	0.8	H	10	HIGH		-	9	90
	5	LEVEL OF AUTONOMY (IN DECIDING AND ACTING)	7.1	HIGH	8	1.5	M	6	MEDIUM		-	5	30
	6	PROPORTION OF BENEFICIARIES	7.1	HIGH	8	1.6	L	9	HIGH		-	8	72
	7	CONTINUITY IN TIME OF PROJECT OUTCOME	7.8	HIGH	8	0.9	H	8	HIGH		-	6	48
	8	LEVEL OF RESILIENCE	8.4	HIGH	8	1.2	M	10	HIGH		-	8	80
	9	INTEGRATION WITH OTHER POLICY DOMAINS	7.5	HIGH	8	1.4	M	8	HIGH		-	8	64
	10	PARTICIPATION OF TARGET POPULATION	8.5	HIGH	8	1.1	M	9	HIGH		-	6	54
B SUGGESTED "COMPLEMENTARY" VARIABLES	1	ATTENTION TO MOST VULNERABLE GROUPS	7.9	HIGH	8	1.2	M	9	HIGH		-	9	81
	2	LEVEL OF ENVIRONMENTAL PROTECTION	6.8	MEDIUM	8	1.0	M	7	HIGH		-	7	49
	3	REPEATABILITY	5.6	MEDIUM	8	1.8	L	5	MEDIUM		-	8	40
	4	INCORPORATION OF LOCAL/TRADITIONAL KNOWLEDGE	6.0	MEDIUM	8	1.9	L	4	MEDIUM		-	2	8
5		-	not defined					-	not defined		-	-	
6		-	not defined					-	not defined		-	-	
7		-	not defined					-	not defined		-	-	
8		-	not defined					-	not defined		-	-	
9		-	not defined					-	not defined		-	-	
10		-	not defined					-	not defined		-	-	
C USER ADDED VARIABLES	1	STRENGTHENING COOPERATION AMONG STAKEHOLDERS	-	not defined				8	HIGH		-	7	56
	2		-	not defined				-	not defined		-	-	-
	3		-	not defined				-	not defined		-	-	-
	4		-	not defined				-	not defined		-	-	-
	5		-	not defined				-	not defined		-	-	-
	6		-	not defined				-	not defined		-	-	-
	7		-	not defined				-	not defined		-	-	-
	8		-	not defined				-	not defined		-	-	-
	9		-	not defined				-	not defined		-	-	-
	10		-	not defined				-	not defined		-	-	-
IUPA - integrated scores											0.0	7.4	

Figure 2.17 Index for the Evaluation of the Usefulness of Adaptation Practices IUPA

2.1.5 Summary

In the present work conducted for TWINLATIN under Work Package 8 for the Chilean Case, different steps were undertaken in order to address the topic of climate change impacts and associated social vulnerability: (i) a hydrological modelling application was built for 2 sub-basins of Biobío, with different hydrological regime; the Lonquimay sub-basin which is located in the Andes and which receives important snowmelt contributions is considered to represent an interesting case study for what may also happen under climate change in the Baker River Basin (which is located further south, but for which current hydrometeorological data availability does not allow conducting detailed modelling

work); *(ii)* climate changes scenarios were generated and discussed for both the Biobío and Baker basins, based on output from both RCM and GCMs; *(iii)* for the Biobío sub-basins, the hydrological impacts of these change scenarios were modelled by means of the SWAT tool; *(iv)* an interpretation of the model results was made, and a basic assessment of what may also happen in Baker –based on the obtained change signals- was conducted; *(v)* the role of scenario modelling for the quantification of the exposure component of the vulnerability equation was indicated, and additional information was provided on the occurrence of GLOFs in the Baker Basin during 2008; *(vi)* information from the work under TWINLATIN was shared with stakeholders in the Basin, and an exercise was conducted in which the perception of the adaptive capacity among stakeholders was evaluated; *(vii)* an index was developed which may help identify optimum adaptation options in future work.

The wide range of values for the change signals that can be obtained in an impact assessment study such as the one presented for the Biobío and Baker Basins is a direct consequence of the uncertainties that persist with respect to the intensity and even direction in which change in climatic variables will manifest itself at the local and regional level, under global warming: information based on different GCMs provides different regional change patterns for a single change value in mean global temperature (MAGICC/SCENGEN). For a given study site, change results obtained from a finer-scale modelling exercise (RCM runs) may also differ considerably from what is obtained from the GCMs (although in this case, only the magnitude and not the direction of change was affected). In addition to this, the hydrological model itself (through its conceptualization, parameterization, calibration,...) also influences in the final range of values of the changes in mean annual or monthly discharges. The modeling that was conducted in this case with the SWAT tool is deterministic, in the sense that one input delivers a single output, so the uncertainty that is inherent to the model approach is not even reflected in the final results.

Even so, important conclusions can already be made from the conducted work, which may be useful for defining adaptation measures in the field of water management: different sensitivity to climate change could be observed in the snow-fed (or mixed) versus the rainfall-fed sub-basins, and proportionality factors between changes in annual precipitation and discharge (~elasticity) could be obtained. These may be helpful for making quick assessments of what may happen in similar basins in other parts of the country. The quantification –through modeling- of the potential hydrological effects also proves useful in awareness building and in a stakeholder evaluation of exposure, sensitivity, adaptive capacity and the resulting vulnerability. Specifically for the Baker Basin, it can be assumed that an increase in temperature may lead to a significant change in the annual distribution of discharge, as a consequence of reduced snowfall and earlier and increased snow and glacier melt; the frequency (and magnitude?) of phenomena such as GLOF may be increased, posing a threat on human communities living downstream. For this reason, a complete inventory of peri-glacial lakes in the Basin which may be subject to GLOFs becomes highly desirable.

For similar studies as this one conducted under TWINLATIN, we find it important to consider multiple change scenarios, as to take into account the existing uncertainty with regard to the precise manifestation of local or regional consequences of global change. The combined use of output from GCMs and an RCM proves very useful in this case. The RCM allows for a better preliminar evaluation of its skill, as – due to its scale – a comparison of its results from the baseline run with locally observed meteorological data sets becomes more feasible; however this does not guarantee a correct modelling of future climates, and thus the consideration of alternative possible outcomes through the inclusion of results from different GCMs is recommended. This is even more the case as the RCM runs typically only consider 2 different emission scenarios, instead of the larger sets e.g. included in MAGICC/SCENGEN.

Finally, it is important to indicate how in many cases the currently existing meteorological network and available time series data sets will severely limit the possibilities for model calibration, validation as well as its application for impact assessment. Too often, parts of the basin that are hydrologically very important (i.e. parts that may be isolated geographically but that receive very important input contributions to the total water balance) are very little or not monitored at all.

2.2 CATAMAYO-CHIRA RIVER BASIN (PERU – ECUADOR)

2.2.1 Introduction

2.2.1.1 Short description of the basin

The binational Catamayo-Chira river basin has an extension of 17,199.18 km², 7,212.37km² of which, are in Ecuadorian territory (66.82% of the Loja province), the Peruvian part occupies an area of 9,986.81 km² and it is located in the department of Piura (corresponding to 30% of the department).

The river basin is located between 03°30' and 05°08' South latitude and 79°10' and 81°11' West longitude, with a altitudinal rank that goes from sea level, in the outlet of Chira river (in the Pacific Ocean), to 3,700 m. in Podocarpus National Park (Loja). The river basin limits North with the binational river basin Puyango - Tumbes, East with the Zamora - Chinchipe province in Ecuador, South with the provinces of Piura and Huancabamba in Peru and West with the Pacific Ocean.

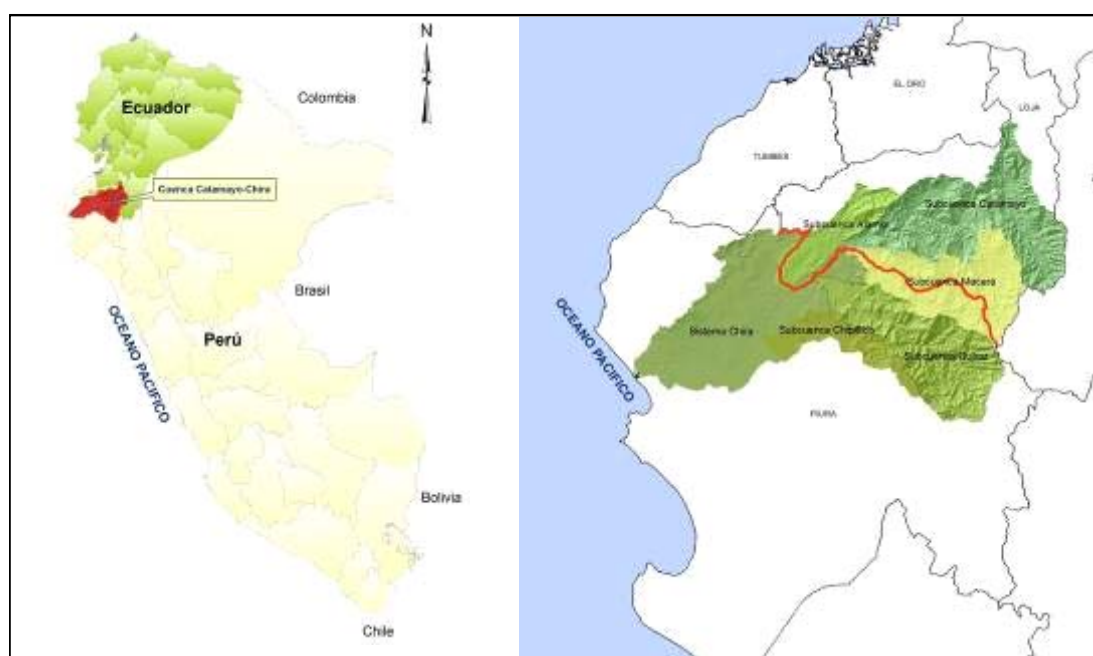


Figure 2.18 Location of Catamayo Chira river basin

The territory of the Catamayo-Chira river basin comprises the old Ecuadorian-Peruvian volcanism that comes off the Azuay Knot (located in Ecuador) and is crossed by Western and Eastern Andean mountain ranges. These mountain ranges, to the south, 3°40' S, and in Ecuadorian territory diminish considerably in altitude. In the North-eastern end of Peru, the western mountain range has a very irregular relief. From the central axis in this point the mountain range of the Andes diminishes towards the West, giving rise to long secondary mountain range arms, plateaus of Piedmont, hills and micro hills.

The plains are rare and of little extension in the Eastern and central part of the region, but towards the low and western sector of the river basin, with altitudes below 500 m, shows quite extensive plains, with very differentiated biomass and vegetal cover.

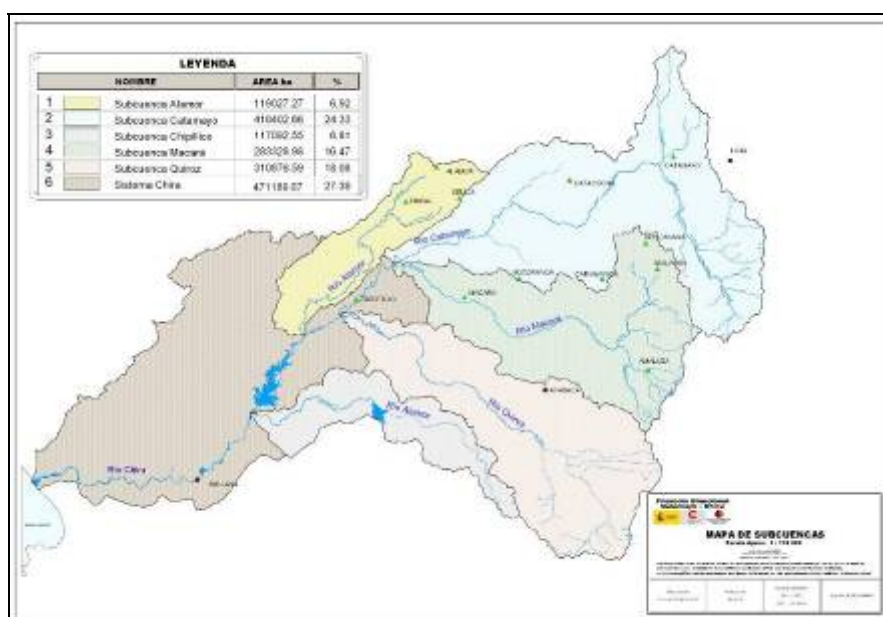


Figure 2.19 Map from the Catamayo Chira sub basins

The Catamayo Chira river basin, consists of the sub river basins of Quiroz (3,108.77 km²), Chipillico (1,170.27 km²), Alamor (1,190.27 km²), Macará (2,833.29 km²), Catamayo (4,184.03 km²) and the Chira System (4,711.90 km²). The main course is the Catamayo Chira river, with an overall length of 315 km, of which 196 km are located in Ecuadorian territory, in which it takes the name of Catamayo river, and the rest 119 km, in Peruvian territory, where it takes the name of Chira river (see hydrological information in section 4).

The river basin precipitations and temperatures present noticeable variations in space and time. In the lower river basin the rainy periods are short and scarce and, with the exception of the years of the phenomenon EL NIÑO, it rains from January to April with an annual average of 10 to 80 mm. In the river basin medium zone the rainy period goes from December to May with annual average precipitations of 500 to 1,000 mm. On the other hand, in the high river basin, rains happen from October to May with annual averages superior to 1,000 mm. With regards to temperatures, the annual average temperatures of the river basin oscillate between 24°C in the low River basin, 20°C in the medium River basin and 7°C in the high part of the River basin. In the following table the climatic characteristics are divided in a total of 17 climatic zones as combinations of their mean annual precipitation and mean annual temperature:

Table 2-2 Climatic zones in Catamayo Chira river basin

Range mean annual Precipitation [mm]	Range mean annual Temperature [°C]	Area [ha]	Area %
0 - 125	18 - 24	25,005.5	1.5 %
	> 24	76,411.0	4.4 %
125 - 250	18 - 24	71,767.1	4.2 %
	> 24	192,533.5	11.2 %
250 - 500	< 12	4,336.3	0.3 %
	12 - 18	16,822.7	1.0 %
	18 - 24	99,182.3	5.8 %
	> 24	209,517.5	12.2 %
500 - 1000	< 12	30,653.3	1.8 %
	12 - 18	192,992.2	11.2 %

Range mean annual Precipitation [mm]	Range mean annual Temperature [°C]	Area [ha]	Area %
1000 - 2000	18 - 24	345,077.6	20.1 %
	> 24	99,153.8	5.8 %
	< 12	29,875.7	1.7 %
	12 - 18	177,648.8	10.3 %
> 2000	18 - 24	135,131.7	7.9 %
	< 12	10,375.1	0.6 %
	12 - 18	3,433.8	0.2 %

It has been estimated that there is considerable underground water potential but the basic information available is insufficient for a definitive characterization. The resource is operated, in a neither rational nor planned form, in some sub river basins for farming, domestic and industrial uses.

The land use/land cover in the river basin varies due to the big differences in climatic and topographic conditions and includes farm land, pastures, forests, brush vegetation, Andean 'Páramo' and others. In general the forest land cover predominates with 698,602.12 ha (40.6% of the River basin). Next come the pasture areas with 501,639.1 ha (29.2%), followed by the brush vegetation with 232,277.54 ha (13.5%). Farming occupies 177,731.35 ha (10.3%) and Andean 'Páramo' covers an area of 25,740.44 ha (1.5%). Finally there are areas dedicated to other uses (eroded areas or in erosion process, urban areas, water bodies, etc.) which occupy an area of 83,927.06 (4.9 %) (Consorcio ATA-UNP-UNL, 2003). The spatial distribution of those classes can be observed on the following map – where it must be mentioned that due to the high variability of natural conditions especially the forest areas have very different characteristics all over the basin. Those areas range from dry forest in the low part to dense mountain rain forests in the upper part. Also the distinction between brush land and forest as well as pastures is not always very clear, as brushes also serve for grazing and are similar to a very light dry forest area.

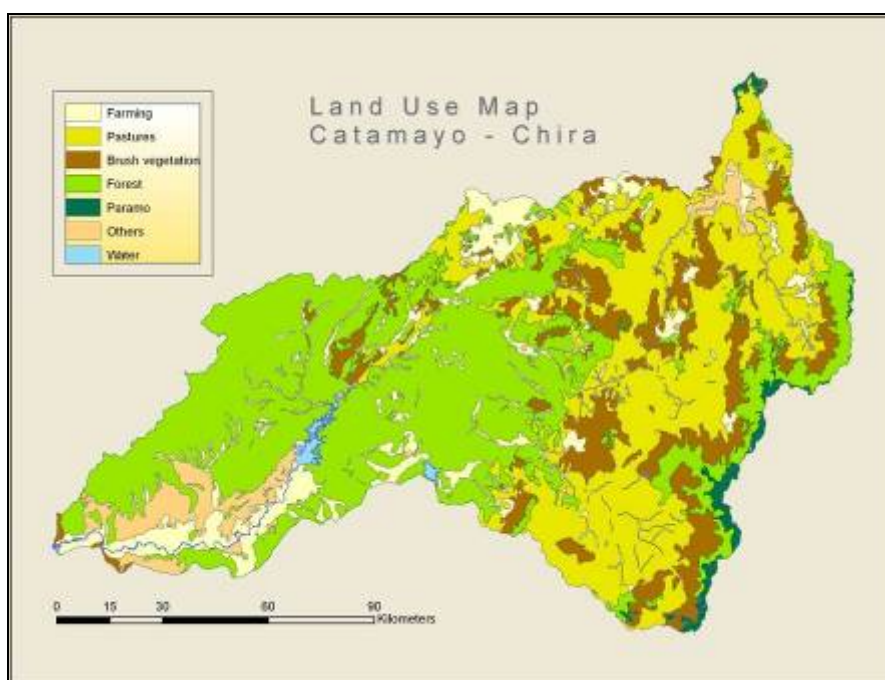


Figure 2.20 Land Use in the Catamayo-Chira basin

In the Ecuadorian part of the river basin, the population rises to 191,487 inhabitants, whereas in the Peruvian side it is 303,565 inhabitants, which supposes a total population in the river basin of 585,052 inhabitants. In addition, the population of the Area of influence (population which also uses the water

of the river basin) constituted by the city of Loja, with 142,271 inhabitants and by the low and medium Piura, including the city of Piura, presents a population of 620,725 inhabitants. The total population of the Catamayo-Chira River basin, and its area of influence, is 1.348.048 inhabitants (in 2001).

59.4% of the economically active population (PEA) works in the primary sector (agriculture, cattle ranch, forestry, hunt, fish and in the extraction sector). 32.5% of the PEA works in the tertiary sector (commerce, hotel profession, tourism, restaurants, services of repair, transport, etc.) and the 8.1% are located in the secondary sector, which includes industrial activity, and crafts.

2.2.1.2 Special issues and problems

A Limited hydrological and meteorological data availability

The Catamayo Chira is a river basin that has been intensely studied in its lower parts; because of the great hydraulic infrastructure existing as it is Poechos reservoir. In spite of this, there are gaps of quality information within the river basin and a lack of continuity in the registry of certain parameters, which are exposed next.

Hydrology is a subject which has never been studied in a systematic form in the river basin. There are some isolated studies, of very small portions of the river basin and also some wells of underground water operation but there is no knowledge of the hydro geological processes that occur in the basin.

There is a meteorological stations network not sufficient for the river basin scope, in addition, many of the stations have discontinuous registries or have been removed from operation at some moment. In a binational river basin that can pass from a serious drought alarm situation to a flood alarm situation in three days (as it has happened in the first week of February 2006), there is an unavoidable need of sharing hydro meteorological information (see “WP02 Monitoring and Database construction – Archydro Database”). Especially for Peruvian institutions dealing with water management in the lower part of the catchment it would be important to have access to information from the upper part of the river basin. As those areas are predominantly located in Ecuador a binational interchange of information needs to be established.

Hydrological parameters are an aspect that has a good level of registries by the operation of the reservoir, but there are only registered data at gauging points on times of avenues. Generally, in dry periods, the stations stop to operate and only the entrance to the reservoir is measured. On the other hand, in the high river basin there are no water gauge stations. With respect to the precipitation registries, these have the same characteristics that the meteorological parameters, and in general are very few stations equipped with rain gauges. There is no information on the types of predominant storms, or the intensities of these.

B Erosion and Sediment Deposition

As consequence of the decomposition of magmatic rocks, soils in the basin mainly are sandy soils that in general are highly erosionable (Consortio ATA-UNP-UNL, 2003). Young Entisols are predominant with more than 55% of the total area. These soils types “have little or no evidence of the development of pedogenic horizons”. It is therefore typical for eroded landscapes/landscapes susceptible for erosion as they appear generally where “the soil material is not in place long enough for pedogenic processes to form distinctive horizons” (USDA, 1999).

Combined with a high percentage of steep slopes (especially in the upper area of the basin), resulting in extreme erosion rates. The majority of terrain in the upper part of the basin is characterized by slopes greater than 30% (717,866 ha) - with 214,068 ha steeper than 58%. Those conditions have to be seen alongside with a high percentage of inadequate use. In the case of the sub basin Chira for example 37 % and in the sub basin Catamayo 39% of the area have been classified as overused. These areas for example are to be found in the steep slopes of the central cordillera which are – instead of forest and conservation areas – occupied by agriculture and pasture (Consortio ATA-UNP-UNL, 2003).

The combination of those factors has a fatal effect on the possibilities of agricultural land use: due to constant erosion as well as extreme erosion events the soil resources get lost in the upper part of the basin. Specially affected is hereby the sub basin Catamayo where ca. 116,478 ha have been identified as eroded in the year 2003. But also in the lower part, for example in the Chira basin ca. 90,845 ha have been classified with the same problem. For the whole basin a total of 362,117 ha can be considered as being in process of erosion, which makes up more than 20% of the total area (Consortio ATA-UNP-UNL, 2003).

On the other hand there exist grave problems caused by the sedimentation in the majority of irrigation structures. This affects specially the lower part, where big plane areas are used for irrigated agriculture. The most important project is hereby the irrigation of over 80,000 ha of agricultural land through the Poechos reservoir. This reservoir since 1976 has lost about 45% of its original capacity. This is specially contributed to two strong phenomena de El Niño that produced a multiple of the normal sediment yield but also during normal years the sediment yield is considerably high.

C ENSO (El Niño Southern Oscillation)

As the River basin Catamayo Chira is located in vicinity to the Pacific Ocean, the sea has big influence on the local climate. As generally the cold Humboldt Current is dominating at the Peruvian coastline the climate is characterized by the absence of greater rainfall between May/June to December. In contrast when warmer water accumulates at the coastline the El Niño phenomenon occurs. The warming of sea water (about 1-4 °C over normal level) stimulates the evaporation and intense rainfalls are the consequence (Consortio ATA-UNP-UNL, 2003). The other phase of the ENSO phenomenon, called La Niña, has the contrary effect as it brings droughts. Due to an accumulation of warm water in far western Pacific the water along the coastline of Peru and Ecuador is cooler than in normal state and as a consequence evaporation and rainfall are impeded.

In the second part of the 20th century 13 phenomena of El Niño have been identified after a method by Rossel regarding the influence on Ecuadorian and Peruvian rain gauge measurements. The most disastrous of them have been recorded ultimately in 1982/1983 and 1997/1998 lasting eleven respectively eight months. This most recent El Niño event lasted from March 1997 to June 1998 and globally it was considered the most intensive and destructive of the 20th century (Consortio ATA-UNP-UNL, 2003) – in the case of the Catamayo Chira basin for example irrigation infrastructure was damaged by landslides or the power of high waters (Consortio ATA-UNP-UNL, 2003).

As mentioned above, a constant problem for the irrigation infrastructure is erosion and the following deposition of sediments in channels and specially water reservoirs. Unfortunately there is no control about where the sediments come from and only few data of the exact amount of sediment production. On sediments, isolated measurements of the Peruvian part of the river basin have been made, since the solid load in suspension has been registered previous to the installation of the reservoirs. In the Peruvian part therefore some studies (e.g. INADE, 1994) have been conducted but in the Ecuadorian part there exist no sedimentation data. In “WP 03 – Hydrological Modelling” and “WP 06 – Pollution Pressure and Impact Assessment” this lack of information is tried to be removed by the application of the Erosion and Sedimentation Models SWAT and WaTEM/SEDEM. But as there is a registry of the annual sedimentation of the reservoirs, the annual behaviour of the sediment transport can be inferred. And here the dramatic effects of the El Niño phenomenon on the hydrologic infrastructure become obvious.

While in “normal” years an amount of 7-8 m³ yr⁻¹ of sediments reach the reservoir Poechos, in the El Niño years 1982/1983 and 1997/1998 the sedimentation rate went up to 79 m³ yr⁻¹. In this context those intense rain events cost the Reservoir about 15 years of valuable lifetime. It is even estimated that by two more similar El Niño events big part of the agriculture in the valleys ‘Chira’ and ‘Low Piura’ could collapse as the reservoir can’t fulfil it’s functions anymore (Consortio ATA-UNP-UNL, 2003). The following graph visualizes the problem of sedimentation in the Poechos reservoir where the effect of the El Niño years is clearly visible.

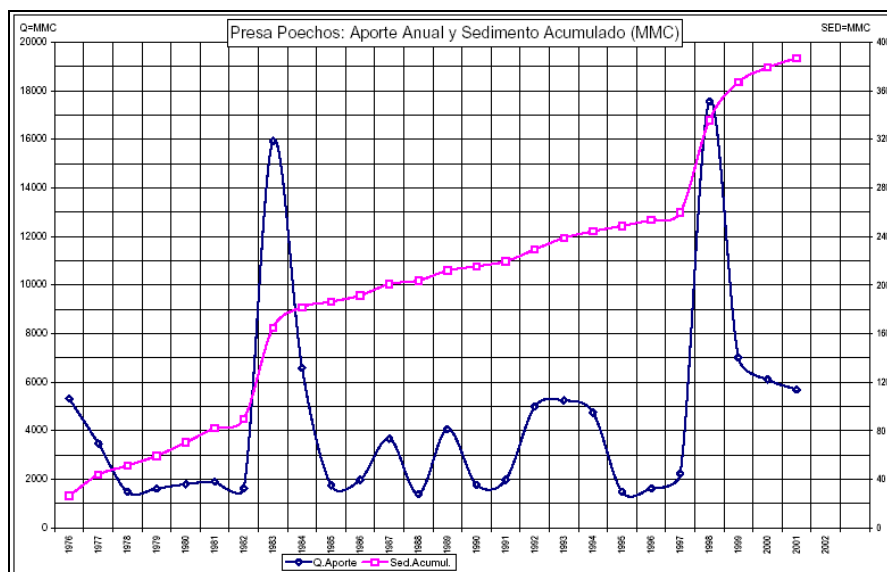


Figure 2.21 Yearly sediment entry and accumulated sediment load in the Poechos reservoir (Consortio ATA – UNP – UNL, 2003)

The impact of climate and extreme climate phenomena is therefore extremely high on the Catamayo Chira basin, on one hand on the soil resources, and on the other hand on water availability in the reservoirs and the involved agricultural systems, the main source of income and guarantee the economic stability of the region.

D Water use

On the agricultural water use, there are global demands data, and established irrigation modules, but these data obey to calculations and/or inferences of the people in charge of distribution of the water. There are no real consumptions data, because of the lack of structures of gauging at field level. With regards to population use, there is no general inventory of the population supplies systems. The situation is more problematic in rural areas where, in general, the few supplying systems are only conductions from the sources to the towns which generally have no purification systems. The populations waste waters, do not count with treatment, reason why there is a constant pollution of the channels. There is no information of the spilled volumes, or of the source points.

E Lack of awareness

On the basis of studies that the trans national Project has made in the River basin (like the biophysical and socioeconomic diagnosis and of the work that is still developing), there have been identified, for the different scopes, the needs for training, awareness raising and education for the different stakeholders related to water resources that is described briefly.

The described activities must be developed from a gender and participative perspective to assure the presence of men and women in the different spaces (training, awareness raising, education), as actors who impact on water resources in a differentiated way, due to their different roles, their necessities and interests, the access to resources and control that they have on them. This means letting spaces in which people can access the information and knowledge in order to change attitudes that are contributing to the deterioration of the environment. Therefore, it is necessary to promote the participation of women, who have generally not been taken into account in the natural resources planning and management actions. Spaces must then be generated which give opportunities to those who are in unequal conditions to the access and control of the resources and in the decision making in the environmental scope.

The river basin presents serious erosion problems in its different manifestations, which entails to the degradation of land and the sedimentation of the hydro agricultural infrastructure works (regulated and

not regulated). In this sense, it is necessary to sensitize the agriculturists and rural agents about the importance of taking care of vegetation and soil, and to undertake training activities related to the good use and handling of natural renewable resources, and the use, adapted maintenance and operation of social and productive infrastructure works. In addition, with the development of the commitments acquired within the framework of the TWINLATIN project, the training of the Catamayo Chira project and the main institutions technicians will be necessary. Topics in this context should be theoretical and practical concepts on erosion, including modelling, possible mitigation performances, etc.

2.2.1.3 Types of changes and effects that are modelled and assessed

In the frame of TWINLATIN, two types of changes are being modelled. First, those related to land use change, measuring the impact that different scenarios of land use would have on the sediment and water production. Second, those related to climate change. Different scenarios of Greenhouse Induced climate change will be evaluated, calculating the impacts of every one of them on the sediment and water production.

The land use change in this study are absolute changes between defined land use classes and do not imply land use modifications, like intensification of agriculture or forest degradation. The modelled climate changes are absolute changes in temperature and relative changes in precipitation, including data that can be generated from this change like the changes in intensity of rainfall.

The effects that those changes have on the study area are assessed by the analysis of production and deposition of sediments as well as the production of water. As described above in ‘special issues’ those phenomena are one of the gravest problems in the basin.

2.2.1.4 Limitation of the study area

The area that is covered by the Hydrologic Modelling as well as the Impact Assessment and Modelling of Change effects is limited to certain parts of the Catamayo Chira basin.

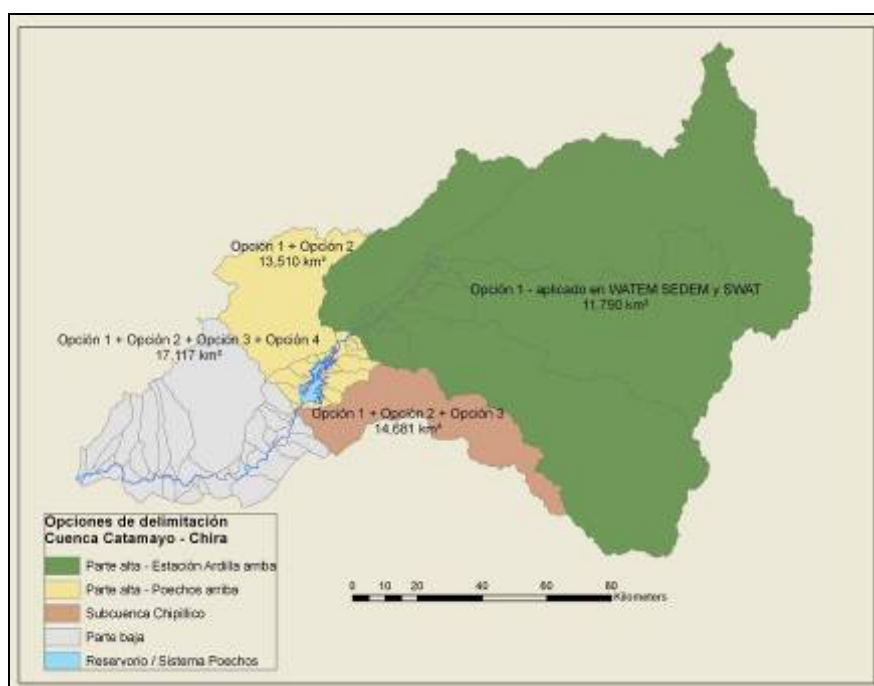


Figure 2.22 Study areas for Impact Assessment, Hydrologic Modelling and Change Effects

As described in the respective reports (see WP 03, WP 06) the modelling of the whole basin is made impossible by the presence of reservoirs that feed irrigation systems outside of the basin and irrigation channels that alter the natural course of water. For those activities data availability is insufficient to allow integration in the two models used. In the following map various options for study areas can be observed. The study areas selected for the Hydrologic and Impact Assessment Modelling both reach

from the upper limits of the basin to just above the ‘Pochos’ reservoir at about 125 m altitude. Here the study area is marked by the sediment and flow volume gauging station ‘Ardilla’. The total size of the study area is therefore reduced to about 11,790 km².

2.2.1.5 Models used to analyse the effects of change

As mentioned above the *Soil Water Assessment Tool* (SWAT) and the *Water and Tillage Erosion Model/Sediment Delivery Model* (WaTEM/SEDEM) are the tools that have been chosen to model the effects of changes in the Catamayo Chira basin.

SWAT quantifies the impact of land use management on water production and soil erosion while WaTEM/SEDEM produces maps of sediment production and sedimentation areas. Therefore the model results complement each other showing both how much and where erosion takes place and sediments are produced.

2.2.2 Scenario creation

2.2.2.1 Climate change

A Introduction

Climate change is expected to show considerable influences both on the provision of water and the production of sediments in the basin. Possible changes are represented particularly by a variation of the rainfall and temperature, which could possibly cause various change effects. A rise of temperature might for example result in higher ratios of evapotranspiration with the consequence of reduced water recharge rates and an elevated risk of droughts. Spatial and temporal variation of rainfall may both aggravate the same problem in some areas or may in other areas result in higher agricultural productivity. At the same time it also may result in higher rainfall intensities and therefore expose soils to greater risk of erosion processes.

To identify the most probable future development various scenarios of climatic change are elaborated and the resulting changes are applied on the baseline climate. Then the simulated climate change scenarios are introduced into both the SWAT model and WaTEM/SEDEM to compare the effects of climate change to the results of “WP 03 – Hydrological Modelling” and “WP 06 – Pollution Pressure and Impact Assessment”, which are considered the baseline situation.

B Climate trends in the Catamayo-Chira basin

Climate trends have been analyzed for the period 1970 – 2000 using data from five meteorological stations inside and one station in the vicinity to the basin with the goal to find indications for climate change happening in the basin. Therefore the tendency for the past development of temperature and precipitation was investigated by the application of a filter based on the moving average of 4th order to obtain a softened diagram of the historic registry. The variation of the tendency is expressed as the difference between initial and final value of the straight line calculated on basis of the data generated by the moving average (Oñate-Valdivieso, 2008).

The maximum temperature of all six investigated meteorological stations show an increase of temperature between 0.6° C and 1.7° C (Figure 2.23). In the case of the mean temperature five of the six stations show an increase of temperature, while only the station ‘Malacatos’ shows a decrease. So tendencies of climate change in case of the registry of temperature are quite unambiguous and indicate a rise of temperature in the study area. Therefore it is considered possible that a relationship between green house gas emissions and the raising temperatures exists (Oñate-Valdivieso, 2008) and the elaboration of climate change scenarios based on the future variation of respective human behaviour seems justified.

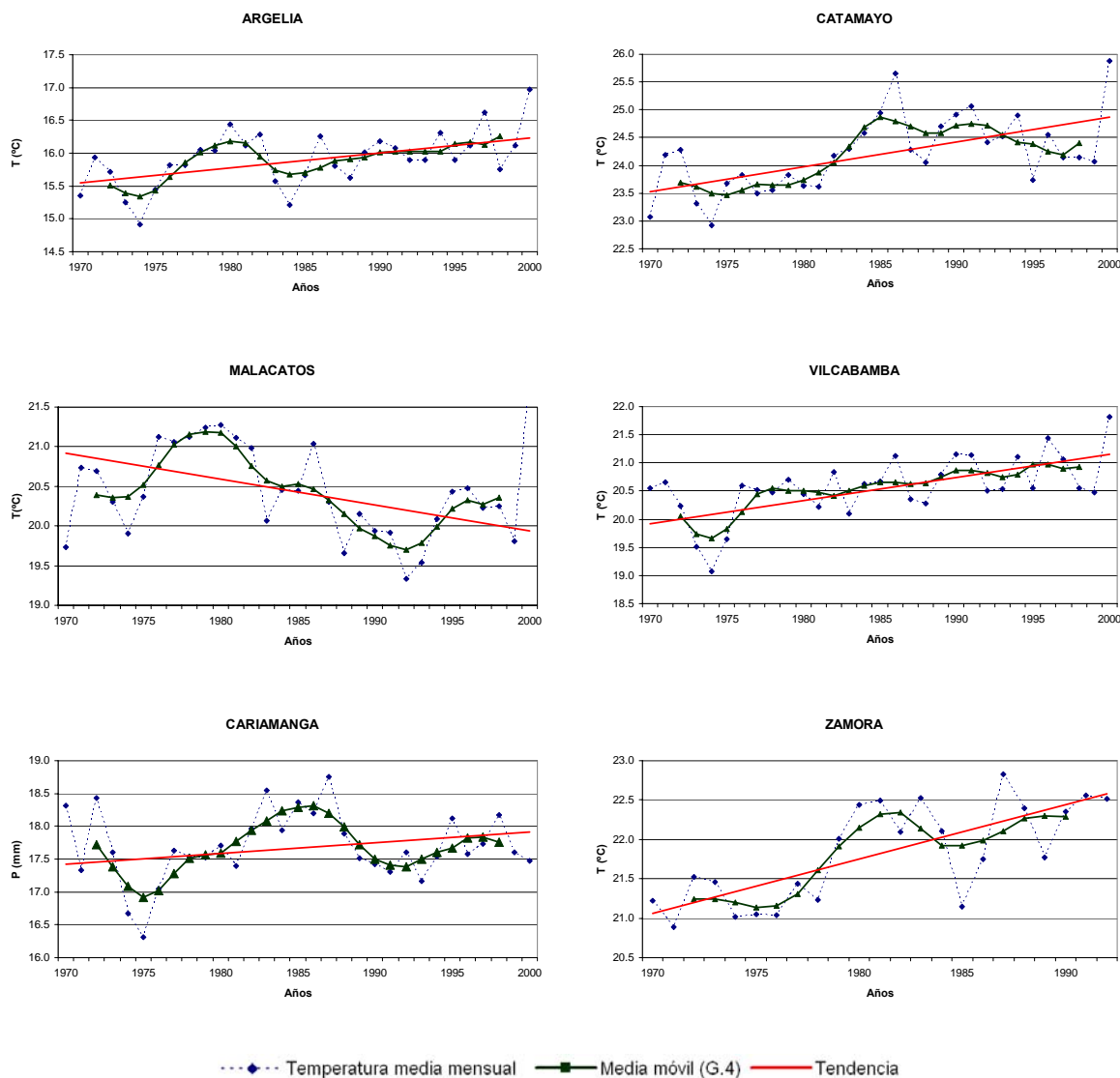
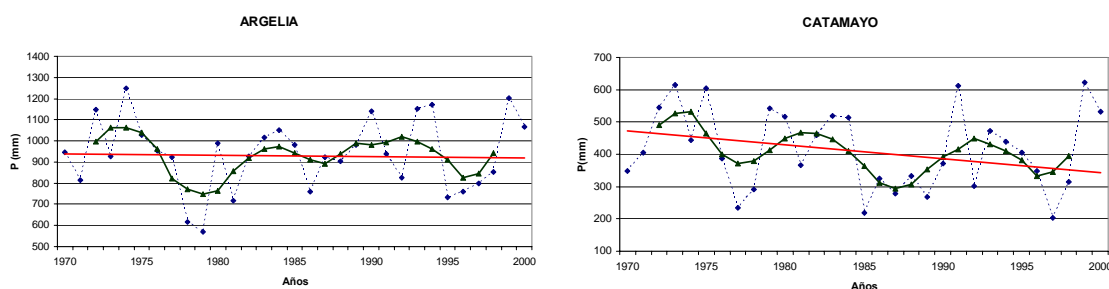


Figure 2.23 Tendencies of mean monthly temperature in the study area 1970 and 2000 (Oñate-Valdivieso, 2008)

In the same period the tendency of precipitation is not very clear. Although a decrease of rainfall is observed in four of the six analysed gauging stations, the tendency is not significant in any of the cases (Figure 2.24). In the station ‘Argelia’ it only sums up to -2.1% and is therefore almost stable. In ‘Catamayo’, ‘Malacatos’ and Zamora the tendencies of rainfall represents a decrease between -11.7 and -25.3 %. An opposite tendency with a similar magnitude can be observed in the stations ‘Vilcabamba’ and ‘Cariamanga’.



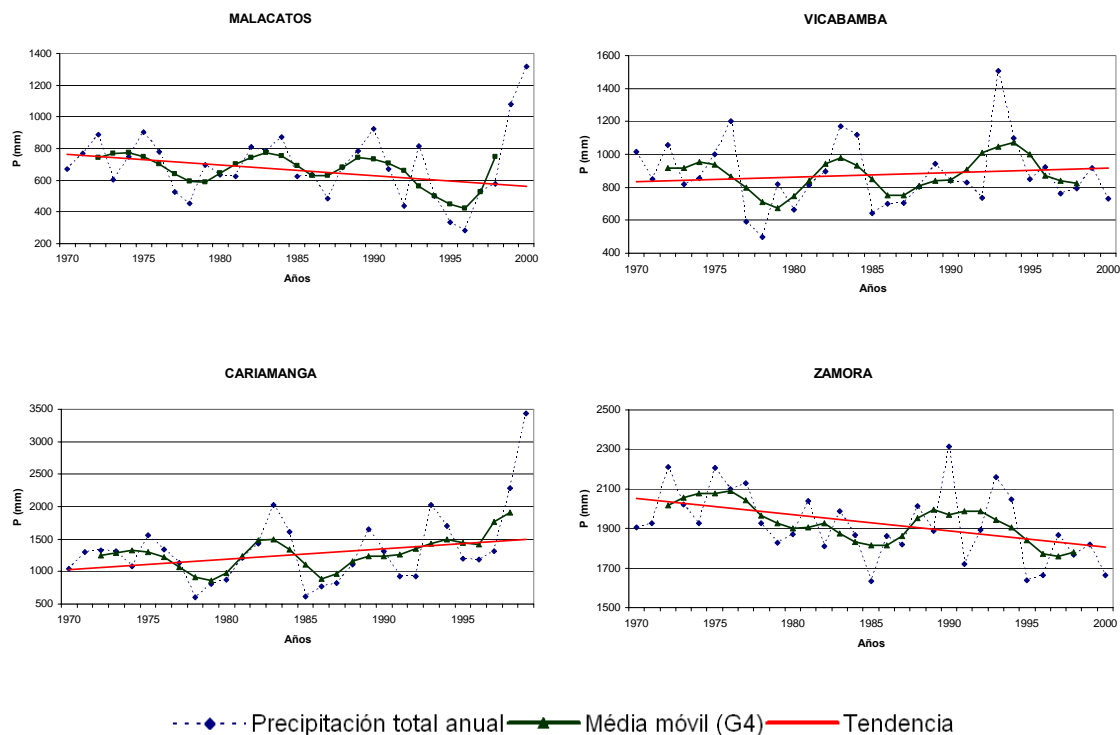


Figure 2.24 Tendencies of mean annual precipitation in the study area 1970 and 2000 (Oñate-Valdivieso, 2008)

Although no unambiguous trends in precipitation can be observed, in the same study the tendencies of water discharge in two nearby river gauging stations show a clear decreasing trend for the measured water amount (-29% and -25.6% respectively) (Figure 2.25). This persistence of a negative tendency in the water amount allows the assumption that also in other meteorological stations, that have not been analysed, a falling tendency of rainfall amount prevails (Oñate-Valdivieso, 2008). So at least there are hints that rainfall is decreasing since 1970 as a result of climate change.

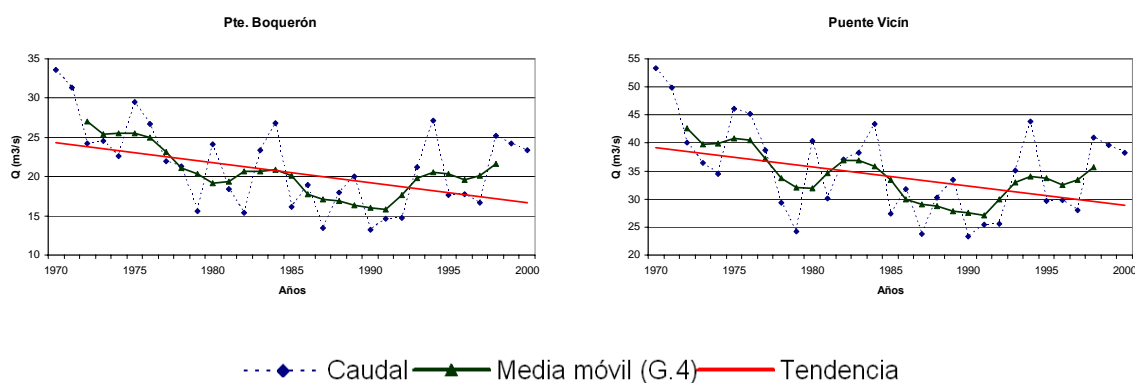


Figure 2.25 Tendencies of water discharge in the study area 1970 and 2000 (Oñate-Valdivieso, 2008)

Overall data from the same analysis of climate characteristics show a decrease in precipitation of 4% and an increase in the mean temperatures of 1.1° C. Even if it is impossible to attribute these alternations with absolute certainty directly to the green house gas emissions, it is considered possible that the two phenomena are related (Oñate-Valdivieso, 2008). According to the IPCC it is also likely that human influence contributed to a global trend towards increases in area affected by drought since the 1970s and the frequency of heavy precipitation events (IPCC, 2007). As a consequence the tendencies observed in the Catamayo-Chira basin (in the case of temperature more clear, in the case of

precipitation more diffuse) are compatible with the intention to model climate changes scenarios in the study area.

C Description of climate change scenarios

With the objective to analyze the performance of the 17 available models in the Catamayo-Chira basin, the variation of temperature and rainfall were modelled for 2025, 2050 and 2080. Graphics of the dispersion of the projected precipitation and temperature, as well as the monthly variation of each parameter, were analyzed. The comparison of the obtained future scenarios with the formerly mentioned tendencies in the historic data, taking into consideration the spatial resolution and climatic sensibility of each model, permitted to select the GCM used in the elaboration of climatic scenarios (Oñate-Valdivieso, 2008). Finally, the following four GCM's were chosen as they adjusted best to the local conditions of the basin Catamayo-Chira:

- CSSR96
- ECH498
- BMRC2
- HADCM2

Two SRES scenarios were chosen to generate future climate change scenarios for the Catamayo Chira basin: the A1 and the B2 scenario. The A1 scenario is based on very rapid economic growth, global population that peaks in mid-century and declines thereafter, and rapid introduction of new and more efficient technologies. The B2 scenario considers a future world in which the emphasis is on local solutions to economic, social, and environmental sustainability, with continuously increasing population and intermediate economic development.

Even though the following analysis of change effects only concentrates on the year 2050, the SWAT model needs some years of fore-running to adjust to local hydrologic conditions, so it was considered to elaborate climate change data for a period at least 5 years before the reference year 2050. Therefore, the model is used to simulate the hydrologic effects of the climate change from 2045 – 2055 with the central year 2050 compared to the model results of WaTEM/SEDEM.

The MAGICC/SCENGEN outputs for both the A1 and the B2 SRES scenario clearly indicate a further increase of temperature in the study area around the year 2050. In the case of the A1 scenario this temperature increase however shows much larger variation (between 1.4 °C in February 2045 and 2.7 °C in July 2055) (Figure 2.27). In the B2 scenario, the range of temperature increase is from 1.1 (February 2045) to 2.0 (August 2055) (Figure 2.26). The relatively warmer months such as December to March are the ones that present lower temperature increase while the colder months June to August present the strongest increase.

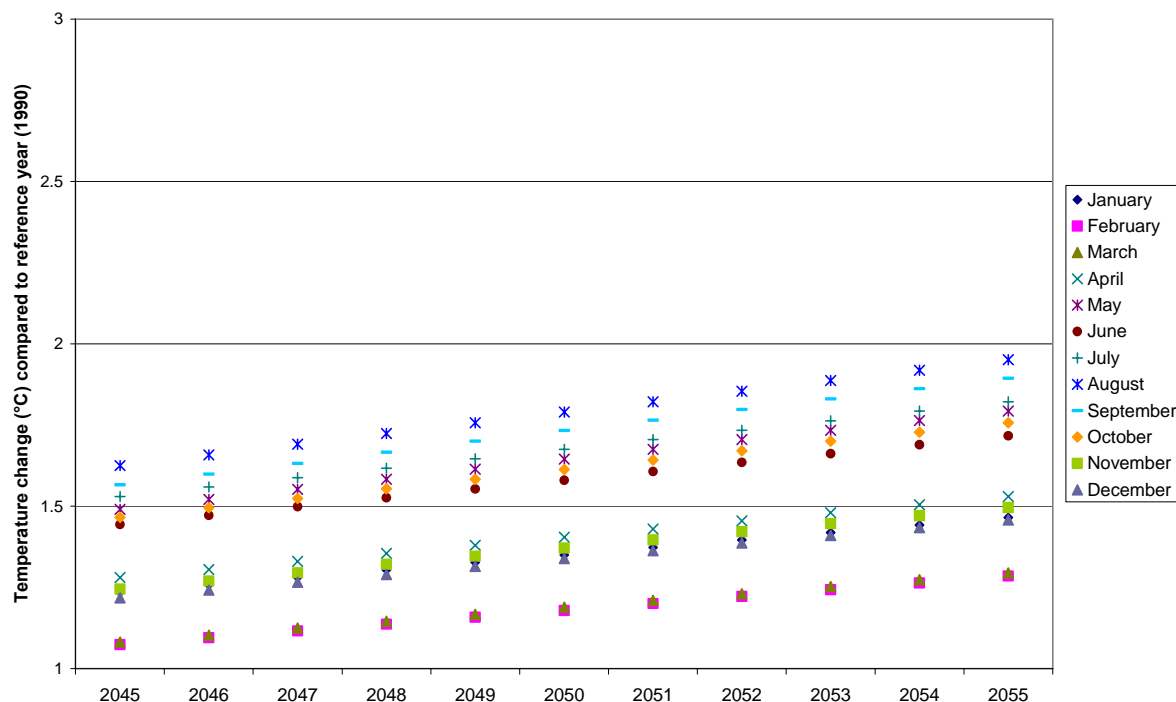


Figure 2.26 Simulated monthly temperature change for 2045 – 2055 – B2 scenario



Figure 2.27 Simulated monthly temperature change for 2045 – 2055 – A1 scenario

The effects of a greenhouse induced climate change on the local rainfall characteristics seem more ambiguous. The model results indicate again more moderate changes in the B2 scenario than in the A1 scenario but in the course of the years contradictory tendencies can be observed.

In the *B2 scenario* the months with a tendency of increasing rainfall and months with a tendency of decreasing rainfall are clearly differentiated (Figure 2.28). Here only the months of February to March and June to July present positive figures, while for the rest of the months the model indicates decreasing rainfall. The consequence in the local context could be that the rainfall period, that actually

presents maximal rainfall amounts from February to April or October to December changes its temporal distribution pattern slightly.

For most gauging stations, where the peak rainfall can be observed between February and April, the rainfall season might become shorter as the relatively low rainfall amounts of September to December decrease. On the other hand rainfall amount and intensity might get extremer to the end of this season, since February and March already present high rainfall rates and show positive change rates for the simulated timeframe. The precipitation increase in the months of June and July might indicate a smaller second rainfall period in the actual dry season – but, as the modelled results present *relative* increases for very dry months, the absolute increase of precipitation would remain low.

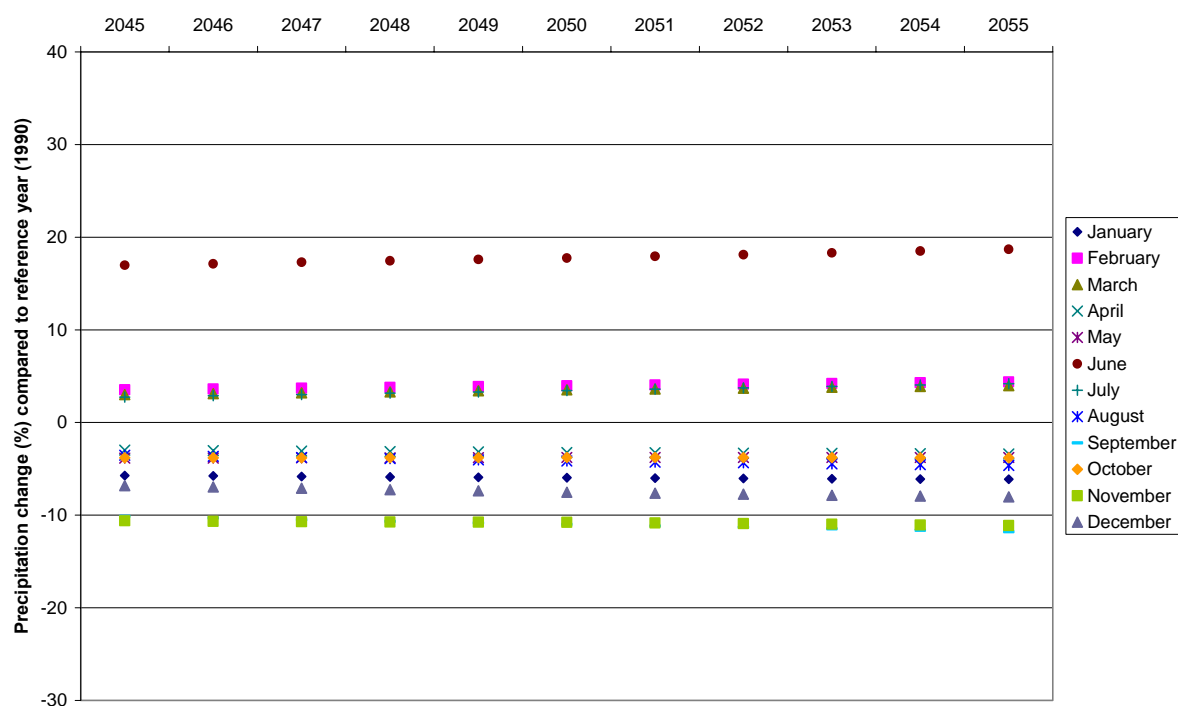


Figure 2.28 Simulated monthly rainfall change for 2045 – 2055 – B2 scenario

The *A1 scenario* presents the same tendencies although the values for increasing rainfall in June are considerably higher than in the B2 scenario and also the expected decrease of precipitation, for example in November is extremer (Figure 2.29).

In both cases an overall decrease of rainfall amounts can be expected as 8 of 12 months (B2 scenario) or 7-9 of 12 months (A1 scenario) present negative tendencies for the period 2045 – 2055. The consequences on the basins potential of water provision would therefore be negative in future, while consequences on sediment production are not clear. With diminishing rainfall amounts, the rainfall intensity might also decline but on the other hand, the increasing rainfall intensities during the dry period, when vegetation cover is low, sediment production might as well increase. A tendency that is assumed as ‘very likely’ by the IPCC is, that heavy precipitation events become more frequent in the 21st century (IPCC, 2007). As a consequence, independently of a greenhouse gas emissions scenario, an increase in erosion rates might be expected in the future. Unfortunately this hypothesis can not be verified with the data obtained by MAGICC/SCENGEN and was therefore not simulated neither by SWAT nor by WaTEM/SEDEM.

“Pollution Pressure and Impact Assessment” the respective monthly rainfall would be introduced into the regression equation that explains best the relation of rainfall amount and measured rainfall intensities and yearly rainfall erosivity maps are introduced into the model calculations. In this yearly timescale however the monthly rainfall variation that was simulated by MAGICC/SCENGEN is smeared out and an overall rainfall intensity decrease would be introduced into WaTEM/SEDEM. Due to the coarse scale of the climate change simulations this decrease would be applied uniformly throughout the whole study area. This is why climate change scenarios could not be evaluated with WaTEM/SEDEM. The effects of climate change are therefore only evaluated with SWAT.

2.2.2.2 Land use change

A Introduction

The most impacting land use changes in the last centuries in the Catamayo-Chira basin has been the deforestation to open up new agricultural and also pasture areas. This process often ends up in degraded and eroded soils – especially in areas with steep slopes. Documentation of this phenomenon is difficult as the maps available are not very detailed and use different legends. Nevertheless for the Ecuadorian Part of the Basin, Feijó and Chalán (2008) describe a forest area to pasture conversion of 20,000 ha between 1992 and 2002, while for the sub basin Quiroz on the Peruvian Side a conversion of forest and brush area to cultivated land of 6,592 ha is reported by Gruber (2008) for the period 1994 – 2007.

The two land use change scenarios applied in this study therefore also focus on these aspects. The *first* land use change scenario “Development based on actual Trends” emphasizes on an unmanaged development of the agricultural production activities and considers a continuation of actual land use change tendencies. The *second* scenario “Sustainable Development Scenario” includes a river basin management plan, with both protection and conservation activities that would contribute to sustainable development of the basin. Consequently in certain regions this scenario shows possibilities to move against this historic trend, whereas in other parts the typical scheme of agricultural development is still applied.

The scenarios were developed based on (i) expert judgment of actual tendencies and (ii) an ecologic/economic landscape value study (‘Zonificación Ecológica – Económica de la Cuenca Catamayo-Chira’).

- (i) The first land use change scenario is based on the past developments and actual land use change tendencies and no land use management actions are integrated. In general this scenario represents an unattractive situation, where the actual problems in the basin persist. Moreover, this scenario implies a constant deterioration of natural resources and a slow expansion of agricultural land without changes in the behaviour of local institutions and land use actors.
- (ii) The ecologic/economic landscape value study that serves as basis for the creation of the second land use change scenario is thought as an instrument for the sustainable development of the Catamayo-Chira basin and is therefore one of the main sources for the “Plan of Land regulation, Management and Development of the Transnational Basin Catamayo-Chira” (POMD in its Spanish abbreviation). It results in an integral landscape classification with the goal to reach the “harmony between the welfare of the population, the optimal use of the natural resources and the protection of the environment” (Consultores ZEE, 2006). In this context the best suited land use is identified in a process of balancing the three mentioned interests.

This to a certain extent includes a counter steering of past the land use changes. In terms of the elaboration of the scenario this means that on the actual land use map some areas are assigned for natural conservation, protection of water recourses and the regeneration of degraded soils. In these regions, the area of forest and brush land is increasing which promises a positive impact on erosion and sediment production problems. This issue is within the focus of the

work packages “WP 03 – Hydrological Modelling” and “WP 06 – Pollution Pressure and Impact Assessment”.

The second part of the scenario represents ongoing deforestation processes that respond to economic/agricultural needs. Hereby areas, identified as suitable for arable land and pasture, are converted into these land use classes. Consequently in these areas higher net erosion rates can be expected.

The idea behind the combination of both needs is to find equilibrium between increasing agricultural productivity with less impact on ecosystems and natural resources. This is why this scenario is named the “Sustainable Development Scenario”. Through the application of the SWAT and WaTEM/SEDEM models, change effects can be investigated concerning the impact on production of water resources, the loss of soil resources and the contamination of aquatic ecosystems.

B Description of land use change scenarios

(i) Development based on actual trends

In this scenario actual trends in land use change and land use conflicts are taken into consideration. Land use conflicts mostly occur where areas are overused, which means land use is too demanding for the soil to support it on a long timescale. This is a typical phenomenon in past and actual land use development in the basin and causes long term degradation of soils. The phenomenon is characterized by

- the loss of the vegetation cover – principally by deforestation processes
- the loss of soil fertility and consequently low agricultural production
- the abandonment of unproductive agricultural areas that are partly used for pasture and the expansion of agricultural areas

These tendencies lead to a vicious circle with successive disappearing of the natural vegetation and degradation of soil resources.

This slow development is integrated in this land use change scenario, as well as the introduction of some new crops like pineapple, onion, olive and ‘tamarindo’, which is a tree species appreciated for its hard wood and nutritive fruits. New agricultural areas are introduced mostly near existing ones. The installation of a new planned irrigation project, named ‘Zapotillo’, was included. This irrigation system would convert 6.800 ha into profitable agricultural land in the western part of the basin. Natural conservation areas, for example the ‘Páramos’, remain untouched.

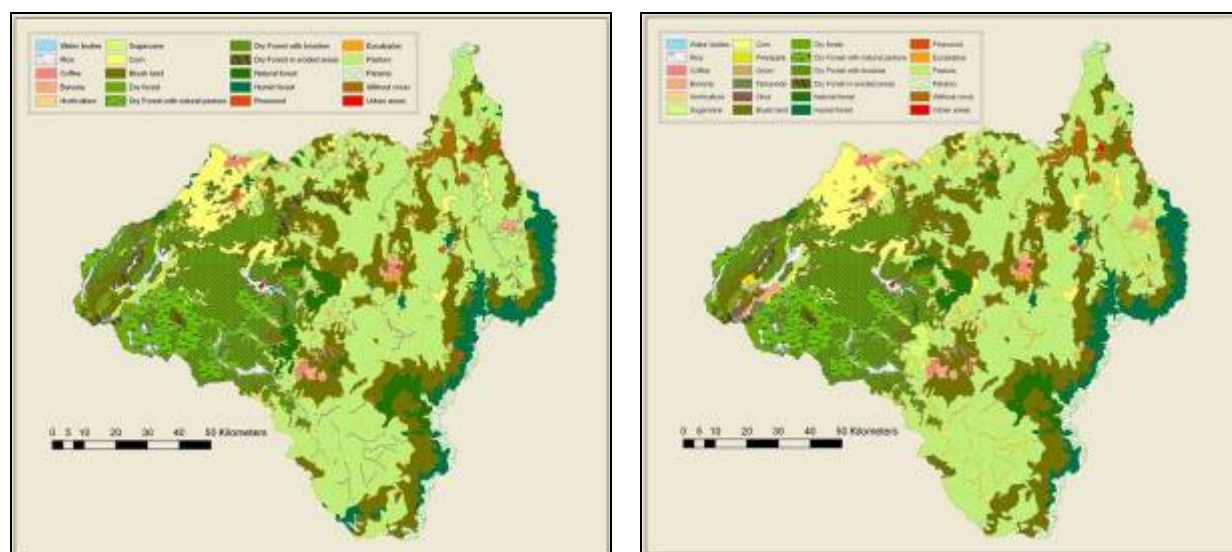


Figure 2.31 Actual land use map (left) and modified land use map – Development based on actual trends

As a result the scenario represents the slow expansion of agricultural areas that substitute the brush and forest areas. Also the abandonment of arable land and the reactivation of formerly abandoned areas can be observed. Some areas covered by dry forest in higher areas that have been strongly disturbed by grazing activities are converted into pasture and brush areas. The scenario includes the increase of corn and loss of natural forest in the ‘Alamor’ subbasins in the western part and the ‘Quiroz’ subbasin in the southern part of the basin.

Table 2-3 Changes applied to land use classes – Development based on actual trends

Land Use Classes	Land Use 2007 [ha]	Actual Trend Scenario [ha]	Change [ha]	Change [%]
Water Bodies	300.38	300.38	0.00	0.00
Rice	16,829.41	17,937.79	1,108.38	0.07
Coffee	5,816.75	5,816.75	0.00	0.00
Banana	9,426.00	12,988.82	3,562.82	0.38
Horticulture	1,197.77	1,426.02	228.25	0.19
Sugarcane	8,128.60	16,101.91	7,973.31	0.98
Corn	66,508.11	71,195.57	4,687.46	0.07
Pineapple	0.00	1,965.73	1,965.73	-
Onion	0.00	904.86	904.86	-
Tamarindo	0.00	1,028.06	1,028.06	-
Olive	0.00	1,288.34	1,288.34	-
Brush Land	217,205.31	227,825.89	10,620.58	0.05
Dry Forest	13,675.59	11,412.81	-2,262.78	-0.17
Dry Forest with brushes	144,139.48	143,331.28	-808.20	-0.01
Dry Forest with natural pasture	62,953.91	62,953.91	0.00	0.00
Dry Forest in eroded areas	21,490.46	7,572.03	-13,918.43	-0.65
Natural Forest	48,933.12	36,549.40	-12,383.72	-0.25
Humid Forest	53,110.62	49,035.47	-4,075.15	-0.08
Pinewood	2,471.42	2,471.42	0.00	0.00
Eucalyptus	4,176.59	4,176.59	0.00	0.00
Pasture	461,856.87	461,937.37	80.50	0.00
Páramo	23,254.98	23,254.98	0.00	0.00
Without Cover	16,289.37	16,289.37	0.00	0.00
Urban Area	1,273.31	1,273.31	0.00	0.00

To visualize the expected effects of this land use change scenario, the land use classes are categorized as “Non Eroding” and “Eroding” based on their RUSLE C-Factor in the same way as the calibrated WaTEM/SEDEM model. Land Use Classes with an RUSLE C-Factor below 0.14 are considered “Non Eroding”, classes with a C-Factor value above 0.14 are considered as “Eroding” (for further details see “WP 06 – Pollution Pressure and Impact Assessment”) (Figure 2.32). The green areas show the conversion from ‘dry forest’ to ‘brush land’, which due to the assigned C-factors will show an improvement of the WaTEM/SEDEM modelling results, whereas in reality the effect of these changes should be minimal. The effects that are detected in this case by the SWAT model are considered to be more realistic.

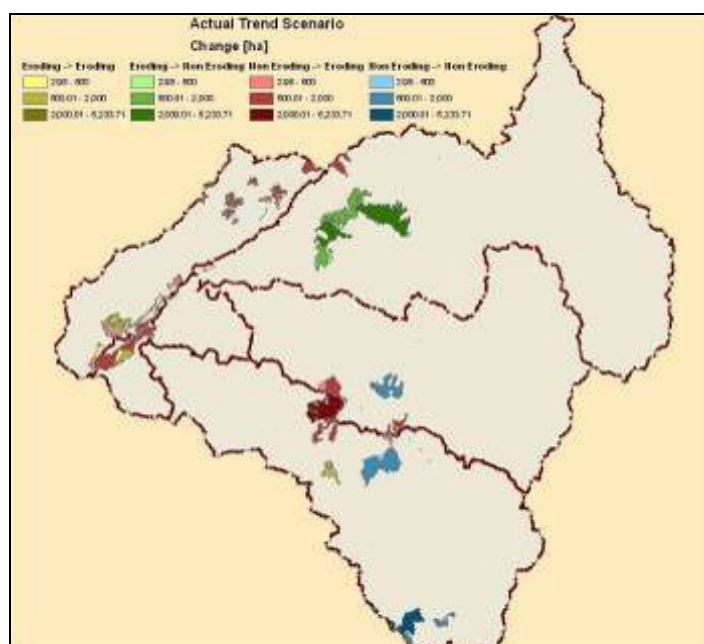


Figure 2.32 Categorized land use changes – Development based on actual trends

(ii) Sustainable Development Scenario

The scenario creation was done by the introduction of various types of land use into the actual map of land cover. On one hand they represent the goal of protection of biologic, soil and hydrologic resources or an intensified production of forest products. This scenario includes more areas with dense vegetation like forest and brush land, therefore a reduction of erosion can be expected.

The classes that are introduced into the map are:

- Areas for natural protection and conservation
- Reforestation in degraded areas
- Regeneration of degraded forests
- Areas for forestry development

These classes of land use are translated into already existing land use classes in the actual maps to guarantee the comparability with the baseline situation and the applicability in the SWAT model and WaTEM/SEDEM. The already existing land cover classes of natural forests, reforestations and – in the case of protection measures also the ‘Paramo’ vegetation – are assigned to the new areas. When for example a pasture area is replaced by a forest area, the specific type of forest is chosen considering the location of the specific area. Areas for reforestation and forestry are not only the regional types of forest but also plantations of Pine and Eucalyptus as those two genera are commonly used for forest plantations in the basin.

The development of agricultural productive areas is represented by the following types of agricultural activities:

- Crop farming with zones designated to a development of coffee, sugarcane or corn
- Pasture farming
- Both crop and pasture farming

As mentioned before, the result of the Ecologic/Economic Landscape Value Study is a combination of both ecologic and economic development. In the scenario creation it integrates two tendencies: protection and increase of production areas. Therefore the two resulting land use maps are combined. The land use transformation processes represent an ecologically compliant way of economic and agronomic development.

Although the suitable areas for agricultural growth are larger, the increase of areas designated for coffee, sugarcane and corn is restricted. The same happens for the woodland classes, which for conservation purposes would embrace greater areas, but is also restricted by the growing agricultural and pasture areas. Emphasizing the interrelations of socio-economic and ecological needs it shows a perspective for a development at a large time scale (Consultores ZEE, 2006). In the following table the changes in area of each land use class is displayed:

Table 2-4 Changes applied to land use classes – Sustainable Development Scenario

Land Use Classes	Land Use 2007 [ha]	Sustainable Development Scenario [ha]	Change [ha]	Change [%]
Water Bodies	295.35	295.35	0.00	0.00%
Rice	16,822.23	13,017.96	-3,804.27	-22.61%
Coffee	5,816.75	26,090.06	20,273.31	348.53%
Banana	9,426.00	2,552.64	-6,873.36	-72.92%
Horticulture	1,197.77	404.24	-793.53	-66.25%
Sugarcane	8,128.60	24,959.11	16,830.51	207.05%
Corn	66,851.64	83,031.46	16,179.82	24.20%
Brush Land	210,641.43	162,111.85	-48,529.58	-23.04%
Dry Forest	241,897.13	242,209.56	312.43	0.13%
Natural Forest	48,933.12	72,501.73	23,568.61	48.16%
Humid Forest	53,110.62	68,630.52	15,519.90	29.22%
Pinewood	2,471.42	6,404.27	3,932.85	159.13%
Eucalyptus	4,176.59	7,150.12	2,973.53	71.20%
Pasture	468,420.77	436,194.92	-32,225.85	-6.88%
Páramo	23,254.98	23,254.21	-0.77	0.00%
Without Cover	16,289.37	9,199.86	-7,089.51	-43.52%
Urban Area	1,273.31	1,246.50	-26.81	-2.11%

The areas of cropland and woodland and forest plantations increase considerably. In contrast, brush areas show a decline. This is a result of the combination of conservation and production tendencies, since both the ecologic and economic value of brush land is limited. Also pasture areas reduce noticeably. Areas without cover are partially converted into forest, and partially into arable land. The 'páramo' ecosystem, which is important for regulating headwater hydrology (Podwojewski and Poulénard, 2000), remains almost entirely untouched.

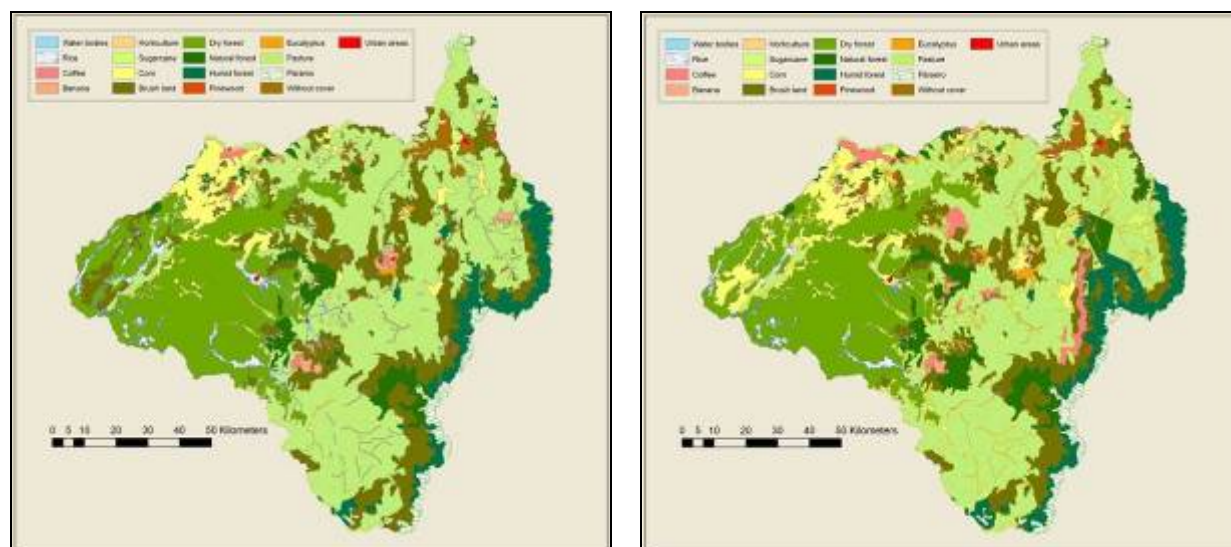


Figure 2.33 Actual land use map (left) and Sustainable Development Scenario (right)

Reclassifying the land use changes in this scenario into “Eroding” and “Non Eroding” land use classes, changes and their supposed effects can be observed in Figure 2.34. Areas that are introduced to fulfil the ecologic aspect of the scenario are all considered as “Non Eroding”. Arable land is considered as “Eroding”. Since Pasture and Forest land use classes both are categorized as “Non Eroding”, the effects of the conversion from Forest to Pasture or vice versa will not show large change effects when comparing WaTEM/SEDEM modelling results. In the SWAT model the interactions between vegetation and surroundings are described in a much more complex manner, so clearer change effects can be expected.

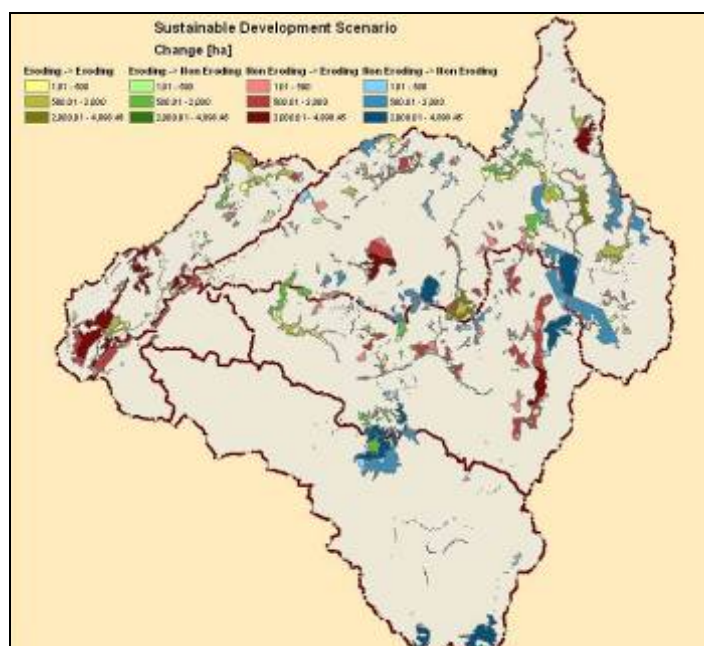


Figure 2.34 Categorized land use changes – Sustainable Development Scenario

Blue areas mark areas with land use changes between different “Non eroding” land use classes, for example the conversion of Páramo into pasture. Changes between two “Eroding” land use classes, for example two different crop types, appear as *yellow* areas. In *green* areas, for example reforested areas, positive effects on soil loss can be expected. Areas where “Non Eroding” areas are converted into agricultural land are marked in *red*. The equilibrium between ecologic and economic development is represented by equal proportions of changes with expected positive and negative effects on soil erosion. In case the Ecologic and Economic Landscape value study also took into account for example

slope factors during the new distribution of agricultural and conservation areas, a positive balance of erosion production still might be possible.

2.2.3 Scenario impact assessment

2.2.3.1 Methods used for impact assessment

A SWAT

(i) Introduction

The SWAT model (Soil and Water Assessment Tool) is a semidistributed hydrological model, which was developed by the USDA-ARS (Agricultural Research Service) in collaboration with the University of Texas to assist water resource managers in assessing the impact of management on water supplies and nonpoint source pollution in watersheds and large river basins (Arnold et al., 1998). The application of SWAT in the Catamayo-Chira basin is described extensively in the report “WP 03 – Hydrological Modelling”.

SWAT has been already successfully applied for water quantity and quality issues for a wide range of scales and environmental conditions around the globe. A comprehensive SWAT review paper summarizing the findings of more than 250 articles is written by Gassman et al. (2007).

SWAT consists of a set of sub models, used to simulate different hydrological processes. The model is based upon the general hydrological balance equation. Division of the basin into subbasins and hydrological response units allows introducing differences in evapotranspiration for various crops, soils etc. Run-off is predicted for each hydrological response unit (HRU) by using the curve number equation. The HRU are created by the model on subbasin level, improving representation and defining smaller areas with homogenous physical and climatic characteristics, which allows SWAT to produce a better physical description of the hydrological balance. The necessary parameters to estimate daily potential evapotranspiration are calculated based upon monthly values of climatic data included in the model, using internal equations managed by SWAT.

Vegetative growth is an important factor for SWAT, so a lot of biophysical parameters had to be adapted from the original SWAT database for the Catamayo Chira basin, since this information couldn't be collected for the study zone.

(ii) How SWAT is used to assess the effects of change

The SWAT model, when calibrated and validated to fit the local conditions, is able to assess the effects of changes using various types of change scenarios.

In the case of land use changes, the vegetation cover and land use input can be alternated in order to assess possible effects of those changes on the hydrologic cycle. Especially the effects of changes in forest cover and other land use conversions on the mean annual soil loss is of interest, because those results can be compared to the WaTEM/SEDEM results. Also the effects of these changes on water discharge and evapotranspiration are of interest.

SWAT allows varying climatic variables, most importantly precipitation and temperature, but also solar radiation or relative humidity. Through daily or monthly variation of those factors it is possible to evaluate the effect of climate change scenarios on the hydrologic processes in the catchment. As described in paragraph 2.2.2.1, the monthly outputs of MAGICC/SCENGEN allow alternating the temperature and rainfall data of the baseline situation to create different climate change scenarios. In this study the climate change scenario was based on the projected changes of rainfall and temperature from 2040 to 2050

(iii) Limitations

The most time consuming aspect was the gathering and digitalisation of climatic and hydrologic information. Efforts were concentrated on digitalisation of daily precipitation and pluviograms. Unfortunately, not all climatic data could be digitized, due to limited time and resources.

In the Ecuadorian part of the basin, no sediment measurements were available, and the network of hydro meteorological stations is limited. Additionally, flow stream measurements have a high degree of uncertainty, since direct measurements are taken every trimester, and daily water level readings on any moment of the day. Detailed hydrometeorological and sedimentological information exist from 1972 till 1990. Since 1990 some stations went out of order, which reduces information availability for some areas in the basin.

Another problem was the lack of information related to biophysical parameters, describing the hydrological characteristics of the different soil use types that need to be incorporated in SWAT. The by SWAT developers generated database does not consider crops and soil uses of some soil covers in the basin (e.g. coffee, banana, dry forest etc.). Therefore it was necessary to introduce these new land uses in the SWAT database, although information for CN, LAI, USLE C and some other parameters were not available. Therefore, these land uses were associated with other existing crops in the SWAT database and drawn from a few existing studies developed in the basin.

The existing soil information showed a lot of inconsistencies such as a lack of correspondence between similar zones on both sides of the border, which generated large uncertainties about map quality. This conclusion, together with the absence of hydrophysical data on each soil type, emphasised the need of a soil study to homogenize available information, with focus on hydrological model implementation.

(iv) Data requirements

To start working with SWAT it was necessary to recollect information, which in a lot of cases was not available in digital formats, e.g. soil information and precipitation data. Therefore, the digitizing of necessary information formed a large part of the implementation process. Data requirements of SWAT are large, but the most important input information is the following:

- Digital Elevation Model

Initially, contour lines each 200 m, at a 1:250.000 scale was available for the basin. To improve the quality of the DEM it was necessary to lower the scale of the base map. For that purpose, additional topographical information was processed at a 1:50.000 scale with contour lines every 40 m at the Ecuadorian side of the basin and at a 1:100.000 scale with contour lines every 50 m at the Peruvian side. An integration of the contour lines was done in ArcView, using curve interpolation techniques, which resulted in a single map with contour lines every 40 m.

The greatest difficulty was the difference of detail between the topographical maps generated in both countries. It was a time and effort consuming job integrating both maps into a single map for the basin.

The DEM, used for SWAT was elaborated in ArcView 3.2 and had a spatial resolution of 100 m x 100 m. The DEM basically permitted to define the draining system and the subbasin borders.

- Hydrography

A validation of the river network was done in vector format. Correspondence between new 40m contour lines and the existing river network was verified. During this analysis some inconsistencies were found (especially in the Ecuadorian part, due to different information sources) such as rivers crossing contour lines and incomplete river courses.

To correct these errors, information at 1: 50.000 at the Ecuadorian side was used, which allowed matching the information with the contour lines. Not all of the existing rivers could be used because this would have generated large differences at the border, since Peruvian river network information was on a smaller scale. A new visual validation was done till obtaining a product adjusted to the needs of the model.

- Climate and hydrological data

A quality analysis of climatic and hydrological data with daily and monthly resolution from the 19 Peruvian and 24 Ecuadorian stations was done. Process simulation requires a considerable amount of climatic, meteorological and hydrological data, including precipitation, temperature, wind speed, dew point temperature, and solar radiation, all on daily and monthly level. This information is used by the model to simulate model entries and outputs. Additionally, flow stream and sedimentation data are required for calibration and validation. Register uniformization was done by statistic procedures. This way, 15 monthly parameters characterizing the climate were obtained to prepare the model for the basin.

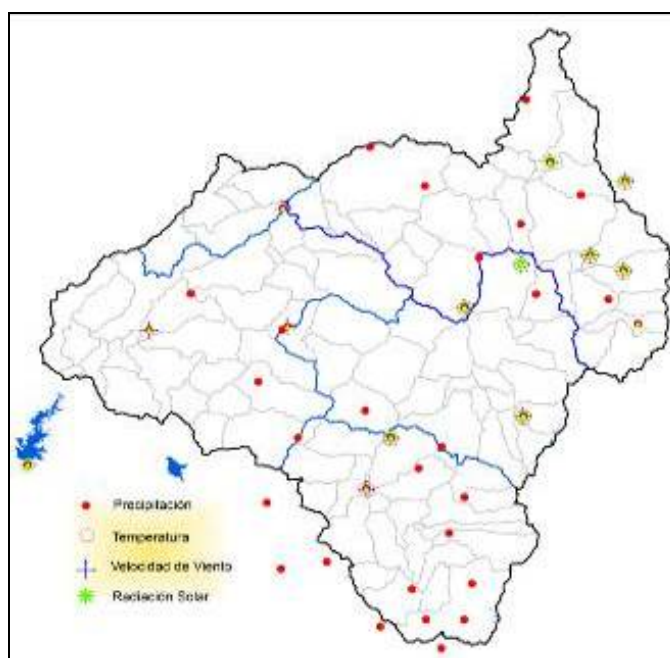


Figure 2.35 Meteorological stations used for SWAT application in the Catamayo-Chira basin

To determine evapotranspiration, the Hargreaves method was used. This method basically requires minimum and maximum temperatures.

The analysed pluviometric stations present a rainy period between October and April, with March being the wettest month. The stations in the lower part of the basin present the biggest absolute differences between dry and wet months, in comparison to the stations in the upper part where precipitation is more uniformly distributed through the year. In the lower stations, the ENSO effect is much more important.

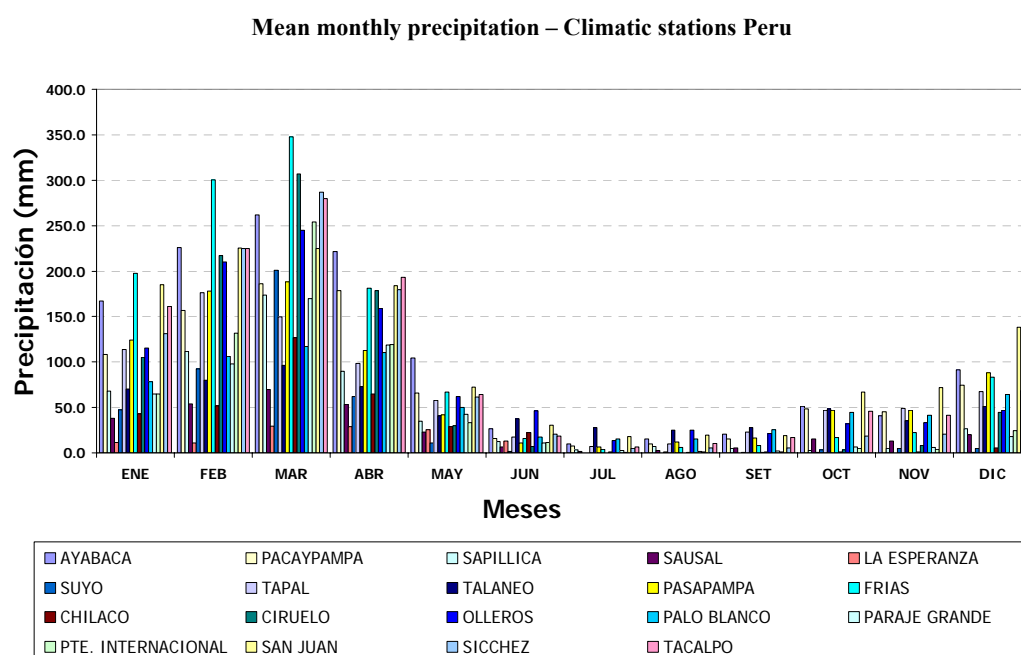
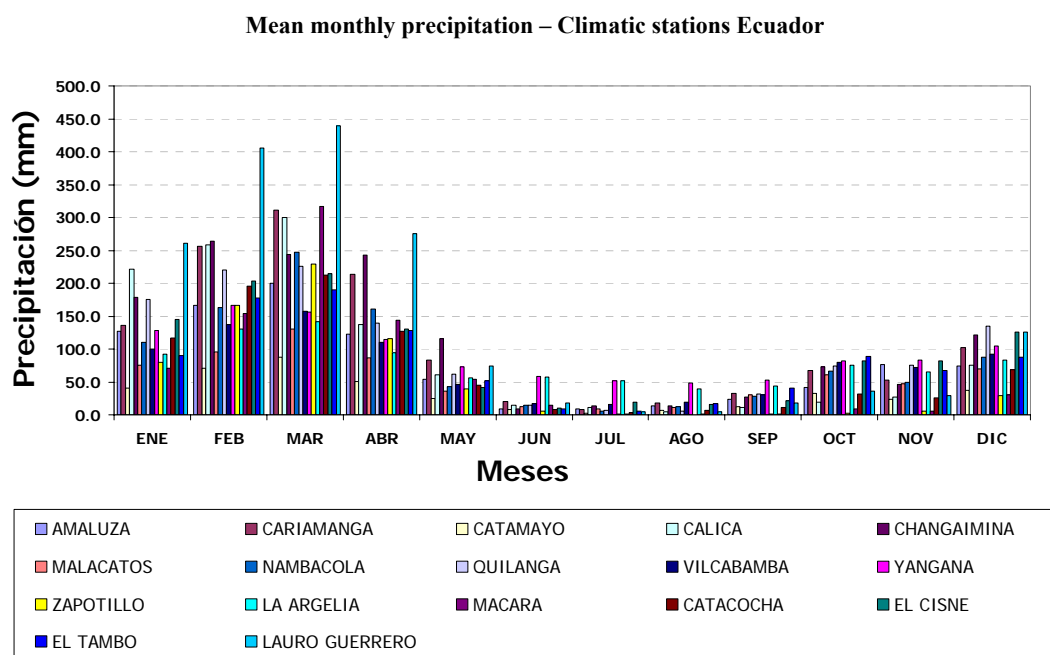


Figure 2.36 Visualization of precipitation regimens – Stations used for SWAT

▪ Soil use

Basic information was the soil use map, elaborated by the Catamayo Chira project in 2002. This map was actualised with Landsat images from 2006. Additionally, field verification was done. The largest problem in this part of the process was the lack of information for the biophysical parameters describing the hydrological characteristics of the different soil uses in the basin, which are needed for SWAT. The by the SWAT developers generated database does not consider crops nor soil uses present in the study area (e.g. coffee, banana or dry forest). Therefore it was necessary to introduce these data in the SWAT data base. For these crops no Curve Number (CN), Leaf Area Index (LAI), Cover and crop managing factor (USLE C) and other parameters were available. To cover the lack of information, these parameters were estimated, comparing existent crops in SWAT and small local studies.

▪ Soil types

As a start a soil map realized in the year 2002 by the Catamayo Chira project was used. This map was based upon various studies carried out by different institutions in Peru and Ecuador, but this information was not detailed enough for SWAT, basically because the most important information needed were hydrophysical data of the different soil units identified on the map.

For this reason a specific soil study was planned, to incorporate data into SWAT, and concentrated in the area, determined for the study (see Annex in “WP 03 Hydrological Modeling”: Validación y Complementación de los Estudios de Suelos de la Cuenca Binacional Catamayo Chira con miras a Implementar El Modelo SWAT).

From field samples and laboratory analysis, profile characterisation was obtained, consisting of: general characteristics, soil unit description (including morphological, physical and chemical soil aspects and taxonomic classification), and verification and correction of soil units. This permitted the generation of a data base that could be used for SWAT.

The K factor (in $\text{ton ha h ha}^{-1} \text{ MJ}^{-1} \text{ mm}^{-1}$) defined as soil resistance to erosion by direct impact of rain drops, was calculated for this study using the EPIC model (Sharpley and Williams, 1990):

$$K = \frac{1}{7.6} \left\{ 0.2 + 0.3 \exp \left[-0.0256 \text{SAN} \left(1 - \frac{\text{SIL}}{100} \right) \right] \right\} \left(\frac{\text{SIL}}{\text{CLA} + \text{SIL}} \right)^{0.3} \left(1.0 - \frac{0.25\text{OM}}{\text{OrgC} + \exp(3.72 - 2.95\text{OM})} \right) \left(1.0 - \frac{0.7\text{SN}}{\text{SN} + \exp(-5.51 + 22.9\text{SN})} \right)$$

Where $\text{SN} = 1.0 - \text{SAN}/100$, SAN, SIL, CLA, OM and OrgC are percentages of sand, lime, clay, organic matter and organic carbon content respectively.

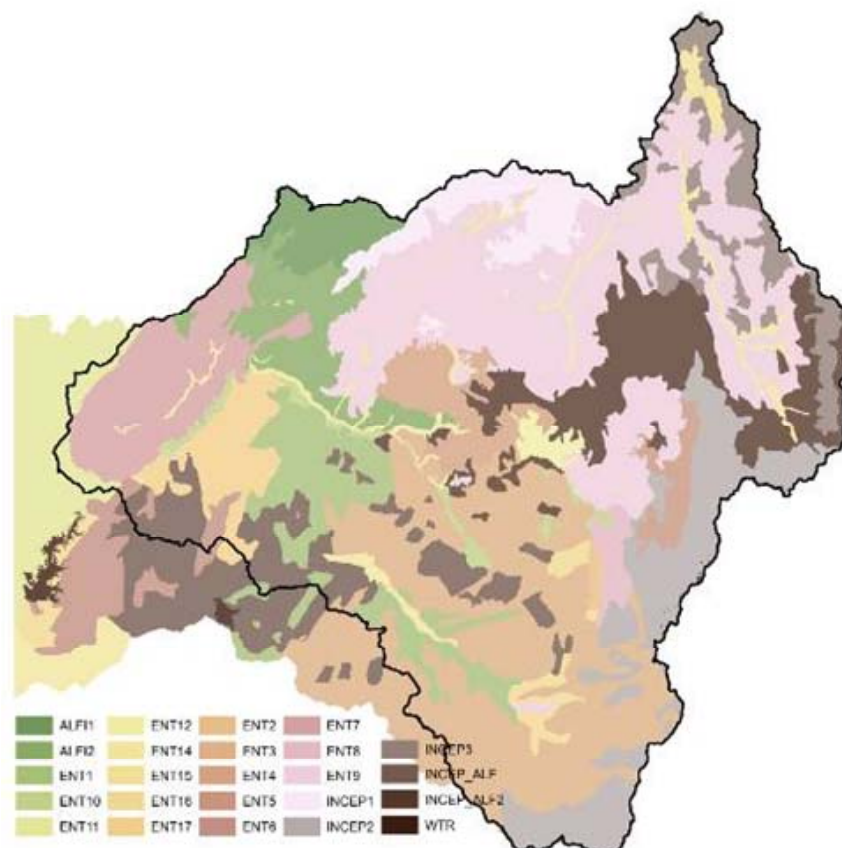


Figure 2.37 Soil types used in SWAT

(v) Output – Baseline situation

SWAT is a rather powerful model that produces a lot of output information. These output data depend on the type of simulation; this can be daily, monthly or annual, for each hydrological response unit, and for each sub basin. In this study a monthly analysis of the information was made for each of the 111 microbasins defined. For each one the model predicted sediment production (in $t\ ha^{-1}$) and the net amount of water contributed by the micro basin to the flows (in mm), besides some other hydrological variables characterizing the water cycle.

Data are organized according to the hydrological year (September-August) to represent hydrological behaviour in the basin and to allow comparing results with results from the WaTEM/SEDEM application, run in the same study area.

Years are classified in very dry years, dry years, wet years, normal years and ENSO years. This was done to differentiate and analyse hydrological behaviour of the basin in different periods and climatologic conditions.

Table 2-5 Classification of hydrological years

period	Sep/76 – Aug/77	Sep/77 – Aug/78	Sep/78 – Aug/79	Sep/79 – Aug/80	Sep/80 – Aug/81	Sep/81 – Aug/82	Sep/82 – Aug/83	Sep/83 – Aug/84	Sep/84 – Aug/85	Sep/85 – Aug/86	Sep/86 – Aug/87	Sep/87 – Aug/88	Sep/88 – Aug/89	Sep/89 – Aug/90	Sep/90 – Aug/91	Sep/91 – Aug/92	Sep/92 – Aug/93	Sep/93 – Aug/94
ENSO year							x											
Wet year								x										
Normal year	x										x		x			x	x	x
Dry year		x	x	x	x				x	x				x	x			
Very dry year						x						x						

Concerning sediment production in dry and normal years erosion rates of $37.3\ t\ ha^{-1}\ yr^{-1}$ were calculated. In wet years erosion rates were about $61.0\ t\ ha^{-1}\ yr^{-1}$. The maximum erosion rate for the analysed periods was $185.7\ t\ ha^{-1}\ yr^{-1}$ during the period September '82-august –'83 (ENSO year).

In the same manner the annual contribution was estimated at 5 different river sections for the years 1976 to 1988. Results can be seen in Table 2-6. The ENSO year (1983) delivers the highest sediment rates, due to greater runoff and the consequently greater erosion, basically in the middle part of the basin. This year contributions are up to $20\ 10^6\ t$ which is compared to a wet and a dry year respectively 3 and 10 times more. Likewise, 1983 registers the highest sediment contributions compared to other years for all analysed points.

Table 2-6 Sediment contribution in 5 measurement stations in the basin

Year	Sediment contribution [$t\ yr^{-1}$]				
	Station Santa Rosa	Station Puente Internacional	Station Alamor en Saucillo	Station Paraje Grande	Station Ardilla (Inlet at Pochos)
1976	2,149,647.03	2,741,987.41	768,185.24	416,598.49	7,844,674.68
1977	1,165,959.31	1,678,083.94	463,187.32	278,773.72	6,119,269.33
1978	78,092.83	540,949.98	69,276.50	32,435.78	877,663.05
1979	584,147.21	1,277,856.25	326,718.24	50,317.49	2,517,391.82

1980	460,190.51	698,063.39	122,633.48	45,450.90	2,888,220.97
1981	775,588.99	2,068,855.34	351,933.22	240,215.55	5,760,970.41
1982	330,556.61	2,246,234.19	206,817.38	119,463.46	4,575,773.78
1983	2,302,537.99	3,490,550.99	1,705,591.16	541,839.86	20,043,617.60
1984	1,885,625.43	2,748,078.24	570,061.77	145,985.81	8,875,487.54
1985	192,733.68	598,780.16	281,689.94	3,056.62	1,774,978.10
1986	685,798.23	895,794.29	797,790.16	23,600.12	3,483,040.74
1987	610,755.65	1,290,597.50	683,154.76	124,955.34	6,896,996.46
1988	650,559.71	1,039,416.19	231,555.80	21,200.37	2,260,666.96

From these results the 15 micro basins that contribute most to sedimentation generation were determined. The discrimination criterion was $3 \text{ t ha}^{-1} \text{ yr}^{-1}$, considering lower values are low erosion rates. A historical series was analysed by SWAT (1976 – 1988) representing different hydrological conditions.

Areas with a higher erosion rates at microbasin level were located in the Alamor, Catamayo and Macara subbasins (microbasins No. 33, 15 and 106), representing an area of 170,291.00 ha with a mean soil loss of $36.5 \text{ t ha}^{-1} \text{ yr}^{-1}$.

Table 2-7 Largest sediment contributing microbasins in different hydrological conditions

Subbasin	Micro basin	Area [ha]	Normal year	Dry year	ENSO year (82-83)	Wet year	Multiannual mean
			(76-77)	(80-81)	(82-83)	(83-84)	
$\text{t ha}^{-1} \text{ yr}^{-1}$ (SSY)							
Alamor	15	13076.00	14.325	10.185	50.943	12.579	22.376
Alamor	16	14610.00	13.693	8.844	42.493	11.201	20.19
Catamayo	28	8438.00	21.378	8.833	9.116	5.215	10.386
Catamayo	33	19500.00	37.152	19.665	185.686	13.636	34.24
Macará	45	17980.00	3.119	14.295	0.829	7.418	6.393
Macará	48	13560.00	2.550	1.751	1.984	6.111	4.303
Macará	59	19333.00	2.066	2.748	2.031	5.607	4.72
Macará	60	13607.00	13.934	6.829	9.848	4.679	8.337
Macará	66	2760.00	2.123	1.180	7.552	1.104	2.936
Macará	72	3060.00	9.239	4.729	6.073	2.792	5.658
Macará	77	8133.00	7.517	3.694	5.131	2.390	5.479
Alamor	105	14035.00	6.223	4.940	26.157	5.984	14.149
Alamor	106	3522.00	13.933	10.693	55.802	12.978	22.909
Alamor	107	11586.00	11.141	4.751	51.184	2.368	5.567
Alamor	109	7091.00	5.624	2.942	2.289	1.957	4.937
Total		170,291.00					

The $1.7 \cdot 10^5$ ha affected by erosion are located in Alamor in the maize and coffee areas on hill sides with moderate slopes. The identified zones in the Catamayo and Macara subbasin are those corresponding to depredated forest with trees and scarce pastures.

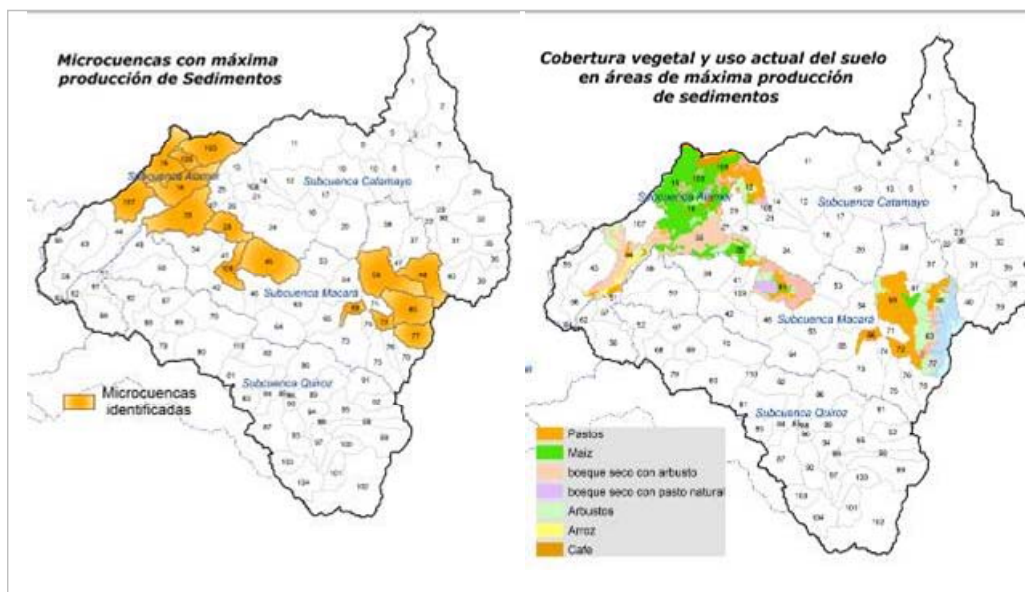


Figure 2.38 Microbasins with largest predicted soil losses

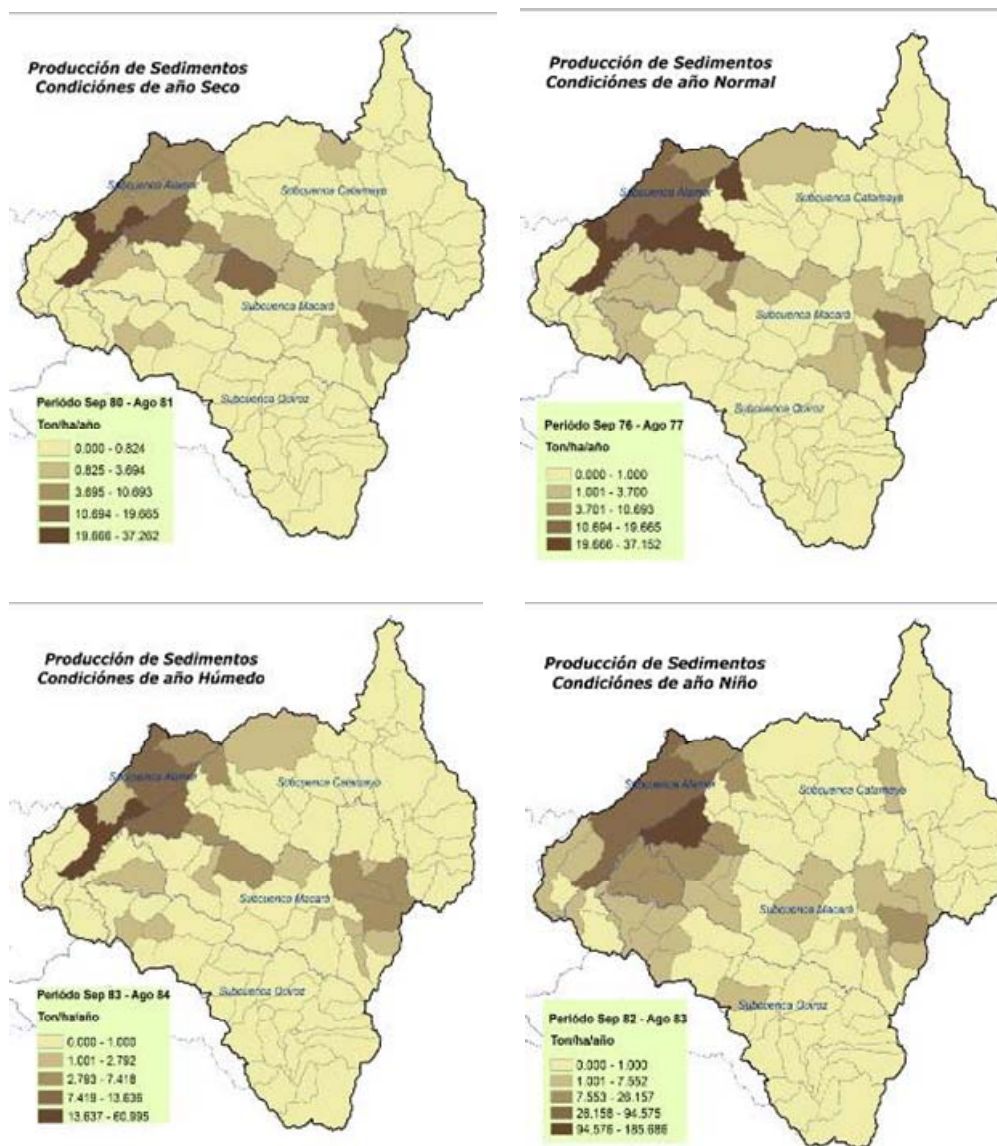


Figure 2.39 Predicted sediment production in different hydrological years

As can be observed in Figure 2.39, in dry year conditions (Sep '80 – Aug '81) as well as in normal year conditions (Sep '86 – Aug '87) there is no remarkable difference related to most contributing microbasins. Also in a wet year the Alamor, Macara and Catamayo subbasins always represent the largest contributions. If we analyse erosion rates from the different micro basins there are a large differences, especially between a normal or dry years and a wet year. Sediment yield per ha is almost duplicated. In a year affected by ENSO, area specific sediment yields reach extremes such as $186 \text{ t ha}^{-1} \text{ yr}^{-1}$, which is 5 times the value of a normal year. Nevertheless, in spite of the differences between hydrological conditions between different years, some microbasins are always affected.

The output maps of predicted water production for each micro basin for different hydrological years are shown in Figure 2.40. In this case the difference in spatial distribution between an ENSO year and other years is notorious. A large water production in the lower and middle part areas can be seen as a direct consequence of the climate alterations caused by ENSO, resulting in heavy rains in the – in normal conditions– dry coastal area.

On the other hand, in a normal, dry and wet year, the spatial distribution of water production is more similar, with the largest predicted water production in the middle and higher part of the Catamayo, Macara and Quiroz subbasins, contributing up to 1444 mm water in the period Sep '83 – Aug '84.

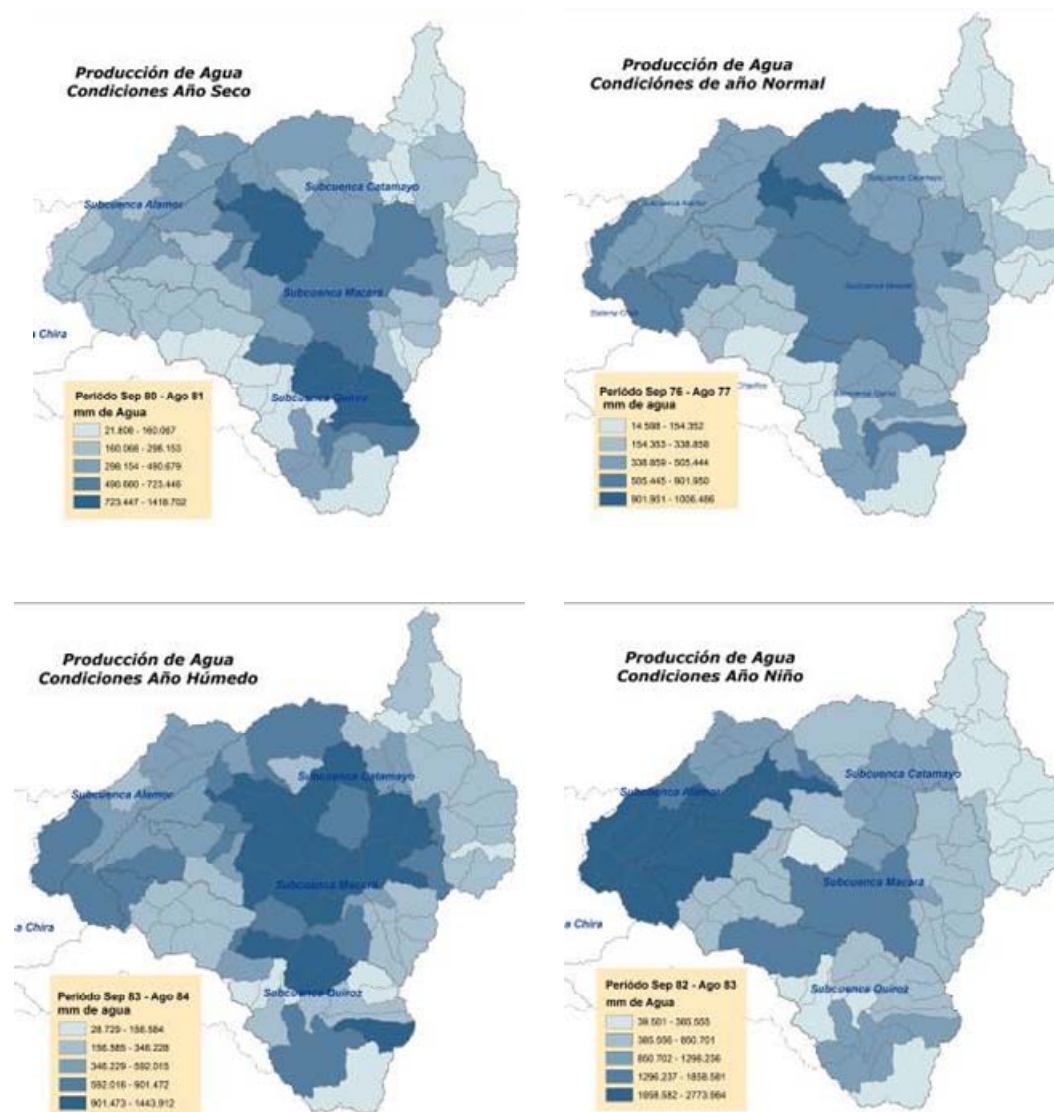


Figure 2.40 Water production in different hydrological years

Based upon these results, 20 micro basins were determined as the largest water contributors. A historical series of 21 years (1976 – 1994), representing different hydrologic conditions, was simulated in SWAT.

Table 2-8 shows the water production for each sub basin. Production in four different hydrologic periods is compared. The table shows the amount of water expressed in mm (WYLD = runoff + lateral flow + subterranean water contribution – transmission loss), which results in the net water contribution of the micro basin to the flows.

Table 2-8 Water production in microbasins

Subbasin	Micro basin	Area [ha]	Normal year (76-77)	Dry year (80-81)	ENSO year (82-83)	Wet year (83-84)	Multiannual Mean *
			mm (WYLD)				
Catamayo	14	5,086.00	659.155	466.627	1462.599	670.259	626.778
Catamayo	21	8,411.00	1006.063	756.654	2340.973	935.901	970.521
Catamayo	24	25,762.00	719.495	1418.702	494.301	1443.912	671.327
Catamayo	25	6,825.00	953.305	723.446	2294.628	893.005	932.662
Catamayo	26	3,946.00	1003.938	756.210	2340.019	934.903	969.496
Catamayo	27	1,092.00	1006.486	757.566	2340.609	936.667	970.866
Catamayo	28	8,438.00	758.561	682.995	825.002	731.663	538.831
Macará	37	9,625.00	381.180	540.876	587.157	1078.313	543.255
Macará	38	19,181.00	484.437	648.858	692.314	1224.872	647.333
Macará	41	4,608.00	737.403	664.223	817.415	722.372	527.784
Catamayo	45	17980.00	576.030	1138.793	385.555	1138.692	616.620
Macará	53	11,855.00	630.139	574.965	1296.236	992.240	596.586
Macará	54	12,903.00	660.950	612.306	1381.019	1044.297	631.623
Macará	59	19,333.00	459.728	619.954	656.946	1197.761	620.523
Macará	65	8,927.00	606.684	578.494	1708.006	1244.596	693.570
Macará	73	18,598.00	577.067	634.776	1389.526	625.859	547.654
Quiróz	86	17,402.00	468.689	837.736	805.326	1041.587	764.027
Quiróz	89	11,816.00	466.536	841.878	811.667	1049.220	769.175
Macará	99	2,300.00	727.013	519.876	1145.460	912.708	442.030
Catamayo	108	495.00	630.877	442.807	1398.000	645.402	596.919

* Multiannual mean of the 21 simulated years

As can be seen in Figure 2.41, the 20 micro basins identified as important for water production, are located in the Catamayo, Macará and Quiroz subbasins. The most important microbasins are located in the Catamayo subbasin (No. 25, 26 and 27).

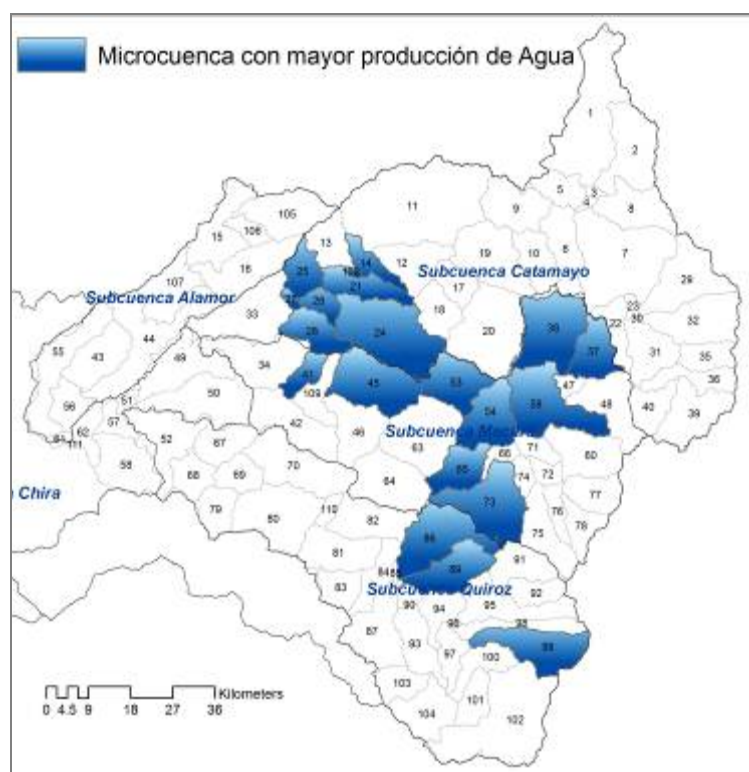


Figure 2.41 Most water producing microbasins

In Figure 2.42, the amount of water (in $10^6 \text{ m}^3 \text{ yr}^{-1}$) for each modelling year can be appreciated. The ENSO year 1983 had the largest contributions, summing up to $12 \cdot 10^9 \text{ m}^3 \text{ yr}^{-1}$. For a year in normal conditions, the mean contribution is $4 \cdot 10^9 \text{ m}^3 \text{ yr}^{-1}$, measured in the Ardilla station at the inlet of the Poechos reservoir. The most important contributions are from the Macara subbasin (Puente Internacional) with contributions up to $2.4 \cdot 10^9 \text{ m}^3 \text{ yr}^{-1}$ and the Catamayo subbasin (Santa Rosa Station) with contributions up to $1.5 \cdot 10^9 \text{ m}^3 \text{ yr}^{-1}$. These two sub basins represent a 70 % contribution.

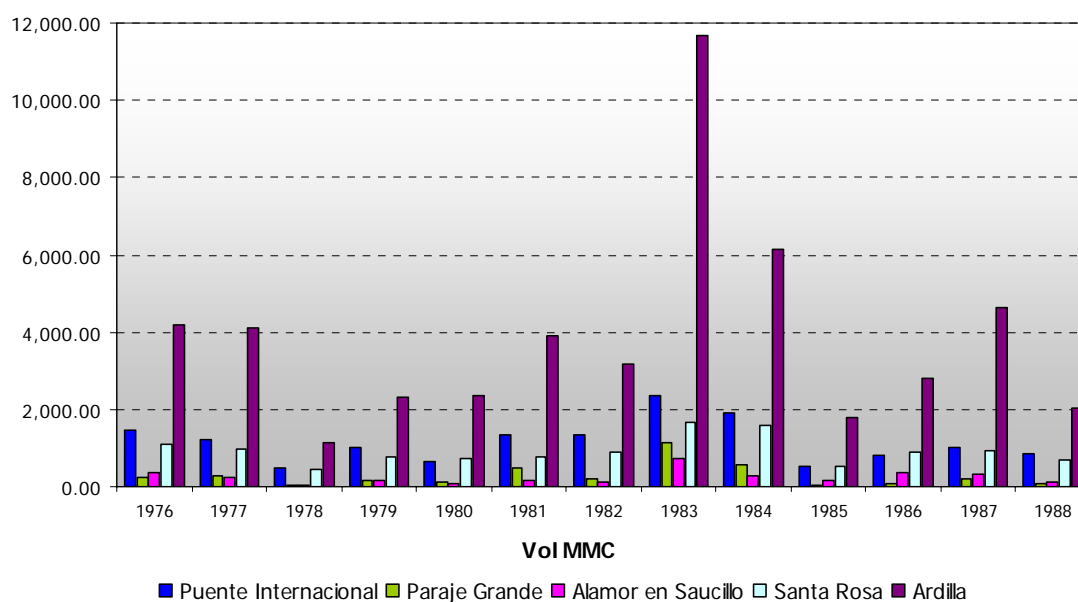


Figure 2.42 Water production [$10^6 \text{ m}^3 \text{ yr}^{-1}$]

B WaTEM/SEDEM

The WaTEM/SEDEM model was created by a team of experts of the ‘Laboratory for Experimental Geomorphology’ of the Katholieke Universiteit Leuven, Belgium. It consists of two parts as can already be deduced by the name. In the first component Water- or Tillage-Erosion is calculated on basis of the ‘Revised Universal Soil Loss Equation’ (RUSLE) (Van Oost et al., 2000). The second component integrates a simulation of sediment accumulation and distribution based on a transport capacity that is assigned to every pixel (Van Rompaey et al., 2001).

The WaTEM/SEDEM model has three main components: (1) the assessment of a mean annual soil erosion rate for each grid cell (based on RUSLE), (2) the assessment of a mean annual transport capacity for each grid cell, and (3) a sediment routing algorithm that redistributes the produced sediment over the catchment taking into account the topology of the catchment and the spatial pattern of the transport capacity (Van Rompaey et al., 2001).

In “WP 06 – Pollution Pressure and Impact Assessment” the model functionality, the inputs and the calibration/validation process is described more extensively as the model is used to evaluate the River pollution by diffuse sources – in this case the sediment load.

The soil erosion rate is calculated in tons per hectare and year with the widely used Revised Universal Soil Loss Equation (Renard et al., 1997)

$$A = R * K * LS * C * P \quad (1)$$

where:

- A: average annual soil loss [$t \text{ ha}^{-1} \text{ a}^{-1}$]
- R: rain erosivity factor [$\text{MJ mm ha}^{-1} \text{ a}^{-1}$]
- K: soil erodibility factor [$t \text{ h MJ}^{-1} \text{ mm}^{-1}$]
- LS: topographical slope and length factor
- C: crop management factor
- P: erosion control factor

To model the effects of the described scenarios, at least one of those factors has to be varied to be able to evaluate the effects of change. In the case of the climate change scenarios the predicted rainfall amount is transmitted into values of rainfall intensity, whereas in the case of land use change scenarios, the crop management factor is varied.

The variation of land use patterns will not only affect the absolute sediment production, but also will have an effect on sediment routing, deposition processes and river pollution evaluation. The WaTEM/SEDEM model bases on the mean annual transport capacity that is evaluated for each cell depending of its land use:

$$Tc = Ktc * Eprg = Ktc * R * K * (LS - 4.12 * Sg * 0.8) \quad (2)$$

where:

- Ktc is the transport capacity coefficient (m)
- Eprg is the potential gully erosion ($\text{kg m}^{-2} \text{ a}^{-1}$)
- Sg is the local slope (meter per meter)
- R, K, and LS are the factors from the RUSLE

In the calibration process values of Ktc are defined for two different land use categories – for (highly) eroding and non-/less eroding land use classes. The transport capacity coefficient for cropland and other highly erosive land use classes was defined to be 15m, while for pastures, páramo, brushes and forests a value of 3m has been identified (for more details on calibration refer to the WP06 report).

The modeled baseline situation in the case of WaTEM/SEDEM represents the relatively recent time period from September 1999 to August 2000, that was characterized by high precipitation values and

therefore high rainfall intensities (see WP 06 – “Pollution Pressure and Impact Assessment”). The annual soil loss for 111 microbasins was predicted to be between 1.3 and 239.3 t ha⁻¹ yr⁻¹. For the whole study area the average annual soil loss is predicted to be 40.4 t ha⁻¹ yr⁻¹. As the model considers deposition processes, the sediment load that effectively reaches the river system can be evaluated. This sediment yield is considered to be between 0.4 and 144.8 t ha⁻¹ yr⁻¹, which averages 19.2 t ha⁻¹ yr⁻¹ for the whole study area. Only about half of the sediment that is produced by erosion in one year effectively reaches the aquatic systems.

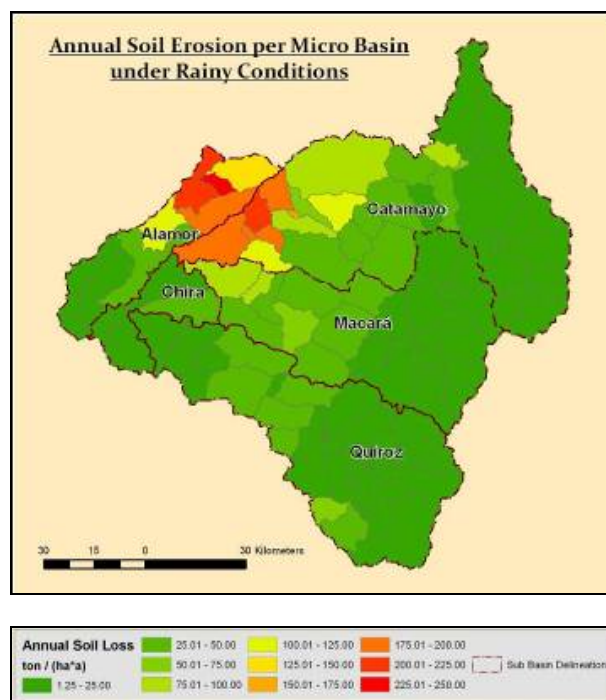


Figure 2.43 Mean annual soil loss predicted by WaTEM/SEDEM - baseline situation

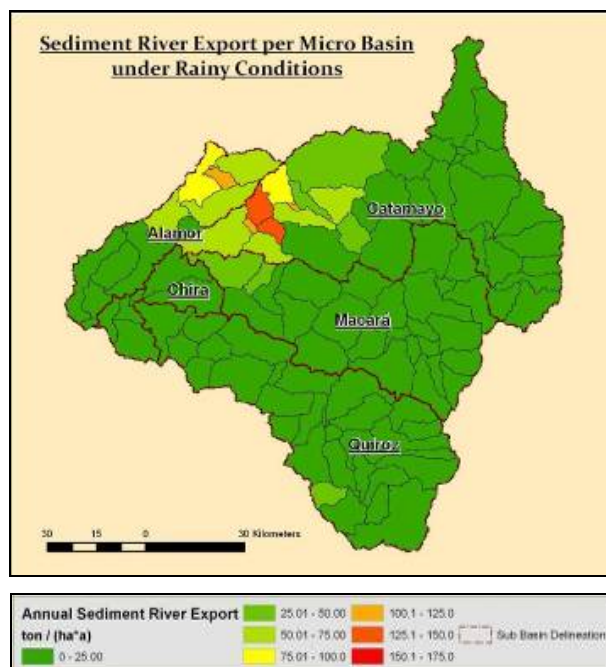


Figure 2.44 Mean annual sediment river export predicted by WaTEM/SEDEM – baseline situation

Throughout the modelling of annual soil loss under different climatic conditions, the spatial distribution of the microbasins with the highest sediment production values did not change

considerably. Those microbasins are therefore not only representative for the baseline climate but for the whole climatic spectrum of the study area. Most of these microbasins are located in the sub basin Catamayo (14) whereas 6 are located in the sub basin Alamor, 3 in the sub basin Macará and 1 in the sub basin Quiroz.

Additionally, the microbasins that showed the highest sediment export values are practically located in the same areas.

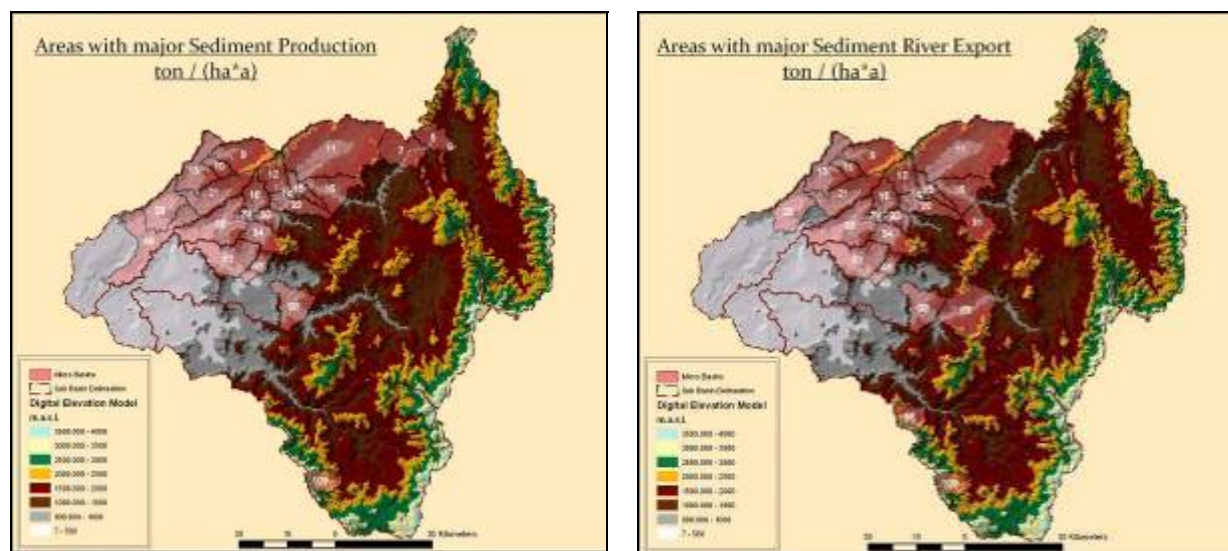


Figure 2.45 Microbasins with highest soil erosion (left) and sediment export (right) – baseline situation

2.2.3.2 Separate effects

A Climate change

(i) SWAT

The results of the MAGICC/SCENGEN model are expressed as an absolute value referring to an increase or decrease of temperature and as a percentage to identify an increase or decrease in the precipitation level related to 1990 data (see Figure 2.26 p. 2-31, Figure 2.27 p. 2-31, Figure 2.28 p. 2-32 and Figure 2.29 p. 2-33). SCENGEN was run for two zones: region 1 (5.0° – 0.0° S, 80.0° – 75.0°W) and region 2 (10.0° – 5.0°S, 80.0° – 75.0° W). These results were used to deform meteorological data in the basin.

MAGICC/SCENGEN results show for both the A1 and the B2 scenario a tendency of decreasing precipitation in the study area. In the case of the A1 scenario this decreasing precipitation oscillates between -1.3% (March 2045) and -21.9% (November 2055). In the case of B2 scenario the range of reduction in precipitation varies from -3.5% (august 2045) to -11.8% (September 2055). For both the A1 and the B2 scenario a raise in temperature in the study area is predicted. In the case of the A1 scenario this raise in temperature varies between 1.4 ° C (February 2045) and 2.7 ° C (July 2055). In the B2 scenario, the range of raise varies from 1.1°C (February 2045) to 2.0°C (August 2055).

These values of predicted change precipitation estimated by MAGICC/SCENGEN were applied to 31 rain gauging stations located in the area of the Catamayo-Chira basin. For 28 Peruvian and Ecuadorian stations the results obtained for region 1 were applied and in another 3 Peruvian stations the results obtained for region 2 (Figure 2.46). In the same way absolute values for the temperature change estimated by MAGICC/SCENGEN were applied to 8 climatic stations in Peruvian territory and 6 in Ecuador. All temperature stations correspond to Region 1 (Figure 2.46). The perturbations were applied to the 1990 reference year in each station, which allowed the generation of a new historical temperature and precipitation series in the basin for the period 2045-2055.

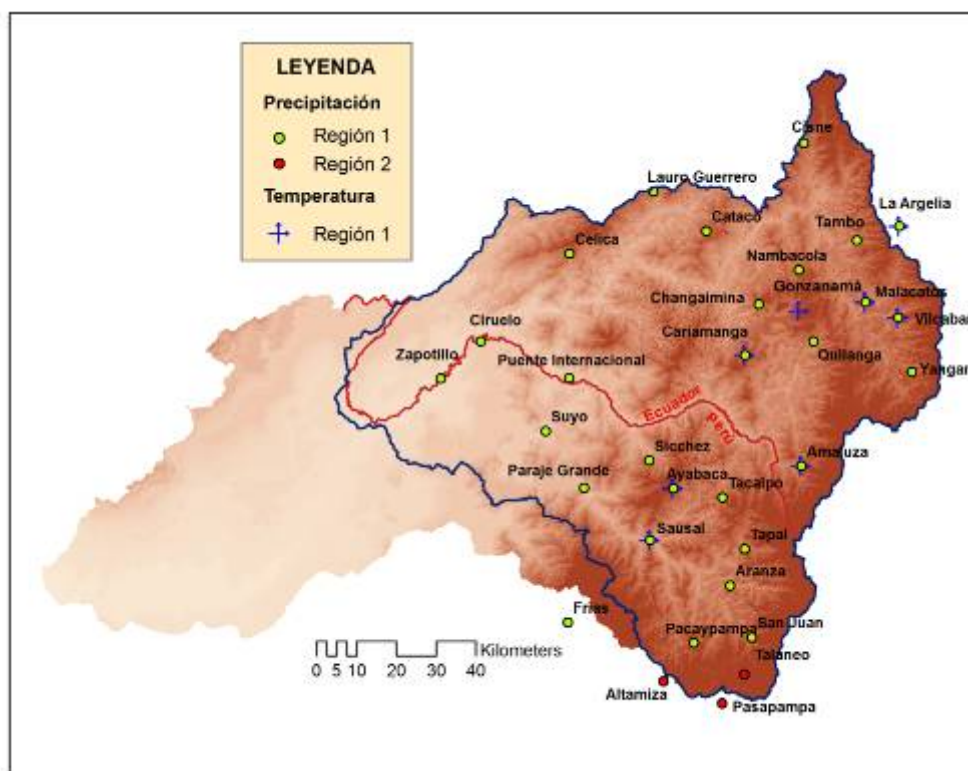


Figure 2.46 Climate stations where climate changes estimated with MAGICC/SCENGEN were applied

Once the SWAT model was calibrated and validated, data from these new series were incorporated for temperature and precipitation, to subscribe actual climatic data. However, information corresponding to actual land use and soil type was conserved. Results of the application of climate change scenarios A1 and B2 in SWAT were analysed using the differences in percentage obtained in climatic change scenarios, compared to the baseline situation.

Table 2-9 Predicted effects of climate change on water balance (SWAT)

Water balance components	Actual conditions	Climate change scenarios (2050)			
	1990	A1		B2	
Precipitation (PCP)	707.87	585.54	- 17.3 %	549.77	- 22.3 %
Water Yield (WY)	225.82	143.25	- 36.6 %	130.93	- 42.0 %
Sediment Yield (SY)	0.89	0.66	- 25.8 %	0.63	- 29.3 %
Runoff	38.25	19.25		17.24	
Percolation	93.48	40.83		36.99	
Evapotranspiration	429.14	426.07		402.32	

Table 2-9 shows the results of climate change scenario modelling using SWAT for the two climatic change scenarios generated with MAGICC/SCENGEN. A reduction in the mean annual precipitation can be seen for both A1 and B2 scenarios, compared to the baseline situation. Water yield in the basin (net water import contributing to flow streams) decreases also, with more severe decreases in the B2 scenario. On the other hand, the simulated climate scenarios present a decrease of the sediment yield: results for 2050 show a reduction of 29% and 26% for the B2 and A1 scenarios, respectively. In general, no large differences between both scenarios are observed.

The spatial distribution of water yield at microbasin level for the baseline situation and for simulated climate change scenarios A1 and B2 are shown in Figure 2.47. In the baseline situation, absolute values reach 883 mm for microbasins located in the centre and upper parts of the basin. In case of A1 scenario the maps show a predicted reduction in water yield in various microbasins that for actual

water production are very important. In A1 scenario absolute values reach a maximum of 593 mm, while in the B2 scenario it reaches up to 599 mm.

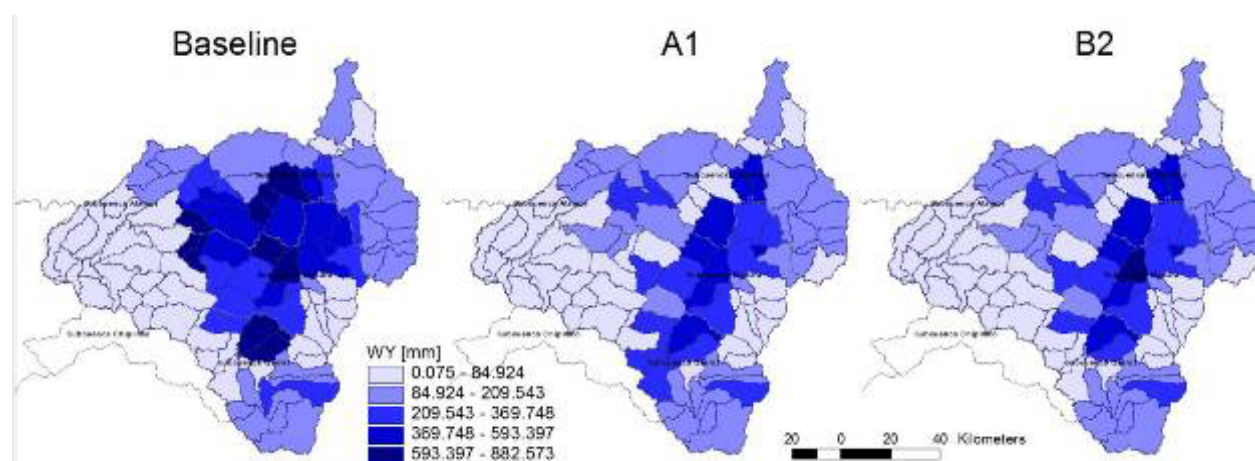


Figure 2.47 Predicted water yield in different climate change scenarios (SWAT)

Figure 2.48 shows the spatial distribution of sediment yield at microbasin level for the baseline situation in the reference year as well as for simulated A1 and B2 change scenarios. For the baseline situation, the highest values reach $44.2 \text{ t ha}^{-1} \text{ yr}^{-1}$ and are located in the Alamor subbasin in Ecuador. In the case of A1 and B2 scenarios, the maps show a predicted reduction in erosion rates in the microbasins that under actual conditions are highly affected by erosion. Absolute values reach $9.8 \text{ t ha}^{-1} \text{ yr}^{-1}$ and $9.9 \text{ t ha}^{-1} \text{ yr}^{-1}$ for the A1 and B2 scenarios respectively. This reduction can be explained by the important predicted reduction in precipitation for both scenarios A1 and B2, as rain is a basic element causing water erosion. Nevertheless, the predicted reduction in precipitation amount does not necessarily imply a reduction in rainfall intensities. Heavy precipitation events will ‘very likely’ become more frequent in the 21st century (IPCC, 2007), with increasing sediment production rates as a consequence.

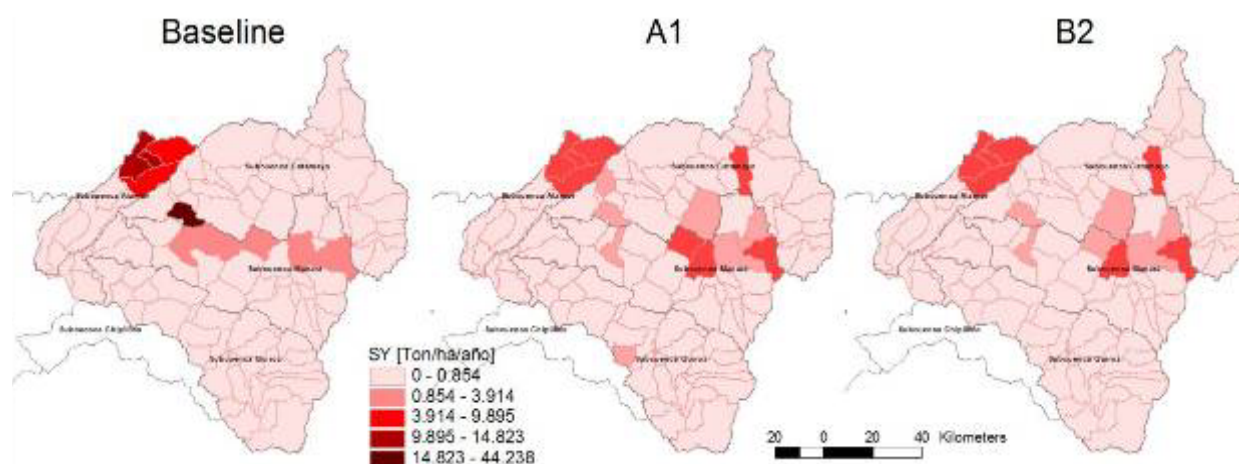


Figure 2.48 Predicted sediment yield in different climate change scenarios (SWAT)

B Land use change

(i) SWAT

As described previously, two land use change scenarios were generated to analyze the effects of land use changes in the basin Catamayo-Chira. The first scenario is based on the actual land use tendencies, mainly the deforestation of dry, natural and humid forests and their conversion to pasture areas and cropland. The second scenario was based on an economic and ecologic landscape value study, which

represents a “Sustainable Development” since both economic and ecologic developments of the basin are considered.

The meteorological data (precipitation, temperature, wind speed etc.) are maintained constant in the evaluation of the land use change scenarios. Only land use input data are adapted using the two land use change scenarios. The simulation with SWAT was applied on a period of 21 years (1976 – 1994), which is the same period that was used for model calibration and validation. Consequently, the predicted water discharge and sediment production can be compared to the baseline situation, to evaluate change effects. The change of the land use input map required an adaptation in the calibration of some parameters in the SWAT land use database, especially related to biophysical parameter of newly introduced agricultural crops.

In the following results, scenario 1 refers to the scenario based on ‘actual trends’, while scenario 2 is based on ‘sustainable development’.

Table 2-10 shows the results of SWAT simulations for the baseline situation (1987), and for the two land use scenarios. Both scenarios show higher predicted production of water. For the first scenario this increase is larger, probably due to the higher percentage of cropland (+ 20%), combined with the decrease of woodland (- 5%). The effects of these changes can also be observed in the decreasing values of evapotranspiration and an increase in runoff.

Predicted sediment production shows different results for the two scenarios: the effect of scenario 2 (‘sustainable development’) is a decrease of erosion, while for scenario 1 (‘actual trends’) an increase in erosion is modelled. A positive effect on soil erosion in scenario 2 is observed, even with the expansion of arable lands with sugarcane, corn and coffee. Since this increase occurs on areas less susceptible to erosion and accompanied with an expansion of woodland and forest areas, overall erosion reduces.

Table 2-10 Predicted effects of land use change on the water balance (SWAT)

	Baseline condition (1987)	Scenarios			
		Scenario 1		Scenario 2	
Precipitation (mm)	946.04	946.04	-	946.04	-
Runoff (mm)	131.48	140.87	+ 7.1%	146.72	+ 11.6 %
Lateral flow (mm)	163.23	164.86	+ 1.0 %	166.11	+ 1.8 %
Percolation (mm)	219.36	210.18	- 4.2 %	221.77	+ 1.1 %
Evapotranspiration (mm)	451.28	450.74	-0.1 %	431.45	- 4.4 %
Water production (mm)	432.83	450.77	+ 4.1 %	448.77	+ 3.7 %
Sediment production (t ha ⁻¹)	2.68	3.42	+ 27.6 %	2.11	- 21.3 %

Effects of land use changes were analyzed on microbasin scale, which allows the identification of the areas most affected by the simulated land use change scenarios. Figure 2.49 shows the distribution of runoff values for the baseline situation and two land use change scenarios. In general, the effect of land use change on the spatial distribution of runoff generation is low. In some microbasins runoff increases due to the conversion of brush vegetation into corn, while in other regions the transformation of pasture into shrubby vegetation causes a decrease of the runoff. The installation of a new irrigation system in the Zapotillo area in the lower part of the basin (scenario 1) raises runoff values.

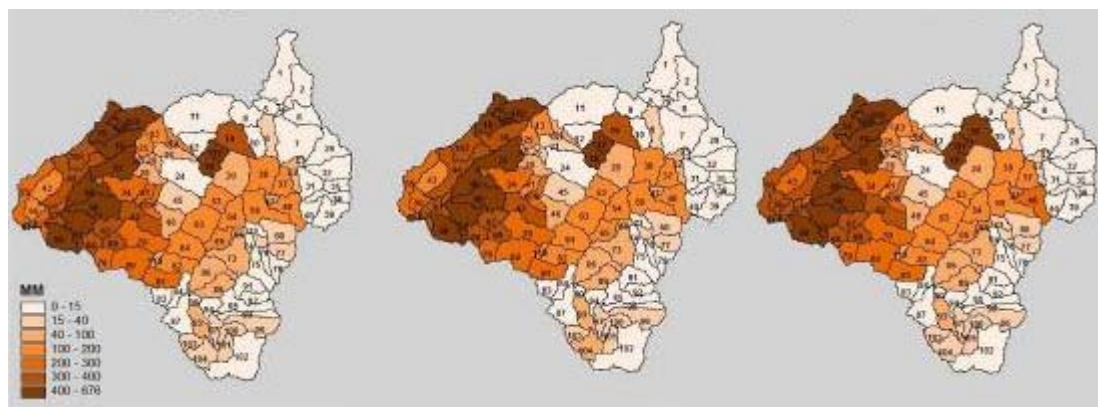


Figure 2.49 Predicted runoff for baseline situation (left), scenario 1 (centre) and scenario 2 (right)

The spatial distribution of evapotranspiration at microbasin scale can be observed in Figure 2.50. The highest values reach up to 996 mm and can be observed in the elevated part of the basin where large woodlands are located. The brush land areas show values of about 400 mm and the cropland areas show the lowest evapotranspiration values. In both scenarios a decrease of evapotranspiration values can be observed. In the first scenario the decrease is due to the deforestation of humid forests, whereas in the second scenario, the transformation of pasture areas into cropland has an even stronger effect. However, in the same scenario reforestation activities in other areas raise the evapotranspiration rates locally, so overall changes compared to the baseline situation remains small (see Table 2-10).

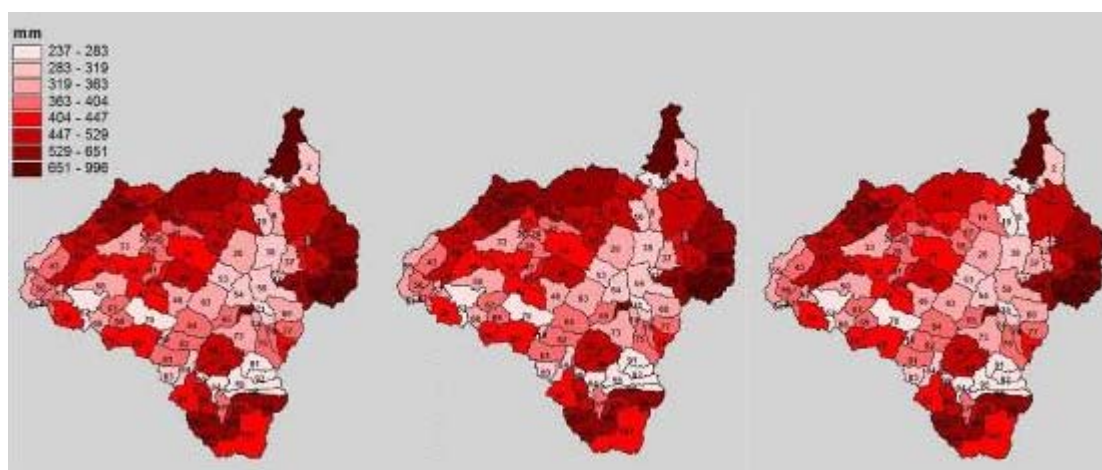


Figure 2.50 Predicted evapotranspiration for baseline situation (left), scenario 1 (centre) and scenario 2 (right)

The expected effects of both land use change scenarios on water discharge and soil loss were analysed. Mean monthly values of the baseline situation and of the two modelled scenarios were examined for a two year period. Figure 2.51 shows the effect of the two land use change scenarios on water discharge at the Ardilla station at the inlet of the Poechos reservoir.

Both scenarios show an increase of water discharge in the wet period, due to deforestation (scenario 1) and an increase of arable land (scenario 1 and 2). However, the effect on peak discharges of scenario 2 is lower. In the dry months, the first scenario shows a decrease of the baseflow (-10 – -34 %), while the second scenario results in an increase in baseflow up to 15 % in August and September.

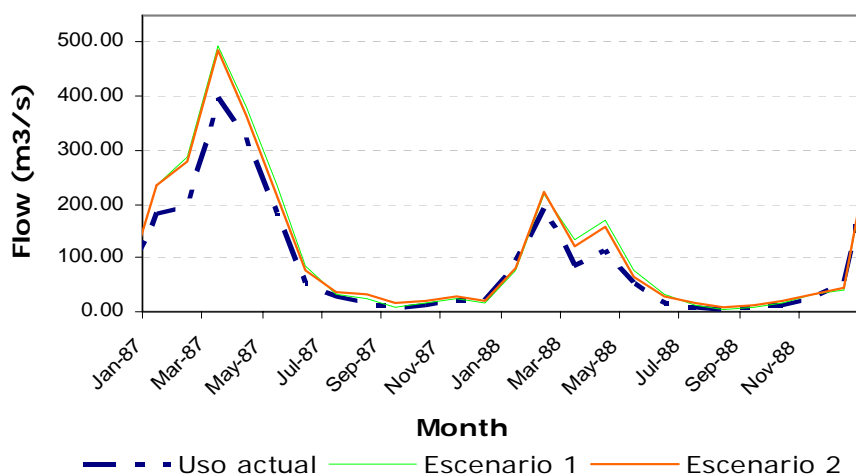


Figure 2.51 Simulated water discharge at Ardilla station for the baseline situation and two land use change scenarios – 1987-1988(SWAT)

In Figure 2.52 the simulated soil loss of the baseline situation is compared with the two land use change scenario modelling results. The first scenario shows larger amounts of soil losses, while the second scenario modelling results remains below the baseline sediment yields.

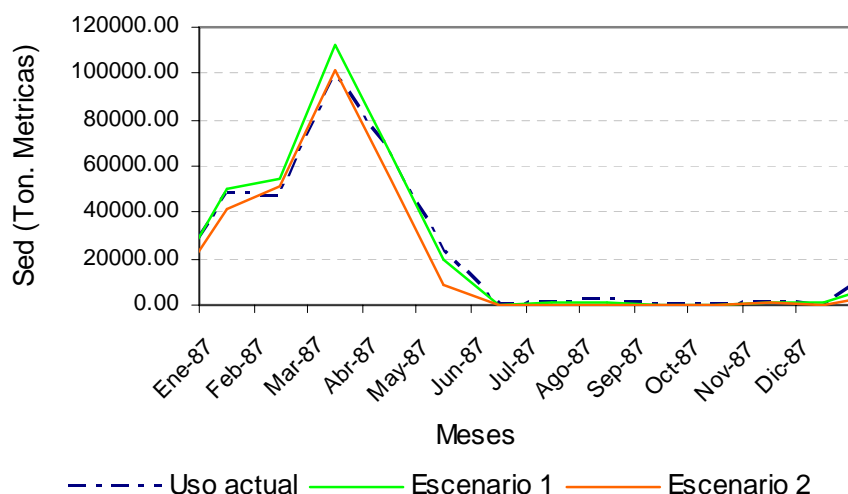


Figure 2.52 Simulated soil losses [t ha⁻¹] for the baseline situation and two land use change scenarios – 1987-1988 (SWAT)

The spatial distribution of predicted soil losses are shown in Figure 2.53. Scenario 1 shows an increase of sediment yields compared to the baseline situation. The affected areas are located in the centre of the basin, where new cropland areas (corn, sugarcane, banana, other fruit crops) were introduced, and forest areas decrease. In some areas soil losses are multiplied by 3 due to the conversion of dry forest into fruit crops, or even multiplied by 19 (from 0.3 t ha⁻¹ yr⁻¹ to 4.9 t ha⁻¹ yr⁻¹) due to the conversion of forest areas into sugarcane and banana.

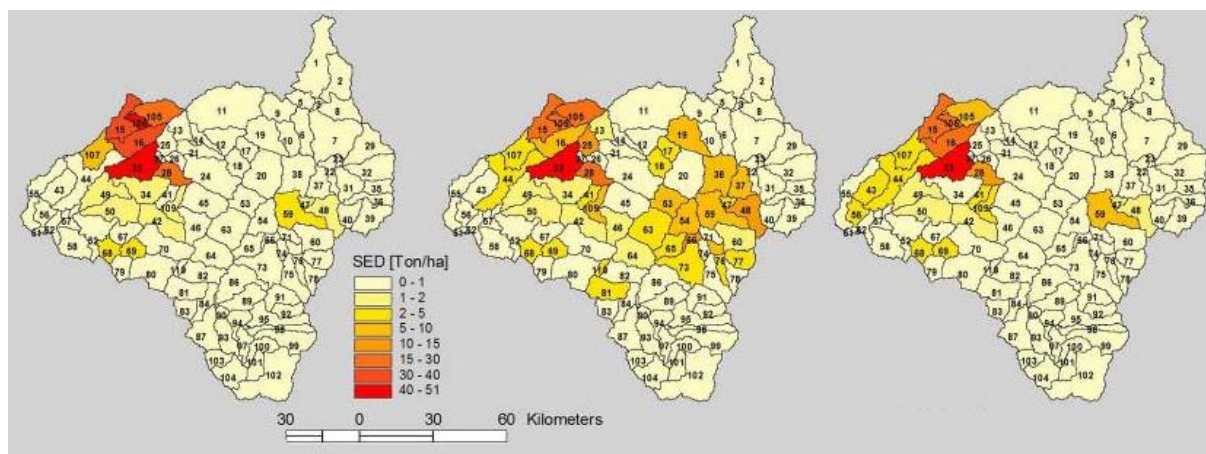


Figure 2.53 Predicted soil losses [$\text{t ha}^{-1} \text{yr}^{-1}$] for baseline situation (left), scenario 1 (centre) and scenario 2 (right)

In general, soil losses are expected to decrease with scenario 2 (-21 %, see Table 2-10). Additionally, the same microbasins showing important soil losses in the baseline situation are highlighted here. These microbasins are mainly located in the upper Alamor subbasin.

In microbasins where pastures are converted into brush land and dry forest, or from corn to coffee, a decrease in soil losses is predicted. Soils in this area have a loamy clay texture, causing poor drainage potential and high soil erodibility. However, some microbasins show an increase in comparison to the baseline situation, due to the conversion of brush vegetation and dry forest into corn areas.

(ii) WaTEM/SEDEM

WaTEM/SEDEM was used to assess the effects of both land use change scenarios on erosion and sedimentation processes. The first scenario is based on the actual land use tendencies, mainly the deforestation of dry, natural and humid forests and their conversion to pasture areas and cropland. The second scenario was based on an economic and ecologic landscape value study, which represents a “Sustainable Development” since both economic and ecologic developments of the basin are considered.

WaTEM/SEDEM estimates mean annual soil loss for the baseline conditions to be $40.37 \text{ t ha}^{-1} \text{yr}^{-1}$. At microbasin scale, annual soil losses range between 1.25 and $239.29 \text{ t ha}^{-1} \text{yr}^{-1}$. If deposition processes are taken into consideration, WaTEM/SEDEM predicts the sediment yield that effectively reaches the river system. For the baseline conditions, the average sediment river export is estimated $19.20 \text{ t ha}^{-1} \text{yr}^{-1}$ for the entire study area. Values range between 0.36 and $144.83 \text{ t ha}^{-1} \text{yr}^{-1}$ at microbasin scale (see also the WP06 report).

In Table 2-11 the results of scenario modelling are compared to the baseline condition. The first scenario shows almost no changes compared to the baseline condition, whereas WaTEM/SEDEM predicts a considerable decrease of mean annual soil loss and mean annual sediment river export for the second scenario.

Table 2-11 Predicted effects of land use change on soil loss and sediment river export (WaTEM/SEDEM)

	Baseline condition (Sep '99 – Aug '00)	Scenarios			
		Scenario 1		Scenario 2	
Mean annual soil loss ($\text{t ha}^{-1} \text{yr}^{-1}$)	40.37	40.65	+ 0.7 %	32.45	- 19.6 %
Mean annual sediment river export ($\text{t ha}^{-1} \text{yr}^{-1}$)	19.20	18.85	- 1.8 %	15.13	- 21.2 %

Although in general the same microbasins are prone to water erosion (see below), both in the baseline condition and in the two future land use change scenarios, there are important change effects in the predicted absolute amounts of soil losses and sediment yields (Figure 2.54 and Figure 2.55).

Even though the predicted quantitative change effects of the first scenario on the basin scale initially were thought to be small, when looking at the spatial distribution of soil losses and sediment river

export, some microbasins show a considerable increase. These areas with large change effects are mainly microbasins with conversions from forest areas into sugarcane and other crops. The underestimated change effects of this scenario on basin scale are caused by conversions from dry forest into brush land, which cause a predicted decrease of soil loss and sediment yield due to the values of the crop factor dedicated to these land use classes. In fact, this decrease is in reality not thought to be so large.

The second scenario shows a decrease of annual soil loss and annual sediment yields in almost all the microbasins, mainly thanks to the reforestation and recultivation of bare land, brushes and pasture areas, and crop type changes. Only a few microbasins show larger soil losses, due to the intensification of agricultural activities in these areas.

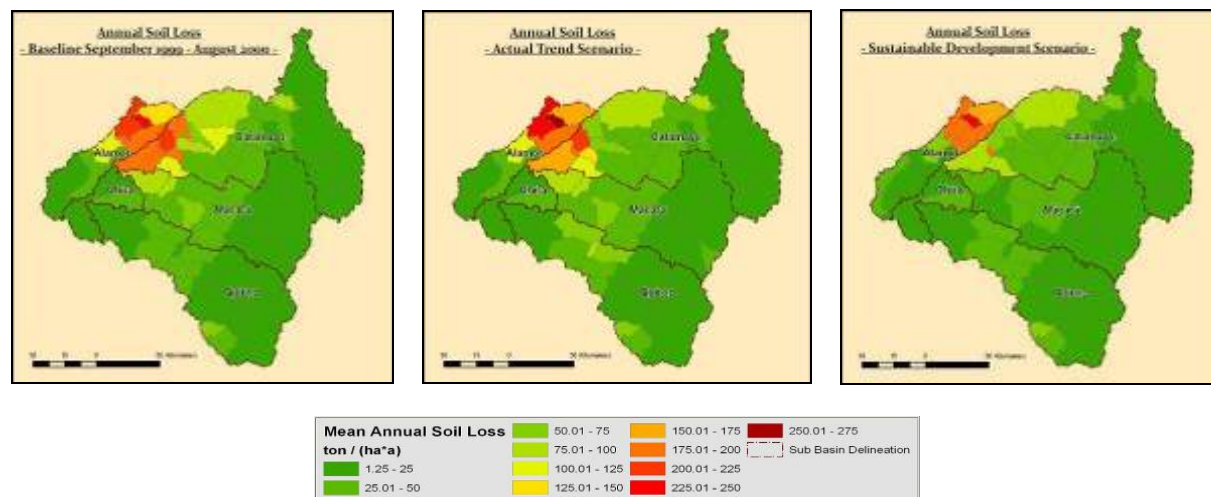


Figure 2.54 Mean annual soil loss for baseline situation (left), scenario 1 (centre) and scenario 2 (right) (WaTEM/SEDEM)

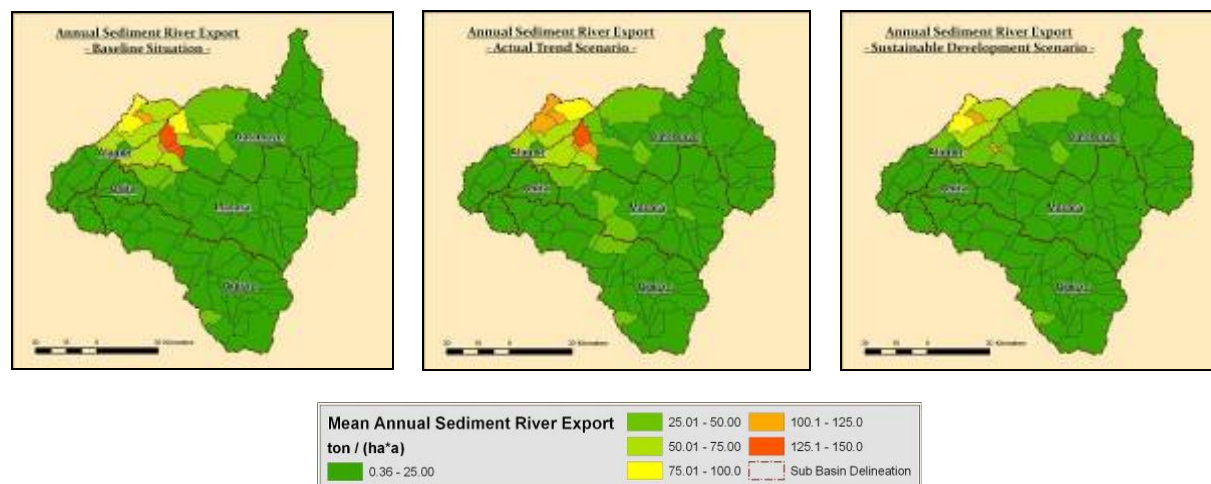


Figure 2.55 Mean annual sediment river export for baseline situation (left), scenario 1 (centre) and scenario 2 (right) (WaTEM/SEDEM)

In general, WaTEM/SEDEM predicts a small difference in spatial variation between the most affected microbasins by water erosion between the baseline conditions and the two future scenarios (Figure 2.56).

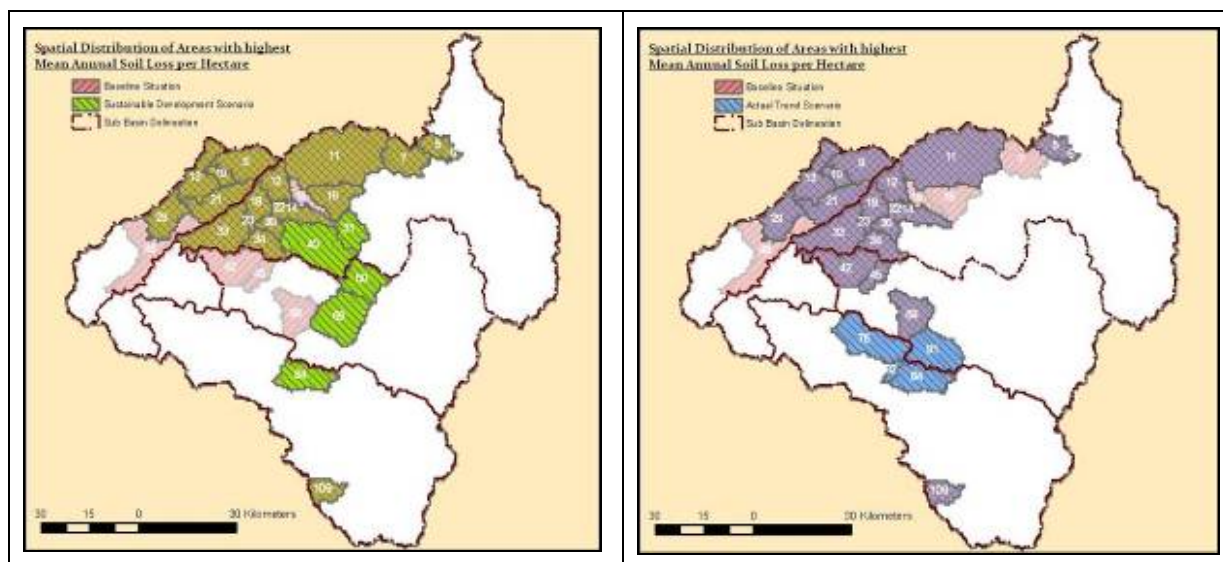


Figure 2.56 Most affected microbasins by water erosion – baseline condition compared to scenario 1 (left), baseline condition compared to scenario 2 (right) (WaTEM/SEDEM)

2.2.3.3 Combined effects

Because of limited time and resources, no assessment of combined effects was done through modelling. However, an assessment of combined effects can be preliminary formulated considering the outcomes of separate effects modelling.

A combination of the first land use change scenario (based on actual tendencies) and the A1 climate change scenario will most probably result in a slightly decreasing water yield, especially decreasing base flows. Also, an increasing sediment yield can be expected. The negative effects of the A1 climate change scenario on water yield and sediment yield might be counterbalanced by the positive effects of the second land use change scenario ('sustainable development' based on the river basin management plan). The same counts for the B2 climate change scenario. A combination of the first land use change scenario with the B2 climate change scenario will probably lead to a decrease in water yield and an increase in sediment yield.

Based on the results of separate change effects assessment, we might draw the conclusion that the second land use change scenario might possibly counterbalance the negative effects of both climate change scenarios on water yield and sediment yield.

2.2.4 Conclusions

For the Catamayo-Chira basin, the effects of two climate change scenarios, and two land use change scenarios were assessed.

To generate future climate change scenarios, two SRES scenarios were selected: the A1 and the B2 scenario (IPCC, 2000). The A1 scenario is based on very rapid economic growth, global population that peaks in mid-century and declines thereafter, and rapid introduction of new and more efficient technologies. The B2 scenario considers a future world in which the emphasis is on local solutions to economic, social, and environmental sustainability, with continuously increasing population and intermediate economic development. Both scenarios, created using MAGICC/SCENGEN, consist of a raise in temperature, and an overall decrease in precipitation, with shorter but more intense rainy seasons.

Also, two land use change scenarios were created. The first scenario is based on the actual land use tendencies, mainly the deforestation of dry, natural and humid forests and their conversion to pasture areas and cropland. The second scenario was based on an economic and ecologic landscape value study, which represents a "Sustainable Development" since both economic and ecologic developments of the basin are considered.

The SWAT model was used to assess the effects of land use change and climate change on water discharges. In both land use change scenarios, an overall increase in water discharge is expected. However, the first scenario would result in a decrease of the base flow and an increase of discharge during the rainy season. This could raise the risks of flooding. The second scenario shows a more equilibrated increase of water discharge, both during the rainy season and during the dry season. The reduction of drought during the dry months would be a very positive development. Basically the same microbasins, mainly located in the centre of the basin, remain the ones with highest water yields in both scenarios. In contrast, the effects of both climate change scenarios consist of a decrease of water yield. Decreases are more pronounced in the B2 scenario.

Both the SWAT model and WaTEM/SEDEM were used to assess the effects of changes on soil losses and sediment production. Both models show comparable results. The first land use change scenario would result in a slight increase of sediment yield; while the second (sustainable development) land use change scenario would lead to a decrease of soil losses around 20 %. This reduction of soil losses in the Catamayo-Chira basin would be very important, since the use of the Poechos reservoir will be limited due to siltation. The spatial distribution of microbasins with largest erosion problems remains more or less the same in both scenarios, compared to the baseline situation. For both climate change scenarios, small reductions of soil loss rates were predicted. Nevertheless, these results are not reliable, since the impact of an increase in rainfall intensities could be modelled neither by SWAT nor by WaTEM/SEDEM, while heavy precipitation ‘very likely’ will become more frequent in the 21st century (IPCC, 2007).

In any case, the results of this scenario impact assessment need to be analysed with caution. Especially the uncertainty of the assessment of the impact of climate change is high. First, the simulations of MAGICC/SCENGEN refer to 1990 as the baseline year. This year was one of the driest of the last 30 years. Second, the same climate change factors for temperature and rainfall were applied for the whole basin, without differentiation between lower and upper part of the basin. Third, we have no estimations on future frequency or intensity of ENSO events. These events cause special concern in the Catamayo-Chira basin, where extremely high soil losses were registered during the last ENSO events.

The application of both SWAT and WaTEM/SEDEM also is a source of uncertainty, since the coarse resolution of baseline data affected the calibration and validation process of both models. In the reports of Work Package 3 (Hydrological Modelling) and Work Package 6 (Pollution Pressure and Impact Assessment) these uncertainties are addressed in more detail.

Future investigation should now be focussed on the areas identified as predominantly affected by soil losses and mostly important in terms of water production. Mitigation and protection measures should be formulated and implemented in these areas.

2.3 CAUCA RIVER BASIN

2.3.1 Introduction

The Cauca River basin is the second most important river basin in Colombia with a length of 1,204 km. and 59,074 km² of drainage basin. More than 16 million persons live in this basin, representing 25 % of Colombian inhabitants. The Cauca River goes through the Departments of Cauca, Valle del Cauca, Quindío, Risaralda, Caldas, Antioquia, Córdoba, Sucre and Bolívar.

The Upper Cauca River basin extends from the Salvajina Dam, in Cauca, until the municipality of La Virginia, in Risaralda. One of the main environmental authorities in the Upper Cauca is the “Corporación Autónoma Regional del Valle del Cauca” (CVC), which works on the integrated management and information of water bodies in its jurisdiction area.

This area has important human settlements and important industries located in the western part of Colombia, such as paper and food products manufacturing, the sugar cane agro-industry and coffee growing in the foothills of the basin.

In the development of Work Package 8 on the Global Changes effects, a methodology application is made at the Tuluá River pilot basin due to lack of information required for the analysis and study of variables in the work package in the Upper Cauca Basin. There are important data limitations for example in soil use coverage and socio-economic data.

The study mentioned in the present report corresponds to the climatic variables, specifically rainfall, and includes soil use and socio-economic variables of the basin.

2.3.1.1 General basin characteristics

The Upper Cauca River basin is located in the south-western part of Colombia. The Cauca River flows 445 km in its geographic valley and descends from an altitude of 1,000 m a.s.l., down to 900 m a.s.l. This section of the river has an average width of 105 meters ranging from 80 meters in the upper part of the basin (Salvajina – La Balsa) to 150 meters in the lower area (Anacaro – La Virginia). The full river depth may range from 3.5 to 8 meters.

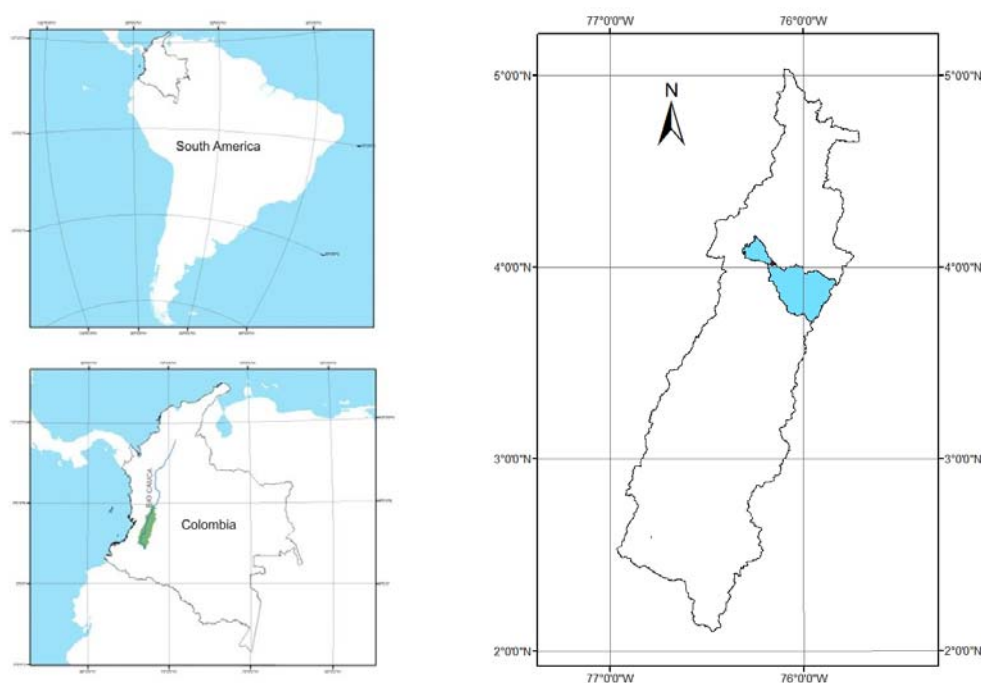


Figure 2.57 Location of the Tuluá river basin, pilot basin for WP 8

The Tuluá River basin, where Work Package 8 was developed, is located in the right margin of the central zone of the Upper Cauca River basin, as illustrated in Figure 2.57. The northern limit of the basin comprises the Morales and Bugalagrande River basins. The east border is the Department of Tolima, the south borders the Amaime, Guabas, Guadalajara and San Pedro river basins, and the western border is the Cauca River basin.

2.3.2 Scenario creation

Analysis of climatic and socio-economic factors to evaluate water supply and demand in the Tuluá River pilot basin are associated with climate change prediction backed up by global scale change models, and with the evolution of land use, agricultural, animal husbandry and industrial activities, as well as population growth in the studied area. These are the important factors having an impact on water resource supply in the zone. The study is developed taking into consideration information available on the different environmental variable forecasts. These are later jointly analyzed through an actual or baseline water demand and supply balance and considering a future plan for 2020 and 2050.

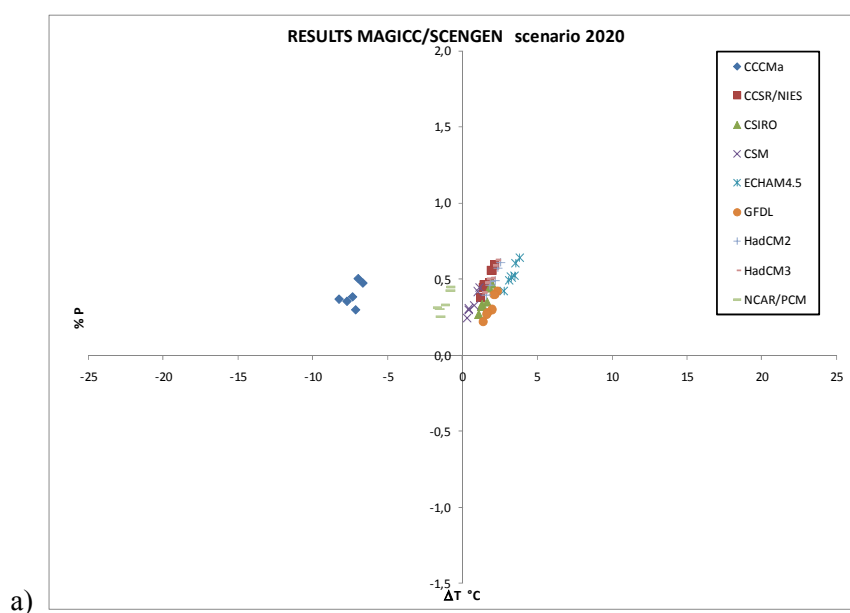
A joint study held between CVC and “Universidad del Valle” (Inter-Administrative Agreement 110 of 2007) for the socio-economic and soil use change variable planning was used in the vulnerability assessment (CVC and Universidad del Valle, 2007).

2.3.2.1 Climate change

Climatic change is reflected in the basin in terms of water resources supply analyzed with the MAGICC/SCENGEN model results and basin observations according to historic rainfall data registered for the last 30 years in the different river basin stations.

Figure 2.58 shows the results of the MAGICC/SCENGEN v 4.3 model application (see Annex 1). Results of runs made for future scenarios applying MAGICC/SCENGEN used the 1990 global temperature and rainfall data as reference and proposed future climatic scenarios for 2020 and 2050. All cases show a wider range of rainfall increase directly proportional to time. The analyzed grid corresponds to the area located at (0 to 5°) latitude and (-75 to -80°) longitude, where the Upper Cauca River basin is located.

All scenarios present a temperature increase ranging from 0.2 – 0.6 °C and 0.8 – 1.5 °C for 2020 and 2050, respectively. Also, most cases show an increase in rainfall, except for the GCMs CCCMa and NCAR/PCM. When we exclude these GCMs, the basin shows rainfall increases between 0 – 4% and 0 – 10% for years 2020 and 2050, respectively.



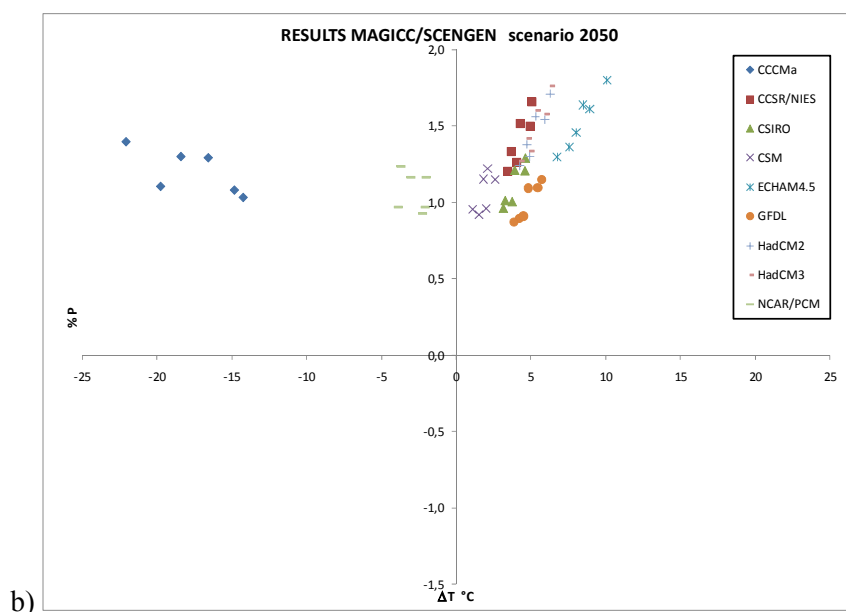


Figure 2.58 Results of MAGICC/SCENGEN: (a) 2020 and (b) 2050

2.3.2.2 Land use change

Changes in the land use are relevant bio-physical and socio-economic factors that determine water resources and soil demand in the river basin. One of the main activities demanding soil resources in the basin is industrial agriculture, such as sugar cane plantations. There are other crops found in a large area of the study zone.

The main crops were identified for this study and forecasts were made for the area covered in the Tuluá River basin. A digital map dated 1996 and 2006 exists for this basin (Gobernación del Valle del Cauca, 1996-2006; Gobernación del Valle del Cauca, 2006-2007). Crops, which represent 98.4% of the agricultural area in 2006 include: sugar cane, potato, corn, sorghum, coffee and soy bean.

Two procedures were used in creating the land use change scenarios: (1) the implementation of a statistical model that allows estimating change patterns in the variable according to recorded historic data, and (2) a model which determines maximum areas per crop, according to environmental conditions such as altitude, temperature, soil type and precipitation. Both models were combined to create a land use change scenario for 2020, the critical condition being the largest area resulting from the two procedures.

This methodology was adopted because different land use maps which would allow direct land use change modelling were not available. Likewise, it was not possible to determine an expert panel to facilitate understanding the different points of view of the basin inhabitants in order to construct scenarios. Historical census data were consulted, and information was analysed using GIS.

Annual census data was analysed for the period 1988-2007, containing area information by crop, using ARIMA lineal and robust regressions, which highlight atypical points in the registers, in order to determine its behaviour compared to land use maps of 1996 and 2006 (Box and Jenkins, 1976). As a result, the censused areas within each crop of the basin were determined and helped determine the crop areas by municipality of the basin in the 2020 plan.

The Law of Limiting Factors was established as a modification to the Law of the Minimum (Dent and Young, 1981), which states that the distribution of a certain crop is controlled by environmental factors for which the crop has its own adaptation range, or a closer control, depending of the technology used. Therefore, limits and possible expansion areas for agricultural land use for 2006 and 2020 were based on temperature, precipitation, altitude, and soils (Figure 2.59).

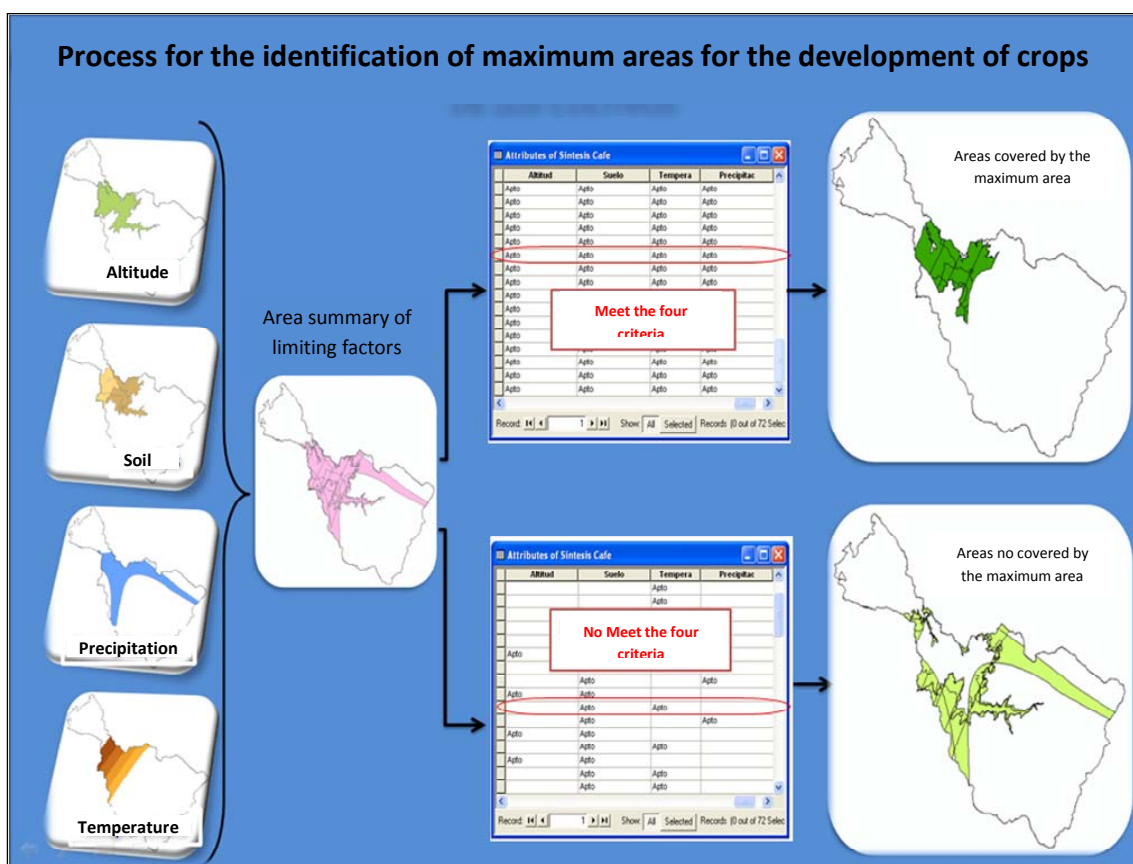


Figure 2.59 Identification of maximum areas for land use change scenario creation

Finally, a cross-section of the projected areas in the two previous stages was made. When the projected area for a crop, according to census registers was larger than the area estimated by the limiting factors, this was used for the 2020 land use scenario (Table 2-12).

The year 2006 was used as the baseline situation, since this was the most recently updated cartography available.

Table 2-12 Use of land for agriculture in 2006 and 2020

Crop	Area 2006 [ha]	Area 2020 [ha]	% change	% of cultivated area (2020)
Sugar cane	8.591	10.352	20,5%	25%
Sorghum	491	296	-39,7%	1%
Soy bean	81	0	-100,0%	0%
Corn (flat land)	745	1227	64,7%	3%
Coffee	977	986	0,9%	2%
Native grass	36.984	26.819	-27,4%	66%
Feeding grass	462	12	-97,5%	0%
Potato	4.159	1.194	-71,2%	3%
Total	52.491	40.886	-22,1%	100%

The analysis shows that area designated for agriculture tends to decrease in the future. Sugar cane will be the most important crop in the agricultural area of the basin, representing 25% of the total area. The native grass figure was estimated in order to associate it with extended livestock breeding in the basin and establishing bovine demand for 2020. Therefore, the estimated area is representative, covering 66% of the total projected area. Coffee plantations also show a growing trend towards 2020. This crop is located in the most vulnerable area associated with climate change and variability. This is an

important factor to be considered in future studies in order to estimate local impact on coffee production systems. Census registration of potato crops was a projected area of 63 ha, while land use cartography shows an area of 4,159 ha. The average of these areas was used, considering that the census area has a decreasing trend and affected the cartography area in 2006. As a result of this, it is of vital importance to confirm the 2006 data. Figure 2.60 shows the productive systems and the maximum areas according to environmental limiting factors. Changes are mainly noticed for coffee and potato. Although native grass occupies the largest area in the basin, it is expected to experience no noticeable change.

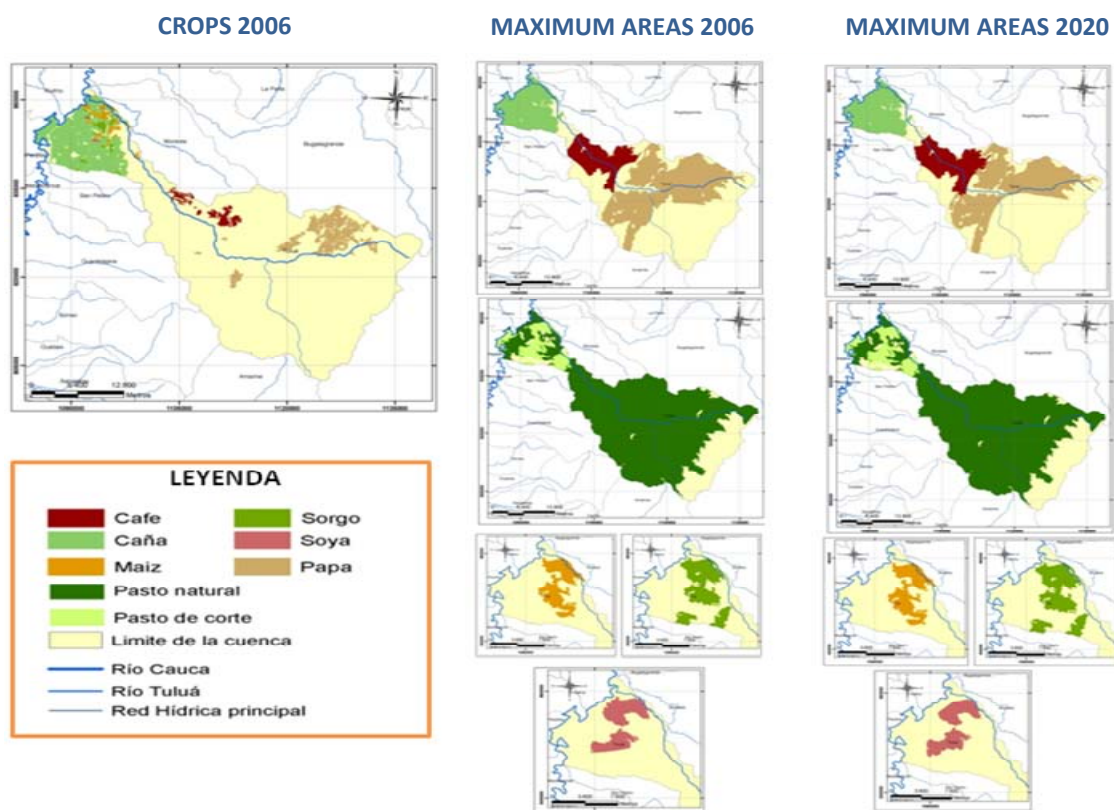


Figure 2.60 Productive systems and maximum productive areas according to limiting factors (2006 and 2020)

The projected changes in agricultural land are used to predict agricultural water demands. Additionally, the effect of de/afforestation is evaluated. Therefore, scenarios were created through expert judgment. In the baseline situation (scenario 1) 35 % of the basin is covered by forest. A second scenario includes afforestation (40 % forest coverage), and a third scenario considers deforestation (25 % forest coverage).

2.3.2.3 Changes in water demands

Environmental and socio-economic factors determining water demand in the Tuluá River basin are linked to land use, agricultural, animal husbandry and industrial activities and to population growth. Historical information was collected from the census in order to understand how pressure is generated on the water resource supply in the study zone.

The water demand for each of the socio-economic factors identified (agricultural, industrial, bovine and domestic use) in the Tuluá River Basin was estimated in order to study the combined effects of socio-economic factors. The environmental demand (ecologic floor) was also calculated in order to present a more comprehensive summary of the water resource demand factors and to integrate them into an offer-demand analysis. Following are the results for each demand, using as a basic reference for this analysis the methodological analysis of CVC (2000), in which the Tuluá river basin is divided into two areas : Production and Consumption (Figure 2.61).

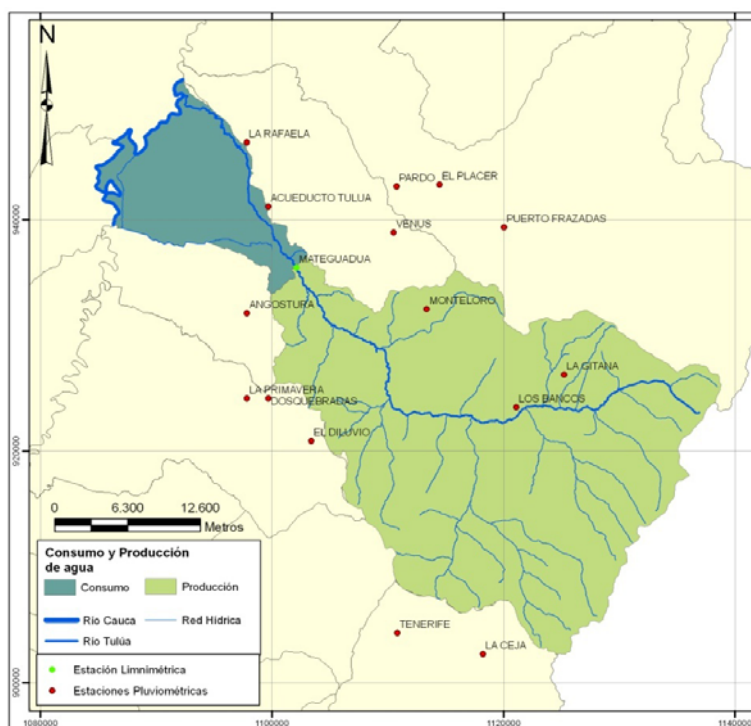


Figure 2.61 Production and consumption and hydrologic stations in the Tuluá river basin

A Population growth

Population projection was done based on 1985, 1993 and 2006¹ census data for the headwaters and rural population in each of the four municipalities (political-administrative divisions) located in the Tuluá river basin. Based on the population data per municipality and information on territorial extension of the municipalities, population density was estimated. Population density data was then applied to the municipal zone of the basin in order to assign rural densities when the municipality zone of the basin corresponded to this category in the political and administrative division. This also allowed to estimate the basin population by adding the four municipalities' data and its corresponding projection based on the censal rate of the model developed by CVC (1995):

$$r_i = \frac{\ln(P_{fi}) - \ln(P_{ii})}{t}$$

Where: r_i :Municipal area censal growth rate

P_f : Final population in municipality

P_i : Initial population in municipality

t : Period

i : Municipality: Buga, El cerrito, San Pedro, Tuluá

The period of time was calculated in a year scale according to the following equation:

$$t = \frac{C_f - C_i}{365}$$

Where: C_f : Date with days, month and year of the final census

C_i : Date with days, month and year of the initial census

¹ Source: National Statistics Department - DANE

Once the inter-census data was calculated, the municipal population annual growth was estimated:

$$P_{f_i} = P_{i_i} \cdot x \cdot e^{rt}$$

Where: P_i : Initial population in the urban area
 P_f : Urban population of the year to be planned
 r : Inter-census growth rate
 t : Projection time, in years

The rural population of the basin was projected for the same period of time. Table 2-13 shows the projection, with a total increase of 5,970 inhabitants in the rural area of the Tuluá River Basin. Data shows a larger population density in San Pedro and a larger amount of inhabitants in Tuluá.

Table 2-13 Actual and projected rural population in the Tuluá river basin

Municipality	Rural Population		Average Census Population Density	Basin Population	
	2008	2020		2008	2020
Buga	16,013	23,751	0.20	8,700	12,904
Cerrito	22,047	16,354	0.39	2,742	2,034
San Pedro	10,008	12,476	0.49	3,214	4,006
Tuluá	26,981	31,103	0.28	11,009	12,691
<i>Total</i>	<i>75,049</i>	<i>83,684</i>		<i>25,665</i>	<i>31,635</i>

Estimated domestic water demand for 2020 is shown in Table 2-14. The water demand was estimated according to population projection in the river basin municipalities². A water consumption reference figure simulating a high demand scenario was used, considering daily water consumption per person of 250 liters.

Table 2-14 Projected rural and urban domestic water demands in the Tuluá river basin (2020)

Municipality	Population	Demand	Demand	Demand	Demand
	2020	l/day	l/s	m ³ /s	mm/month
Rural	31,635	7,908,750	91.5	0.092	0.026
Buga	12,904	3,226,000	37.3	0.037	0.011
El Cerrito	2,034	508,500	5.9	0.006	0.002
San Pedro	4,006	1,001,500	11.6	0.012	0.003
Tuluá	12,691	3,172,750	36.7	0.037	0.010
Municipal Head					
Tuluá Aqueduct	193,122		700.0	0.700	0.199
<i>Total Domestic Demand</i>			<i>791.5</i>	<i>0.883</i>	<i>0.251</i>

This indicates that the monthly domestic consumption in 2020 will be 0.24 mm month⁻¹, or 2.9 mm yr⁻¹. Tuluá consumption will represent 90 % of the total. At the rural level, the municipality of Tuluá is the most populated one. Therefore, the rural demand percentage of Tuluá in 2020 is projected to be 45 % of the rural demand.

² Water demand in the municipality of Tuluá is provided in Regulatory Resolution No. No.SGA.006 dated January 17, 2003, assigning a volume of 700 l/s, valid for 2020.

At the moment, the Tuluá basin has an estimated population of 193,000 inhabitants and a demand of 0.22 mm/month. A 16 % population increase (31,757 inhabitants) and a 14 % domestic requirement increase equivalent to 17 l/s in domestic requirements are projected for 2020.

B Bovine water demand

A 1996-2006 bovine inventory was made in the municipalities in the Tuluá River basin, based on information collected from surveys made by UMATA (Gobernación del Valle del Cauca, 1996-2006). Results in Table 2-15 show milk production has the highest water consumption, with 60 % of the total consumption. Water consumption is estimated to increase from 2008 to 2020 by 8 %, or 7,000 l/day.

Table 2-15 Inventory and 2020 estimate of bovine water demand in the Tuluá river basin

year	Meat		Dairy Products		Double Purpose		Total consumption (l/day)
	Amount	Consumption (l/day)	Amount	Consumption (l/day)	Amount	Consumption	
1996	7332	21263	12591	50366	1184	7576	79205
1997	6820	19777	12429	49716	2528	16180	85673
1998	5782	16768	16490	65958	1140	7295	90021
1999	5878	17047	17130	68521	1204	7705	93273
2000	7657	22206	11787	47148	5216	33385	102738
2001	8381	24304	10420	41681	2811	17988	83973
2002	8084	23442	18327	73307	1895	12126	108875
2003	8385	24315	10613	42453	2393	15313	82081
2004	8856	25681	10880	43520	1655	10591	79792
2005	9993	28981	11444	45774	1756	11237	85992
2006	9796	28408	11917	47668	1811	11593	87669
<i>2020 estimate</i>							961991

C Agricultural water demand

Agricultural demand estimate is shown in Figure UC 2.6. Results show native grasses (associated to extended livestock breeding) and sugar cane are the productive systems that will have a larger coverage of the basin area, representing as well the highest estimated agricultural demand.

It can also be noticed that the month October shows the highest demand due to the higher evaporation. Agricultural demand in the consumption area represents 70.5 % of the total, with sugar cane being the most representative crop. Natural grass shows the highest water demand in the future. The 2020 total estimated agricultural demand of the basin is 1,358 mm.

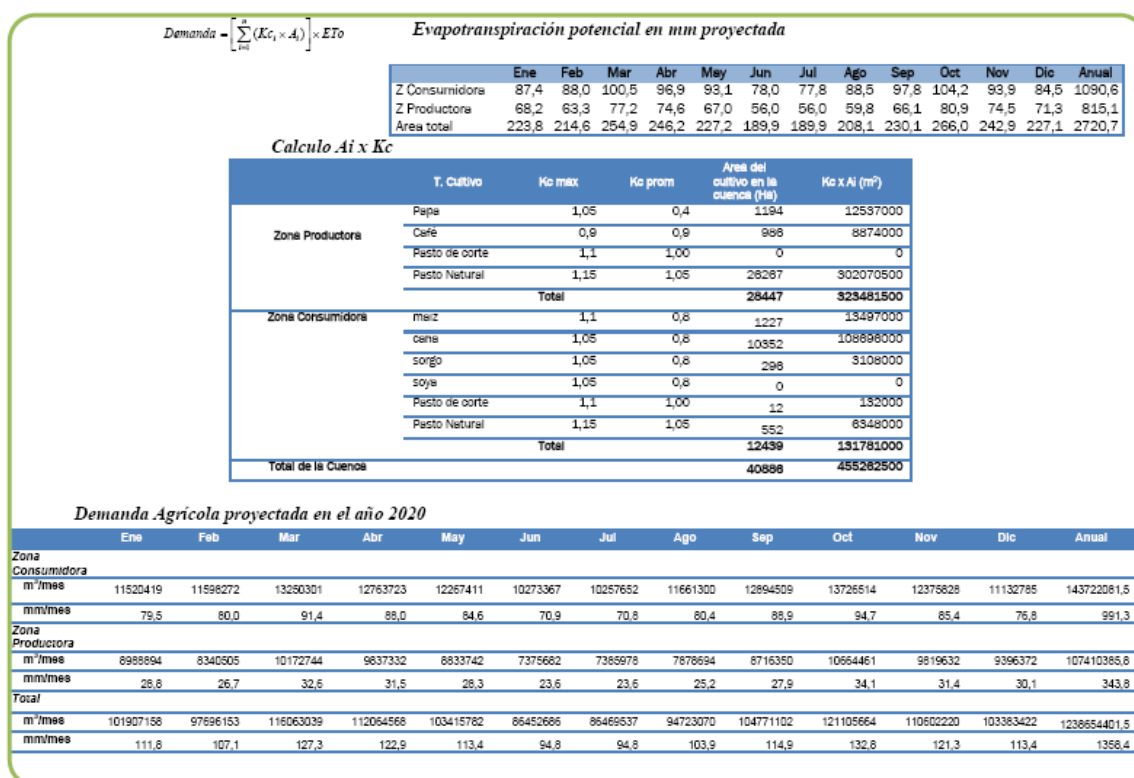


Figure 2.62 Projected agricultural water demands in the Tuluá river basin (2020)

D Industrial water demand

Table 2-16 shows the 2020 estimated industrial water demand based on consumption data by each of the industries in the area. It is important to have detailed information about the location of the industries, water consumption, discharges, etc. Since this information is not available in many cases, as it occurs for the Tuluá River Basin, CVC has worked based on studies made (INCOL S.A. et al., 1993), considering that the industrial water demand is 8 % of the agricultural water demand, both for the supply as well as the consumption in the basin. The production zone was considered in the industrial demand calculation since supply systems for coffee, potato and animal husbandry in the basin also contribute to the industrial demand for water in the basin.

Table 2-16 Projected industrial water demands in the Tuluá river basin (2020)

	Jan	Feb	Mar	Apr	May	Jun	Jul	Aug	Sep	Oct	Nov	Dec	Annual
Consumption zone	6.4	6.4	7.3	7.0	6.8	5.7	5.7	6.4	7.1	7.6	6.8	6.1	79.3
Production zone	2.3	2.1	2.6	2.5	2.3	1.9	1.9	2.0	2.2	2.7	2.5	2.4	27.5
Total	8.7	8.5	9.9	9.6	9.0	7.6	7.6	8.5	9.3	10.3	9.3	8.5	106.8

Results show a total demand of 106.8 mm per year, with October and March having the highest water demand. The average future industrial demand is estimated at 8.9 mm/month.

2.3.3 Scenario impact assessment

2.3.3.1 Methods used for impact assessment

Scenario impact assessment was made estimating a water balance for 2020.

The calibrated HBV hydrologic model (see the WP 2 report) was used to evaluate water supply in 2020, using the MAGICC/SCENGEN model output. Input data series of the HBV model were altered and the water flow for the analysis of the water balance in the future scenario was generated.

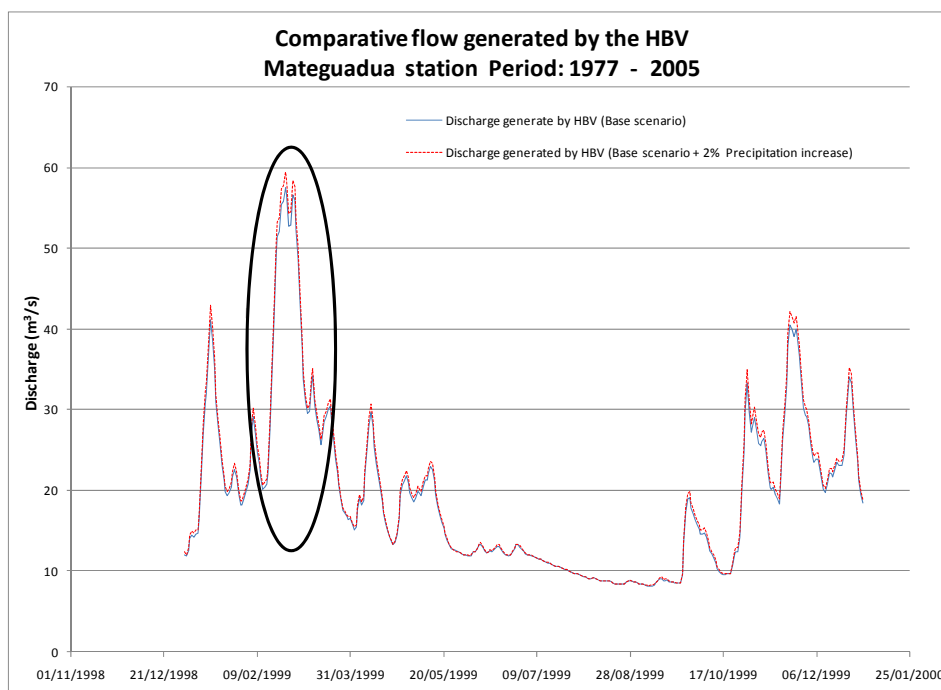
This study did not include an analysis of future diffuse source contamination impact (see erosion modelling in WP 6 with WaTEM/SEDEM), due to lack of information for the Tuluá River basin. However, the results presented in WP 6 in the neighbouring Bugalagrande river pilot basin could be interpreted in the same manner for the Tuluá River basin, considering their similarity in terms of topography, morphology, hydrology, etc. The implementation of this erosion model, complying with all requirements required for good calibration, would have allowed calculation of the direct incidence of soil loss and the effects of change related to agricultural and animal husbandry activities. Evaluation of erosion and the related problems causing soil resource deterioration in the future will allow the identification of sensitivity to change relevant to this aspect within the basin.

2.3.3.2 Separate effects

Projected changes are analyzed separately in each of the studied components: the change in the water supply characterized in the precipitation and water flow of the basin, as well as the water demand related to land use and population changes.

A Climate change

According to the results of the MAGICC/SCENGEN climatic change model, precipitation historic series were modified, and the HBV previously calibrated hydrologic model was used as described in the WP 3 report. The model was run using estimated rainfall changes, and the flow series were obtained. This allowed determining flow changes in the Mateguadua station at the Tuluá basin, according to 2020 estimated climatic changes. Figure 2.63 shows a 3 % increase in flows, considering a 2 % precipitation increase at the study basin. Impact of increased precipitation is expected to be larger on high flows than on low flows.



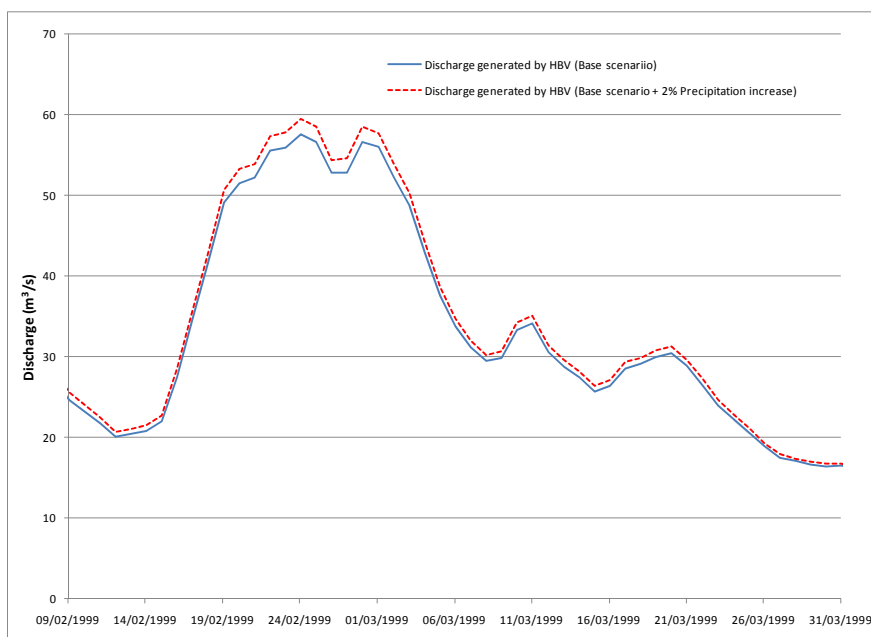


Figure 2.63 Predicted effects of climate change on discharge

B Land use change

A sensitivity analysis of the HBV model was made for the flow generation, modifying land use according to three scenarios, considering changes in forest coverage percentage in the basin (25 % - 35 % and 40 % forest coverage).

Figure 2.64 shows HBV model runs for the analysis of sensitivity to de/afforestation. Water flow generated at the Mateguadua station does not show sensitivity in the model considering changes in forest coverage.

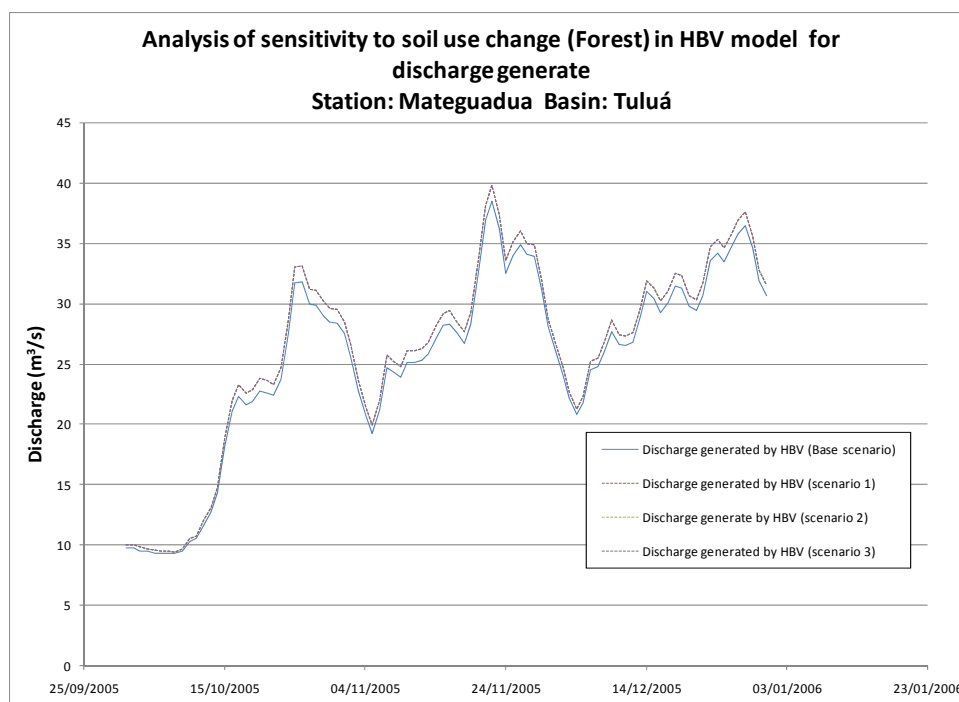


Figure 2.64 Predicted effects of de/afforestation in the Tuluá river basin

C Changes in water demand

Agricultural Demand

Agriculture is one of the main activities having an impact over the basin. Therefore, it is of crucial importance to analyse the effects of changes in the agricultural demand. Average monthly precipitation and the agricultural demand for 2006 and 2020 are shown in Table UC 3.2 and figure UC 3.3.

Table 2-17 Water balance in 2006 and 2020 considering agricultural demands in the Tuluá river basin

	Jan	Feb	Mar	Apr	May	Jun	Jul	Aug	Sep	Oct	Nov	Dec	Annual
2006													
<i>Consumption zone</i>													
Precipitation	84.0	93.5	141.0	163.9	136.4	76.1	56.4	55.8	108.8	173.6	147.9	97.2	1334.5
Demand	79.3	76.5	82.3	70.9	67.6	64.9	75.4	82.1	78.0	71.1	65.8	69.8	883.7
Balance1	4.7	17.1	58.7	93.0	68.8	11.2	-19.0	-26.3	30.7	102.5	82.1	27.3	450.8
<i>Production zone</i>													
Precipitation	113.6	112.5	163.7	196.0	155.7	85.7	60.0	64.2	109.7	214.1	201.3	142.0	1618.5
Demand	36.9	32.2	35.5	29.9	30.6	30.8	35.9	37.6	34.3	31.7	28.6	32.8	396.7
Balance1	76.7	80.3	128.2	166.1	125.1	54.9	24.1	26.6	75.3	182.5	172.7	109.2	1221.7
2020													
<i>Consumption zone</i>													
Precipitation	93.9	92.6	142.2	148.0	123.7	81.6	68.7	64.6	115.2	147.2	147.4	96.3	1321.4
Demand	79.5	80.0	91.4	88.0	84.6	70.9	70.8	80.4	88.9	94.7	85.4	76.8	991.3
Balance1	14.4	12.6	50.8	60.0	39.1	10.7	-2.1	-15.8	26.3	52.5	62.0	19.5	330.0
<i>Production zone</i>													
Precipitation	128.3	119.7	166.3	192.9	151.6	99.1	72.7	72.5	116.1	203.6	201.4	144.8	1668.8
Demand	28.8	26.7	32.6	31.5	28.3	23.6	23.6	25.2	27.9	34.1	31.4	30.1	343.8
Balance1	99.5	93.0	133.7	161.4	123.3	75.5	49.1	47.2	88.2	169.4	170.0	114.7	1325.0

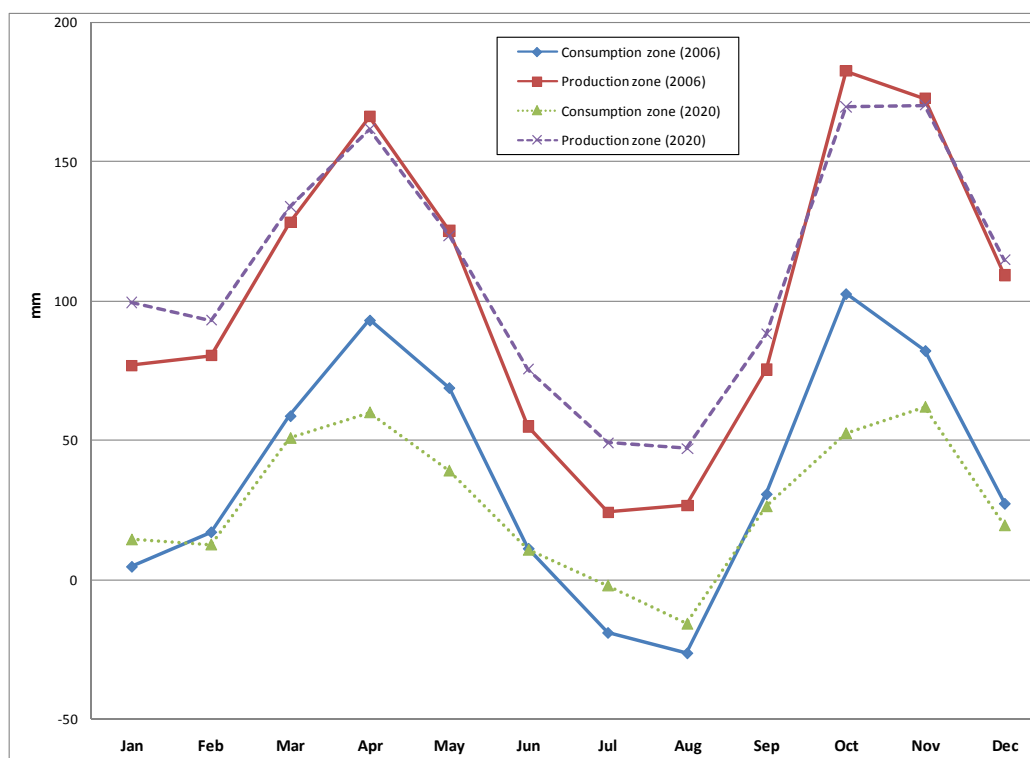


Figure 2.65 Water balance in 2006 and 2020 considering agricultural demands in the Tuluá river basin

In the production zone, water availability in 2020 will be 8 % higher than in 2006. This is a consequence of the reduction of agricultural demand caused by the reduction of area covered by crops and an increase of precipitation by 3 %. The water balance is especially higher in the dryer months (Jan-Feb and Jun-Sep).

In the consumption zone, on the other hand, water availability is estimated to be reduced by 27 %. The reduction can above all be noticed in the wetter months (Mar-May and Oct-Nov). The dry season (Jul-Aug), in contrast, shows higher water availability. Water availability seems to be better spread out over the year.

2.3.3.3 Combined effects

According to the precipitation-agricultural demand balance, the net basin water demand is shown in Table 2-18. The ecological flow is included in the water demand, with an estimated value corresponding to 10% of the multiannual monthly average registered at the Mateguadua station. The agricultural demand was estimated using a 1/0.33 factor resulting from the fact that sugar cane is the crop with the largest extension, and its irrigation is mainly done by gravity. The project efficiency was estimated 33 %, corresponding to a gravity irrigation system, which includes conduction, distribution and application efficiencies. The highest demands occur during the dry season, in July and August, both in 2006 and 2020, showing water deficits.

Table 2-18 Actual and predicted water demand associated to socio-economic factors

	Jan	Feb	Mar	Apr	May	Jun	Jul	Aug	Sep	Oct	Nov	Dec	Annual
2006													
Agricultural	0.0	0.0	0.0	0.0	0.0	0.0	57.4	79.6	0.0	0.0	0.0	0.0	137.1
Bovine	0.1	0.1	0.1	0.1	0.1	0.1	0.1	0.1	0.1	0.1	0.1	0.1	0.9
Domestic	0.2	0.2	0.2	0.2	0.2	0.2	0.2	0.2	0.2	0.2	0.2	0.2	2.6
Industrial	9.3	8.7	9.4	8.1	7.9	7.7	8.9	9.6	9.0	8.2	7.5	8.2	102.4
Environmental	4.2	3.7	3.9	4.7	4.4	3.4	2.7	2.3	2.1	3.1	5.1	4.6	44.3
<i>Net</i>	<i>13.7</i>	<i>12.7</i>	<i>13.6</i>	<i>13.1</i>	<i>12.5</i>	<i>11.4</i>	<i>69.4</i>	<i>91.8</i>	<i>11.4</i>	<i>11.6</i>	<i>13.0</i>	<i>13.1</i>	<i>287.3</i>
2020													
Agricultural	0.0	0.0	0.0	0.0	0.0	0.0	6.4	48.0	0.0	0.0	0.0	0.0	54.4
Bovine	0.1	0.1	0.1	0.1	0.1	0.1	0.1	0.1	0.1	0.1	0.1	0.1	1.3
Domestic	0.2	0.2	0.2	0.2	0.2	0.2	0.2	0.2	0.2	0.2	0.2	0.2	2.9
Industrial	8.7	8.5	9.9	9.6	9.0	7.6	7.6	8.5	9.3	10.3	9.3	8.5	106.8
Environmental	4.3	3.8	4.0	4.9	4.5	3.5	2.8	2.4	2.2	3.2	5.4	4.8	45.7
<i>Net</i>	<i>13.3</i>	<i>12.7</i>	<i>14.3</i>	<i>14.8</i>	<i>13.9</i>	<i>11.4</i>	<i>17.0</i>	<i>59.2</i>	<i>11.9</i>	<i>13.8</i>	<i>15.0</i>	<i>13.7</i>	<i>211.1</i>

An estimated net demand of 211 mm is estimated for 2020. August shows the highest water demand (59.2 mm) in the year. Water demand in 2020 is 27 % less than the demand of 2006, mainly due to the decrease in agricultural demand. The highest percentage increases in water demand are expected in the bovine sector (50 %).

At inter-annual level the greatest water demand increases (approximately 20%) are projected for October and November, being mainly affected by greater demand in the industrial sector. In general, the domestic, industrial and environmental demand for 2020 is expected to increase 10 %, 4 % and 3 %, respectively.

Consequently, an offer-demand water balance was analysed (Table 2-19 and Figure 2.66).

Table 2-19 Actual and predicted water balance in the Tuluá river basin

	Jan	Feb	Mar	Abr	May	Jun	Jul	Aug	Sep	Oct	Nov	Dec	Annual
2006													
Surface water offer	15	13	14	17	15	12	10	8	7	11	18	16	156
Ground water offer	36	36	36	36	36	36	36	36	36	36	36	36	432
Total Offer	51	49	50	53	51	48	46	44	43	47	54	52	588
Net Demand	14	13	14	13	13	11	69	92	11	12	13	13	288
Net Balance - mm/month	37	36	36	40	39	37	-24	-48	32	35	41	39	301
2020													
Surface water offer	15	13	14	17	16	12	10	8	8	11	19	17	160
Ground water offer	36	36	36	36	36	36	36	36	36	36	36	36	432
Total Offer	51	49	50	53	52	48	46	44	44	47	55	53	592
Net Demand	13	13	14	15	14	11	17	59	12	14	15	14	211
Net Balance - mm/month	38	36	36	38	38	37	29	-15	32	33	40	39	381

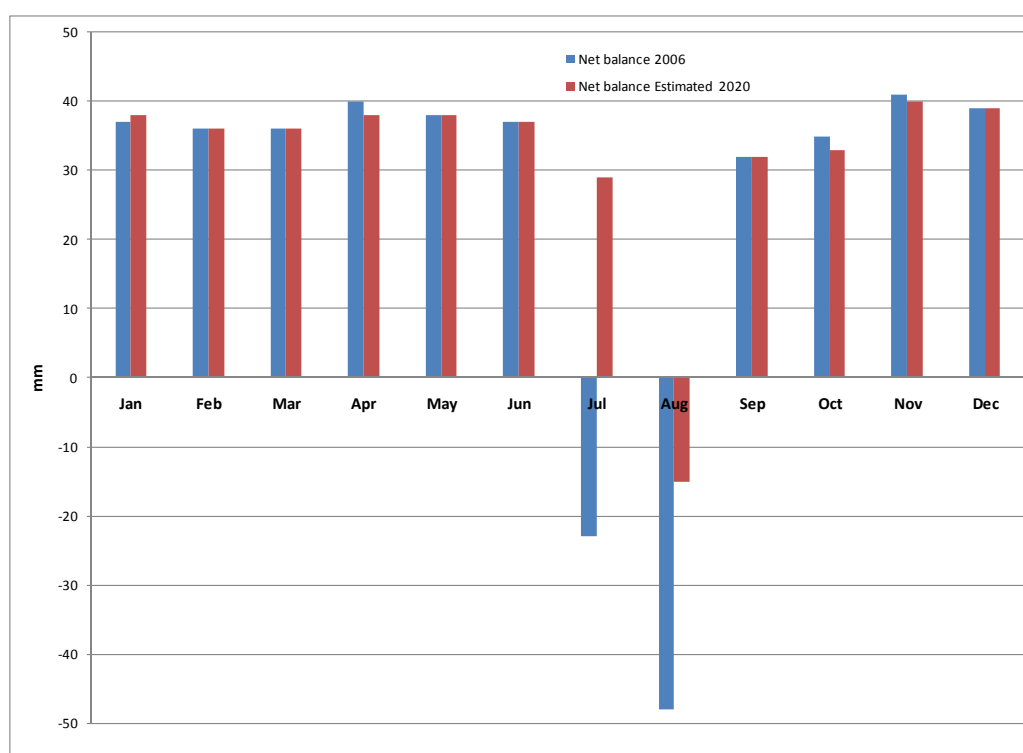


Figure 2.66 Actual and predicted water balance in the Tuluá river basin

Results of the predicted water balance in the Tuluá river basin show an increase of the net yearly availability to 382 mm in 2020, compared to an actual availability of 301 mm. The month of August is the only month with a -15 mm deficit. In the actual situation, two months show an important negative balance (July and August). Compared to 2006, net water availability is expected to increase with 27 %, mainly as a result of the reduction of agricultural practices and an expected increase of rainfall. However, a small reduction in water resources is expected during the months of January, February and June.

2.3.4 Vulnerability assessment

According to the results shown in the scenario impact assessment, the Tuluá river basin is not expected to experience important damages from future climate change, land use change and changes in water demand. From these results we might therefore conclude the basin is not very vulnerable to change, considering the future scenarios evaluated in this study. The Tuluá basin is representative of

the Upper Cauca Basin study area. The analysis seems to demonstrate that different water dependent stakeholders will not suffer larger deficits in the future compared to the actual situation.

One of the main stakeholders having an impact on land use due to the demand of raw material production for the manufacturing of bio-diesel is the sugar cane producing sector. This sector is presently adapting new technologies to reduce the use of irrigation water, using more efficient irrigation systems such as aspersion irrigation, precision agriculture systems and irrigation by windows.

In general terms, the productive sector activities create a basin not very sensitive to change. However, it would be interesting to study other factors experiencing change, such as the ecological factors, that also depend on the water supply and demand in the basin, and that may be much more sensitive to – for example – climate change. More specific research is required on the impact of climate change on forest and moorland vegetation, which may have a significant impact on the still unknown water resources conservation and the biodiversity of the basin.

2.3.5 Summary

Climate change results for the pilot basin are expected to cause higher discharges that can be replicated in the Upper Cauca River Basin and in general, in the entire south-western zone of Colombia, according to global scale models. Climate change impact assessment resulted in larger water availability at the Mateguadua station in the Tuluá pilot basin, as was shown by data obtained using the model calibrated in the context of Work Package 3. However, these results should be interpreted with certain care, since the input of the hydrologic model was created by using the future climate change scenarios of the MAGICC/SCENGEN model.

According to climate variable data and compared to the demand-offer balance of the land use and socio-economic variables, the most sensitive crops to climate changes (precipitation and temperature) in the Tuluá River basin are coffee and potato. The environmental limiting factors of the future climate change scenario in 2020 forecast an increase in coffee production and a decrease in potato crops. In general terms, food products are more sensitive and vulnerable to changes in the river basin.

Results shown by the WaTEM/SEDEM erosion model in the Bugalagrande pilot basin (see WP 6 report) corresponds to a basin that progressively loses soil and may turn into a critical scenario in terms of land use due to the increase in agriculture for food and agro-industrial purposes, as well as grass feeding areas. The final result is production decreases and therefore, a slower economic development in the region.

According to demand-offer water balances for the present conditions and the 2020 scenario, the Tuluá River pilot basin does not evidence severe vulnerability to global change. No significant impacts are to be found in terms of the environmental and socio-economic variables of the basin. However, the estimates of the analyzed variables represent certain degree of uncertainty and therefore, require complementary studies in order to reduce the uncertainty and obtain better future scenarios.

It is acknowledged that climate change is represented through future climate prediction in terms of precipitation and air temperature patterns that has a high degree of uncertainty. That is what is shown by the results of global circulation models in the Andean Region. Large climate variations are present in our region, making it very hard to estimate the magnitude of the expected changes. Although the TWINLATIN project shows a base analysis for the possible changes in precipitation and temperature, it is important to make progress in the reduction of uncertainty levels, as well as the inclusion of variations associated to extreme hydro-climatic phenomena such as droughts, floods, events associated to ENSO. This would help to improve the reliability of the analysis of water supply, which is an important tool for the environmental and territorial management.

For the analysis of socioeconomic variables involved in the demand-offer balance, some factors were assumed; such is the case of the industrial demand which according to previous studies have been adopted as demand values. It is important to update or have more accurate data in order to have a more accurate model and change impact.

Additionally, it is important to consider the impact of change on productive systems in the basin. One should consider the economic value of possible changes associated with crop yield and production. This is an important process that must be considered for the different environmental and technological present and future activities. Different management scenario should be considered through the creation of a panel of experts in order to reach an agreement on socio-economic and environmental variables and to analyse the impact of water resources availability related to the actual local situation, reducing uncertainty in results. The so-called POMCH, a plan of integrated basin management for the region (Planes de Ordenamiento de las Cuencas Hidrográficas) is currently under construction.

2.4 COCIBOLCA LAKE BASIN (NICARAGUA – COSTARICA)

2.4.1 Introduction

The Cocibolca Lake Basin (approx. 22.000 km²) is shared between Nicaragua and Costa Rica (Figure 2.67); however, the Cocibolca Lake itself is completely located within Nicaragua. With a surface area of approximately 8,000 km² it constitutes the second-biggest lake in Latin-America. It directly drains a land surface area of approx. 14.000 km² (the occasional connection between the Xolotlan Lake Basin further north and Lake Nicaragua is not considered here). In the new Nicaraguan Water Law (2007), the Cocibolca Lake is mentioned as a priority area for protection, as it constitutes a very important freshwater reserve for the country and the Region (future production of drinking water).

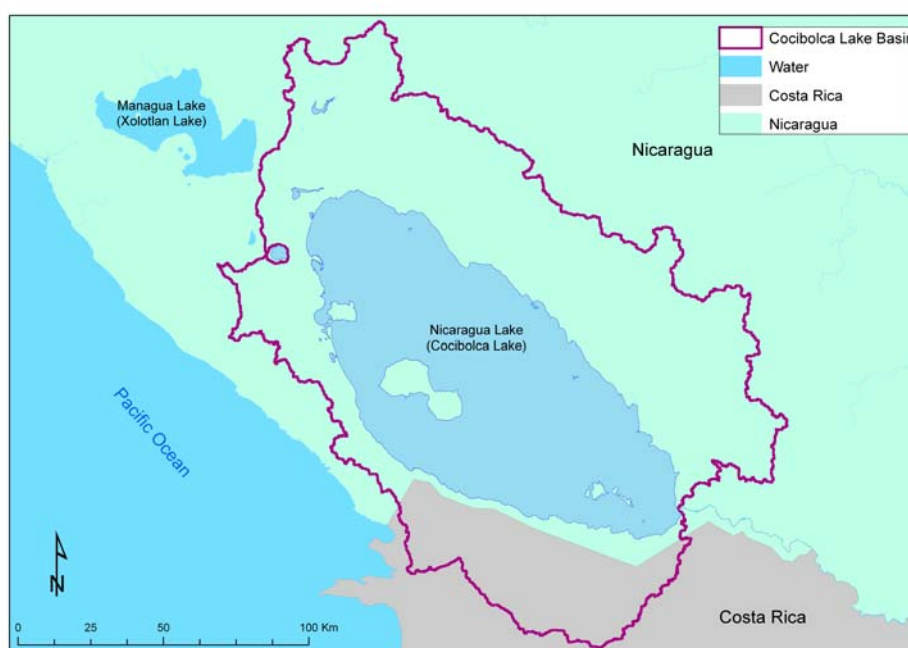


Figure 2.67 The Cocibolca Lake Basin³

In Nicaraguan society, the idea is widespread that the water quality of the Cocibolca Lake has deteriorated significantly over the past decades. In addition to the increasing presence and effects of human pressures in the Basin (see also the Work Package 6 report), changes in the lake and the basins' water balance itself may also play a fundamental role in such a process, and may also pose additional threats on ecosystems and human society (droughts, extreme events,...). For this reason, and considering the logistical and time constraints under TWINLATIN, for the analysis of the potential impacts of change scenarios on the water resources in the Cocibolca Basin the following approach was proposed and used:

- As a first approximation, under TWINLATIN climate-change scenarios for the Cocibolca Basin were prepared based on output from the MAGICC/SCENGEN v4.1 scenario generation tool (Hulme et al., 2000; Wigley, 2003a; Wigley, 2003b; Wigley et al., 2000); this was done as part of a harmonized approach towards scenario generation applied by the different TWINLATIN partners. A step-by-step manual on the use of the MAGICC/SCENGEN tool v4.1 for the generation of change signals was developed at EULA-Chile and CIEMA,

³ Sometimes the Río Frio drainage area (in the SSE of the map) is included in the delineation of the Lake Basin; however the Frio river drains directly to the San Juan River and is therefore not included in the figure here.

Nicaragua, and made available as a “twinning contribution” to the other Latin-American project partners (see Annex 1, in Spanish).

- Output from MAGICC/SCENGEN consists of change signals with regard to a simulated 1961-1990 reference period; absolute and percentage change are obtained for mean annual temperature and precipitation for future 30-year time windows; the change values are obtained for two 5° x 5° cells which both contain parts of the Cocibolca Basin: [90° - 85° W | 10° - 15° N] and [85° - 80° W | 10° - 15° N]
- In addition to this, “*reference period*” and “*future*” daily precipitation time series for 0.5° x 0.5° grid cells covering the entire study area have been obtained from the RCM runs covering Central America and the Caribbean which have been executed by the Cuban Meteorological Institute (PRECIS tool⁴; SRES scenarios A2 and B2); a first assessment of the differences between “*downscaled*” versus “*coarse-scale*” change scenarios for the Cocibolca Basin climate is made.
- Even without conducting hydrological impact assessment by means of a calibrated and validated mathematical model application (quality and availability of input and calibration data for the Cocibolca Basin was not sufficient for this purpose), the change signal information itself was analyzed as it already provides very useful information which allows making a first estimation of the potential local and regional hydrological impacts of climate change.
- The information obtained from the RCM run for the Cocibolca Lake Basin was incorporated in the Georeferenced Environmental Database for the Cocibolca Basin SIGACC using for this purpose the ArcHydro toolset, and is available at INETER for future reference.
- A basic vulnerability assessment exercise was conducted with the stakeholders during the twinning workshops which were held in the Basin.
- An index for the evaluation of adaptation practices is proposed.
- A list with important actions for future research is provided.

2.4.2 Water balances and hydrological modelling

2.4.2.1 Introduction

The establishment of water balances for Nicaragua and for the Cocibolca Basin is seen as a priority action for the Nicaraguan Institute of Territorial Studies (INETER). In order to support the activities of INETER with regard to this aspect, under Work Package 3 a series of activities have been conducted, ranging from *(i)* the establishment of a simple water balance for the basin based on the generation (through interpolation) and mathematical combination of GIS-layers representing mean annual values for the meteorological variables derived from measured and remote-sensing data sets; *(ii)* the testing of a simple hydrological model (WASMOD) on a sub-basin, the Mayales, in combination with a Monte Carlo analysis, in order to evaluate the effects of uncertainties related to the quality of the calibration data sets; *(iii)* the application of a more classical spatially-distributed modeling approach for this same sub-basin. All these activities aimed at providing additional information for the establishment of improved water balances.

2.4.2.2 Input data

The hydrometeorological datasets (available time series of discharge, precipitation and temperature; for station locations see the Work Package 2 report) used for the mapping of the reference period climatology and for model calibration and validation were obtained from INETER (daily time series for the Nicaraguan part of the Basin) and from NOAA (monthly time series only, mostly for the Costa Rican part of the Basin). Cleaning of these time series was conducted (the cleaning process consisted of quality control, elimination of low- or dubious quality data sets and gap-filling) and the accepted data sets were incorporated in the Environmental Database for the Cocibolca Basin (SIGACC). From

⁴ <http://precis.insmet.cu/Precis-Caribe.htm>

these data sets, stations with more than 30% complete years of precipitation data for the 1975-1994 time window were selected and used in a GIS-based interpolation exercise, from which the map with the reference period annual precipitation for the Basin was obtained (see Figure 2.74 p. 2-84).

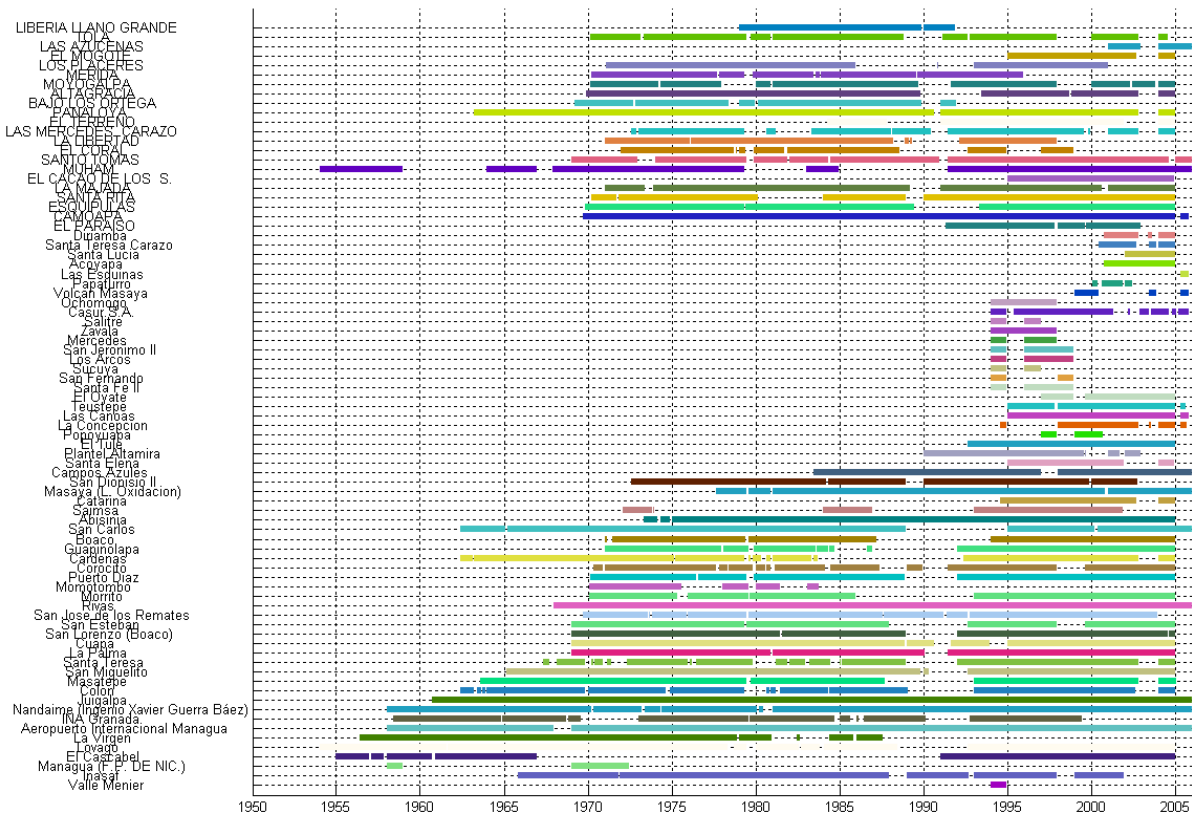


Figure 2.68 Availability of time series of monthly precipitation data for the Cocibolca Basin and immediate surroundings (SIGACC database, after quality control and gap-filling)

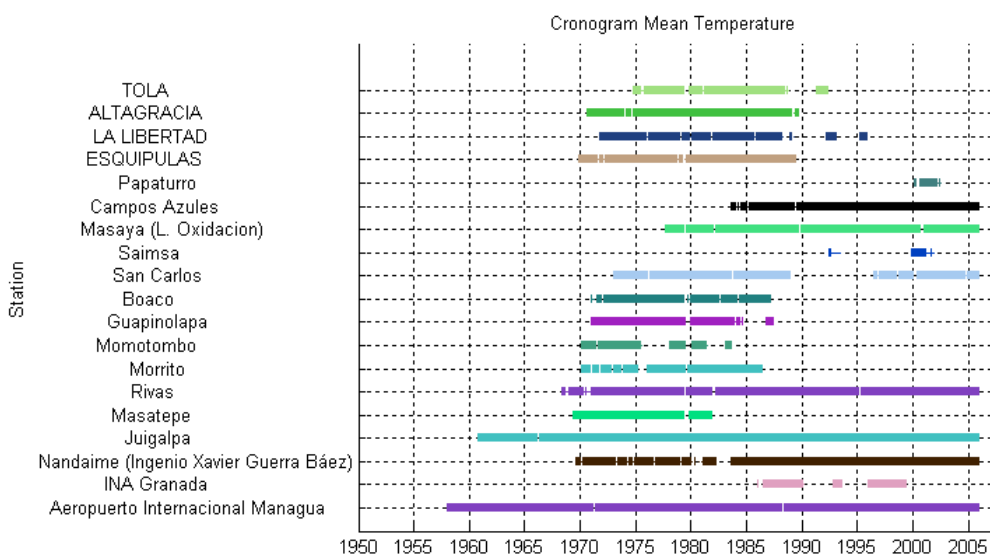


Figure 2.69 Availability of time series of mean daily temperature data for the Cocibolca Basin and immediate surroundings

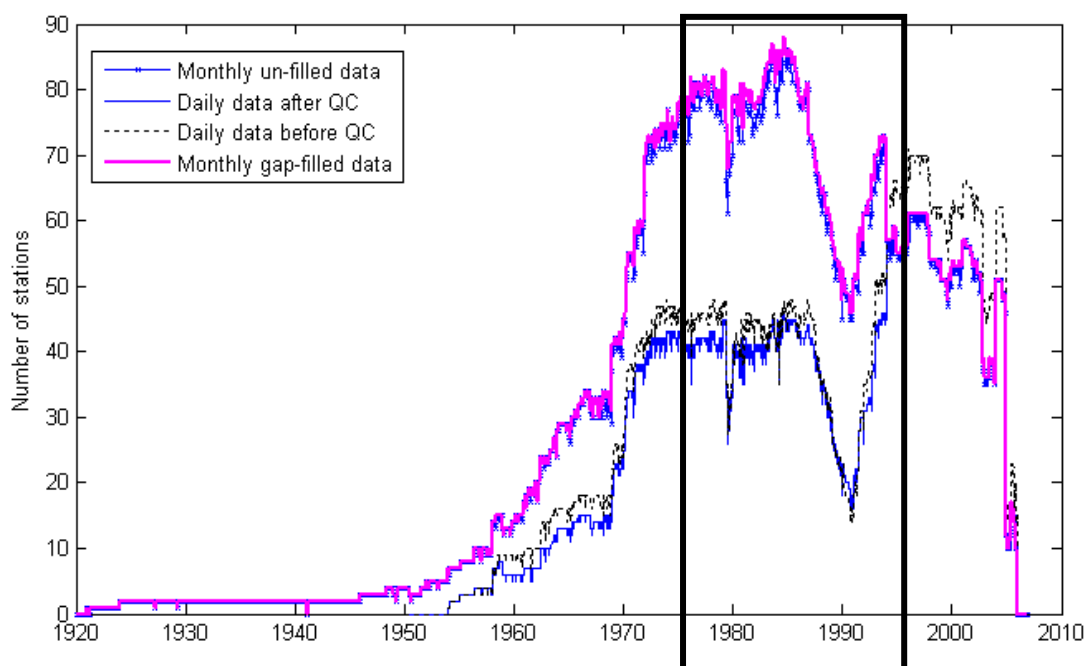


Figure 2.70 Number of stations per year with available time series of precipitation data before and after quality control and gap filling respectively; a considerable part of the data was of too poor quality to be used

The black box in Figure 2.70 shows the 1975-1994 time window from which time series data were selected for the preparation of the SIGACC-based mean annual precipitation map. The window was selected based on the good availability of data over a 20-year time period.

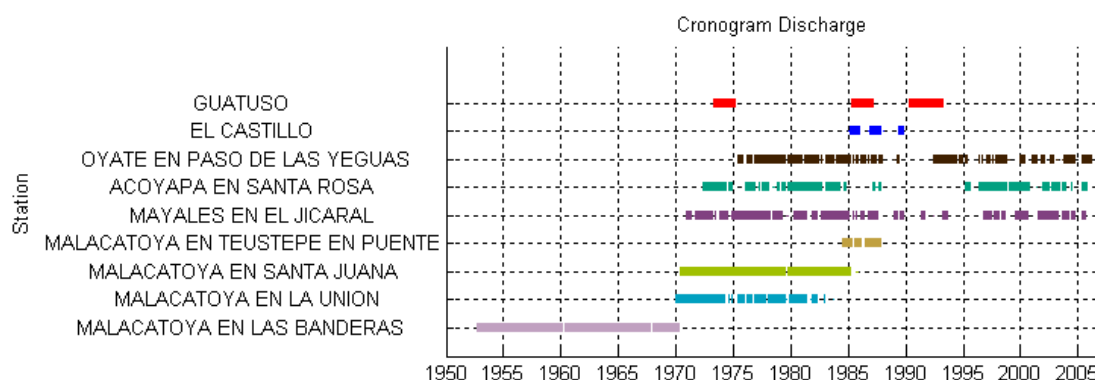


Figure 2.71 Availability of discharge data for the Nicaraguan part of the Cocibolca Lake Basin

2.4.2.3 Results

The reference period precipitation map obtained from the observed and cleaned data sets is shown in Figure 2.74 (p. 2-84). The pronounced spatial N-S gradient in mean annual precipitation can clearly be observed in this figure.

Reference period discharge values for the Mayales sub-basin are shown in Figure 2.72 (the Mayales is one of the few Nicaraguan sub-basins for which both a long discharge time series and corresponding precipitation data were available, see also Figure 2.71). Figure 2.72 also indicates the “limits of acceptability” ranges around the “observed” discharge values, i.e. all discharge values obtained from hydrological modelling that for a given period in time fall within the corresponding range are considered as equally good, due to the estimated uncertainty on the discharge measurements. Rating curve points were available for low and medium discharge values only; therefore uncertainty on the higher, extrapolated discharge values is large.

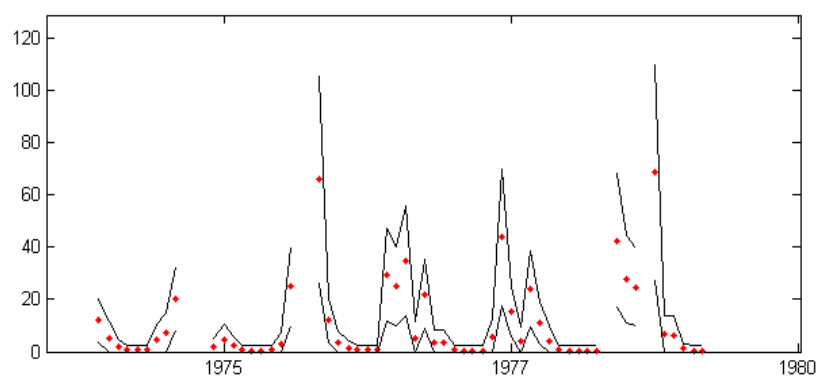


Figure 2.72 Limits of acceptability around the observed monthly discharge [mm] in the Mayales catchment

Results from the spatially distributed hydrological modelling exercise that was conducted on the Mayales sub-basin by means of the WASMOD model are shown below (for further details, see the Work Package 3 report).

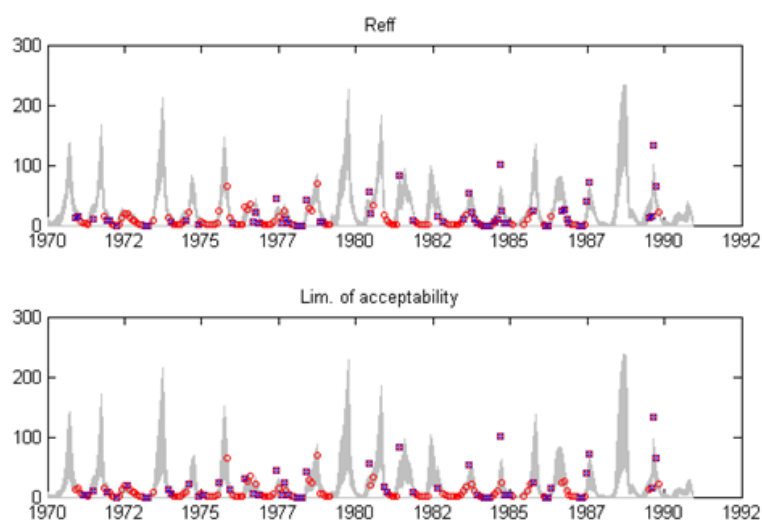


Figure 2.73 Discharge [mm] from the WASMOD validation (1970-1990)

The top graph shows the simulated uncertainty bound for the Reff-criterion and the bottom graph the uncertainty bound for the limit of acceptability criterion⁵ (red rings with a black cross mark months where the model fails and the observations fall outside the limits of acceptability).

The results show how the uncertainty with regard to the observed time series influences the calibration exercise: a considerable amount of possible value combinations for the different model parameters delivers discharge values that lay largely within this uncertainty bound; all these combinations are considered for further modelling and as a consequence of this, large uncertainties will also exist (the grey bands) for the simulation results obtained from WASMOD. Even so, it can be observed how during validation a considerable amount of the observed data points fail to fall within these large uncertainty bounds (this occurs both for high as well as for low discharge values).

Considering (i) these large uncertainties already associated to the simulated model outcome, and the added uncertainty that would be obtained under scenario modelling due to the existence of multiple plausible scenarios for climate change; and considering (ii) the fact that calibration and validation – due to limited data availability – could only be conducted for a single sub-basin, it was decided that spatially distributed modelling for the assessment of hydrological impacts from climate change in the Cocibolca Basin by means of the WASMOD tool should not be a priority action under TWINLATIN.

⁵ For more specifications on both criteria and on the conducted modeling work, see the Work Package 3 report.

Instead, a simpler approach was made, consisting of the evaluation of the representation of the reference climate by means of the RCM model runs, and an analysis of change values obtained from the different used scenario generation tools and first logical deduction of their potential impacts. Once also the RCM time series for temperature can be obtained, a complete water balance can be made, representing plausible future conditions and spatial patterns of water availability in the basin. In the current context, however, more attention was given to preparing the Basin's Environmental Database, so that a good departure point becomes available for easily conducting more detailed modelling work once the required input information becomes available.

2.4.2.4 Baseline

The baseline climatology for the Cocibolca Lake Basin is shown in the following figures. Figure 2.74 shows the mean annual precipitation for the 1975-1994 reference period, obtained from the data-quality controlled time series of the SIGACC database. Figure 2.75 originates from the climatological map set for Nicaragua obtained from INETER, whereas Figure 2.76 and Figure 2.77 show the RCM-simulated mean annual precipitation for the 1961-1990 reference period. Temperature data from the RCM runs could not be obtained yet.

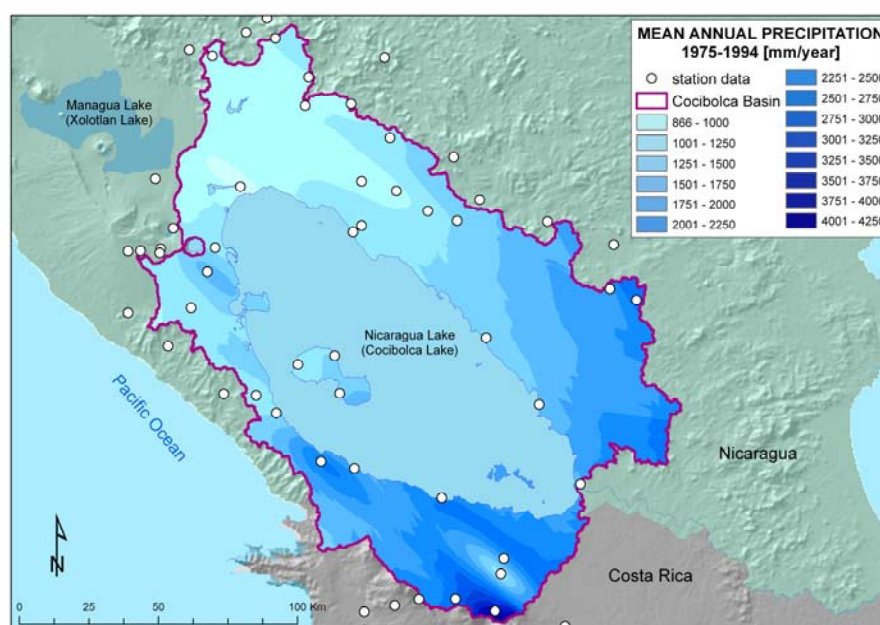


Figure 2.74 Mean annual precipitation [mm yr⁻¹] for the Cocibolca Basin (1975-1994) interpolated by means of Universal Kriging from the data contained in the Cocibolca Basin Environmental Database

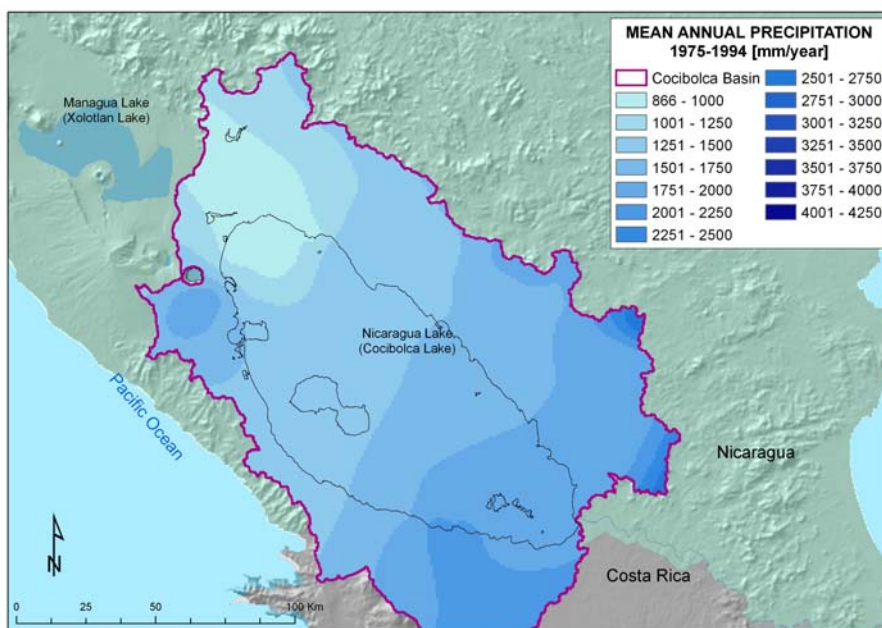


Figure 2.75 Mean annual precipitation [mm yr⁻¹] as interpolated from the INETER isolines (valid for the Nicaraguan part of the Cocibolca Lake Basin only) (INETER water balance)

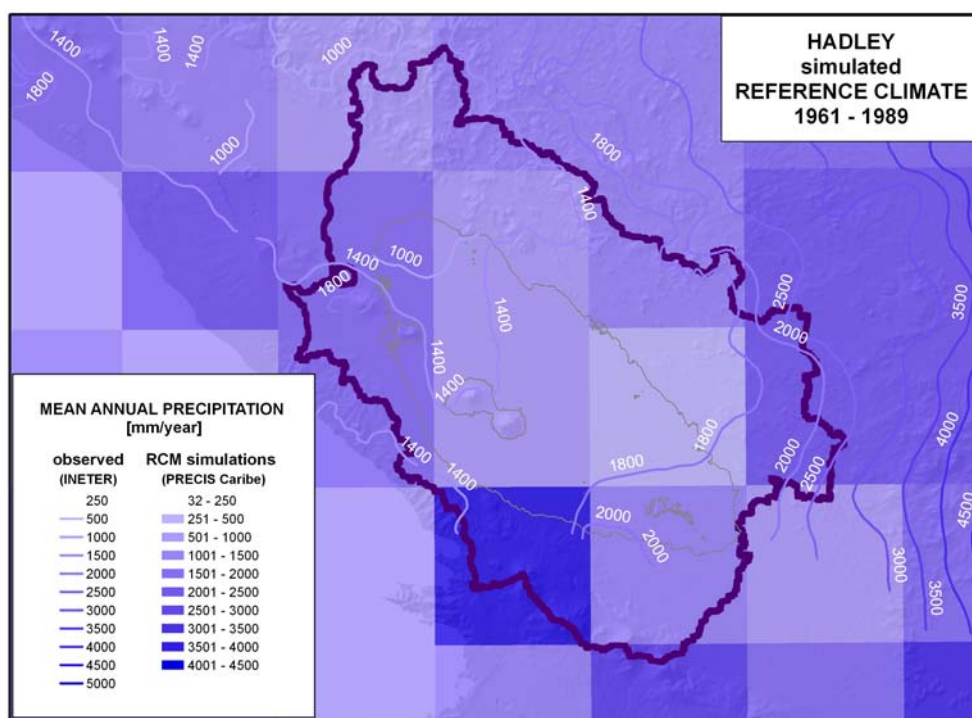


Figure 2.76 PRECIS/Hadley: simulated mean annual precipitation patterns over the Cocibolca Basin for the reference period 1961-1989 the isolines indicate observed precipitation patterns (isolines source: Water Balance INETER)

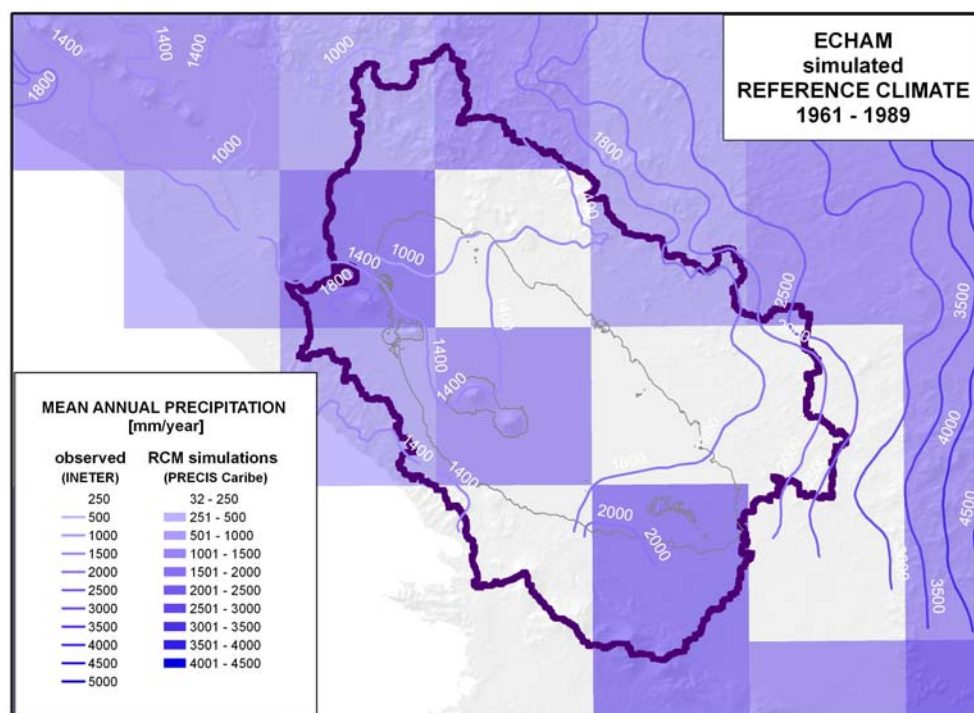


Figure 2.77 PRECIS/Echam: simulated mean annual precipitation patterns over the Cocibolca Basin for the reference period 1961-1989
the isolines indicate observed precipitation patterns (isolines source: Water Balance INETER)

When comparing the results from Figure 2.74 and Figure 2.75 with the results from Figure 2.76 and Figure 2.77 (and taking into account the summary data from Table 2-20 p. 2-92), the HADCM3-driven RCM model run for the reference period seems to provide a reasonable approximation of the “real” magnitude and to a lesser degree also the spatial patterns of precipitation over the Cocibolca Basin. This seems to indicate that the simulation of future climatic conditions over the Cocibolca Basin by means of the RCM driven by the HADCM3 may provide the most interesting information for stakeholders (compared to the results from the ECHAM-driven RCM run) with regard to potential future climatic conditions in the Basin. However, it needs to be indicated here that a reasonable representation of the reference climate does not necessarily guarantee a good prediction of future climatic conditions.

2.4.3 Scenario creation

2.4.3.1 Climate change

A generic methodological framework initially developed under TWINBAS was further implemented under TWINLATIN. The framework is shown in Figure 2.78. The way in which (and if) the different components of the framework are specifically implemented however may be case study-specific, as this will depend on the quality and availability of input data sets.

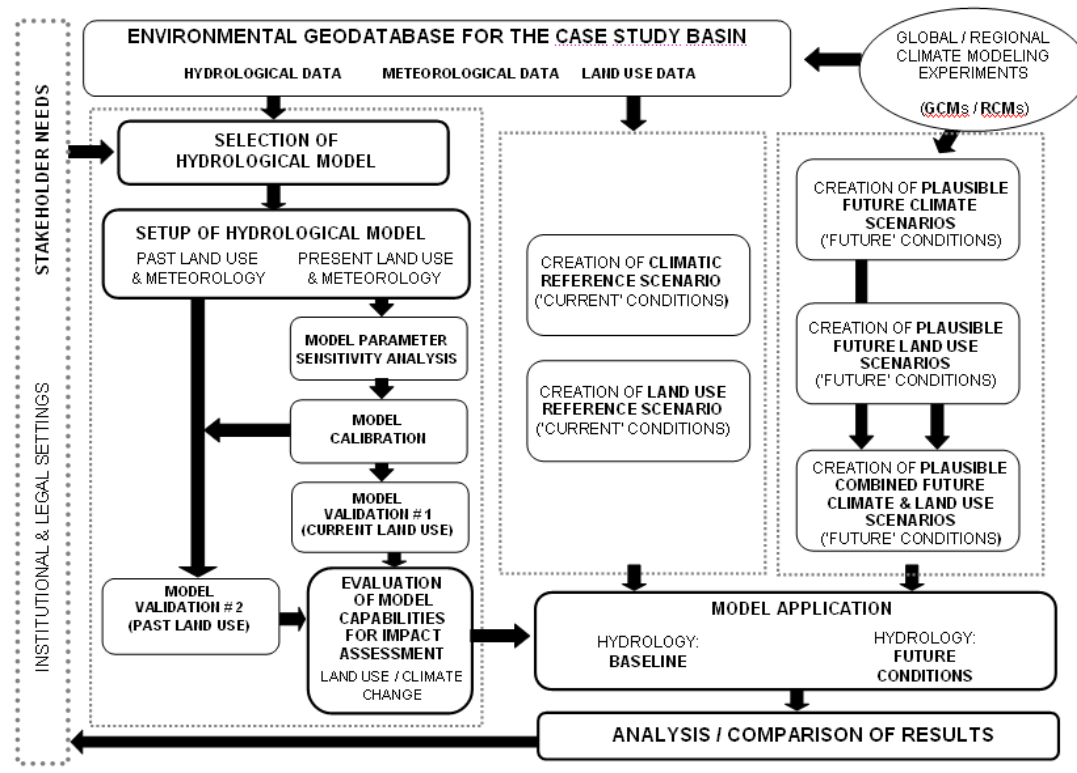


Figure 2.78 Generic framework for change impact assessment for basin hydrology (Debels et al., 2007)

In the case of the Cocibolca Basin, ongoing post-TWINLATIN efforts will be required in order to achieve a more complete and in-depth application of this framework. Due to the considerable time investment that was required in order to obtain and clean the necessary data sets, and due to other logistical and time constraints, for the Cocibolca Basin attention under Work Package 8 was mainly focused on the creation of reference and plausible future climate scenarios from GCMs and the PRECIS RCM (under Work Package 3, a model calibration and validation for a selected sub-basin has been conducted, and the possibilities for using model tools in impact assessments are also briefly discussed under 2.4.2.3 p. 2-82). No advanced scenario modelling could be conducted for the Cocibolca Basin in the framework of the TWINLATIN project, but through a simpler approach a first interpretation of potential impacts was made.

A Creation of scenarios with MAGICC-SCENGEN

In the present study – in order to incorporate in our evaluation the impact of uncertainty associated with the conceptualization/simplification of the global and regional climatological processes in the different models, as well as with the existence of different scenarios for the future emissions of greenhouse gases – we analyzed the change signals obtained from MAGICC-SCENGEN for 9 different GCMs. We further considered the combined effects of greenhouse gases and aerosols, and for each GCM we simulated change for the 6 SRES “marker” emission scenarios: A1FI, A1T, A1B, A2, B2, B1 (IPCC, 2001). As such, a total of 54 scenarios were obtained from the tool. Changes for precipitation and temperature were simulated for a future time window of 30 years centered on 2050; the mean annual results are shown in Figure 2.79 and Figure 2.80.

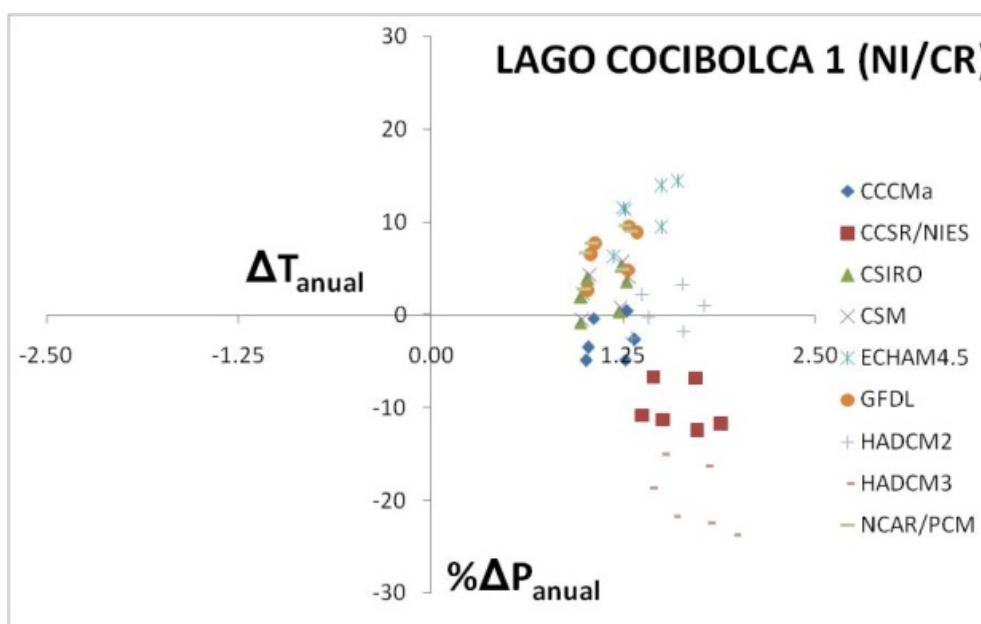


Figure 2.79 Results from MAGICC/SCENGEN for 6 SRES marker scenarios and 9 different GCMs changes in mean annual precipitation [%] and temperature [°C] between a 30-year time window centered on 2050 and the simulated 1961-1990 reference climate (Pacific side, 90° - 85°W | 10° - 15°N)

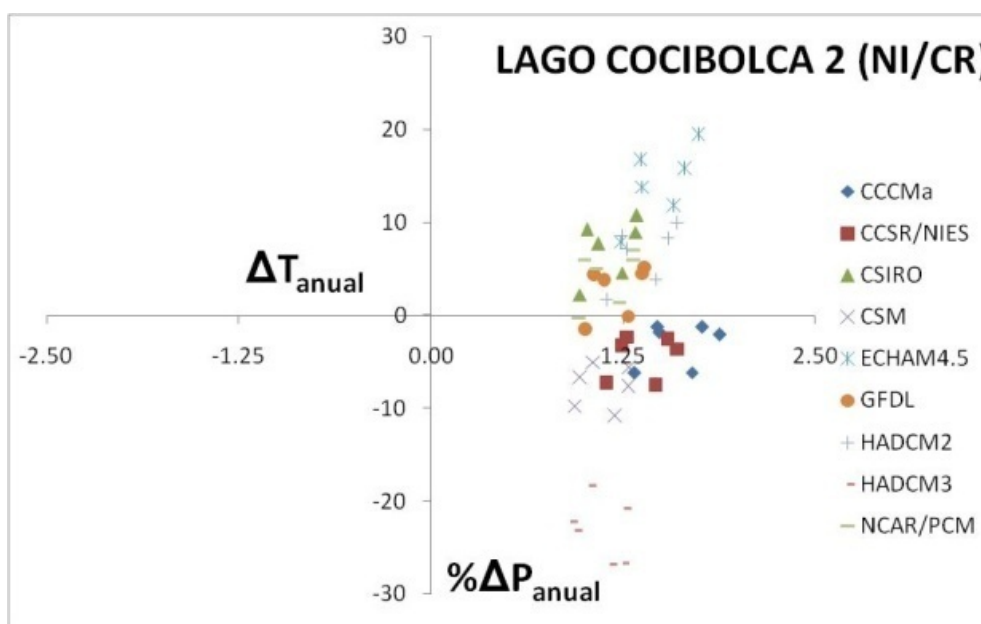


Figure 2.80 Results from MAGICC/SCENGEN for 6 SRES marker scenarios and 9 different GCMs changes in mean annual precipitation [%] and temperature [°C] between a 30-year time window centered on 2050 and the simulated 1961-1990 reference climate (Atlantic side, 85° - 80°W | 10° - 15°N)

B Creation of regional scenarios based on the output from an RCM

Two large-scale GCM models (HadCM3 and ECHAM) were used to force the regional-scale simulations conducted by means of the PRECIS tool at the Cuban Meteorological Institute⁶. Under TWINLATIN, daily time series from these runs for the output variable “precipitation” could be obtained from the Cuban Meteorological Institute for the emission scenarios A2 and B2, for a

⁶ <http://precis.insmet.cu/Precis-Caribe.htm>

rectangular set of grid points which contains the Cocibolca Lake Basin (both Nicaraguan as Costa Rican part).

At each point of the grid, 6 daily time series could be obtained: the first two series correspond to the simulated reference or control climate (“*current*” climate) for the 1961-1989 and 1961-1990 time windows, for the RCM runs driven by the HADCM3 and ECHAM boundary conditions, respectively. The “future climatic conditions” time series obtained from the RCM/Hadley runs are available for the period 2071-2099, for both the A2 and B2 emission scenarios. For the RCM/Echam run, the corresponding time series are available for the 1991-2099 time period. The full time series have been incorporated in the ArcHydro-based Environmental Database for the Basin, and have been handed over to INETER for future research activities.

From the ArcHydro database, spatial and thematic queries were conducted as to construct data layers that represent the spatial patterns of mean annual precipitation over the Cocibolca Basin obtained from the PRECIS/HADLEY and PRECIS/ECHAM model runs, for the common reference period (1961-1989) and for the common future time window 2071-2099. From these data layers, percentage change factors were calculated. The resulting figures are given below.

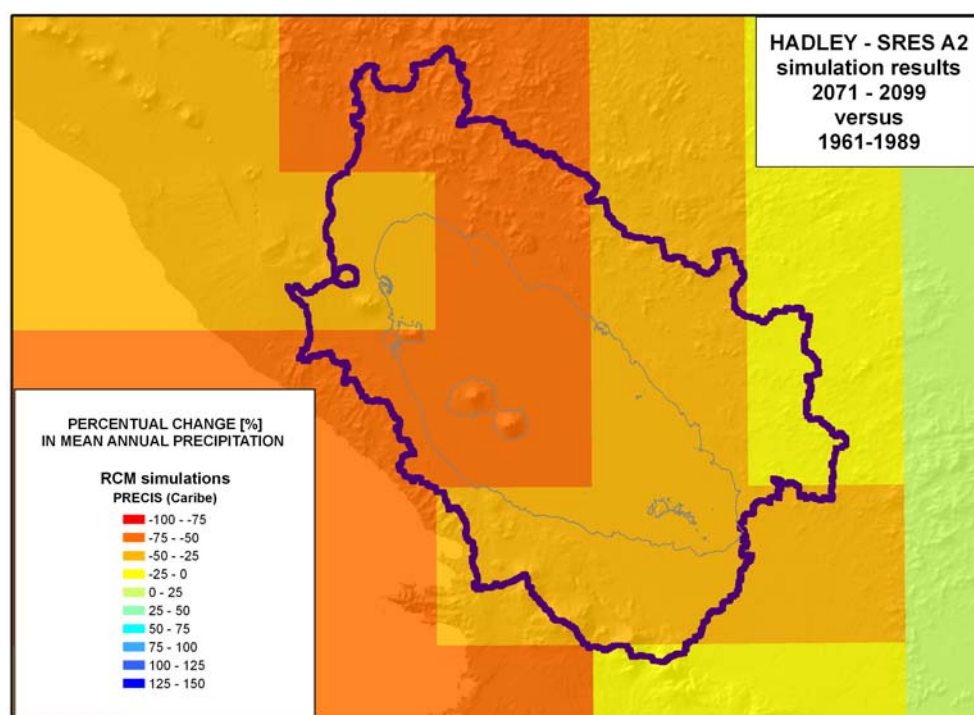


Figure 2.81 PRECIS/Hadley SRES A2 emission scenario
Change [%] in simulated mean annual precipitation patterns over the Cocibolca Basin between the future time windows 2071-2099 and the reference time window 1961-1989

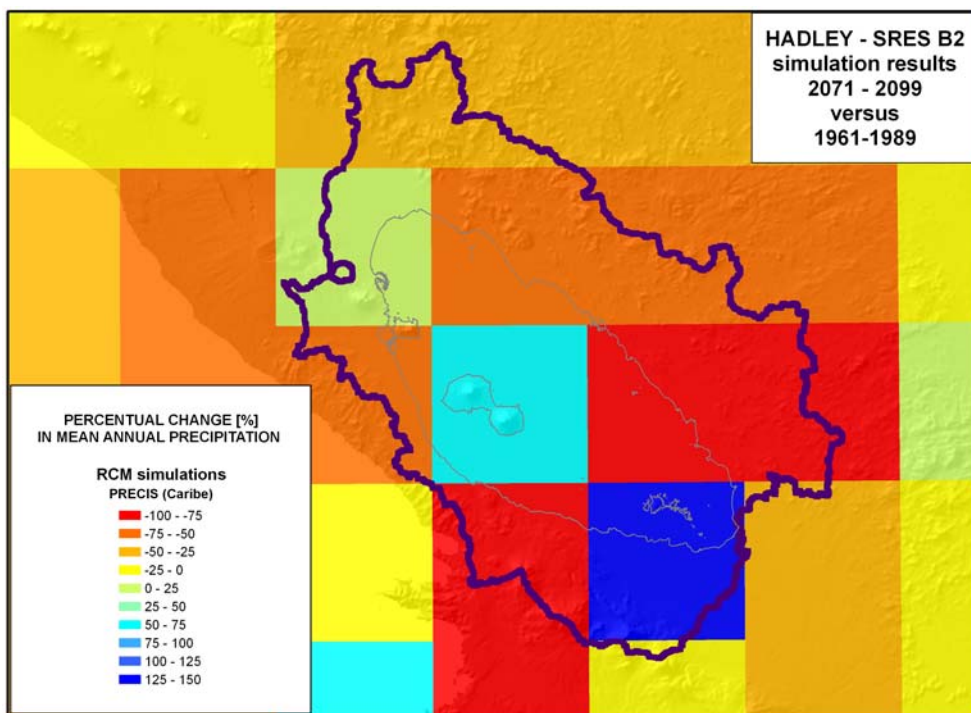


Figure 2.82 PRECIS/Hadley SRES B2 emission scenario
 Change [%] in simulated mean annual precipitation patterns over the Cocibolca Basin between the future time windows 2071-2099 and the reference time window 1961-1989

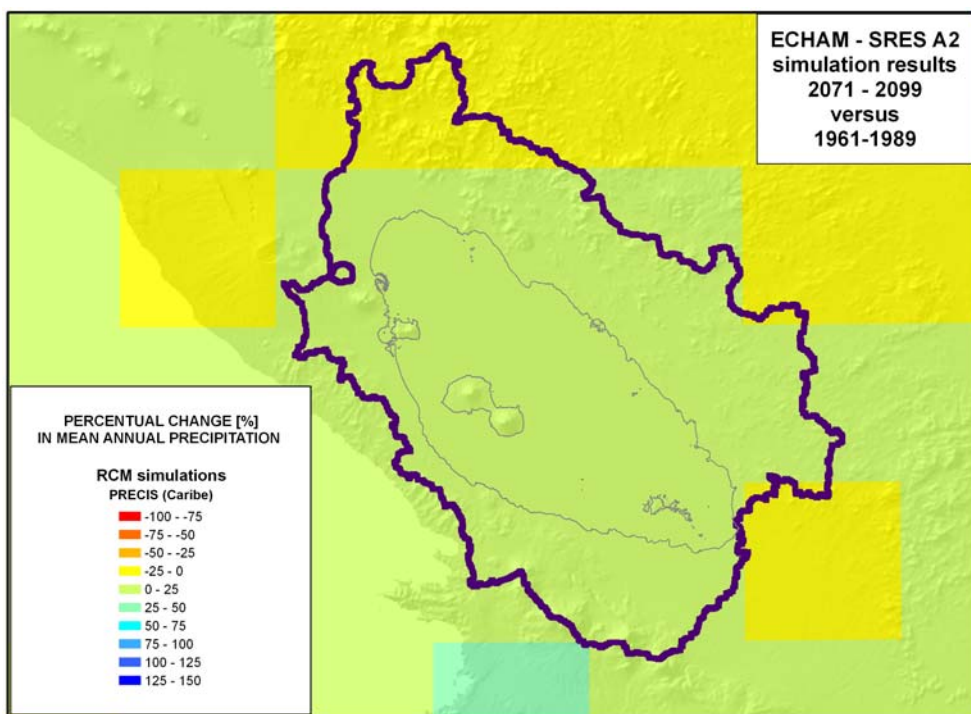


Figure 2.83 PRECIS/Echam SRES A2 emission scenario
 Change [%] in simulated mean annual precipitation patterns over the Cocibolca Basin between the future time windows 2071-2099 and the reference time window 1961-1989

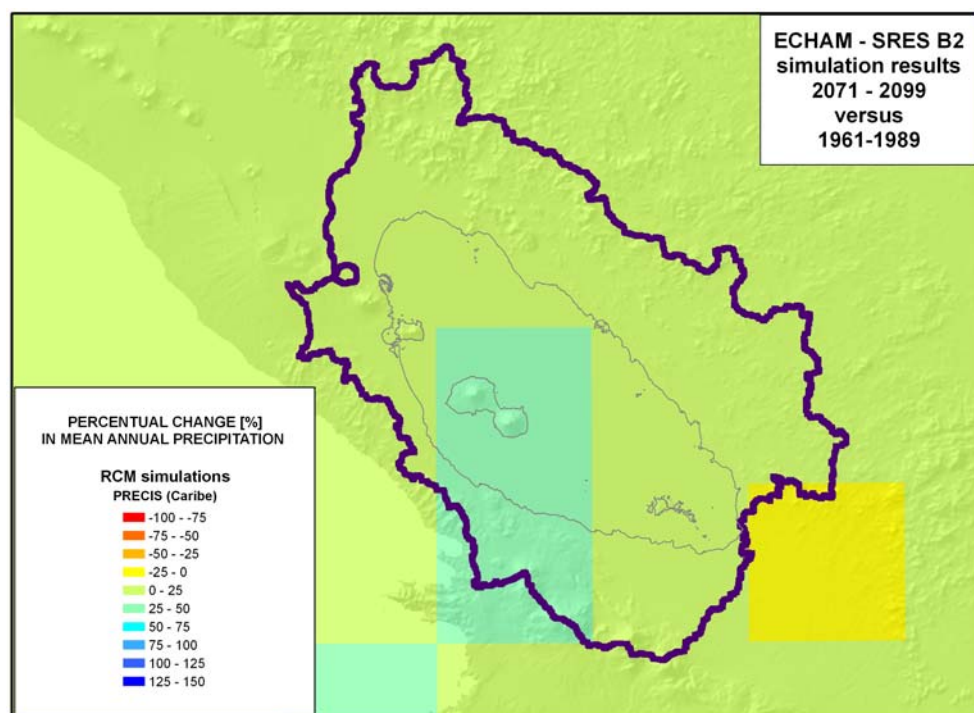


Figure 2.84 PRECIS/Echam SRES B2 emission scenario
Change [%] in simulated mean annual precipitation patterns over the Cocibolca Basin between the future time windows 2071-2099 and the reference time window 1961-1989

2.4.3.2 Land use change

Due to the variable spatial coverage of the existing historical and current land use maps for the Cocibolca Basin area, the highly heterogeneous interpretation techniques and classification schemes that have been used in the preparation of these maps, and the lack of validation data or quality assessments (see also the Work Package 6 report), no land use change modelling was conducted for the Cocibolca Lake Basin under TWINLATIN. Instead, the recommendation is formulated here for the use of a bi-national, well-established and agreed-upon protocol, and a uniform classification scheme in all future work.

2.4.3.3 Changes in water demands

Selected aspects have been incorporated in the Work Package 9 report.

2.4.3.4 Water resources developments

No major coherent and imminent water resources development projects are known for the Cocibolca Basin.

2.4.4 Scenario impact assessment

2.4.4.1 Separate effects

A Climate change

For the Cocibolca Lake Basin, it can be seen from Figure 2.79 and Figure 2.80 how for both 5° x 5° cells different GCMs produce different change signals for precipitation, whereas all GCMs produce a rise in temperature. The MAGICC-SCENGEN output for **HADCM3** produces a considerable decrease in precipitation for the **2050** time window, between approx. - 15 % and - 25 % for the western cell, and between approx. - 18 % and - 28 % for the eastern cell. The MAGICC-SCENGEN simulations of

the **ECHAM** results, however, project an increase in mean annual precipitation in both cells, with a magnitude between + 5 % and + 22 %.

The results from the RCM runs driven by the **HADCM3** also show a decrease in precipitation over the Cocibolca Basin for the time window centered on **2085**, but by the end of the century these would be of a larger magnitude: values range from - 30 % to - 44 %. For the same time window, RCM runs driven by **ECHAM** deliver an estimated increase in mean annual Basin precipitation between + 14 % and + 20 %. The spatial patterns over the Basin obtained from the RCM are not clear; therefore no further interpretation of these has been made. Instead, the conclusions that were formulated are based on the mean change values over the Basin (Table 2-21).

In the Cocibolca Basin, the divergence in results obtained for mean annual precipitation from MAGICC-SCENGEN for the different GCMs complicates an unambiguous evaluation of the potential impacts of climate change on water resources; however increased temperatures and associated changes in the basin hydrology and in the lake physics/chemistry/biology can be foreseen. In addition to this, we can indicate here that the HADCM3-driven RCM runs gave a much more realistic representation of mean annual precipitation over the Cocibolca Basin for the reference period (Table 2-20). Climate change signals directly or indirectly derived from the HADCM3 indicate a considerable reduction in annual precipitation over the Cocibolca Lake Basin. Under such a scenario, the combination of reduced precipitation and increased temperature can be expected to generate considerable impacts in the basin's water balance and in the physical-chemical and biological characteristics of the lake.

Table 2-20 Mean annual precipitation over the Cocibolca Lake Basin [mm yr⁻¹] for the reference climate and a simulated change scenario (2071-2099) obtained from the Regional Climate Modeling exercise PRECIS-Caribe (Insmet)

mean anual precipitation Cocibolca Lake Basin [mm yr ⁻¹]	REFERENCE CLIMATE		CHANGE SCENARIO (2071-2099)	
	STATION DATA	RCM (simulated)	SRES A2	SRES B2
PRECIS – HADLEY* (RCM)		1323	922	745
PRECIS – ECHAM* (RCM)		454	518	545
TWINLATIN*	1758			
INETER*	1566			

* the reference period is 1961–1989 for the PRECIS data set, 1975–1994 for the TWINLATIN observations data set; data from 1980–2000 were used for the INETER Water Balance calculations

Table 2-21 Changes in mean annual precipitation over the Cocibolca Lake Basin [%] for the reference climate and a simulated change scenario (2071-2099) obtained from the Regional Climate Modeling exercise PRECIS-Caribe (Insmet)

% change in mean annual precipitation	CHANGE SCENARIO (2071-2099)			
	SRES A2		SRES B2	
PRECIS – HADLEY (RCM)	-30.3		-43.7	
PRECIS – ECHAM (RCM)	+14.3		+20.2	
MAGICC/SCENGEN - HADLEY	-45.7 (P [*])	-54.5 (A [*])	-26.4 (P [*])	-32.4 (A [*])
MAGICC/SCENGEN - ECHAM	+14.9 (P [*])	+18.8 (A [*])	+14.9 (P [*])	+18.8 (A [*])

* output from MAGICC/SCENGEN is for 5° x 5° pixels; P corresponds to output that approx. covers Nicaragua's Pacific side (model pixel 90° - 85° W | 10° - 15°N); A corresponds to the Atlantic side (pixel 85° - 80°W | 10° - 15°N)

The results of this work show how climate change can and most probably will constitute an additional stress factor to ecosystems and human society in the Cocibolca Basin, clearly indicating the importance and usefulness of anticipated mitigation and adaptation actions, such as a major awareness building among stakeholders on the needs for rational land and water use, and a further promotion of the concepts of integrated and adaptive water resources management practicing.

2.4.4.2 Combined effects

Considering the observations already mentioned, no such modelling was or could be conducted under TWINLATIN.

2.4.5 Vulnerability assessment

2.4.5.1 Exposure of society

Results obtained from the climate change scenario analyses documented in the previous chapter relate to the “exposure” component of vulnerability, in the specific field of global warming impacts on regional climatology (with logical deductions towards impacts on water resources and basin hydrology). The generated regional climate change scenarios for the Cocibolca Lake Basin area show a high probability of a considerable increase in the mean annual temperature, which may result in an exposure of society to considerably different future conditions of availability and quality of water resources in the Cocibolca Lake and its surrounding basin.

2.4.5.2 Vulnerability of water stakeholder

Without having conducted major, quantitative analyses on the “sensitivity” component of vulnerability, the magnitude of the “*plausible*” impacts obtained from the scenario analyses for the Cocibolca Lake Basin in combination with the high levels of poverty and the probability of associated low adaptive capacity allow us to assume that a considerable vulnerability potential exists for both human society as well as the natural ecosystems in this basin.

It can thus also be assumed that a considerable amount of adaptive capacity would need to exist or to be generated in the basin if vulnerability towards the impacts from climate change on water resources is to be maintained at, or reduced/brought down to levels which are acceptable for society.

Indications of existing and potential future vulnerability of society in the Cocibolca Lake Basin to the water resources-related effects of climate change and variability already exist indeed: fish mortality in the lake has repeatedly been observed, and has been associated to changes in the lake water temperature in the past; hurricane pathways have crossed the lake basin area in the past, causing floods

and damage to human infrastructure and productive systems; water scarcity, seasonal and/or periodical droughts have already seriously affected the water provision to households in several of the major cities in the Basin over the past – a solution based on the production of drinking water from the Cocibolca Basin will be influenced by the future quality of water resources in the lake and on costs for pumping water from the lake to the higher-laying cities.

2.4.5.3 Public participation and the perception of vulnerability

During the public participation workshops held in the Cocibolca Basin in the second half of the year 2008 in the Municipalities of Granada and Rivas, an exercise was conducted as to evaluate the existing perception of vulnerability towards the effects of climate change among the participating basin stakeholders. For this purpose, through a questionnaire, stakeholders were allowed to express their perceptions with regard to the importance of different factors that are known to influence vulnerability towards the (water resources-related) effects of climate change (Figure 2.85 up to Figure 2.88). Previously to the application of the enquiry, a PowerPoint presentation was given in which the concepts of vulnerability, exposure, sensitivity and adaptive capacity were explained in simplified terms. The enquiry then was applied twice, once before and once after results from the work on the exposure component in TWINLATIN (described in previous chapters of this report) were shown (also in a simplified manner). The aim here was to see if the provision of information from site- or region-specific research influenced the stakeholder's perception of vulnerability.

This twinned approach was also applied in other TWINLATIN basins, e.g. the Baker Basin in Chile. Assistance of stakeholders at the public participation workshops in Nicaragua however was considerably higher than in e.g. Baker (historical-political reasons can explain this). For the Granada and Rivas workshop respectively, 36 and 15 opinions could be collected. These numbers are still relatively small, but allow already obtaining a first impression on which factors – according to the opinion of stakeholders – are insufficiently developed in the basin and, as such, contribute to a low adaptive capacity.

Figure 2.85 up to Figure 2.88 show the outcome from this public participation process. Each axis in the graph represents a factor which is considered to influence the adaptive capacity of stakeholders. Participants were asked to assign a high value to those factors whose current conditions in the basin or country positively contribute to their adaptive capacity, whereas a low score needed to be assigned to those factors whose current condition is seen as a cause of low adaptive capacity, and which thus contribute to higher vulnerability.

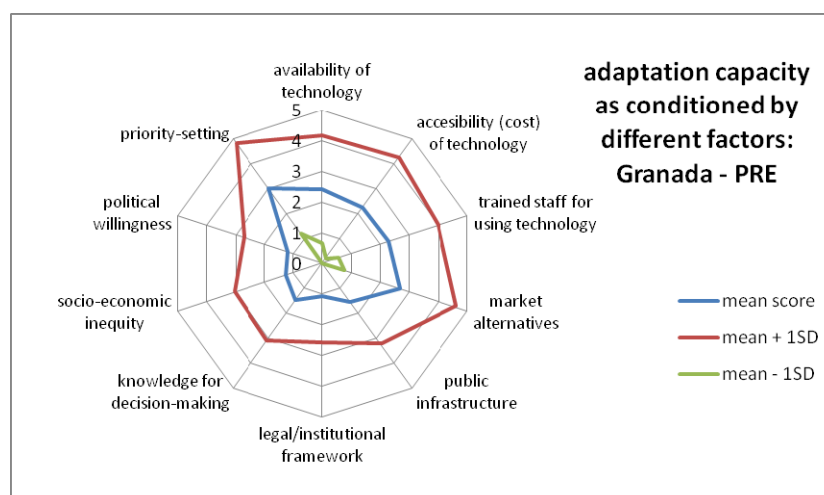


Figure 2.85 Cocibolca Lake Basin's stakeholder perception with regard to vulnerability - factors that condition adaptive capacity to climate change (Granada workshop, previous to showing results from WP08; n = 36)

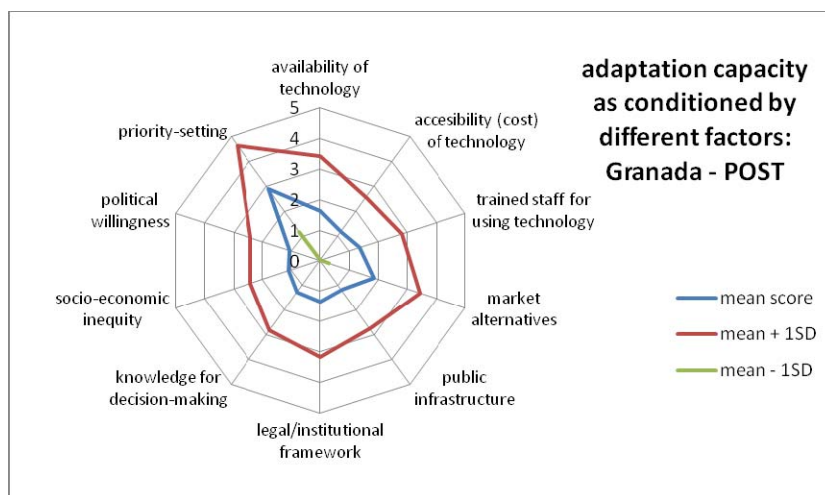


Figure 2.86 Cocibolca Lake Basin’s stakeholder perception with regard to vulnerability - factors that condition adaptive capacity to climate change (Granada workshop, after results from WP08 have been shown; n = 32)

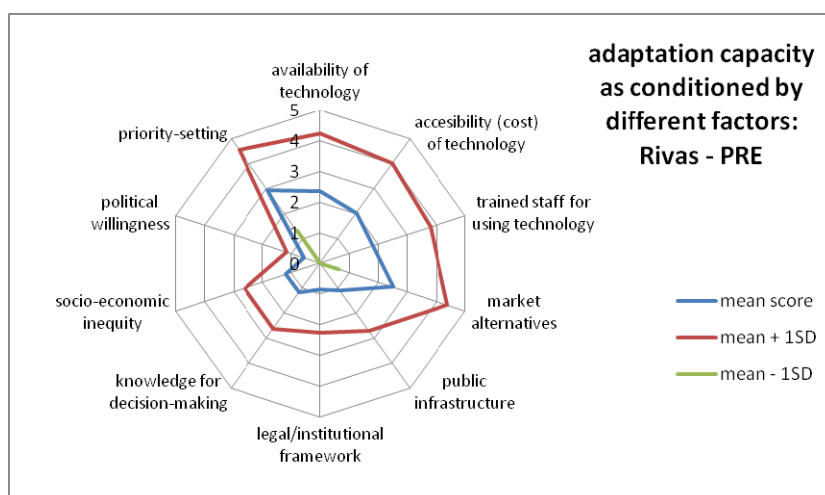


Figure 2.87 Cocibolca Lake Basin’s stakeholder perception with regard to vulnerability - factors that condition adaptive capacity to climate change (Rivas workshop, previous to showing results from WP08; n = 15)

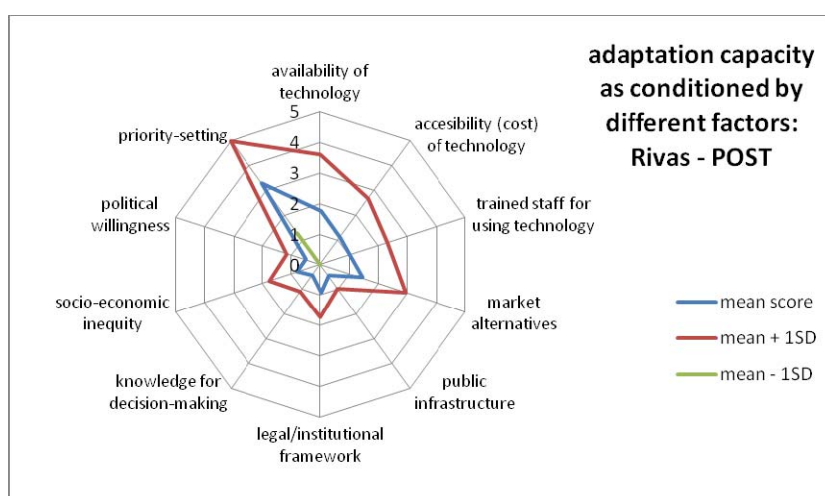


Figure 2.88 Cocibolca Lake Basin’s stakeholder perception with regard to vulnerability - factors that condition adaptive capacity to climate change (Rivas workshop, after results from WP08 have been shown; n = 15)

Factors were: (i) the existence of technology which would enable adaptation; (ii) the availability of this technology at accessible costs; (iii) the existence of qualified personnel to make use of such technology; (iv) the existence of market alternatives (e.g. good market prices for more drought-resistant crop alternatives in case of predictions of a drier climate); (v) the availability of adequate public infrastructure (e.g. flood protection dams, early warning systems, etc.); (vi) and adequate legal/institutional framework; (vii) adequate knowledge for decision-making (e.g. results from research on climate change impacts; adequate monitoring networks); (viii) socio-economic equity (inequity is a negative factor as the poor tend to have less adaptive capacity); (ix) political willingness to act; (x) the importance the stakeholders themselves give, or are able to give –due to priority setting– to the topic of climate change.

In all cases and for most factors, rather low mean scores were obtained (nearly almost ≤ 3). A remarkable result is also how for factors in the lower half of the graph (especially from the “political willingness”-“market alternatives” diagonal downwards) typically the lowest scores were given (“market alternatives” itself however, does not get this typical low score). Somewhat surprising is also how the “priority setting” systematically gets the highest score. The evaluation of this factor was conducted to see if stakeholders consider that other worries than climate change (and variability) are much more urgent, with the result that not sufficient attention can be given to this topic. This exercise however seems to indicate that stakeholders in the Basin do consider climate change and variability a high-priority topic.

In many cases, scores obtained after the results from the TWINLATIN research on the exposure component had been shown tend to be lower than during the first application of the enquiry. This seems to indicate that through the awareness building exercise the perception of vulnerability (due to lack of adaptive capacity) is higher than before.

The mean value for the “knowledge for decision-making” was low in all cases, and did not increase after information from the research was provided. This seems to indicate that a high demand exists among the basin stakeholders for additional, probably higher-resolution and more specific information on the topic of regional, local and sectorial impacts of climate change.

It is important to indicate that the current results are based on a small amount of questionnaires; even so the exercise provides interesting preliminary information on what factors of the vulnerability equation future efforts should be focused. As such, it can also assist in defining topics for future research.

2.4.5.4 Adaptation to reduce vulnerability

In order to reduce vulnerability, a timely adaptation to probable new environmental conditions under climate change becomes imperative. Adaptation in the context of human society can be defined as: ‘adjustments in human systems in response to actual or expected climatic stimuli (*~exposures*) or their effects (*~exposures + sensitivity*), in order to moderate harm or exploit beneficial opportunities’ (IPCC, 2001). It is an integral part of the implementation of the United Nations Framework Convention on Climate Change (UN, 1992), and ‘requires urgent attention and action on the part of all countries’ (UNFCCC, 2002).

After the evaluation of vulnerability, a next logical step in the preparation of society for the potential impacts of climate change thus consists of the definition of adaptation practices for stakeholders in the water resources sector. Through the implementation of such adaptation practices, vulnerability can be addressed and reduced.

In this context, at CIEMA-UNI/EULA-Chile under TWINLATIN and through a collaborative research effort with a group of non-TWINLATIN researchers from the Latin-American and Caribbean Region brought together by the Inter-American Institute on Global Change Research **IAI**, starting from a common interest in impacts in the water resources sector a prototype multi-purpose index was developed and proposed for use in the evaluation of practices for adaptation to climate variability and change. The Index of Usefulness of Practices for Adaptation (**IUPA**) allows the user to assign weights and scores to a set of user-defined criteria for evaluating the general usefulness of adaptation practices.

Individual criterion scores are then aggregated into a final index value. Both the final value and the individual parameter scores provide useful information for improved decision making in the context of the definition of adaptation measures for climate change. An innovative aspect of this IUPA index is that guidance is given to the user through the inclusion of recommendations on evaluation criteria and criterion-specific weight factors. This guidance is provided by the aforementioned expert panel from the Latin-American and Caribbean Region (LAC). Although the index has not been applied yet in any of the TWINLATIN case study basins (no major adaptation practices are known), its usefulness for both TWINLATIN and other basins in the world was demonstrated through a practical application for an existing adaptation practice well-known to one of the research group members. The proposed index is particularly practical for a quick first assessment or when limited financial resources are available, making the tool especially useful for practitioners in the developing world. The index is flexible both from the perspective of its construction and use, and additional expert opinions can easily be included in future versions of the tool. The excel worksheet used for calculating the index value is shown in Figure 2.89. The index and its application are described in detail in Debels et al. (2008).

Index for the evaluation of the Usefulness of Practices for Adaptation - IUPA v1.0													
Case Study: Improving Disaster Management, Chile													
I VARIABLES			II SUGGESTIONS OF THE PANEL					III EVALUATION BY THE USER					
NAME OF THE VARIABLE			SUGGESTED WEIGHT (0-10)	SUGGESTED RELEVANCE	n	σ	level of agreement	ASSIGNED WEIGHT	ASSIGNED RELEVANCE	SCORE (design phase)	WEIGHTED SCORE (design)	SCORE (post-implementation)	WEIGHTED SCORE (post-)
A	B	C	D	E	F	G	H	I	J	K	L	M	N
A SUGGESTED "CORE" VARIABLES	1	ACCOMPLISHMENT OF THE OBJECTIVES	8.3	HIGH	8	1.0	M	9	HIGH		-	8	72
	2	REQUIRED IMPLEMENTATION TIME	6.8	MEDIUM	8	0.7	H	7	HIGH		-	8	56
	3	TOTAL COST	6.6	MEDIUM	8	1.3	M	7	HIGH		-	9	63
	4	ROBUSTNESS AND/OR FLEXIBILITY OF THE SOLUTION	8.9	HIGH	8	0.8	H	10	HIGH		-	9	90
	5	LEVEL OF AUTONOMY (IN DECIDING AND ACTING)	7.1	HIGH	8	1.5	M	6	MEDIUM		-	5	30
	6	PROPORTION OF BENEFICIARIES	7.1	HIGH	8	1.6	L	9	HIGH		-	8	72
	7	CONTINUITY IN TIME OF PROJECT OUTCOME	7.8	HIGH	8	0.9	H	8	HIGH		-	6	48
	8	LEVEL OF RESILIENCE	8.4	HIGH	8	1.2	M	10	HIGH		-	8	80
	9	INTEGRATION WITH OTHER POLICY DOMAINS	7.5	HIGH	8	1.4	M	8	HIGH		-	8	64
	10	PARTICIPATION OF TARGET POPULATION	8.5	HIGH	8	1.1	M	9	HIGH		-	6	54
B SUGGESTED "COMPLEMENTARY" VARIABLES	1	ATTENTION TO MOST VULNERABLE GROUPS	7.9	HIGH	8	1.2	M	9	HIGH		-	9	81
	2	LEVEL OF ENVIRONMENTAL PROTECTION	6.8	MEDIUM	8	1.0	M	7	HIGH		-	7	49
	3	REPEATABILITY	5.6	MEDIUM	8	1.8	L	5	MEDIUM		-	8	40
	4	INCORPORATION OF LOCAL/TRADITIONAL KNOWLEDGE	6.0	MEDIUM	8	1.9	L	4	MEDIUM		-	2	8
5		-	not defined					-	not defined		-	-	
6		-	not defined					-	not defined		-	-	
7		-	not defined					-	not defined		-	-	
8		-	not defined					-	not defined		-	-	
9		-	not defined					-	not defined		-	-	
10		-	not defined					-	not defined		-	-	
C USER ADDED VARIABLES	1	STRENGTHENING COOPERATION AMONG STAKEHOLDERS	-	not defined				8	HIGH		-	7	56
	2		-	not defined				-	not defined		-	-	
	3		-	not defined				-	not defined		-	-	
	4		-	not defined				-	not defined		-	-	
	5		-	not defined				-	not defined		-	-	
	6		-	not defined				-	not defined		-	-	
	7		-	not defined				-	not defined		-	-	
	8		-	not defined				-	not defined		-	-	
	9		-	not defined				-	not defined		-	-	
	10		-	not defined				-	not defined		-	-	
IUPA - integrated scores											0.0	7.4	

Figure 2.89 The Index for the Evaluation of the Usefulness of Adaptation Practices (IUPA)

2.4.6 Summary

In the present work conducted for TWINLATIN under Work Package 8 for the Cocibolca Lake Basin, different steps were undertaken in order to address the topic of change impacts and associated vulnerability: (i) outcome obtained from the activities conducted under Work Package 3 was analyzed, and based on this analysis a feasible and meaningful strategy – within the context of TWINLATIN – for activities under Work Package 8 was defined; (ii) climate change scenarios for the Cocibolca Lake Basin were generated and discussed, based on results indirectly obtained from GCMs as well as those directly obtained from a regional RCM run; (iii) a basic interpretation was made of these climate

change scenarios in terms of their potential hydrological consequences; (iv) the role of the previous steps for the evaluation of the exposure component of the vulnerability equation was briefly described; (vi) information from the work under TWINLATIN was shared with stakeholders in the Basin, and an exercise was conducted in which the perception of the adaptive capacity among stakeholders was evaluated; (vii) an index was developed which may help identify optimum adaptation options in future projects; (viii) to conclude, important aspects and topics that could not be addressed under TWINLATIN and which should be considered for inclusion in ongoing or future research on the Cocibolca Lake Basin are summarized (see below).

The wide range of values for the change signals that can be obtained in an impact assessment study such as the one presented for the Cocibolca Basin (this conclusion was also obtained for most other case study basins under TWINLATIN) is a direct consequence of the uncertainties that persist with respect to the intensity and even direction in which change in climatic variables will manifest itself at the local and regional level, under global warming: information based on different GCMs provides different regional change patterns for a single change value in mean global temperature (MAGICC-SCENGEN). On top of this, the existence of a multitude of scenarios for the future emission of greenhouse gases adds additional uncertainty with regard to the magnitude of this change in global mean temperature. Additionally, for a given study site, change results obtained from a finer-scale modelling exercise (RCM runs) may also differ considerably from what is obtained from the GCMs (although in this case, only the magnitude and not the direction of change was affected).

In the case of the Cocibolca Basin, considerable uncertainties were also associated with the outcome of the hydrological modeling exercise conducted under Work Package 3, as a result of uncertainty with regard to input and calibration/validation data sets; therefore in the current context scenario impact modeling by means of a calibrated and validated hydrological model was not conducted under TWINLATIN. Instead, directly from the change scenario information itself qualitative projections were made with regard to possible impacts: higher temperatures will affect evapo(trans)piration; if this occurs in combination with lower precipitation rates, the water balance in the Cocibolca Basin may be seriously affected, as well as the physical-chemical and biological characteristics of the Cocibolca Lake.

Stakeholders in the Basin seem to perceive a high vulnerability due to a combination of the magnitude of possible change/variability and a low adaptive capacity. Frequency of phenomena such as ENSO and extreme events such as tropical storms and hurricanes may further contribute to increased vulnerability, and this aspect should be further addressed in future research.

Finally, it is important to indicate how the currently existing hydrometeorological network and available time series severely limit the possibilities for model calibration, validation as well as its application for impact assessment. Too often, parts of the basin that are hydrologically very important (i.e. parts that may be isolated geographically but that receive very important input contributions to the total water balance) are very little or not monitored at all. In the case of the Cocibolca Basin, no systematic field measurements of meteorological variables are being conducted for the Cocibolca Lake itself, even when – with a surface area of 8000 km² – its impact on the Basin water balance can be expected to be considerable.

Table 2-22 Some important tasks for ongoing research in the Cocibolca Lake Basin

protocol for the systematic generation and storage of metadata
collection + quality control + incorporation in the SIGACC database of hydrometeorological time series from the Costa Rican part of the Basin
collection and incorporation in the SIGACC database of the reference and future time window time series of temperature (and other variables) from the RCM model run for Central-America and the Caribbean

development of a bi-national, well-established and agreed-upon protocol and uniform classification scheme for the preparation of land use data layers for the Cocibolca Basin; this should be developed as a function of the use that will be given to the information, in such a way as to maximize its usefulness and guarantee its compatibility with other datasets

generation of maps/data layers for the Cocibolca Basin representing the different water balance components under plausible future climate change scenarios based on the RCM time series of meteorological variables

evaporation calculations from the lake surface area with the aid of remote sensing data in order to enable the establishment of a full (terrestrial area + lake) water balance for the Cocibolca Basin

larger-scale application of the vulnerability assessment exercise + inclusion of the topic: climate variability versus climate change, extremes (e.g. ENSO, hurricanes,...)

updating of the results from WP 8 using the new version of the MAGICC/SCENGEN tool

improvements to the hydrometeorological monitoring network (rating curves, station coverage, lake water temperature,...) combined with alternative information sources (remote sensing, ...)

2.5 QUARAÍ RIVER BASIN (BRAZIL)

2.5.1 Introduction

The Cuareim River is a tributary of the Uruguay River on its left margin, which is a part of the La Plata basin, the second largest basin in South America. The Cuareim basin is located on the border between Brazil and Uruguay. The Brazilian part of the basin is to be found at the extreme south of the Federative Republic of Brazil, and the river is known in Portuguese as Quaraí. The Uruguayan part is somewhat larger and is located to the north of the Oriental Republic of Uruguay. Some important tributaries are: Tres Cruces Creek, Cuaró Creek and Yucutiá Creek on the Uruguayan (left) side of the main stream, and the Espinilho Creek, the Sarandi Creek, the Quaraí-Mirim Creek and the Garupá Creek on the Brazilian (right) side. Artigas (Uruguay) and Quaraí (Brazil) are the most important cities in the basin.

Most of the basins upper parts have shallow soils (depth up to 0.5m) which determine low soil water-storage capacity, which consequently generates fast-response run-off that may cause flooding in the cities of Artigas and Quaraí, and very low flows during droughts.

Statistical analysis of stream flow recorded at Concordia Bridge between Artigas and Quaraí shows a maximum flow of $4,813 \text{ m}^3 \text{ s}^{-1}$, a minimum flow of zero, and an average flow of $95.6 \text{ m}^3 \text{ s}^{-1}$. Most of the stream flow occurs during and shortly after the rainfall events.

There are several interests concerning water resources in this basin. Flooding of the city of Artigas, in Uruguay, is one of the most important issues. This problem was preliminary addressed by a pilot project supported by WMO (2004). During the Twinlatin project, however, problems related to water demand and availability and to water quality were raised repeatedly by the participants of the general public, local stakeholders and local government during activities of Work Package 4 and Work Package 5. Therefore, in the context of the Twinlatin project, the main interest in hydrological modelling of the Quaraí basin is water resources in general, with emphasis on water availability related to the widespread use for irrigation of rice fields.

The assessment of change effects carried out in WP8 focused largely on hydrological changes, linked to the presence of a large number of small reservoirs in the basin, and the consequences of widespread water abstraction for rice irrigation. (i) During WP4 (Public Participation) activities it also became clear that the local community is worried about the possible change effects of large scale plantations of eucalyptus, which would replace pastures. The general fear is that large eucalyptus plantations might lead to lower stream flows in the basin, leading to an increase in conflicts concerning water use. (ii) Local stakeholders also would like to know what the effect would be of the construction of a larger reservoir, located upstream of the cities of Quaraí and Artigas. This reservoir would be used at the same time for flood control during winter and regularization of low flows during the summer period. (iii) A final analysis of change effects is related to the hydrological impacts associated with climate change.

The whole basin area down to the confluence with the Uruguay River was modelled, and special attention was given to the influence of the small reservoirs and rice fields on the hydrologic behaviour of the basin.

2.5.2 Scenario creation

Scenario modelling was necessary from the start of the hydrological modelling activities in the Quaraí river basin. This is due to the fact that observed stream flow time series are strongly influenced by the presence of reservoirs and by water abstractions for rice irrigation.

(1) In the first scenario that was simulated, the effort was to represent the actual situation in the basin, with the widespread use of water for irrigation and with the presence of a large number of small

reservoirs. This scenario was used for the calibration of the model parameters, since observed stream flow data is influenced by the presence of the reservoirs and water abstractions.

(2) In the second scenario neither reservoirs nor water abstractions were included in the model. The aim of this scenario was to generate the baseline for comparison of the other scenarios.

(3) The third scenario is similar to the second, except for the reservoirs, which were included in the simulations. The aim of this scenario was to generate stream flow time series which could be compared to the ones obtained with the second scenario, so as to allow the analysis of the effect the reservoirs have on the main river stream flow. No water abstractions were included in the third scenario.

(4) The fourth scenario was similar to the third, except for the water abstractions. Water abstractions in the Quaraí river basin are of two types: river abstractions and reservoir abstractions. In the fourth scenario only water abstractions from the reservoirs were included. The aim of this scenario was to analyze the impact of reservoir water abstractions have on stream flow of the main river.

(5) The fifth scenario included reservoirs and both types of water abstractions but did not include the return flow from the irrigated rice fields. The aim of this scenario was to analyze the impact of return flows on stream flow of the main river.

Additional scenarios concerning land use change and climatic change were also simulated.

(6) Climatic change scenarios were based on expected changes in temperature and precipitation from several climatic models using the regionalization algorithm MAGICC/SCENGEN, as is fully described in the next sections.

(7) The land use change scenarios consisted of changes from pasture to forest plantations, which will be possibly happening in the short future in the region. Concerns have been raised about the expansion of eucalypt plantations in Southern Brazil. Criticism is related to expected biodiversity losses and impacts on water resources availability. In this seventh scenario it was considered that 10% of the land currently covered with pasture would be transformed into eucalyptus plantations in the Quaraí basin. Under this assumption three sub-scenarios were simulated. Scenario 7A considered that the eucalyptus plantations would be managed in order to avoid the contact of the trees to groundwater. Scenario 7B considered that the trees had a moderate access to groundwater and scenario 7C considered that the trees had a facilitated access to groundwater.

The analyzed scenarios of water resources development, including the objective of the simulation, are summarized in Table 2-23.

Table 2-23 Scenarios to be analyzed in the Quaraí river basin

Scenario	Reservoirs	Reservoir water abstractions	River water abstractions	Return flow from rice fields	Climatic change	Land use change	Objective
1	X	X	X	X			Model calibration; actual situation
2							Natural situation of the basin
3	X						Analyze effects of reservoirs
4	X	X		X			Analyze effects of reservoirs and reservoir abstractions
5	X	X	X				Analyze effects of return flows
6					X		Analyze effects of climatic change
7						X	Analyze effects of land use change

2.5.2.1 Climate change

Climatic changes or climatic variability may have major impacts on the hydrologic regime, e.g., increase in floods, dry seasons, erosion, and deterioration of the water quality and diversity of

ecosystems. Social-economic impacts related to alterations in the availability of water resources for domestic and industrial use, production of foods, generation of energy, among others, can occur. Thus, there is a clear need of assessing the effect of possible climate changes on the hydrologic regime.

According to Wagener and Franks (2005), the relation between the emission of greenhouse gases and consequently global heating is the most scientifically accepted anthropogenic cause of climate change. Some uncertainties and differences in the results of the main climate models and general circulation models (GCMs) used for future climate prediction exist. Despite all the uncertainties associated to the prediction of climate changes, it is still important to assess the possible impacts of these scenarios on water resources and several studies have been carried out searching in this direction (e.g. Andersson et al., 2006; Chaplot, 2007; Gellens and Roulin, 1998; Thodsen, 2007). Most of those studies used water balance simulation models to assess the effect of possible climate changes on water resources (mainly in terms of precipitation and temperature of the air). Ideally the water models used for these studies have a physical base and are able to represent the hydrological processes as correct as possible (Xu and Singh, 2004).

An interesting review of methodologies that have been applied to predict the impacts of climate changes on water resources was presented by Xu (1999) and Xu et al. (2005).

In order to measure the sensibility of the watershed to climate changes, the concept of outflow elasticity due to changes in mean precipitation or temperature has been used in other studies (e.g. Chiew, 2006; Fu et al., 2007; Sankarasubramanian et al., 2001). It has been shown that not all basins respond the same way to changes in meteorological inputs. The sensitivity of the hydrologic regime to changes in rainfall and temperature depends on physical characteristics of the watershed as soil types, geology and vegetation cover.

Results of GCMs' climate change predictions are currently available. Besides climate components, GCMs can supply results related to the water cycle. However, the special resolution of the GCMs is usually not compatible with the basin planning scale and some of the hydrologic processes are represented in a very simplified way (Xu, 1999). Alternatively, the results of the GCMs can be used as input data in a large scale water model to assess regional impacts (e.g. Fung et al., 2006) or water and climate models can be used (e.g. Yu et al., 2006). Xu (1999) presents some techniques to adjust the spatial scale of GCMs' results to watershed scale, named "downscaling". These techniques are grouped in dynamic downscaling, based on the use of Regional Circulation Model (RCM), and statistic downscaling (e.g. Tripathi et al., 2006).

GCMs can not perfectly represent the climate and often generate partial results. Thus, many studies opt to use the results of GCMs' climate changes in terms of relative changes in the variables of interest (e.g. precipitation and air temperature).

The values of mean changes in the variables of interest can be used to disturb the observed series that later are used as input record in water models. Alternatively, the scenarios of climate change can be built from climate generators (Weather Generator – WGEN) based on random models (e.g. Kilsby et al., 2007; e.g. Richardson, 1981; Semenov and Barrow, 1997). These models generate dependent meteorological variable synthetic series (e.g. precipitation, temperature of the air, solar radiation). The WGEN parameters are obtained from historical series and modified based on results of GCMs or hypothetical scenarios. The advantage of the WGENs is the possibility to include climate variability changes in climate change scenarios (e.g. number of rainy days, standard deviation of mean precipitation or temperature).

The climate change impact assessment is separated in two analyses. The first is a sensitivity analysis of the river discharge due to hypothetical changes in the annual mean precipitation and temperature. The second analysis is based on climate change scenarios obtained from the generator MAGICC/SCENGEN. In both cases, the water model MGB-IPH (Collischonn, 2001; Collischonn et al., 2007) was used to simulate the watershed considering the observed disturbed series of precipitation and temperature and keeping the observed series of other climatic variables (relative moisture, insolation, wind speed). Following, the observed stream flow time series were compared with simulated ones. The 20 year period from 1980 to 2000 was used during the simulations of climatic change scenarios.

Sensitivity studies are carried out to estimate the potential impacts of climate change on stream-flow and water resources. In particular, these studies analyze the sensitivity of river discharge to rainfall and potential evapotranspiration. The most applied methodology involves using a hydrological model, which is first calibrated against historical stream flow data. Then, the observed input climate data are modified to reflect an enhanced greenhouse environment. After that, the calibrated model is run using the modified input data and the same optimized parameter values. Finally, the simulated stream flow is compared against the historical stream flow to provide an estimate of the climate change impact on stream flow. This kind of method was used by Chiew (2006) and by several other authors cited by him. The input data are almost always modified by scaling the historical rainfall and potential evapotranspiration time series by a constant factor, although it would be desirable also consider changes in the rainfall distribution (Chiew, 2006; Chiew and McMahon, 2002).

Climate change scenarios for the Quaraí watershed were obtained from the MAGICC/SCENGEN generator of climate changes scenarios (Model for the Assessment of Greenhouse-gas Induce Climate Change/SCENario GENERator) version 4.1 (Wigley, 2003b; Wigley, 2003a). This version was used in the International Panel on Climate Change Third Assessment Report (TAR) of (IPCC, 2001; IPCC, 2001).

Figure 2.90, Figure 2.91 and Figure 2.92 show predicted changes in mean temperature (y-axis) and precipitation (x-axis) in the region of Quaraí River basin for years 2020, 2050 and 2085. These are results based on MAGICC/SCENGEN and reflect different climatic models and development scenarios. Each point on the chart is a result related to one of nine GCMs and one of the scenarios of greenhouse gas emission. These data are grouped according the GCMs. The results refer to a space of 30 years with one year of reference.

Most of the GCMs in all emission scenarios show that both temperature and precipitation will increase in the Quaraí basin. There is only one result suggesting a decrease in precipitation, by the GFDL climatic model. With this only exception there is more or less a consensus among the models, scenarios and prediction periods suggesting that temperatures will increase by as much as 3°C in the next 80 years, and that annual precipitation will increase by as much as 40%. Therefore, according to the results of IPCC's TAR and the GCMs, the probability to increase the annual mean temperature and precipitation is high in the watershed of Quaraí River.

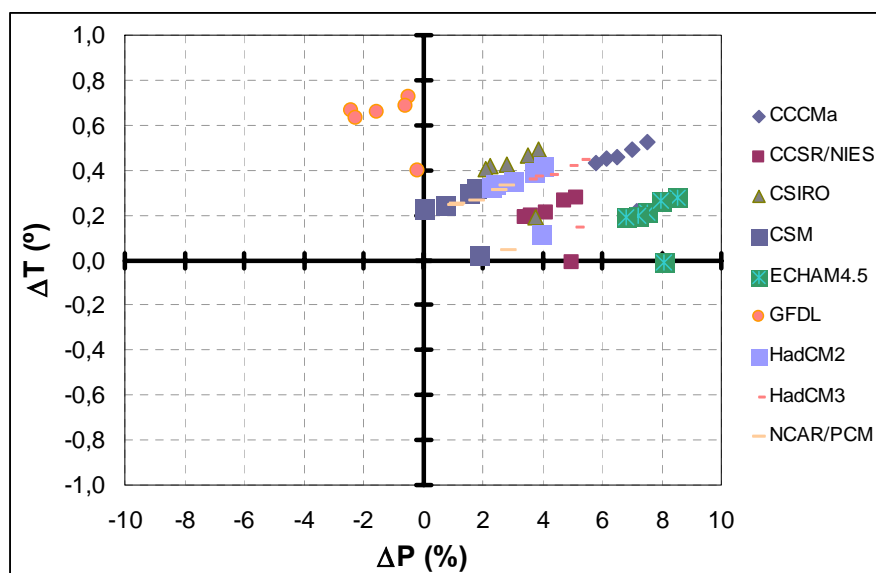


Figure 2.90 Changes in mean temperature and precipitation in the region of Quaraí watershed for 2020

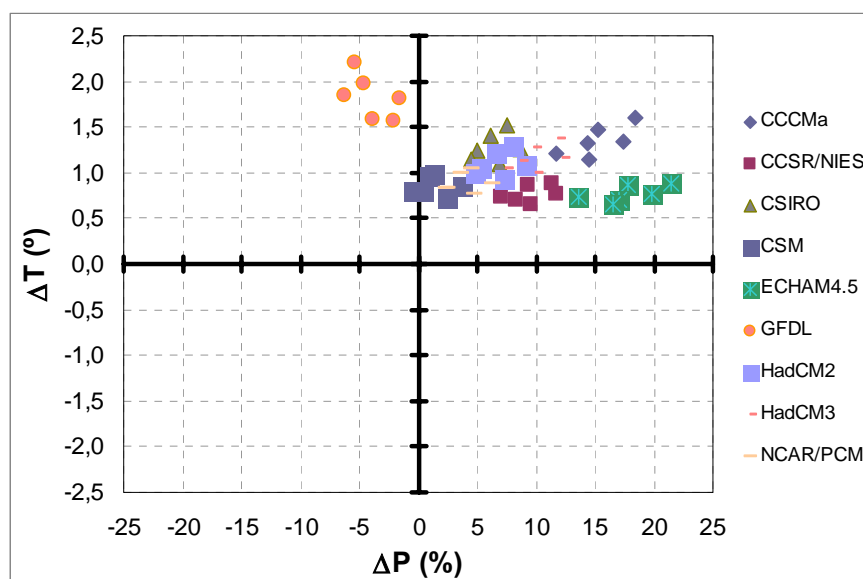


Figure 2.91 Changes in mean temperature and precipitation in the region of Quaraí watershed for 2050

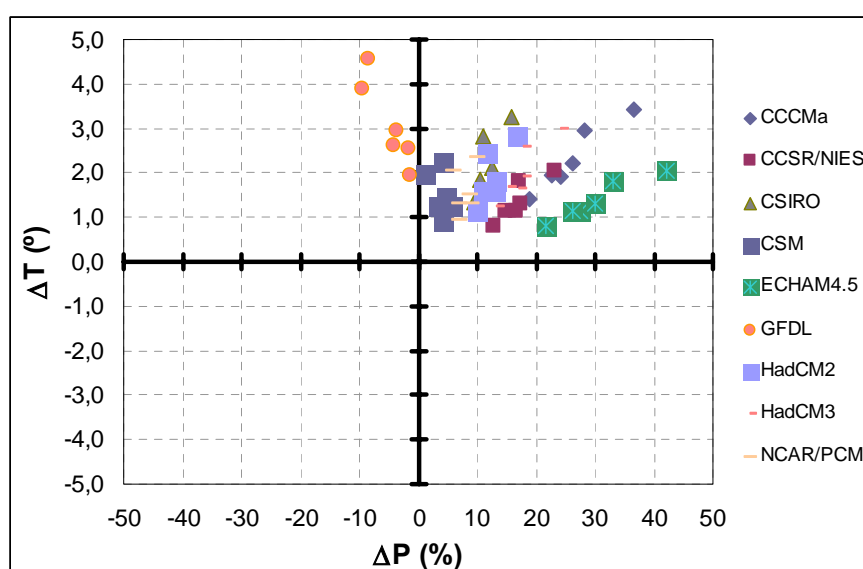


Figure 2.92 Changes in mean temperature and precipitation in the region of Quaraí watershed for 2085

Although most of the results are coherent concerning the direction of modification and indicate an increase both in temperature as in precipitation in the region of the Quaraí basin, these are disparate regarding the magnitude of this modification, mainly in the precipitation. The uncertainty associated with the results is very high, since the difference between the values of different models (for the same emissions scenario) is much larger than the difference in the predictions of a single model, considering different emissions scenarios (when observing charts, it can be observed that the points related to a determined model are all grouped and distant from the groups of points related to the other models). The difference between the results of different models has the same order of magnitude as predictions of climate changes.

Besides the models present discrepancies when predicting the future, they can not precisely represent the current or last climate in the region of Quaraí River. When comparing the annual mean obtained from reproductions of each GCM of the current climate (1961 to 1990) with data observed in temperature (1961 to 1990) and precipitation (1981 the 2000) significant errors are presented. All the GCMs underestimate the annual mean precipitation (error of -46%). The error in the annual mean temperature varies between -1.93°C and 2.99°C. So, the use of values of changes in the temperature

and precipitation and their application in observed series and non-use of gross GCMs results is justified.

Results obtained with MAGICC/SCENGEN also show that the changes will be evenly distributed over the year, suggesting that no sensible modifications of the seasonality will happen. It is therefore expected that winters will be warmer and more humid, while summers will be warmer and more humid.

From the results of the climatic models it is expected that changes in stream flow will be small, because the predicted increase in temperature will increase evapotranspiration and decrease stream flow, while increases in precipitation will lead to increases in stream flow. The two effects will probably cancel each other.

2.5.2.2 Land use change

As long as is known, the original vegetation in the Quaraí river basin was a mixture of natural grasslands and forests. The Spanish and Portuguese settlers found it relatively easy to raise cattle due to the relatively flat relief, and the natural pastures. For hundreds of years, livestock breeding was the most important economic activity in the whole region, and the regional word for cowboy – “*gaucho*” – is now used to identify the people from South Brazil.

During the 20th century, rice growing was introduced in the region and low lying areas, which were normally not valuable for livestock breeding, were slowly changed to rice production.

Currently, the major concern related to land use change in South Brazil is the plantation of forests. Two types of trees (*Eucalyptus* and *Pinus*) are being cultivated for decades now in the State Rio Grande do Sul, mainly for paper and wood production. The extent of eucalyptus plantations will probably grow in the near future in consequence of the setting up of two new paper mills and the enlargement of an already existing one. One of those industries will be located on the border between Brazil and Uruguay, not far from the Quaraí river basin, and part of the forests to sustain this industry will probably be planted in the basin. The plans of increasing area used for eucalyptus plantations coincide with heap criticism on eucalyptus plantations by environmentalists around the world and specifically in Brazil for its high water consumption, and for alleged impacts on biodiversity.

Eucalyptus trees certainly have an impact on water yield as was shown by paired catchment studies and analysis of stream flow data after afforestation or deforestation in several regions in different climatic regions (Andréassian, 2004; Cornish and Vertessy, 2001; Engel et al., 2005; Scott and Lesch, 1997; Sikka et al., 2003). In this sense eucalyptus plantations have similar impacts as other types of forests (Andréassian, 2004).

According to several review studies, the most recent of them being by Andréassian (2004), trees generally use more water than herbaceous species and the afforestation of a catchment previously covered with short vegetation reduces water yield. The impact of forests on floods is to reduce low return period events. Long return period floods seem not to be significantly affected by afforestation or deforestation (Andréassian, 2004). The impact of reforestation on low flows is to decrease low flow while deforestation increases low flows.

The impact of vegetation change seem to be more pronounced in watersheds with deep or very deep soils, where deep-rooted trees have advantages over shallow-rooted grass species in terms of access to water during droughts. The effects of reforestation or deforestation tend to be higher in regions with seasonal rainfalls, when soil water reserves are replenished, and periods with water deficits, when deep soil water is only available to deep-rooted trees (Andréassian, 2004).

There are suspicions that eucalyptus forests can impact water resources more than indigenous forests. Several studies carried out at different regions of the world lead to a suspicion of eucalyptus being major water consumer vegetation. These opinions are based on several studies and by local observation or anecdotal stories of drying out of swamps, wells or springs.

In South Africa Scott and Lesch (1997) described the impacts of eucalyptus afforestation in a 26.2 ha watershed which receives an average of 1167 mm of yearly rainfall and which is subject to 1723

potential evaporation (based on A pan measurements). According to these authors, afforestation of the entire catchment with eucalyptus caused a significant decrease in stream flow three years after planting and forced the stream to dry up completely in the ninth year after planting. More strikingly, perennial stream flow did not return until five years after the plantation was completely clear felled. However, the authors call attention to the fact that the practices used during the afforestation experiment were not representative of those used currently in South African forest industry. While during the experiment the plantation occupied the whole catchment area, the current practice plantations do not use riparian areas, which are kept open under indigenous vegetation. Current practices also seldom occupy more than 75% of a single large catchment.

In India water use by eucalyptus in watersheds originally covered with grasslands has been studied by Sikka et al. (2003) who showed that the presence of the plantations could negatively affect hydroelectric power generation. Water balance studies using paired catchments (32 ha) methodology in a region with 1380 mm annual rainfall have shown that low flows could be reduced by a factor of 2 to 3.75 due to eucalyptus afforestation (Sikka et al., 2003).

In Australia several studies analyzed the impact of eucalyptus afforestation or deforestation on hydrology. One of the most interesting of these studies was published by Cornish and Vertessy (2001) who showed that increase in water yields followed clear felling of old-growth eucalypt forests in Eastern Australia. Forest regrowth resulted in substantial water yield reductions in most of the monitored catchments. Furthermore, Cornish and Vertessy (2001) were able to associate the magnitude of the impacts with forest soil depth, growth rate, and canopy cover. Soil depth seemed to be the most important of those variables, with larger impacts being observed at catchments with deep soils. Impacts of afforestation on catchments with shallow soils seemed to be more pronounced during storms than during low flow periods. Moreover, overall impacts of regrowth on water yield of one of the catchments with shallow soils have been shown to be not significant.

Most of the published studies were carried out in regions outside South America and in climatic regions which do not resemble that of the Quaraí basin, as South Africa, Australia and India. A study by Soares and Almeida (2001) in Brazil showed that evapotranspiration of a eucalyptus plantation was of the same order of magnitude as annual rainfall (~1400 mm) in a region of very deep soils and located in a more tropical region than the Quaraí river basin. Engel et al. (2005) describe a study carried out outside of Brazil, but in a region closer to the Quaraí river basin (in Argentina) than the one described above, where a very old eucalyptus forest has been monitored and compared to the neighbouring grassland vegetation in terms of water use. Their results showed that eucalyptus trees undoubtedly use more water for evapotranspiration than grasslands. Evapotranspiration from eucalyptus was so high it could only be maintained by reducing groundwater levels by more than 50 cm with respect to surrounding grassland.

Unfortunately no published results could be found on the impacts of eucalyptus growing in regions with hydrologic characteristics similar to that of the Quaraí river basin. Furthermore, no reasonable assessment of those impacts in the State Rio Grande do Sul, or in the whole South of Brazil, could be found. In the absence of sound scientific experiments the local debate about the hydrological impacts of eucalyptus is now based more on passionate opinions and political views than on reality. For example, most of the environmentalists repeat what they found in a paper published in the 70's, blaming a single eucalyptus tree of consuming 36.5 thousand litres of water per year. By extrapolating this figure considering 1300 trees per hectare, they expect the evapotranspiration of eucalyptus plantations to be 4745 mm year⁻¹! This value is obviously a unreasonable overestimation, since solar radiation at the top of the atmosphere at the latitude of the South Brazil is equivalent to only 4600 mm year⁻¹.

Annual evapotranspiration in tropical forests is of the order of 1400 mm (Calder, 2002) and is limited by solar radiation. It is not reasonable to expect more evapotranspiration than this in any other kind of large scale vegetating surface in the world. This is truer for a region in the subtropics, where solar radiation is even lower. Calder (2002) presented a review of studies about eucalyptus and water and concluded that this species is not as harmful as often portrayed by environmentalists, though its hydrological disadvantages cannot be ignored.

From the results and reviews found in the recent literature the impacts of eucalyptus plantations on water balance of river basins seem to be more pronounced when some of the following characteristics are fulfilled:

- Deep soils
- Seasonal rainfalls
- Permeable soils
- Access to groundwater
- Forest management

The extent of the impacts will probably be related to the actual eucalyptus species that is planted, since there are a huge number of different species.

Rainfall in the Quaraí river basin is relatively well distributed over the year; however droughts can occur at any season. Soils are generally shallow and impervious. From these two characteristics it can be expected that afforestation will have less impact on stream flow that was observed in other basins. Other characteristics, particularly the sensitivity of the impacts to more or less access to groundwater sources for evaporation can be assessed through simulation of scenarios, as is shown in the following text.

The parameterization of eucalyptus forests that is adopted in the hydrological model affects the results. Within the MGB-IPH model evapotranspiration is calculated using the Penman-Monteith method, according to Shuttleworth (1993). Parameters that affect evapotranspiration are: surface resistance in well watered soil conditions (r_s), Leaf Area Index (LAI), albedo, and vegetation height.

Root depth differences between different types of vegetation can also affect evapotranspiration. Several authors show that evapotranspiration from eucalyptus can be especially high if the roots have access to water stored in deep soils or to groundwater. Therefore, to represent vegetation with very deep roots, the parameter W_m , related to water holding capacity in the soil, should be increased.

Following this considerations the following parameters were adopted to represent eucalyptus forests within the MGB-IPH model. The next paragraphs are summarized in Table 2-24, which shows the adopted values and compares them to values used in the simulation for other types of vegetation.

Bulk surface resistance or canopy resistance controls the capability of the vegetation to transfer water from the soil to the air surrounding the leaves. When the soil beneath the vegetation is not dry, surface resistance takes a minimum value, which is a characteristic of the vegetation itself. We used values of minimum surface resistance in accordance with published results (Kelliher et al., 1995; Shuttleworth, 1993).

Published values for minimum surface resistance for eucalyptus vary among species and according to the region where measurements were taken. Kelliher et al. (1995) suggests a value of canopy conductance which corresponds to 58.8 s m^{-1} of surface resistance, and they refer measurements made in Australia. Measurements in a *Eucalyptus grandis* plantation in Brazil resulted in minimum canopy resistance of 57.8 s m^{-1} (Mielke et al., 1999). Both results are lower than that normally used for natural forests, which are around 100 s m^{-1} ; and are even lower than reference values used for grass: 70 s m^{-1} (Shuttleworth, 1993). A more recent paper published with data from Brazil suggests values as low as 33 s m^{-1} for *Eucalyptus grandis* in a very deep soil (Soares and Almeida, 2001). For simulations in MGB-IPH model we adopted the lowest of those values (33 s m^{-1}) in order to represent the worst situation scenario.

LAI of Eucalyptus is in the range of 2 to 5.8, according to results published by several authors (Kelliher et al., 1995; Soares and Almeida, 2001; Stape et al., 2004). The LAI value adopted for Eucalyptus plantations in the model was the maximum found in literature (5.8), and was adopted throughout the year, in order to maximize losses of evaporation of intercepted rainfall water.

No specific values for albedo of eucalyptus plantations were found. Its value is probably around 0.13, as is normally adopted for natural forests in tropical regions. A value of 0.10 was adopted in the model to represent the worst situation scenario, since this value is typical for water surfaces, and will probably overestimate evapotranspiration.

Table 2-24 Parameter values related to vegetation types adopted in the MGB-IPH model (values for Eucalyptus have been defined in order to create a maximized evapotranspiration scenario)

Vegetation type	Minimum surface resistance (s.m ⁻¹)	LAI	Albedo	Height (m)
Pasture	60 to 90	1 to 6	0.13 to 0.17	1.0
Forest	90	3 to 6	0.13	9.0
Water	0	-	0.1	0.05
<i>Eucalyptus</i>	33	5.8	0.1	9.0

Concerning the extent of land use change, a very drastic land use change scenario was defined in which it was considered that 10% of the area currently covered with grasses or pasture in the Quaraí river basin would be turned into eucalyptus plantations. This would mean a profound change in land cover over 1312 km² of the 14800 km² large drainage area. This area ought to be as much as necessary to feed a pulpwood processing industry unit, which is estimated to be 120 thousand hectares – or 1200 km² – in this region.

Eucalypt plantations have a cycle of several years, from plantation until clear cutting, and then again regrowth from the trunks, until a new clear cutting. It is expected that hydrological impacts vary along this cycle. However, in the scenarios simulated here it was considered that the eucalypt plantations were steady and always at its maximum impact condition.

A preliminary estimate of the impact of this change on the annual water runoff can be made by using the rough figures by Bosch and Hewlett (1982). These authors suggested a 300 to 400 mm yr⁻¹ reduction in stream flow due to afforestation with eucalypt or pine. If we consider that the change affects less than 10% of the basin area, an annual stream flow reduction of not more than 30 to 40 mm should be expected. At the gauging station of Artigas/Quaraí the average annual runoff is of the order of 660 mm year⁻¹. This means that a reduction of 35 mm in annual runoff in this region would represent a 5% decrease in average stream flow.

Due to the shallow soils present in the Quaraí river basin the impacts of reforestation will probably be more pronounced on storm flow than on low flows, as implied by observations in other basins, particularly by Cornish and Vertessy (2001).

Due to the importance that the access to groundwater by eucalyptus trees has on evapotranspiration, three different sub-scenarios have been defined: 7A, 7B and 7C.

In scenario 7A there was no access from eucalyptus trees to groundwater. This scenario corresponds to a situation in which the planted forests are managed in order to avoid parts of the basin where groundwater is shallow, like swamps and regions close to the drainage network. In scenario 7B a moderate access to groundwater was considered. A maximum upward hydraulic conductivity of 0.08 mm day⁻¹ was considered to happen from the aquifer to the soil when the soil was dry. This value was chosen because it is the same as the downward hydraulic conductivity (from the soil layer to the aquifer) which was obtained during model calibration in WP3. In scenario 7C a facilitated access to groundwater was considered. The maximum upward hydraulic conductivity was raised to 2 mm day⁻¹. This value was chosen to represent an extreme scenario, since it is much higher than the expected hydraulic conductivity.

2.5.2.3 Water resources developments

Cultivation of rice has been an important economic activity in South Brazil for the last 100 years. In the Quaraí basin region this type of agriculture is restricted to lower parts of the basin and is combined with livestock breeding.

Since decades rice farmers have built small reservoirs to store water during the winter to supply it to the rice fields during the summer. In the analysis of the basin 402 reservoirs with more than 3 ha of surface area were identified. The surface area of the largest is 845 ha and 34 are larger than 100 ha. Figure 2.93 shows the distribution of surface areas of those 402 reservoirs. It can be seen that the median reservoir area is somewhat more than 20 ha.

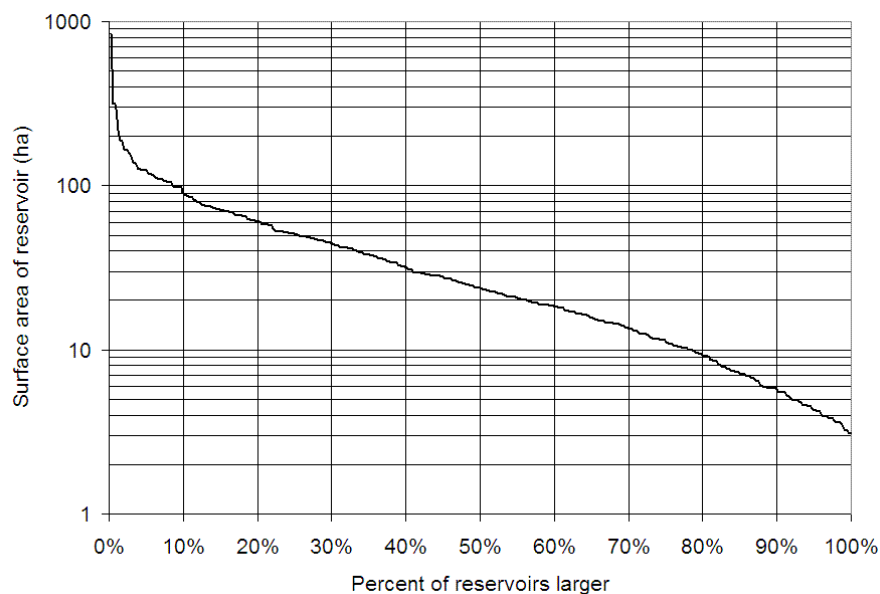


Figure 2.93 Cumulative distribution of reservoir area for 402 reservoirs (surface > 3 ha) in the Quaraí river basin

Five different scenarios had to do with water resources development. Table 2-23 shows the description of the scenarios and it can be seen that scenarios 1 to 5 are related to the presence or absence of water resources structures related to irrigation.

2.5.2.4 Changes in water demands

Population is expected to grow very slowly in the Quaraí river basin. Cities in Uruguay and Brazil are experiencing a standstill in population during the last decades, and rural population is possibly more close to a tendency to decrease than to increase.

The most impacting water demand in the basin is rice irrigation, and this use is already limited by water availability. Therefore water demands can hardly be expected to rise.

2.5.3 Scenario impact assessment

2.5.3.1 Methods used for impact assessment

A MGB-IPH

The hydrological model used in this work package is the same described in WP3: the large scale distributed hydrological model MGB-IPH. The model can be classified as a Hydrology Response Unit model, according to the classification proposed by Beven (2001). The MGB-IPH model is composed of modules for calculation of soil water budget, evapotranspiration, flow propagation within a catchment, and flow routing through the drainage network. The drainage basin is divided into elements of area connected by channels, with vegetation and land use within each element categorized into one or more classes, the number of vegetation and land use types being at the choice of the user. In its original form (Collischonn et al., 2007), the model divides the basin in regular square cells 10x10 km, or 0.1 x 0.1 degrees in size. For the Quaraí basin application a different approach, in which the basin was divided in small catchments, instead of square cells, was used.

The MGB-IPH model uses the Grouped Response Unit (GRU) approach (Kouwen et al., 1993) for hydrological classification of all areas with a similar combination of soil and land cover without consideration of its localization inside the catchment. A catchment contains a limited number of distinct GRUs. Soil water budget is computed for each GRU, and runoff generated from the different

GRUs in the catchment is then summed and routed through the river network. This approach has been used by several large scale hydrological models, such as VIC (Liang et al., 1994; Nijssen et al., 1997; Wood et al., 1992) and WATFLOOD (Soulis et al., 2004).

For the assessment of change effects related to water use the model was specially adapted to represent the small farm reservoirs and the water use in rice fields, as described in WP3.

For the assessment of change effects related to land use the parameters of the vegetation were changed in order to represent the new type of vegetation.

For the assessment of change effects related to climate change, the model inputs were changed and the differences in outputs were assessed.

The model has similar limitations as most hydrological models, but in the case of application in the Quaraí river basin application the most important limitation came from the low stream flow data availability. The model could only be calibrated using a single gauging station for comparison of calculated and observed stream flow. This gauging station is located in the upper part of the basin, controlling more or less one third of the basin area.

(i) Inputs

Data requirements of the MGB-IPH hydrological model are: digital elevation model (DEM); land use; vegetation classes; soil types; river cross-sections; reservoir characteristics; rainfall; stream flow; water quality data; temperature; humidity; atmospheric pressure; radiation; and wind velocity. Data sources were described in WP3.

(ii) Results

The main output of the MGB-IPH hydrological model consists of time series of discharge at several locations on the basin. The model was calibrated with data reflecting the actual situation in the basin, with widespread use of water for irrigation and with the presence of a large number of small reservoirs. We used this scenario to perform the calibration of the model parameters, since observed stream flow data are influenced by the presence of the reservoirs and water uses. Results of the calibration and validation of the model are described in the report for WP3.

(iii) Baseline

The hydrological model was calibrated, taking into consideration the presence of hundreds of small farm reservoirs and rice fields, because these influence the observed stream flow. After the model was calibrated the reservoirs and water abstractions for rice irrigation were removed from the simulation. This new scenario was run to generate the baseline conditions with which every other scenario was compared.

2.5.3.2 Separate effects

A Climate change

In the Quaraí river basin the sensitivity of the stream flow was evaluated by: changing the input data (precipitation and temperature) by a scaling factor; running the model with the optimized parameter values; and then comparing the modelled stream flow for the changed input data with the modelled stream flow using the original data (using data from 1980 to 2000).

Precipitation data were changed by -20%; -10%; -5%; -1%; +1%; +5%; +10%; and +20%. Temperature data were changed from -3 to +3 °C in steps of 1 °C.

Figure 2.94 shows the relation between simulated changes in precipitation ΔP and stream flow changes ΔQ . The three lines show the effect of precipitation changes on average stream flow (red line with triangles), on high flows – as taken from the 5% exceedance time from the flow duration curve (black line), and on the low flows – as taken from the 95% exceedance time (blue line with squares). It can be seen that a 10% change in rainfall results in 18.5% change in medium stream flow. Low flows

are less susceptible to changes in rainfall, showing approximately 13% increase when rainfall is increased by 10%.

This result suggests that the Quaraí river basin is sensitive to rainfall change; however most of the changes are perceptible in medium to high flows. This result may be related to the characteristics of the basin (shallow soils and low base flows).

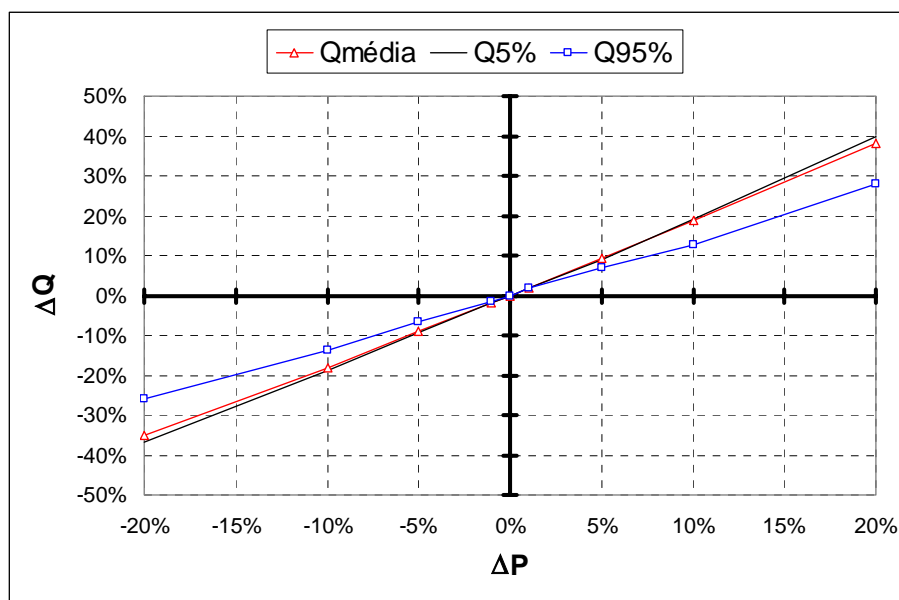


Figure 2.94 Relative changes in stream flow of the Quaraí River related to changes in rainfall

Figure 2.95 shows the relation between simulated changes in temperature ΔT and stream flow changes ΔQ . The three lines show the effect of temperature changes on average stream flow (red line with triangles), on high flows – as taken from the 5% exceedance time from the flow duration curve (black line), and on the low flows – as taken from the 95% exceedance time (blue line with squares). It can be seen that a 2°C increase in temperature results in a 4% decrease in medium stream flow.

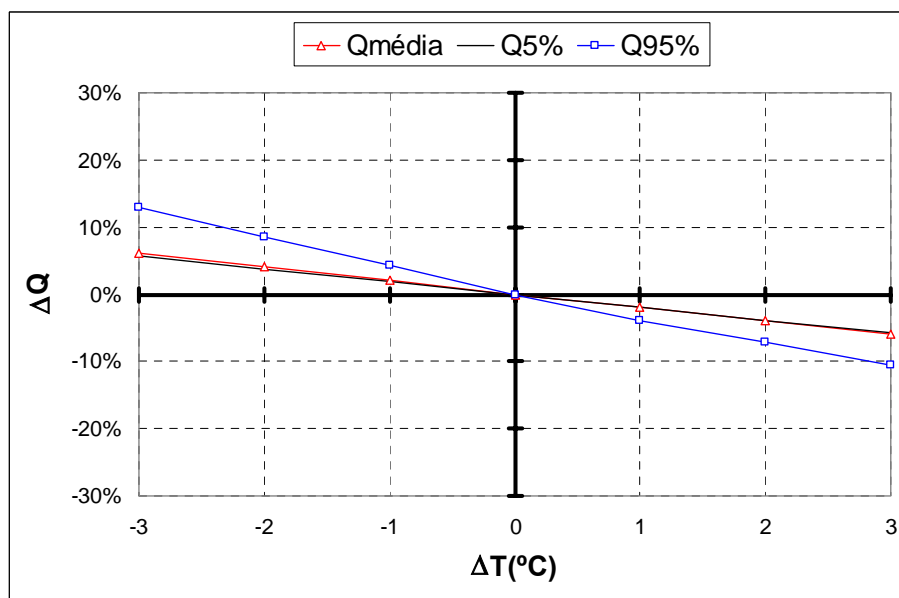


Figure 2.95 Relative changes in stream flow of the Quaraí River related to changes in temperature

Low flows are more sensitive to modifications in the temperature. This can be explained by the fact that evapotranspiration is directly related to temperature, and during non-rainy days, the evapotranspiration rate modifies the soil's moisture. Since the watershed has shallow soils, in a rainy

event these soils are superficially saturated, and thus the previous moisture has less influence in the total volume superficially drained on mean and maximum discharges. On the other hand, the percolation of the volume in the soil to the aquifer depends on the moisture of the soil. So, alterations in the temperature cause more impact on the recharge of the aquifer and indirectly on minimum discharges.

Other authors have shown that the sensibility of a basin to changes in precipitation and temperature is strongly related to the basin characteristics (Chiew, 2006). It is expected that basins with lower runoff coefficients will be more sensitive to climatic changes. The stream flow elasticity related to changes in precipitation can be as high as 4 for basins with low runoff coefficient, meaning that a 10 % decrease in precipitation would lead to a 40% decrease in stream flow. It seems, from these results, that the Quaraí river basin has relatively low sensibility to changes in both precipitation, and this is probably related to its high runoff coefficient.

The monthly results of modification in the mean temperature and precipitation for 2050 in the region of Quaraí watershed obtained by nine GCMs for each one of the six scenarios had been used to disturb the series observed and simulate the impact on the hydrologic regime through MGB-IPH model. Figure 6 shows the impact on the flow duration curve of the river Quaraí. Given the large number of climatic models and scenarios (54) the changes in flow duration curves are shown as the scenario and model average, and the 10 % and 90 % quantiles of all simulations.

It can be seen in Figure 2.96 that expected changes are higher for median to high flows. Median flows are expected to change in the range from -20% to +45%, as can be seen for the 50 % duration in Figure 2.96. The average of the changes predicted by different models and scenarios for Q_{50} (the median flow) is close to +10 %, indicating that an increase in median flow is to be expected.

Low flows, as taken by the Q_{90} flow from the duration curve, are expected to change less than median flows. Only 10 % of the model and scenario combinations predict that Q_{90} will decrease more than approximately 17 %. On the other hand only 10 % of the model and scenario combinations predict that Q_{90} will increase by more than approximately 25 %. The average of predicted changes in Q_{90} is close to 5%. Therefore, an increase is to be expected in low flows, although this increase will be not as clear as for medium and higher flows.

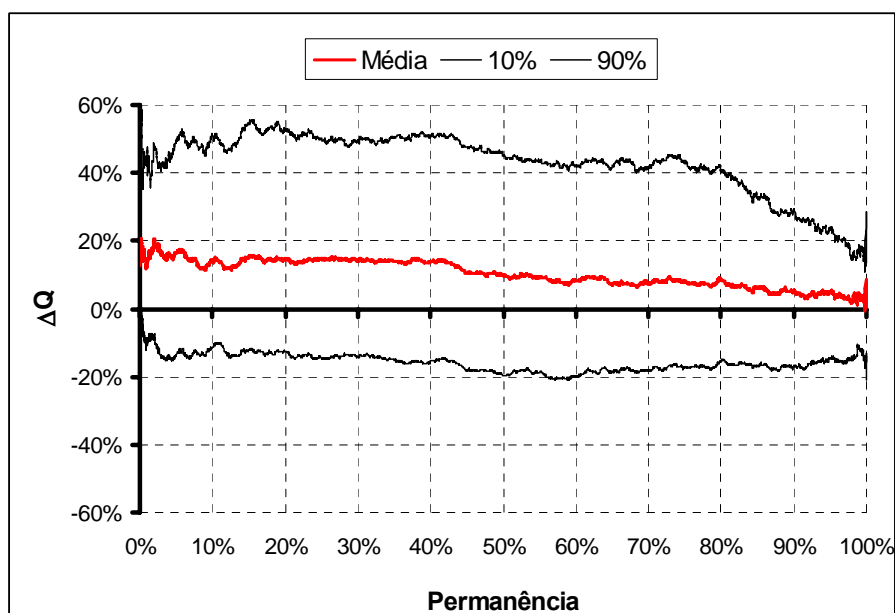


Figure 2.96 Climate change effects on the flow duration curve of the Quaraí River
The red line is the average change for all models and scenarios, the lower line is the 10% quantile and the upper line is the 90% quantile

Especially important in the Quaraí river basin are low flows during the austral summer months, during which a water deficit often occurs in the basin, due to the huge amount of water that is used to irrigate

the rice fields. Therefore, the climatic change results have been calculated for low flows observed during different months. Flow duration curves have been constructed for each month of the year and the changes in the Q95 flow from the duration curve have been calculated for each climatic model, scenario and month. The results are summarized in Figure 2.97. The most distinctive changes are increases of the low flows during the summer months; however the dispersion of the results is large during these months.

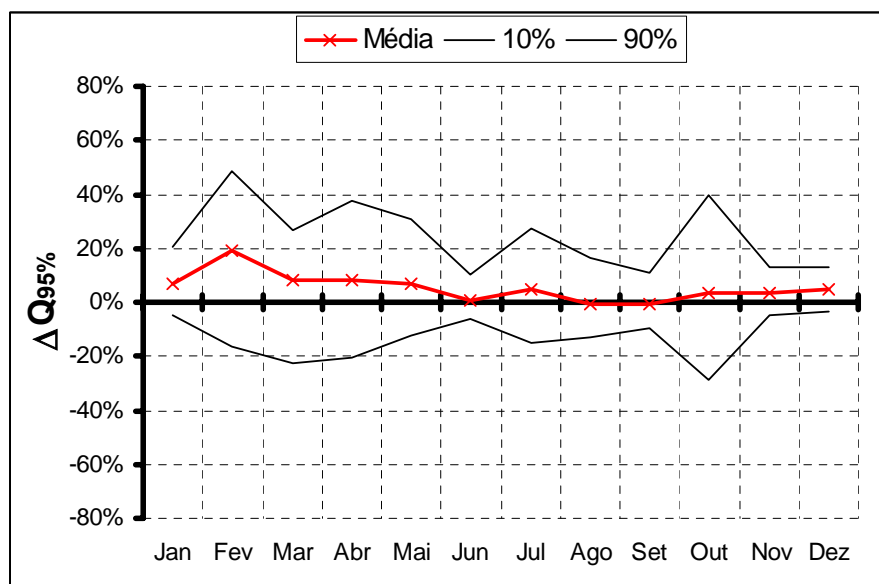


Figure 2.97 Changes in low flows (Q95) for each month using climate change prediction for 2050

From the climatic change results it seems that both increases and decreases can be expected in low flows of the river Quaraí during the more critical part of the year – the summer. The sensitivity analysis showed that due to its high runoff coefficient the basin is on the lower range of susceptibility to climate change. The model runs with climatic change scenarios drawn from MAGICC/SCENGEN suggest that the future climate will result in increases of stream flow in the Quaraí River. Low flows, however, will experiment only slight changes, if any.

It should be noted that this analysis has several limitations. In particular, no assessment of a possible change in rainfall probability distribution was made. It is sometimes stated that climate change will be more clearly observed in terms of changes in the extremes, instead of average values of variables.

B Land use change

The land use change scenarios consisted of changes from pasture to forest plantations, which will be possibly happening in the short future in the region. In these scenarios it was considered that 10% of the land currently covered with pasture would be transformed into eucalyptus plantations in the Quaraí basin. Under this assumption three sub-scenarios were simulated. Scenario 7A considered that the eucalyptus plantations would be managed in order to avoid the contact of the trees to groundwater. Scenario 7B considered that the trees had a moderate access to groundwater and scenario 7C considered that the trees had a facilitated access to groundwater.

Results obtained during model simulations of these scenarios are presented in the following tables and figures. Table 2-25 presents values of average stream flow and two relatively extreme values on the flow duration curve - Q_{95} and Q_{10} – of the Quaraí River at Quaraí, which corresponds more or less to the upper one third of the basin. According to results in scenario 7A, the natural average stream flow of $98.4 \text{ m}^3 \text{ s}^{-1}$ would be reduced to $92.3 \text{ m}^3 \text{ s}^{-1}$ if 10% of the basin pasture area should be replaced by eucalyptus plantations. Low flows would be reduced from 1 to $0.96 \text{ m}^3 \text{ s}^{-1}$ and high flows would also be slightly reduced.

It can be deduced from Table 2-25, that the most impressive change would happen in low flows if the eucalyptus forests had access to groundwater. In scenario 7B (moderate access to groundwater) the reference discharge Q_{95} would be reduced from 1 to $0.71 \text{ m}^3 \text{ s}^{-1}$ while in scenario 7C the new Q_{95} would be only $0.09 \text{ m}^3 \text{ s}^{-1}$.

Table 2-25 Summary of land use change scenario impact assessment at Quaraí (gauging station)
values are in $\text{m}^3 \text{ s}^{-1}$

Scenario	Mean stream flow	Q_{95}	Q_{10}
Natural (scenario 2)	98.4	1.00	253
Eucalyptus no access to groundwater (scenario 7A)	92.3	0.96	235
Eucalyptus moderate access to groundwater (scenario 7B)	91.6	0.71	233
Eucalyptus facilitated access to groundwater (scenario 7C)	90.9	0.09	233

Table 2-26 shows the same results in terms of relative change from the natural condition. It can be seen that changes in average stream flow will be of 6% to 8% reductions, depending on the scenario. Impact on relatively high flows (Q_{10}) would be slightly higher, while impacts on low flows are very dependent on the adopted scenario.

In scenario 7A the reduction of low flows following the eucalyptus afforestation would be of 4%. This reduction is due to larger interception, lower surface resistance and to the other parameter values adopted to represent eucalyptus forests, which boost evapotranspiration. However, the impact is relatively limited because soil moisture deficits restrict evapotranspiration. In scenario 7B it was allowed that upward flow from groundwater to the soil layer partially replenishes soil moisture. As a result the impact on low flows was much higher (29%). Finally, in scenario 7C a very easy access to groundwater was considered and the land use change in less than 10% of the basin drainage area had an impact of more than 90% in low flows.

It is remarkable that results obtained with the hydrological model confirmed that the change in stream flow would be of the order of 5%, as predicted using the values suggested by Bosch and Hewlett (1982).

Table 2-26 Summary of land use change scenario impact assessment at Quaraí (gauging station)
values are in % of change compared to the natural scenario

Scenario	Mean stream flow	Q_{95}	Q_{10}
Eucalyptus no access to groundwater (scenario 7A)	-6%	-4%	-7%
Eucalyptus moderate access to groundwater (scenario 7B)	-7%	-29%	-8%
Eucalyptus facilitated access to groundwater (scenario 7C)	-8%	-91%	-8%

Table 2-27 presents values of average stream flow, Q_{95} and Q_{10} of the Quaraí River at its confluence with the Uruguay River at Barra do Quaraí. According to results in scenario 7A, the natural average stream flow of $304.4 \text{ m}^3 \text{ s}^{-1}$ would be reduced to $285.9 \text{ m}^3 \text{ s}^{-1}$ if 10% of the basin pasture area should be replaced by eucalyptus plantations. Low flows would be reduced from 4.93 to $4.74 \text{ m}^3 \text{ s}^{-1}$ and high flows would also be slightly reduced.

Again in this case, the most impressive change would happen in low flows if the eucalyptus forests had access to groundwater. In scenario 7B (moderate access to groundwater) the reference discharge Q_{95} would be reduced from 4.93 to $3.97 \text{ m}^3 \text{ s}^{-1}$ while in scenario 7C the new Q_{95} would be only $1.60 \text{ m}^3 \text{ s}^{-1}$.

Table 2-27 Summary of land use change scenario impact assessment at Barra do Quaraí (outlet of the Quaraí river basin)
values are in $\text{m}^3 \text{s}^{-1}$

Scenario	Mean streamflow	Q ₉₅	Q ₁₀
Natural (scenario 2)	304.4	4.93	841
Eucalyptus no access to groundwater (scenario 7A)	285.9	4.74	778
Eucalyptus moderate access to groundwater (scenario 7B)	283.7	3.97	773
Eucalyptus facilitated access to groundwater (scenario 7C)	281.7	1.60	771

Table 2-28 shows that relative changes at Barra do Quaraí would follow the general trend observed at Quaraí, with larger impacts during storm flow than during low flows if we consider scenario 7A. A 6% decrease in average stream flow would be probably impossible to detect with the uncertainty in discharge measurements.

However, results from scenarios 7B and 7C show that when relatively free access to groundwater is allowed, the impact of eucalyptus plantations can be practically as high as water abstractions for rice field irrigation.

Table 2-28 Summary of land use change scenario impact assessment at Barra do Quaraí (outlet of the Quaraí river basin)
values are in % change compared to the natural scenario

Scenario	Mean stream flow	Q ₉₅	Q ₁₀
Eucalyptus no access to groundwater (scenario 7A)	-6%	-4%	-7%
Eucalyptus moderate access to groundwater (scenario 7B)	-7%	-20%	-8%
Eucalyptus facilitated access to groundwater (scenario 7C)	-7%	-68%	-8%

Figure 2.98 shows the flow duration curves of the river Quaraí at Barra do Quaraí under the natural condition, without water abstractions, reservoirs and land use change, and the three scenarios of partial land use change with eucalyptus plantations over 10% of the area currently used as pasture. It is clear that differences between scenarios 7A and 2 are barely visible.

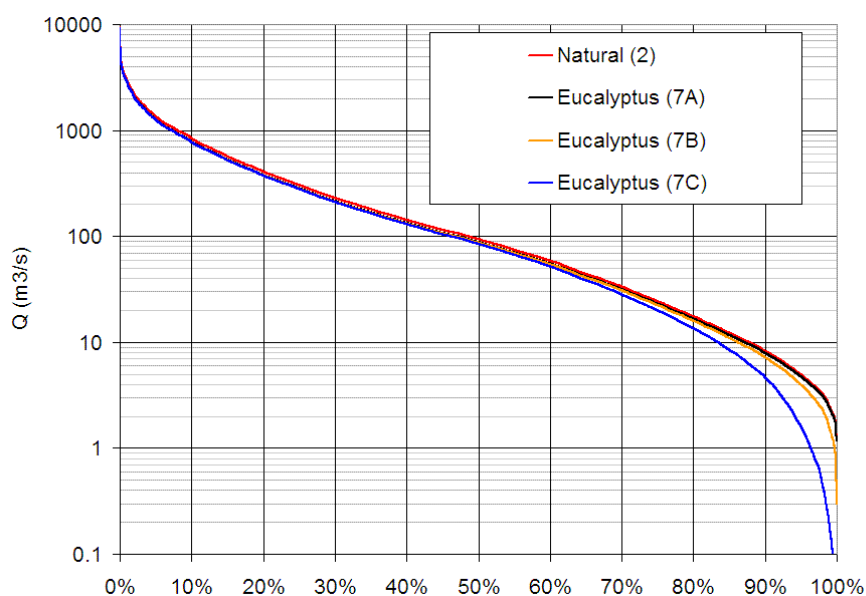


Figure 2.98 Flow duration curves of the Quaraí River at Barra do Quaraí
Under natural conditions – scenario 2 (red line); eucalyptus plantation over 10% of the current pasture land (i) without access from the trees to groundwater – scenario 7A (black line), (ii) with moderate access

to groundwater – scenario 7B (yellow line) and (iii) with facilitated access to groundwater – scenario 7B (blue line)

A moderate access to groundwater by the eucalyptus trees simulated in scenario 7B will result in a clear difference in flow duration curves for discharge values below the Q_{90} .

The results of the land use change scenarios confirm that afforestation with eucalyptus will reduce average stream flow, as is expected for any other kind of forest replacing grasslands. The extent of this impact is relatively low if the forests are planted and managed in order to avoid access to shallow unconfined aquifers. In this case the impact will be more pronounced as a reduction of storm flows than as a reduction in base flow. It can be said that without access to groundwater large scale eucalyptus plantations will have an impact on stream flow that will be undistinguishable, due to the year to year variability and the uncertainty of discharge measurements.

On the other hand, if the eucalyptus forests will be planted in areas of shallow groundwater, the impact will probably be higher. In this case the impacts will be clearly visible on the low flows, which are already very low in the region. If this happens the water availability during the summer, which is already critical, will become worse.

From the hydrological point of view it should be emphasized that planted forests should be avoided in riparian areas, and areas close to the wetlands or swamps. Due to the shallow soils of the basin, the impact of afforestation should be minimal if this recommendation is to be followed.

C Water resources developments

Five different scenarios had to do with water resources development. Table 2-23 (page 2-102) shows the description of the scenarios and it can be seen that scenarios 1 to 5 are related to the presence or absence of water resources structures related to irrigation.

The first scenario, which was used for calibration, included reservoirs, river abstractions for rice field irrigation, reservoir water abstractions and return flows from the rice fields. The second scenario was used to generate the baseline stream flow time series, describing as much as possible the natural situation of the basin. In this scenario reservoirs, water abstractions and return flows were excluded from the simulation.

Results of the comparison between stream flows in scenarios 1 and 2 allow the analysis of the impact of the irrigation activities in the basin. Figure 2.99 shows the difference in flow duration curves for scenarios 1 and 2 in Quaraí, and Figure 2.100 shows the differences in Barra do Quaraí, at the river mouth.

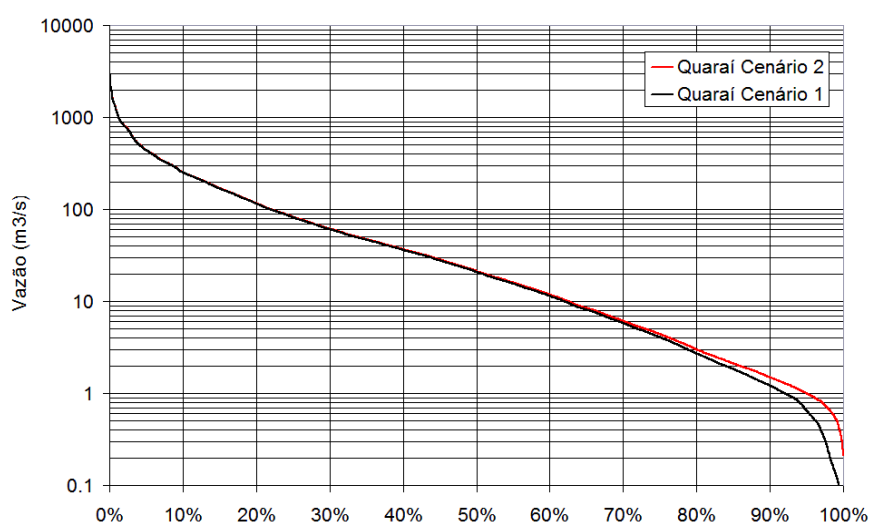


Figure 2.99 Flow duration curves of the Quaraí River at Quaraí/Artigas Scenario 1 (with irrigation and reservoirs - black line) and scenario 2 (natural condition - red line)

The impact of irrigation activities is clearly visible in both the upstream part (Figure 2.99) and downstream part (Figure 2.100) of the basin. Low flows are dramatically decreased at the river mouth, and it is clear that the Quaraí River is probably drying up sometimes.

The reference stream flow Q_{90} at the river outlet, in Barra do Quaraí, in the natural condition of the basin (red line in Figure 2.100) is, approximately, $8 \text{ m}^3 \text{ s}^{-1}$ while in scenario 1, which includes water abstractions and reservoirs, the same reference flow is close to $3 \text{ m}^3 \text{ s}^{-1}$. An even more dramatic difference occurs for Q_{95} , with a drop from 4 to $0.2 \text{ m}^3 \text{ s}^{-1}$, which is practically no flow at all for a river that carries flood flows of the order of several thousands of $\text{m}^3 \text{ s}^{-1}$.

The model simulation results show that the river Quaraí and some of its tributaries eventually went dry during some parts of drier summers. When this occurred, the abstractions were reduced and the rice fields were irrigated with less water than really needed.

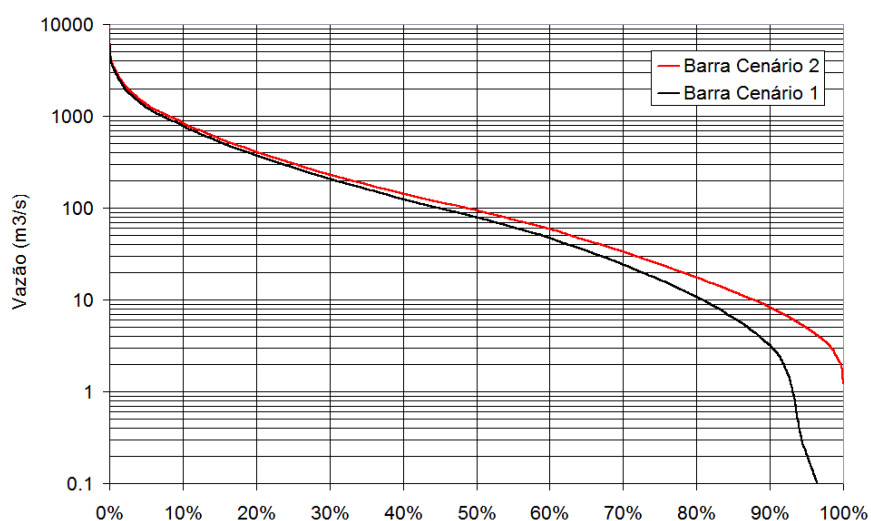
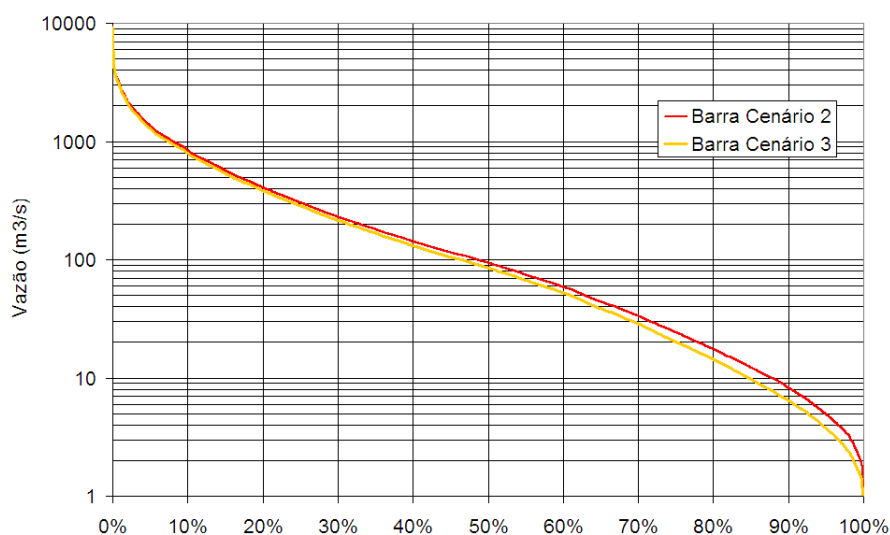


Figure 2.100 Flow duration curves of the Quaraí River at Barra do Quaraí (river outlet) Scenario 1 (with irrigation and reservoirs - black line) and scenario 2 (natural condition - red line)

The third scenario is similar to the second, except for the reservoirs, which were included in the simulations. The aim of this scenario was to generate stream flow time series which could be compared to the ones obtained with the second scenario, so as to allow the analysis of the effect the reservoirs have on the main river stream flow. No water abstractions were included in the third scenario.

Most of the reservoirs in the region do not have any low flow discharge device, so the only possible outflows from the reservoirs occur during flow peaks, after the reservoir is filled. In the model, reservoirs were represented with no outflow during dry periods, and as could be expected the results of scenario 3 show a reduction in low flows, according to the flow duration curves shown in Figure 2.101. The overall effect of the reservoirs is a reduction of stream flow, which could also be expected because evaporation is increased by the available free water surface. The effect is limited because reservoirs only control around a fifth of the whole drainage basin.

The difference in the reference stream flow Q_{90} between scenario 2 (natural) and scenario 3 (with reservoirs but no water use) is $8 \text{ m}^3 \text{ s}^{-1}$ to $6 \text{ m}^3 \text{ s}^{-1}$.



**Figure 2.101 Flow duration curves of the Quaraí river at Barra do Quaraí (river outlet)
Scenario 3 (no irrigation, with reservoirs - yellow line) and scenario 2 (natural condition - red line)**

The fourth scenario was similar to the third, except for the water abstractions. Water abstractions in the Quaraí river basin are of two types: river abstractions and reservoir abstractions. In the fourth scenario only water abstractions from the reservoirs were included. The aim of this scenario was to analyze the impact of reservoir water abstractions have on stream flow of the main river, and differentiate them from abstractions from the river itself.

From the flow duration curves in Figure 2.102 it becomes clear that the water abstraction from the reservoirs is less impacting than the presence of the reservoirs themselves. The blue curve in this figure – which is the flow duration curve in scenario 4 (with reservoirs and with reservoir water abstractions) – is almost the same as the yellow curve, which is the result of scenario 3 (with reservoirs but with no water abstractions).

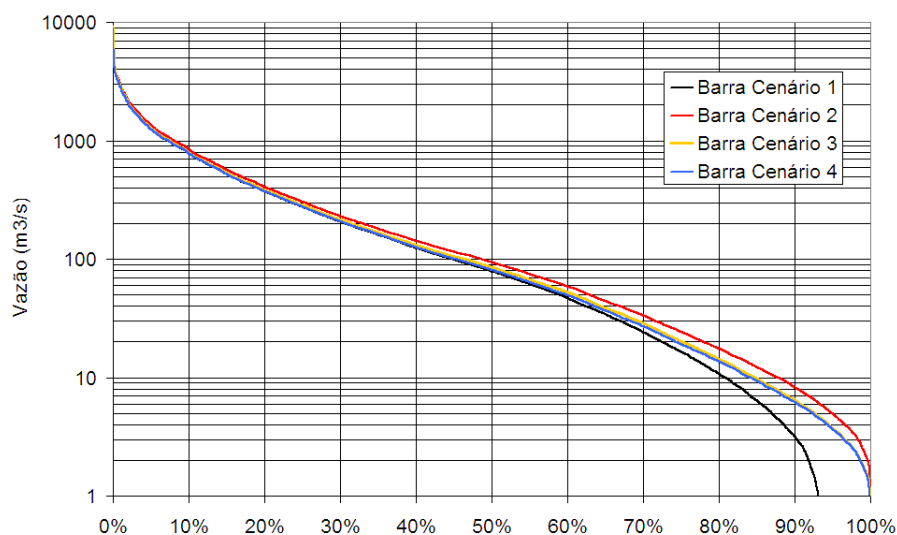


**Figure 2.102 Flow duration curves of the Quaraí River at Barra do Quaraí (river outlet)
Scenario 1 (actual situation, with reservoirs and abstractions – black line), scenario 2 (natural condition red line), scenario 3 (no irrigation, with reservoirs - yellow line) and scenario 4 (with reservoirs and water abstraction from reservoirs - blue line)**

Furthermore, by comparing scenarios 4 and 1 one can examine the relative impact of river water abstractions on the flow duration curves. It can be seen from table 1 that the only difference between

scenarios 1 and 4 is that no river water abstractions are considered in scenario 4. The large differences between flow duration curves for scenarios 1 and 4 and the little difference between scenarios 4 and 3 shows that the impact of the reservoir abstraction is negligible, when compared to the impact of the river abstractions. This result is in accordance with the local experience of the farmers, who very early realized that they needed reservoirs to store water, because the rivers had too low flows.

The fifth scenario included reservoirs and both types of water abstractions but did not include the return flow from the irrigated rice fields. The aim of this scenario was to analyze the impact of return flows on stream flows of the main river.

Scenario 5 is the most severe or pessimistic of all scenarios of water resource development because it imposes water withdrawals of the rivers and reservoirs, but does not consider the return flows from the rice fields. This scenario is similar to scenario 1. The only difference is the presence or absence of return flows, and the differences in flow duration curves can be used to analyze the impact of return flows on the water availability in the basin.

Figure 2.103 presents the flow duration curves for scenarios 1 and 5 at Barra do Quaraí. The two curves are very similar; however the scenario 5 flow duration curve is lower. This result is somewhat surprising, because if we consider a 1 mm day^{-1} return flow from the rice fields, which cover around 700 km^2 in the basin, the return flow alone is equivalent to more than $8 \text{ m}^3 \text{ s}^{-1}$. However, it needs to be remembered that during the driest summers the river actually went dry during the simulations, and the irrigation was temporarily stopped. So, the difference between scenarios 1 and 5 is not to be seen in the flow duration curve, but in the number of days with irrigation lower than needed.

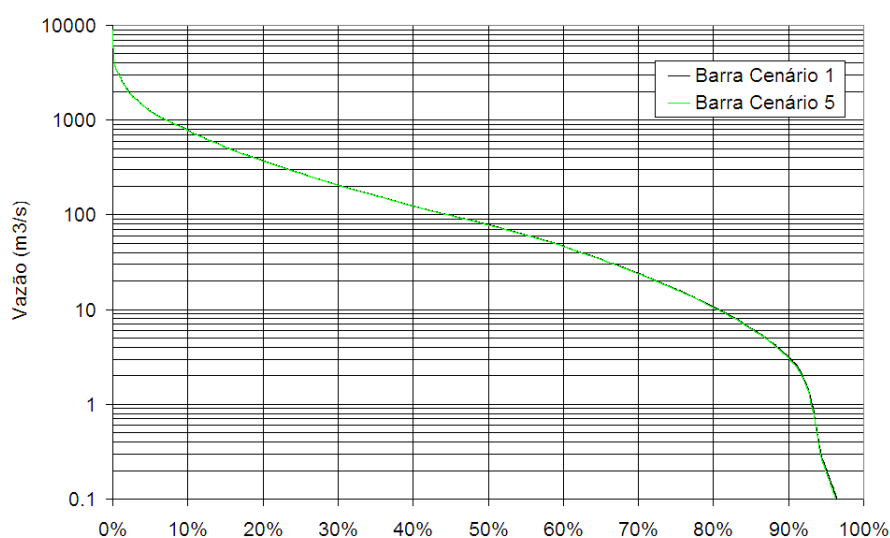


Figure 2.103 Flow duration curves of the Quaraí River at Barra do Quaraí (river outlet) Scenario 1 (actual situation, with reservoirs and abstractions – black line) and scenario 5 (actual situation, without return flows - blue line)

The conclusions about the scenario analysis related to water resources development in the basin is that the use of water already has a large impact on the river Quaraí. The very low base flows of the main river and its tributaries very early motivated the local farmers to build reservoirs for individual use. The impact of the use of the water of these reservoirs seems to be relatively small; however the impact of the presence of the reservoirs is not negligible.

The most important impact related to water resources use in the Quaraí river basin is the direct withdrawals of the rivers, which are drying the river out sometimes. The model results confirm the presence of conflicts among different water users (farmers and public supply) and between the users of the two involved countries. Results of the water resources development scenario confirm outcomes of a prior analysis, which suggested that water is the most important limiting factor to rice growing activity in the basin.

2.5.3.3 Combined effects

Due to the high number of simulated scenarios, and due to the complexity of each scenario, no combined effects have been explicitly simulated. However, an assessment of combined effects can be preliminary made considering that:

- Climatic changes will probably lead to increases in stream flow.
- Land use changes will probably lead to decreases in stream flow.
- Water availability already limits agriculture in the region, and farm reservoirs are used to store water during the winter to use it during the summer.

If the effects would be combined it cannot be clearly stated what the outcomes would be, because the effects of land use and climatic change could counterbalance each other. Nevertheless the uncertainty in results of climatic change is high.

2.5.4 Vulnerability assessment

The people in the Quaraí river basin are exposed to changes in water availability and use. The region faces a situation where its most important economic activity - irrigated rice agriculture - is already limited by water availability. Any decrease in stream flow, especially during the summer months, will result in more frequent crop failures.

Considering that agriculture is the most important economic activity in the basin, the whole region is very sensitive to changes. Should climatic changes lead to lower stream flow availability, or should widespread changes from pastures to forests occur, possibly leading to reductions in base flows, than the local society will face a reduction in income.

In the case of land use change one could possibly consider that part of the reduction in income from agriculture will be counterbalanced by the earnings from forestry.

Farmers in the Quaraí river basin deal with frequent water shortages and droughts, and during the last decades they have learned to overcome this difficulties by storing water in small reservoirs distributed all over the basin, showing that they have the capacity to respond or handle the critical situations.

2.5.5 Conclusions

Scenarios of changes have been simulated for the Quaraí river basin. Changes of land use, climate and water resources use and reservation have been considered. The most important conclusions are summarized in the following paragraphs.

Results of the water resources development scenarios show that water is the most important limiting factor to rice growing activity in the basin. The sensibility of the Quaraí river stream flow to changes in temperature and precipitation was assessed, and compared to published analyses for other basins in the world. From this comparison it can be said that the Quaraí river basin is relatively less sensitive to climatic changes, and this is related to its high runoff coefficient.

The model runs with climatic change scenarios suggest that global warming will result in increases of stream flow in the Quaraí River. Low flows, however, will experiment only slight changes, if any.

The results of the land use change scenarios confirm that afforestation with eucalyptus will reduce average stream flow. The extend of this impact will be relatively low if the forests are planted and managed in order to avoid access to shallow unconfined aquifers. In this case the impacts will be undistinguishable, due to the year to year variability and the uncertainty of discharge measurements. On the other hand, if the eucalyptus forests will be planted in areas of shallow groundwater, the impact will be clearly visible on the low flows, which are already very low in the region.

If the effects would be combined it cannot be clearly stated what the outcomes would be, because the effects of land use and climatic change could counterbalance each other. Nevertheless the uncertainty in results of climatic change is high.

Large uncertainties obviously exist in the analyses shown here. The largest uncertainties are probably present in the climatic change scenarios. Although most climatic models agree suggesting that the region's future climate will be moister and warmer, large differences exist between models and scenarios. Base flows can be reduced or increased in the future in response to the predicted climatic changes, depending on the relative impact of temperature increase, which has a negative impact of stream flow, and precipitation increase, which has a positive impact on stream flow.

Uncertainties are relatively lower in the land use change scenarios. At least in this case the direction of change is known: stream flow will decrease if forests will substitute pastures. However the amount of change is not known accurately.

Relatively lower uncertainties are present in the simulation of water management strategies, however some important questions remain vague, as is the case of the evapotranspiration in rice fields, and the return flows from those fields.

If land use changes would occur in the basin, with eucalyptus plantations partly replacing pastures, than a recommendation should be drawn from this study: access to groundwater by the trees should be avoided by planting the trees far from natural drains and wetlands.

One could say that mitigation measures to reduce the vulnerability to climate are already needed in the basin, due to the frequent occurrence of droughts and floods. Therefore, structural and non-structural measures could be taken, which could result in less vulnerability to both climatic variability and climatic change.

2.6 CUAREIM RIVER BASIN (URUGUAY)

2.6.1 Introduction

Farming and the livestock industry in the Cuareim River basin have always suffered from climate variability and somehow, even though in an implicit way, they have incorporated that factor in the design and management of the production systems.

Nevertheless, in the past years, farmers have been suffering from a double pressure (that of the market and of climate change), increasing the level of risk to adverse climate events, for which they may not be prepared. Only when the agro-climate risk is quantified and considered explicitly in the design and management of the production system, it makes sense to take adaptation measures to climate change or to incorporate climate forecasts. Farming and livestock industry activities are planned with time horizons relatively short compared with the scales that are considered under scenarios of climate change. This is why it is impossible to expect to incorporate climate change information to their making-decision processes. Adaptation will occur if steps are taken to reduce the vulnerability to the current climate variability. As it is through extreme events that we will start to see and suffer the footprints of climate change, following the steps stated above will be the adaptation strategy.

In the Cuareim River basin the socio-economic impact of recurrent forage crisis are well noticed. In addition, this area of Uruguay presents special characteristics: shallow soils, big water deficits during summer even in “normal” years, the highest values of precipitation in the country, the largest interannual variability; the latter even increased in the past decades. Furthermore, it is the region with the highest climate seasonal predictability in the country, highest runoff coefficients and is an area with high topography that allows designing irrigation systems by gravity. From the production point of view, the soils are suitable for rice (already cultivated or not) that let us think of rice-grassland production systems that would jointly justify the cost of any necessary investments to implement them.

There are numerous studies related to the subject in the region and many reports promote irrigation. In particular, a recent thesis (Crisci et al., 2007) designed an irrigation system for the Tres Cruces river basin, subbasin of the Cuareim river basin, that could expand the current area of rice up to 70% with the capacity of irrigating grassland in rotation with rice.

The objective of this study is to contribute to the integral assessment of agro-climate risk in the current production system (individual reservoirs for rice and rain-fed grasslands) and of an alternative system (irrigation system at the basin level with two big reservoirs for rice and grasslands), considering the Tres Cruces basin as a study case, based on the analysis done by Crisci et al. (2007). It is also sought to estimate the value of water in the basin and to do a first approximation to the economic actors, determining who would be potential winners and losers if the alternative system were to be implemented.

Although the availability of water is already a limiting element in the production development the region, it is easy to prove that it is the result of insufficient storage capacity and not because of low water production.

The Tres Cruces basin has the following characteristics:

- (i) The area of the Tres Cruces basin is 1.466 km²
- (ii) The annual average rainfall is 1.400 mm
- (iii) The runoff coefficient can be estimated (in a conservative way) as 0,35

The average water production in the basin is therefore, approximately, $7,2 \times 10^8 \text{ m}^3$, while the sum of all the existing reservoirs in the basin (Table 2-29) is $4,2 \times 10^7 \text{ m}^3$, less than 10 % of average total water production. Although it is not recommended and even not possible to store all the water production, the basin is still far from depleting the resource.

That is why it is of interest to work with an expansion scenario of the storage capacity that is represented by the “alternative system”. This alternative system would approximately quadruplicate the storage capacity of the basin (see Table 2-30 page 2-128), increasing it to just above 20 % of total average water production estimated before. The alternative consists of two big reservoirs at the upper area of the basin (with much poorer and less expensive lands) and an ample gravity irrigation system that reaches an important area of the basin.

It is interesting to examine the alternative system of multisite reservoirs as a future scenario, in particular because it will not develop spontaneously without a governmental policy and intervention, since the management of the water in the basin at the basin level is beyond the possibilities of private agents. An example of the spontaneous development that arose from the initiative of private agents trying to solve the water availability at the parcel level, or the contiguous parcels, is what can be seen at the Brazilian margin of the Cuareim River Basin; in Figure 2.106 the many small reservoirs can be observed. It is important to state that the topography and the soils are different in both margins and therefore it is not possible to extrapolate either results or judgments.

For more details on the physical characteristics and climate of the Tres Cruces basin, refer to Crisci et al. (2007).

2.6.2 Scenario creation

2.6.2.1 Climate change

The Cuareim river basin lies within a region where climate change is already being experienced. This is even more noticeable in the variability than in the mean (IPCC, 2007). For instance, annual precipitation in the basin in the last 20 years was 13% higher than in the previous 20 years, while the interannual standard deviation for the same periods shows a 76% increase.

Not surprisingly then, impacts are already visible. The most vulnerable production sector is the livestock industry, since it depends almost entirely on precipitation for forage and drinking water. Summers show a climatologic deficit in the soil water balance, but droughts are becoming more severe and more frequent, generating social turbulence and claims to the central government. Irrigated crops, mostly rice and also sugar cane, are much less vulnerable to variability in precipitation because they depend on reservoirs and growers make annual decisions according to the available water.

Overall, water production in the basin is far from being the limiting factor, at least on the Uruguayan part. Shallow soils, steep slopes and relatively few reservoirs contribute to a large runoff. Under these circumstances, the most urgent need is to assess the vulnerability of current agricultural practices to climate variability and to analyze how better management of water resources (i.e. improved decision making, increased reservoir capacity) can generate a more resilient production system. In this context, climate change is extremely important, as it influences climate variability, and the basin does not suffer from a mean water deficit but rather from the complexity to deal with year to year variations. Climate scenarios were therefore synthesized reproducing relevant statistics from the past two decades to which the current production system is far too vulnerable.

2.6.2.2 Land use change

On top of the climate tendencies described in the previous section, recently the price of commodities has increased spectacularly, which has created an incentive for and the possibility of introducing irrigation in production systems where it is not the tradition (i.e. grasslands for cattle, summer crops other than rice and sugar cane).

Major tendencies in land use change reflect the pressure of forestry (in poorer soils) and summer crops (in deeper soils) over more traditional extensive livestock farms. In any case, the basin is still on a developing stage and water availability – not production – is clearly one of the limiting factors.

A scenario was therefore constructed assuming that all the land with suitable soil characteristic for farming will change from livestock breeding into summer crops in the Tres Cruces basin. Fortunately,

a detailed study to this point was readily available (Molfino et al., 2000). In this study, we worked only with rice crops since it is by far the most extended in the region and also the most water intensive crop. The growth rate of rice fields in time was fixed at historical values under the assumption that it reflects the capacity of the sector to expand. Figure 2.104 shows current cover of rice fields and its potential to expand in a sub-basin of the Cuareim River.

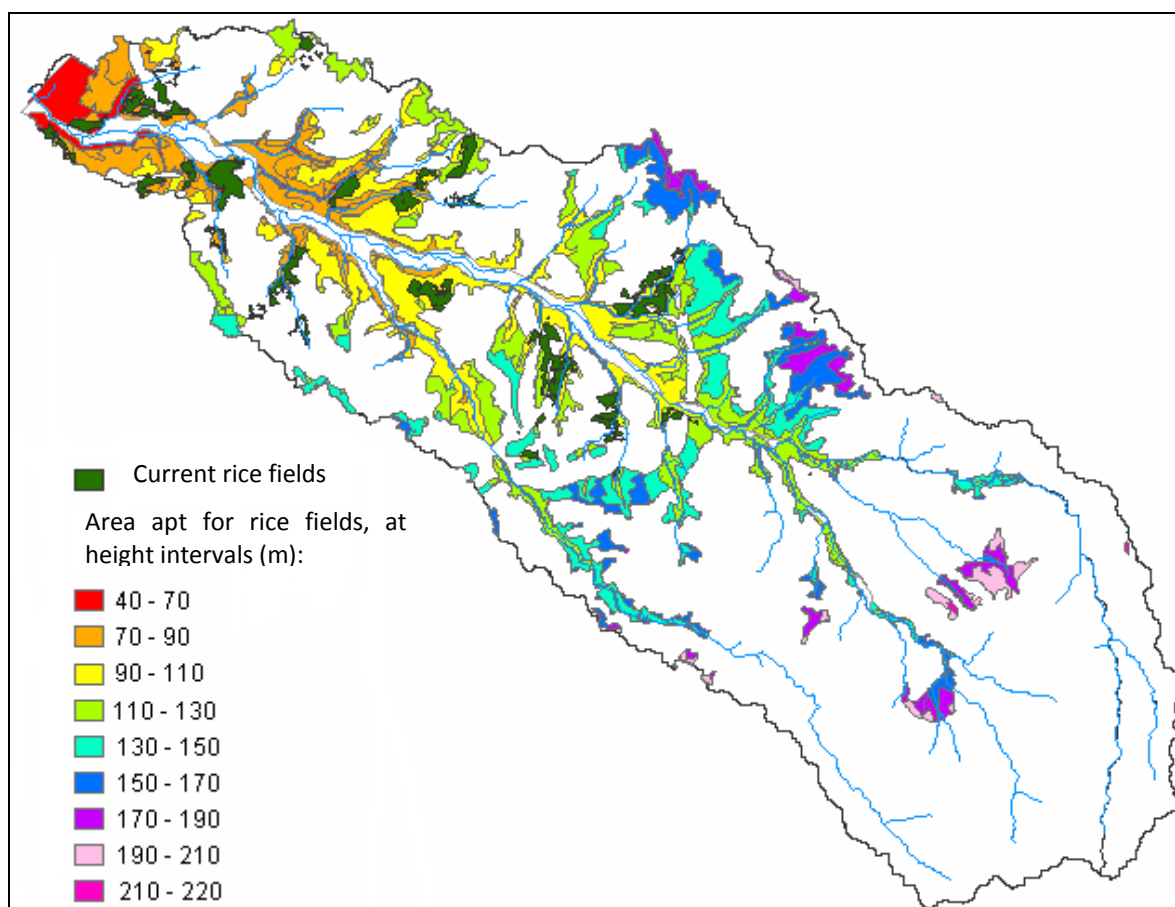


Figure 2.104 Current rice crops (dark green) and potential expansion in the Tres Cruces basin (classified by height intervals)

2.6.2.3 Changes in water demand

From the land use changes described in the previous section it can be inferred that water demand has increased and will most probably keep on growing. The water demand change scenario was constructed based on the land use change scenario and further assuming that the present rotation practice of 2 years of rice and 4 years of grassland remains unchanged. However, grasslands are assumed to be irrigated, which represents a major technological change from current practices. Even though irrigated grasslands are only starting to develop in Uruguay, market incentives and increased climate variability are steadily pressuring the sector in that direction, especially if we consider grasslands in rotation with rice crops where the irrigation infrastructure is already available. Irrigated pastures are critical to render the livestock industry in the region more resilient to climate variations. Water demands per hectare were fixed at $14.000 \text{ m}^3 \text{ ha}^{-1} \text{ yr}^{-1}$ in the case of rice (current standard) and $3.000 \text{ m}^3 \text{ ha}^{-1} \text{ yr}^{-1}$ for grasslands (based on expert judgment).

2.6.2.4 Water resources developments

The land use and water demand scenarios require an increase of irrigation capacity, which in the region can only be attained through the increase of water storage capacity in reservoirs. Currently, all reservoirs are privately owned and serve single farms, or at most a couple (Figure 2.106). They are usually quite close to the rice pads and therefore on the most valuable land with richer soils. If market

forces and individual initiative is left on its own, the only possible outcome is the multiplication of small, individual dams on lowlands (the Brazilian part of the basin serves as an example, see report section 2.5, p 2-101 and onwards). However this scenario is not optimal from a basin wide perspective. Therefore, an alternative development scenario was constructed, with much larger reservoirs in the upper part of the basin where the soil is shallow and unproductive and therefore less valuable. A careful analysis of water production and demand was performed for each sub-basin and the optimal locations of potential reservoirs were identified, so that they could serve the largest possible expansion area by gravity. Results of the water resources development scenario for Tres Cruces basin are shown in Figure 2.107.

A Current system

All the information of the existing reservoirs in the Tres Cruces basin based on the information available at DNH was gathered: height of the reservoir, spillway level, and characteristics of the reservoir for 14 reservoirs that all together correspond to 42 10⁶ m³ stored water (Table 2-29). Figure 2.105 shows a large number of small reservoirs in the Cuareim river basin. In Figure 2.106 the location of the 14 registered reservoirs in the Tres Cruces subbasin is precised.

Table 2-29 Parameters of the registered reservoirs in the Tres Cruces basin

DNH Number	Name	Reservoir Area (ha)	V max (10 ³ m ³)	Spillway Level	Dam Max Height (m)	Crest width (m)	Length of dam (m)	Largest base (m)	Average L (m)	Estimated V dam body (m ³)
27	Leo Cadore	263.0	9,132	56	11.4	4.5	1,869	61	935	307,517
34	Nei Marcos Predebón	61.0	2,256	88	10.4	3.5	686	56	343	92,467
21	YIMA	46.8	1,650	84	9.9	4.0	600	54	300	74,813
30	Hugo Riani	135.0	2,557	100	7.2	3.8	661	40	331	54,168
33	Carlos Silveira Gardet	112.3	4,282	98	12.9	5.0	1,119	70	559	195,607
26	Sergio Paniza (ex Gilberto Martini Refati)	15.9	447	203	7.5	4.0	507	42	254	52,766
20	Selio y Lino Predebón	116.0	3,473	68	9.4	8.0	1,160	55	580	152,934
32	Piriz Araujo	99.7	2,453	87	9.0	5.0	703	50	352	61,555
28	Souza Wagner (ex Ildo Ivo Finger)	20.4	628	131	8.2	4.3	413	46	206	10,900
24	Joaquin Tolosa y otros	128.3	4,317	73	10.2	4.9	850	56	425	115,274
23	Henrique, Nei y Marcos Predebon	81.8	2,605	78	11.1	3.0	664	62	332	104,482
31	Nery Lima (ex vargas hermenegildo)	101.0	906	72	4.2	4.0	215	25	108	5,699
29	Nery Lima	115.5	3,704	92	9.5	4.0	1,336	52	668	154,293
25	Dulisor SA (ex Juan Solari)	94.0	3,790	106	13.3	5.0	450	72	225	100,852

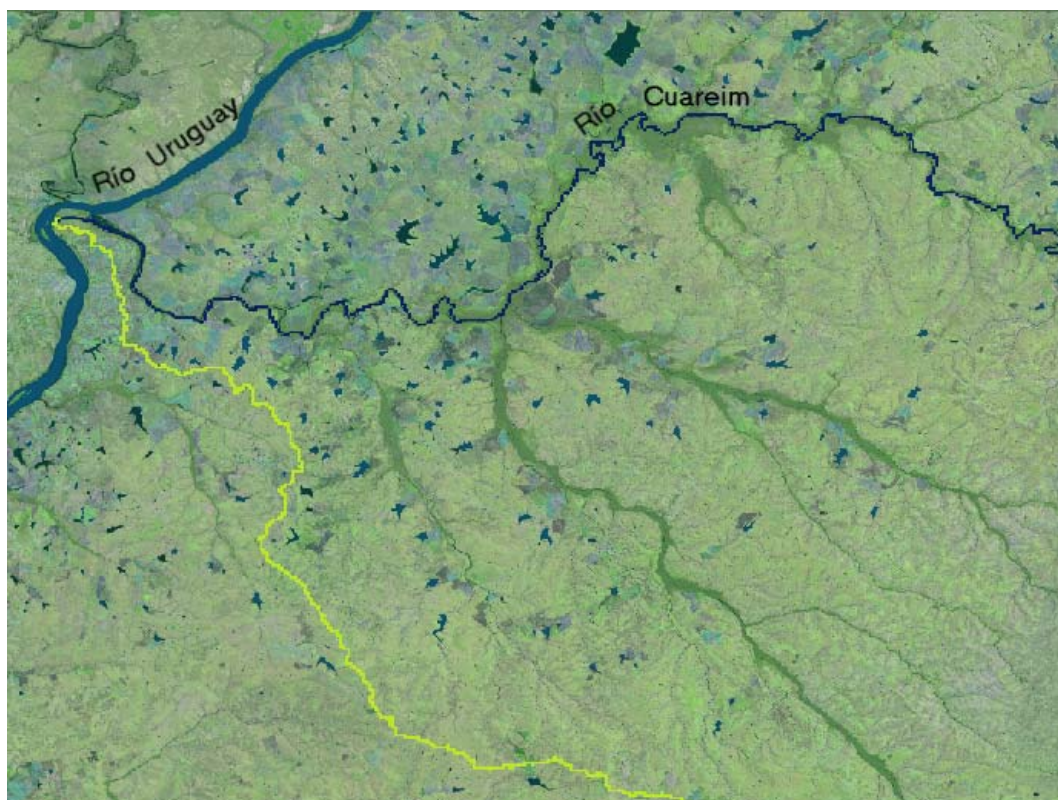


Figure 2.105 satellite image showing a large number of small reservoirs in the Cuareim river basin

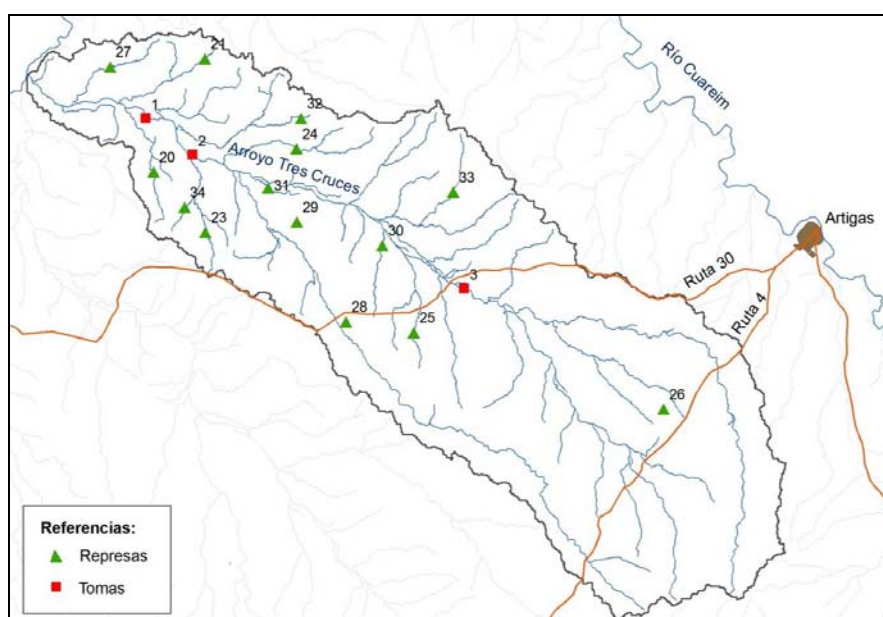


Figure 2.106 Location of the reservoirs and direct intakes in the Tres Cruces basin

In order to calculate the cost per ha, what will be done later on, it is necessary to estimate the volume of the body of the dams. Therefore, it is necessary to know the height, the length, the crest, and the slopes. Most of these data are available at DNH, and those that were not were estimated based on current practices and the topography (see Table 2-29).

The cost of the structure was calculated as follows:

$$C = C_{dam} + C_{secondary_structures} + C_{flooded_land}$$

considering US\$ 2 m⁻³ for the construction of the dam, US\$ 1000 ha⁻¹ to buy the land to be flooded and estimating the cost of secondary structures in 10 % of the cost of the movement of soil.

Although the cost per ha was calculated, and criteria were used to maximize the net returns, these analyses are subject to the huge variations in prices (and relative prices) that have occurred recently. Therefore and when it is possible, the analyses that do not depend on prices are prioritized.

B Alternative system

The motivation for constructing a scenario with two big reservoirs at the upper area of the basin to feed a multisite irrigation system (Figure 2.107) as an alternative system for the basin was explained in the introduction.

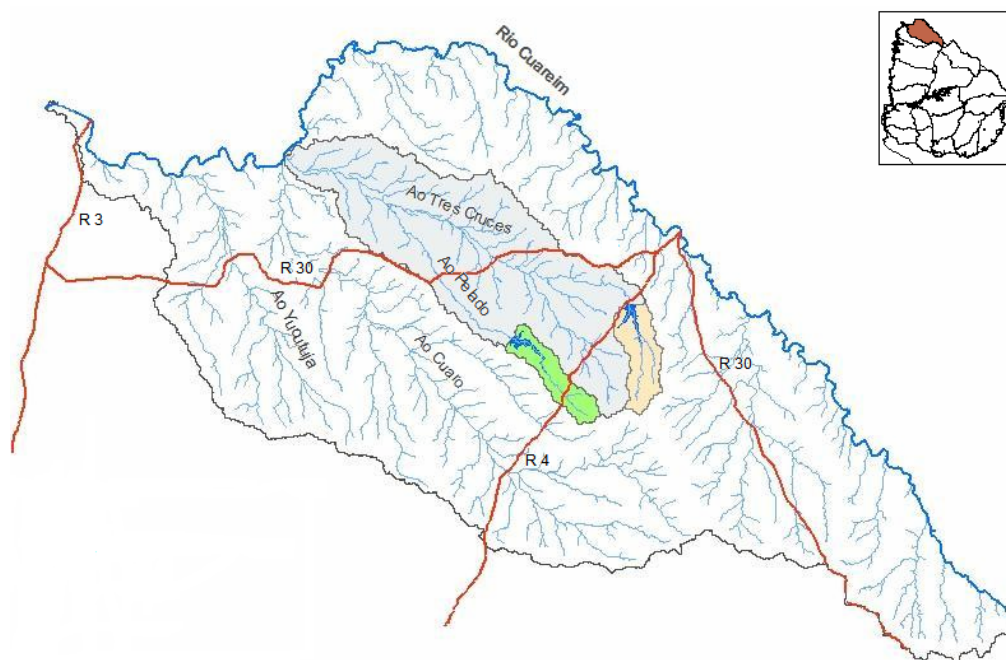


Figure 2.107 Location of the reservoirs and its contributing areas of the alternative system

Details on the climatic, hydrological, hydraulic aspects and of the structure that justifies the selection of those two reservoirs are described in Crisci et al. (2007). In this report, the key information is presented to visualize the system and to be able to do the calculations for risk assessment.

Table 2-30 Parameters of the projected reservoirs in the Tres Cruces basin

Name	Reservoir Area (ha)	V max (10 ³ m ³)	Dam Max height (m)	Crest width (m)	Largest Base (m)
TCch1	620	73,390	36.3	10.3	228
TCp4	651	62,090	36.8	10.4	231

In Table 2-30 one can observe that the capacity of both reservoirs is higher (although of the same order) than the total current storage capacity in many small reservoirs in the Tres Cruces basin. The table also gives an idea of the size of the structures.

2.6.3 Scenario Impact Assessment

2.6.3.1 Criteria to determine the area of rice to be planted in the current system

A Current criteria

The traditional criterion used by producers to determine the area of rice to be planted (when water is really the limiting factor) depends essentially on the water stored at the time to plant (October).

The TEMEZ model was used to determine the runoff in each basin (considering the corresponding soils), the geometry of each reservoir, the precipitation data series (1931-2002) and the values of evaporation to model and program the evolution of the level of water in each reservoir during the whole period. Details of the modelling are presented in Crisci et al. (2007).

With respect to the area to irrigate, two variations of the predominant criterion were used: (i) the available volume for irrigation is the water stored in the reservoir at the end of October and (ii) the available water is the one in the reservoir at the end of October minus the average evaporation during the irrigation season (more conservative criterion):

$$V_{irrigation} = V_{oct} - 4 \cdot \overline{ET} \cdot A_{max.lake}$$

being \overline{ET} the monthly average evaporation in the period Nov-Feb.

The irrigation volume is distributed in equal parts during the 4 months during irrigation season (November to February) and the area of rice ($A_{planted}$) is determined as follows:

$$A_{planted} (ha) = \frac{V_{irrigation} (m^3)}{14.000}$$

In the case of criterion (ii), it is guaranteed that there will never be lack of water for irrigation. Therefore the planted and harvested areas will be identical and thus it is enough to specify the surface that was irrigated each year to determine how the system works. In the case of criterion (i), there may be lack of water in the middle of the season. During the modelling, that surface for which there is not enough water is abandoned and the modelling continues with the rest. That is why the harvested area can be less than the irrigated area.

To compare if one year is better than another one, it is necessary to compare net returns. For example to compare a year when a small area was planted but nothing was lost versus one year when a larger area was planted, but some was lost, it is necessary to look at costs and benefits and the net return in each case. Results are presented for both cases. It has to be said that due to the large variability in prices it is not easy to extrapolate results that depend on future returns.

To do a simple net return analysis, it was considered that:

$$G_{annual} = A_{harvested} \cdot R (bolsas/ha) \cdot P_{bag} - A_{planted} \cdot C_{rice}$$

being the yield R equal to 167 bags ha^{-1} ; $P_{bag} = US\$ 8.5$ y $C_{rice} = US\$ 972 \text{ ha}^{-1}$, including the cost of planning, fertilizing, etc, but neither the land nor the water.

The results for each existing reservoir are presented below (Table 2-31 and Table 2-32).

It can be observed that generally the (i) criterion reports higher net returns. There are exceptions, though, indicated in Table 2-32 (bold values). These correspond to the reservoirs with lowest percentages of planted areas over maximum area. This indicates that the limiting factor is the contributing basin. For those reservoirs slightly over dimensioned for the basin, the most conservative criterion generates, on average, larger net returns.

Table 2-31 Average planted and harvested area for each reservoir using the (i) planting criterion (available volume for irrigation is the water stored in the reservoir at the end of October)
The maximum area that could be planted and the percentage of the average net return and maximum net return is also shown.

Reservoir DNH Number	Maximum area of rice (ha)	Average planted area (ha)	Average harvested area (ha)	Average harvested area / Maximum area of rice	% Max Net Return
27	652	423	409	63%	58%
34	161	145	142	88%	84%
21	118	89	86	73%	67%
30	183	182	173	95%	85%
33	306	303	298	98%	94%
26	32	31	31	97%	94%
20	248	247	242	98%	94%
32	175	146	137	78%	67%
28	45	38	37	82%	76%
24	308	298	287	93%	85%
23	186	184	181	97%	93%
31	65	61	46	72%	23%
29	265	174	165	62%	56%
25	271	249	245	90%	87%

Table 2-32 Average planted and harvested area for each reservoir using the (ii) planting criterion (available water is the water in the reservoir at the end of October minus \overline{ET})
The maximum area that could be planted and the percentage of the average net return and maximum net return is also shown.

Reservoir DNH Number	Maximum area of rice (ha)	Average planted area (ha)	Average harvested area (ha)	Average harvested area / Maximum area of rice	% Max Net Return
27	652	391	391	60%	60%
34	161	126	126	78%	78%
21	118	79	79	67%	67%
30	183	122	122	67%	67%
33	306	254	254	83%	83%
26	32	25	25	78%	78%
20	248	199	199	80%	80%
32	175	117	117	67%	67%
28	45	32	32	72%	72%
24	308	245	245	80%	80%
23	186	149	149	80%	80%
31	65	19	19	29%	29%
29	265	157	157	59%	59%
25	271	217	217	80%	80%

A first approximation to the value of water

The total net return for the whole system can be calculated summing up the net returns for all reservoirs. A weight factor proportionate to the size of the reservoir was used. The total net return is the net return of the whole system, whose total storage capacity was $42 \cdot 10^6 \text{ m}^3$.

Beyond the small net return differences obtained using the different criteria to select the area of rice to plant, a net return per m^3 of water storing capacity can be computed. This calculation has to be done as a function of the capacity of the reservoir and not of the water that was effectively used, because this is the way how irrigation is hired, not mattering whether the water is or not used, because that depends on the climate during the irrigation season.

The net return per m^3 of storing capacity is **0.025 US\$ m^{-3}**

It is interesting to compare this value with the current price of water, that is hired generally by bags of rice, generally around 20.

Price of water = $20 \text{ bags ha}^{-1} \cdot P_{bag} / 14.000 \text{ m}^3 \text{ ha}^{-1} = \mathbf{0.012 \text{ US\$ m}^{-3}}$

This analysis suggests that currently the water gets half of the net returns of the system, and the other half for the land is the other resource not mentioned yet. Nevertheless, the net return of the rice producers (that provide the planting services) and that of the mills are excluded in this calculation.

B Modification of the current criteria using historical rainfall

The criteria used in the previous section are generalized to include within the irrigation volume a portion of the expected runoff during the irrigation period.

$$V_{irrigation} = V_{oct} - 4 \cdot \overline{ET} \cdot A_{lake} + 4 \cdot \lambda \cdot A_{basin} \cdot \overline{C}_{runoff} \cdot \overline{P}_{Nov-Feb}$$

with \overline{C}_{runoff} average runoff coefficient for Nov-Feb and

$\overline{P}_{Nov-Feb}$ average monthly precipitation for the months Nov-Feb and

λ a parameter to adjust two different criteria:

The two different criteria are: (iii) that there will be no failure – understanding by failure that for a year of the period under study and at a certain time during the irrigation season water will lack, and (iv) that the net return be maximized. This second criterion obviously depends on the relative prices. The previously defined criterion (ii) corresponds to the case where $\lambda = 0$.

For the entire period different values of the parameter λ were simulated until the values were defined so that the criteria (iii) and (iv) were met. Results are presented in Table 2-33 and

Table 2-34.

Table 2-33 Average planted and harvested areas for each reservoir using the (iii) planting criterion (no failure)

Average planted and harvested areas are equal with this criterion. The parameter λ , the maximum area that could be planted and the percentage of the average net return and maximum net return is also shown.

Reservoir DNH Number	λ	Maximum area of rice (ha)	Average planted area (ha)	Average harvested area (ha)	Average harvested area / Maximum area of rice	% Max Net Return
27	0.4	652	407	407	62%	62%
34	0.2	161	135	135	84%	84%
21	0.3	118	84	84	71%	71%
30	0.2	183	162	161	88%	86%
33	0.1	306	280	280	92%	91%

Reservoir DNH Number	λ	Maximum area of rice (ha)	Average planted area (ha)	Average harvested area (ha)	Average harvested area / Maximum area of rice	% Max Net Return
26	0.2	32	29	29	91%	90%
20	0.1	248	222	222	89%	89%
32	0.3	175	129	129	74%	73%
28	0.3	45	36	35	79%	78%
24	0.2	308	285	281	91%	88%
23	0.2	186	179	177	95%	93%
31	0.5	65	38	38	59%	59%
29	0.4	265	164	164	62%	62%
25	0.2	271	236	236	87%	87%

Table 2-34 Average planted and harvested areas for each reservoir using the (iv) planting criterion (maximization of net return)

The parameter λ , the maximum area that could be planted and the percentage of the average net return and maximum net return is also shown.

Reservoir DNH Number	λ	Maximum area of rice (ha)	Average planted area (ha)	Average harvested area (ha)	Average harvested area / Maximum area of rice	% Max Net Return
27	0.5	652	411	410	63%	62%
34	0.3	161	140	139	86%	85%
21	0.4	118	85	85	72%	71%
30	0.2	183	162	161	88%	86%
33	0.2	306	306	301	98%	94%
26	0.3	32	31	31	96%	94%
20	0.2	248	245	241	97%	94%
32	0.4	175	133	132	76%	75%
28	0.4	45	37	36	81%	79%
24	0.2	308	285	281	91%	88%
23	0.2	186	179	177	95%	93%
31	0.7	65	46	44	68%	63%
29	0.5	265	166	166	63%	62%
25	0.3	271	246	243	90%	87%

It can be observed that maximizing net return (criterion (iv)) implies planting areas slightly larger (a greater λ) than the criterion of no failure, except for a few reservoirs in which both criteria give the same results (bold numbers in Table 2-33 and

Table 2-34). In all the cases, the criteria (iii) and (iv) generate higher net returns compared to the results of current criteria (i) and (ii). In some cases there are substantial differences. Later on, all the considered criteria are analyzed all together.

Figure 2.108 shows the frequency of the fraction of the net return normalized to the maximum net return with the total water storage capacity for the non-failure criterion (iii). It is verified that nearly half of the years the net return is greater than 90 % of the installed capacity and in 10 % of the cases it is less than 70 % of the maximum.

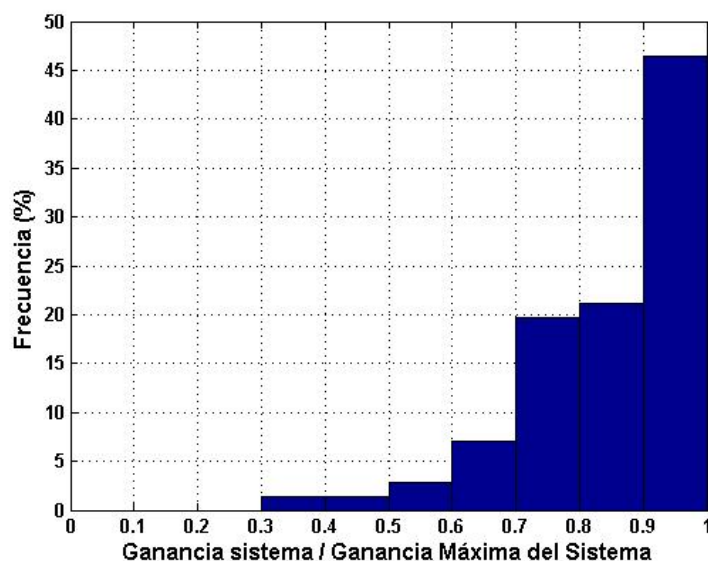


Figure 2.108 Frequency of the normalized net return during the study period for the (iii) planting criterion

In the next section the incorporation of a precipitation seasonal climate forecast during the irrigation season to the decision criterion to determine the area to irrigate is studied. The objective is to check if it is possible to improve the performance of the already analyzed criteria and up to which point.

C Incorporation of climate forecast

The extreme phases of a quasi-periodic oscillation of the atmosphere-ocean coupled system in the equatorial-Pacific zone are known as El Niño and La Niña. The atmospheric component of that phenomenon is called the El Niño Southern Oscillation (ENSO). In the central and oriental equatorial Pacific, the dominant characteristic is the warming (cooling) of the sea surface temperature. ENSO has effects on the whole planet. ENSO also has a high correlation with the precipitations in Uruguay during some seasons. ENSO develops – typically – between July in one year and June the following year.

When an El Niño event occurs (the extreme warm phase of ENSO) there is a tendency to have positive anomalies in the precipitation in Uruguay, although it has a clear seasonal relationship, being maximum in spring (Pisciottano et al., 1994). On the contrary, the La Niña phenomenon (cold extreme phase of ENSO) is associated with negative precipitation anomalies in the region of Uruguay. The seasons when the relationship manifests itself are very similar but not necessarily identical.

Results from research suggest that the impacts of La Niña on precipitation and the yield of rain-fed crops are stronger and/or more constant than the impacts of El Niño. With respect to the impact of the extreme phases of ENSO on temperature, the few studies done in Uruguay suggest that the temperature range in the north of Uruguay is reduced during El Niño years due to the presence of more clouds. This also results in less insolation and is probably the cause of larger yields of rice during La Niña years (Roel and Baethgen, 2005). It has to be remembered that rice is grown always under irrigation, so the lack of precipitation does not affect the yields.

In Figure 2.109 a scatter plot with the relationship between the Niño 3.4 index in the period October-February (months with higher intensity of the phenomenon) and the precipitation registered in the basin of the Cuareim River during the periods July-June and November-October is presented. The lineal fit that was used to forecast the expected precipitation during the irrigation season to determine the irrigated surface instead of using the historical average is:

$$\bar{P}_{Nov-Feb} = 131.7 + 35.4 \cdot [N3.4]$$

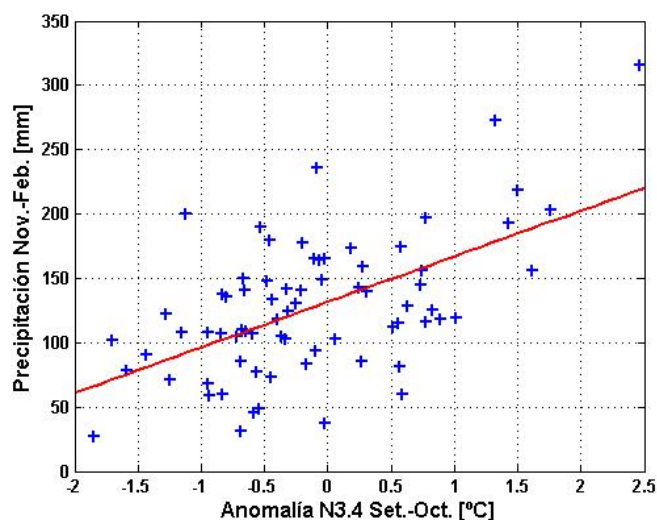


Figure 2.109 Precipitation in Nov-Feb as a function of the average N3.4 index in Sep-Oct
In red, the lineal fit of the forecast used in the criteria (v) and (vi)

With the incorporation of the forecast based on N3.4 in the couple of months prior to the decision on how much to plant, the evolution of the reservoirs for the whole period of study (1931-2002) was simulated, varying the value of λ to satisfy the criteria of no failure (criterion (v)) and maximization of the net return (criterion (vi)), respectively. Results are presented in Table 2-35 and Table 2-36.

Table 2-35 Average planted and harvested areas for each reservoir using the (v) planting criterion (no failure – including climate forecast)

The parameter λ , the maximum area that could be planted and the percentage of the average net return and maximum net return is also shown.

Reservoir DNH Number	λ	Maximum area of rice (ha)	Average planted area (ha)	Average harvested area (ha)	Average harvested area / Maximum area of rice	% Max Net Return
27	0.6	652	418	417	64%	64%
34	0.3	161	141	141	88%	87%
21	0.4	118	86	86	73%	73%
30	0.2	183	162	162	89%	88%
33	0.2	306	306	303	99%	97%
26	0.3	32	31	31	97%	97%
20	0.2	248	245	243	98%	96%
32	0.5	175	138	137	78%	77%
28	0.4	45	37	37	82%	81%
24	0.2	308	285	283	92%	91%
23	0.2	186	178	178	96%	95%
31	0.6	65	42	42	65%	65%
29	0.6	265	169	169	64%	64%
25	0.3	271	247	245	91%	89%

Table 2-36 Average planted and harvested areas for each reservoir using the (vi) planting criterion (maximization of net return – including climate forecast)

The parameter λ , the maximum area that could be planted and the percentage of the average net return and maximum net return is also shown.

Reservoir DNH Number	λ	Maximum area of rice (ha)	Average planted area (ha)	Average harvested area (ha)	Average harvested area / Maximum area of rice	% Max Net Return
27	0.6	652	418	417	64%	64%
34	0.4	161	146	144	89%	87%
21	0.4	118	86	86	73%	73%
30	0.3	183	183	177	97%	90%
33	0.2	306	306	303	99%	97%
26	0.4	32	33	33	103%	99%
20	0.2	248	245	243	98%	96%
32	0.5	175	138	135	77%	77%
28	0.4	45	37	37	82%	81%
24	0.2	308	285	283	92%	91%
23	0.3	186	194	189	102%	95%
31	0.7	65	46	45	70%	67%
29	0.6	265	169	169	64%	64%
25	0.3	271	247	245	91%	89%

Results with criteria (v) and (vi) are very similar, and seem significantly higher to those that do not include climate forecast. A more careful comparison is done in the following section.

In the case of the criterion with maximum net return with climate forecast (vi) it is observed that in certain circumstances larger areas than the maximum (calculated based on the capacity of the reservoir) are planted and even harvested. This means that an area based on the amount of rain is planted, what already was a possibility in the case without forecast even if it was not done for the λ value that maximized the net return. The information added by the climate forecast allows for higher values of λ that maximize the net return and makes that the average harvested area is higher than the maximum area determined by the size of the reservoir. This in particular happens in reservoirs that are small in relation to the contributing areas.

2.6.3.2 Climate change

A future climate scenario was constructed based on the extrapolation of the two significant modes (on the one hand the frequency of ENSO and on the other hand a non-linear tendency) that arose from the analysis of the singular spectrum of the annual precipitation Nov-Oct for the analysis period (1931 – 2002). The annual cycle (of secondary importance in the presence of the reservoirs) and the intensity of the noise below the signal was maintained (for details see Crisci et al., 2007). The synthesized scenario is closer to the characteristics observed in recent decades – with slightly higher averages and significantly higher variability – compared to the first decades of the study period.

The behaviour of the existing reservoirs in this scenario was analyzed using the criterion (iii): no failure, without climate forecast. Results are presented in Table 2-37.

Table 2-37 Effect of climate change on average planted and harvested areas for each reservoir using the (iii) planting criterion (no failure)

The parameter λ , the maximum area that could be planted and the percentage of the average net return and maximum net return is also shown.

Reservoir DNH Number	λ	Maximum area of rice (ha)	Average planted area (ha)	Average harvested area (ha)	Average harvested area / Maximum area of rice	% Max Net Return
27	0.3	652	461	461	71%	71%
34	0.2	161	142	141	88%	87%
21	0.2	118	90	90	76%	76%
30	0.2	183	171	168	92%	88%
33	0.1	306	286	285	93%	93%
26	0.2	32	30	30	93%	92%
20	0.1	248	227	227	91%	91%
32	0.3	175	140	139	80%	79%
28	0.2	45	37	36	81%	81%
24	0.1	308	272	272	88%	88%
23	0.1	186	167	167	89%	89%
31	0.4	65	39	39	60%	59%
29	0.3	265	185	185	70%	70%
25	0.2	271	246	246	91%	90%

Results are slightly higher than the observed results for the current climate (see Table 2-33). These results reflect that the physical characteristics of the reservoirs were not modified while the average precipitation in the climate scenario is slightly higher, therefore generating higher runoff. The relationship between the size of the reservoirs and the production of water is less clear. The climate change scenario presents a somewhat larger variability, but in this case of a system under irrigation, the effect of the average is predominant.

2.6.3.3 Rice-grassland production system

The principal physical data of the projected reservoirs were presented earlier. These were determined after a comprehensive analysis of the water demand as a function of the most productive land, of the water production in the basin and of the difference in levels that makes the conduction of water by gravity possible. It was also considered where to locate the dams from the construction point of view. For details (including the estimated cost of construction per irrigated ha) refer to Crisci et al (2007).

The philosophy of the alternative system responds on one hand to the fact that the potential harvest of water is underused in the basin, and on the other hand that one of the production systems (the livestock industry) has a high vulnerability to climate variability, causing frequent crisis with high socioeconomic costs. The irrigation for production of forage is a substantial change in the production system and there is a need for the development of new technologies. This transformation is just beginning, with one limitation being the guaranteed availability of water. Another characteristic of the alternative system is that it represents – contrary to the current development – a multisite-level solution that is not possible without a decisive participation of the Government.

Although the alternative system was designed for the irrigation of rice-grassland rotation for lands apt for rice that are reachable by gravity, the analysis will be first done for the exclusive use of the reservoirs for rice. Then the impact of that scenario in the reduction of the vulnerability of the livestock industry on grassland will be analyzed.

2.6.4 Vulnerability assessment

2.6.4.1 Assessment of water deficit risks for grasslands in the current system

As was stated before, the most vulnerable production system to climate variability is the livestock industry, due to the non-stable offer of forage due to water deficits in a region with shallow soils.

The soil water balance is simulated with the TEMEZ model for the whole period of study (1931-2002) and for the three predominant soils in the area, with water storage capacity of 76, 34 y 13 mm respectively. As a representative parameter of the water availability is the “Hydrated Well-Being Index” (IBH), during the warm season (October till March): the average quotient between the real and potential evapotranspiration. Figure 2.110 shows the evolution along the years of this water availability index (averaged for the dominant soils); some historic droughts are also shown.

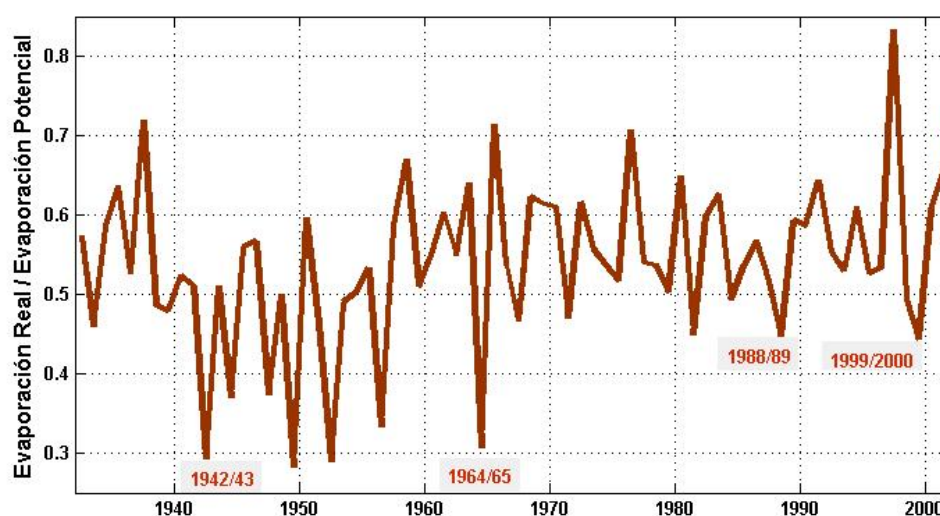


Figure 2.110 Evolution of the mean IBH for Oct-Mar and for the dominant soils in the Tres Cruces basin (1931-2002)

Figure 2.111 presents the frequency of occurrence of IBH during the warm season (October – March) for the dominant soils for the study period. The water deficit during summer is an important climate characteristic of the region that gets worse in exceptionally dry years, with often important water deficits.

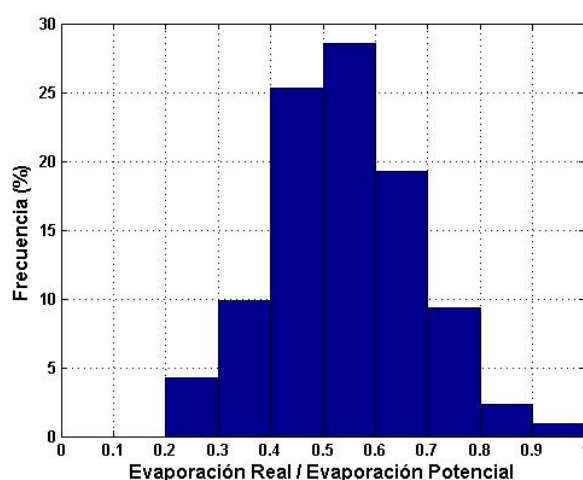


Figure 2.111 Histogram of the mean IBH (Oct-Mar) for dominant soils in the Tres Cruces basin (1931-2002)

Although experience shows the importance of this hydrologic characteristic in the forage production and in the livestock industry, the impact is difficult to assess in a quantitative way. In order to perform a qualitative analysis, a function between the IBH and the meat production per ha (normalized by the maximum production in conditions without water stress, which is 390 kg ha^{-1}), was defined.

The relation between IBH and meat production can be formulated by a polynomial function $P(x)$ of less order that complies with the following conditions (see Figure 2.112):

- $P(0) = 0$ and $P(1) = 1$
- $P'(0) = 0$ and $P'(1) = 0$
- The average historical production (with the distribution of IBH (f_{IBH}) given by the historical data that are shown in Figure 2.111) give a value of 300 kg ha^{-1} . To determine $P(x)$ only the relationship between the average and maximum production matters.

In mathematical terms, this can be expressed as:

$$\int_0^1 f_{IBH}(x)P(x)dx = \frac{\text{Prod}_{\text{Average}}}{\text{Prod}_{\text{Max}}}$$

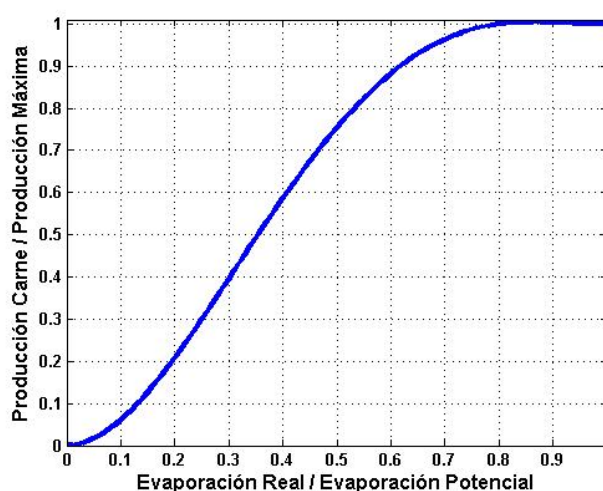


Figure 2.112 Ad hoc function relating IBH with meat production in a rain fed grassland

The ad hoc function – although it is a simplified model – has the expected behaviour, with the highest sensitivity (slope) concentrated in intermediate values of IBH. The function allows us to calculate the histogram of normalized production in the period, by simply multiplying f_{IBH} (Figure 2.111) by $P(x)$ (Figure 2.112). The average is guaranteed by construction and it will be $300/390$, the quotient of average production over specified maximum production.

Figure 2.113 illustrates – within the simplified assumptions – the vulnerability of the system to the inter-annual climate variability. When we compare with Figure 2.108 (the histogram of the net return over the maximum net return for rice for the current reservoirs) the former shows the gross production and in the latter the net returns (except for the cost of water and land). Therefore, the difference in vulnerability is much higher than the one shown by the difference in thickness of the left tail in the distribution. As was stated before, rice is not very much affected by climate variability since it is irrigated.

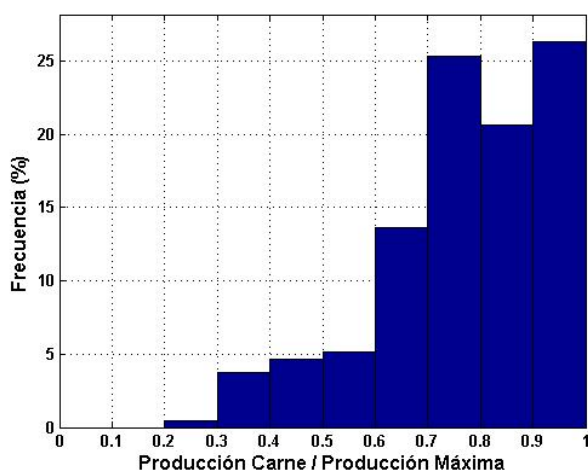


Figure 2.113 Histogram of the normalized meat production in the Tres Cruces basin (1931-2002)

It is impossible to attempt to capture with this analysis the economic impact of the large (and not infrequent) forage crises, when there is cattle mortality and big capital losses as well as other social damages. All the same, Figure 2.113 shows a high vulnerability, with more than 1 out of 4 years with productions less than 70 % of the maximum.

For similar reasons it is not possible to assess the impact of climate change in the livestock industry with sufficient precision. Contrary to the case of production under irrigation (like in the case of rice), the largest impact probably will not be due to changes in the average precipitation but due to the increasing inter-annual variability that is already occurring in the past decades. All the same, the current vulnerability is already unacceptable for the current commodity prices, and a scenario where the vulnerability decreases based on grassland under irrigation has to be imagined. This is precisely the philosophy behind the scenario of the alternative production system with two large multi-parcel reservoirs in the upper area of the basin to supply a rice system with rotation of grassland under irrigation.

2.6.4.2 Assessment of water deficit risks in the alternative system

It is impossible to do the analysis of the use of water in a multipurpose reservoir independent from the relative costs and prices of the involved production systems, in this case rice and grassland. Some initial results are presented below.

The values used for meat production on grassland were the same as those presented before (390 kg ha^{-1} maximum production under irrigation and 300 kg ha^{-1} average for rain-fed production). It should be noted that these values generate a very conservative difference between irrigated and rain-fed production. Installation cost for a hectare of grassland was estimated to be US\$ 45 and the kg of meat at US\$ 1.1. Annual irrigation rate for grassland was estimated at $3000 \text{ m}^3 \text{ ha}^{-1}$. With those assumptions, the net return on the use of water may be calculated as follows:

$$(390-300) \text{ kg ha}^{-1} \cdot 1.1 \text{ US\$ kg}^{-1} / 3000 \text{ m}^3 \text{ ha}^{-1} = \mathbf{0.033 \text{ US\$ m}^{-3}}$$

We observed that with the assumed prices and costs, the value of the return per unit of water used, is essentially the same as the one calculated for rice. Although it is dependent on the variation in input costs and output prices, for the several past years the return per unit of water was similar for rice and for forage. Nevertheless, this parity is not reflected in the use of water that is nearly exclusively used for rice.

The reasons are multiple, but mainly: (i) rice production is only possible under irrigation, while in the case of grassland what is sought with irrigation is an increase in production and a higher resilience to climate variability; and (ii) there is a tradition and a strong know-how in the rice sector that does not exist for irrigation of grassland, in which the economic equation allows for irrigation since a relatively short time.

It is not the goal of this study to determine the optimal use of water, which is strongly related to the rapidly varying relative prices and give very similar returns. In contrast, it is of interest to analyze how the vulnerability of the livestock industry decreases with increasing areas of grassland under irrigation, as it is one of the key motivations for the alternative system. In order to do that, it is necessary to define planting and water use criteria. The behaviour for the historical data was simulated, using various reasonable possibilities (prioritizing in more or less proportion, grassland to rice) and no substantial differences were found. Below one of those cases is presented.

$V_{irrigation}$ was calculated, determining λ with the non-failure criterion. To calculate the area planted with rice, a 2-year rotation of rice and 4 of grassland was assumed; that is 2 ha of grassland per 1 ha of rice. The total portion per hectare of rice is:

$$14.000 + 2 \cdot 3.000 = 20.000 \text{ m}^3 \text{ ha}^{-1} \text{ of rice}$$

As a result of the simulation with optimal λ (maximum λ that makes possible to always have water to irrigate the area planted with rice during the simulation period), the area with rice and under irrigation (both of rice and grassland) for each year is obtained. This criterion implies equal priority for the use of water for the production systems. Nevertheless, there is still a difference between rice and grassland: how much rice to plant is decided every year and, with the selected criterion, it can be always irrigated, whereas grasslands, under the rotation with rice, are always installed. So, it is possible to estimate the index of failure of the irrigation of grasslands, dividing the area under irrigation each year by the maximum area of the system that should be under irrigation. That index, whose evolution during the simulation period is presented in Figure 2.114, indicates the percentage of grassland that could be irrigated each year.

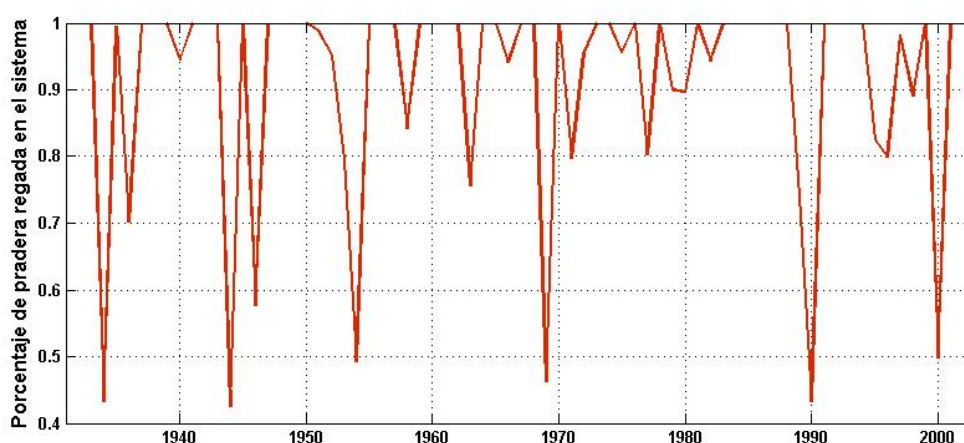


Figure 2.114 Percentage of irrigated grassland in the alternative system (2 large reservoirs) during simulation period

To calculate the water availability index (IBH) of the grasslands, it was assumed to be 1 if the grassland is under irrigation, else it has the value of the rain-fed grassland as calculated before. Therefore, the system's average IBH for one season is:

$$\frac{A_{irrigated}}{A_{max}} + \frac{1 - A_{irrigated}}{A_{max}} \cdot IBH$$

It has to be noted that the correlation between IBH and the percentage of grassland under irrigation is very low (0.01). If during a warm season (Oct-Mar) water availability is low, this affects the volume of water stored and therefore the percentage of irrigated water of the following season. Comparing Figure 2.110 and Figure 2.114, it is interesting to see how the minimums in Figure 2.110 occur in general before the minimums in Figure 2.114 for one year.

Figure 2.115 shows the evolution of the average IBH of the grasslands in the alternative system. The behaviour is dominated by irrigation (similar to Figure 2.114), but with higher values and with some

influence of the direct rainfall on the grassland when there is not enough water to irrigate. Figure 2.116 presents a histogram of the same series.

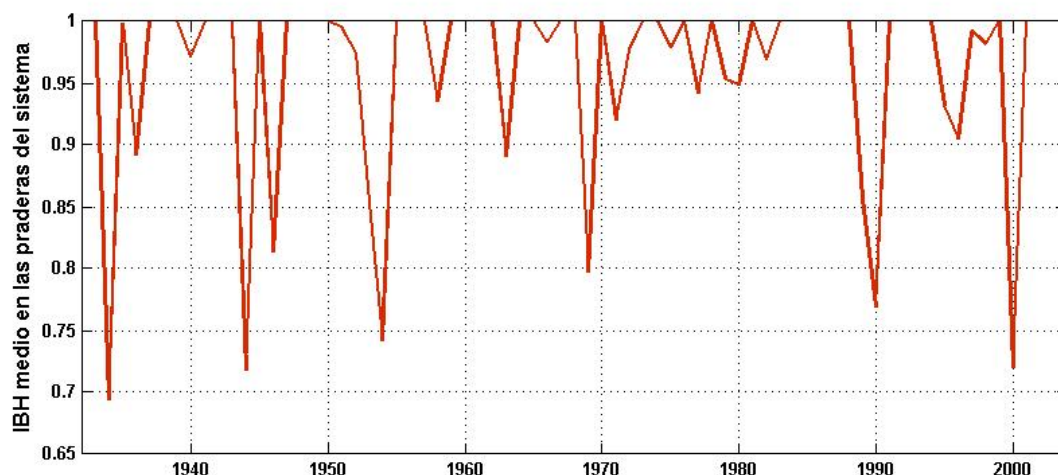


Figure 2.115 Evolution of mean IBH for Oct-Mar for the grasslands of the alternative system (1931-2002)

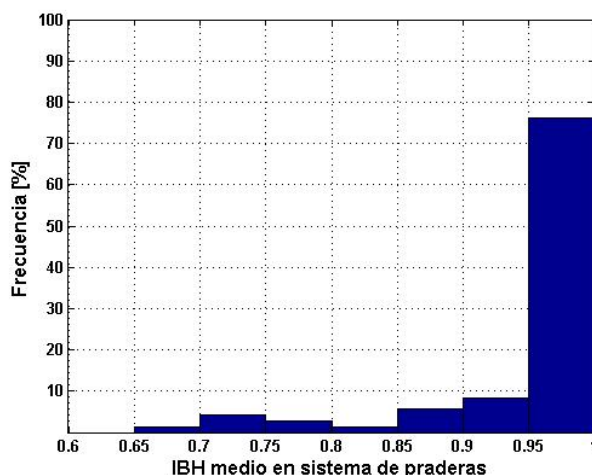


Figure 2.116 Histogram of the average IBH for Oct-Mar and for the 3 dominant soils in the Tres Cruces basin for the grassland of the alternative system

Finally, the histogram of meat production over maximum production based on the evolution of the mean IBH (Figure 2.115 and Figure 2.116) and the ad-hoc function defined before is presented.

The histograms of Figure 2.112 and Figure 2.113 for the rain-fed grasslands are directly comparable with Figure 2.116 and Figure 2.117 in the alternative system with grasslands under irrigation. Essentially, today's high risk due to climate variability would be almost eliminated for that production system. It is also verified that water production in the basins, the storage capacity, and the difference in levels for the conduction of water under gravity are enough to eliminate the climate risk of the system. Details of the distribution of the area of rice that could be planted in the Tres Cruces basin and the one covered by the alternative system are described in detail in Crisci et al. (2007).

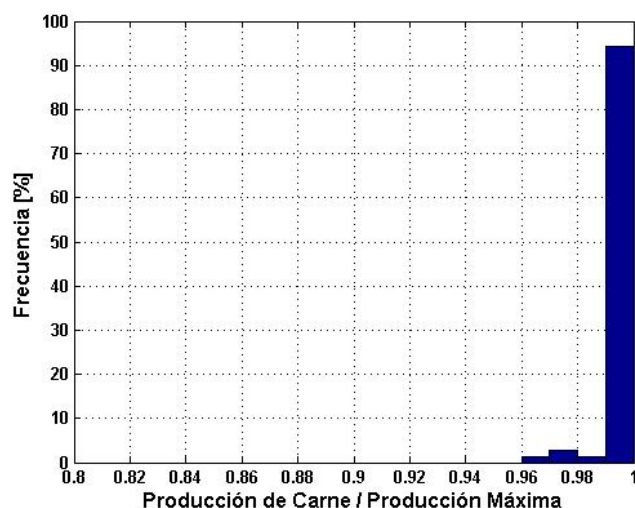


Figure 2.117 Histogram of the normalized meat production in the grasslands under irrigation for the alternative system

2.6.5 Summary

2.6.5.1 Current system

In Table 2-38 a summary of the results obtained for the different criteria to determine the area to plant (with or without information of seasonal climate forecast) and for the climate change scenario for the current total water storage system in the Tres Cruces Basin is presented.

Table 2-38 Parameter λ , percentage harvested area and percentage maximum net return for the different planting criteria under the current irrigation system

	λ	Average Harvested Area / Max area of rice	% Max Net Return
ii: Stored water - evaporation	0	70.8%	70.7%
i: Stored water	-	82.2%	75.7%
iii: No failure	0.26	78.9%	78.3%
iv: Maximum net return	0.34	81.2%	79.2%
v: No failure with climate forecast	0.37	82.1%	81.2%
vi: Max. net return with climate forecast	0.39	83.1%	81.4%
iii: Climate Change	0.21	82.5%	81.9%

The different criteria have a different impact on the reservoirs (some of which have already been mentioned), mostly dependent on the relationship between the reservoir capacity and the size of the contributing area. This is not reflected in Table 2-38. In this section attention is paid in particular to the average effect on the system as a whole. These are the principal results:

- The option of not having any runoff during the irrigation season is too conservative and it is far from producing a maximum net return. The λ optimum values for the different criteria indicate a use of 26 % to 39 % of the rainfall.
- The criterion of growing rice as a function of the stored water at the end of October (somehow assuming the cancellation of the evaporation with the runoff during the irrigation season) is much closer to the best criterion, but it is not recommended either as it does not take into account the characteristics of each reservoir. Comparing it with (i), we see that in (iii) we have less harvested area but higher net return. This reflects that in (i) much more of the initially planted area was lost,

which indicates that for many reservoirs (with worse relationship of contributing area to capacity) the criterion is excessively risky.

- Both with and without climate forecast, the criterion of maximum net return (where risk is taken growing areas somewhat bigger), gives marginally better results; the difference is more noticeable in the case without climate forecast.
- Both with the criterion of no failure and with the criterion of maximization of net return, the incorporation of the seasonal climate forecast based on the N3.4 index, improves the net return for all the reservoirs, with a global impact of a little more than 2 % increase in the net return.
- In the climate change scenario, the efficiency of the system slightly improves due to the small increase in the precipitation and, because of that, there is improvement in the relationship between water production in the contributing areas and the volume of the reservoirs, whose capacities were not changed.

2.6.5.2 Alternative system

Below the results of the historical balances of the basins and the reservoirs of the alternative system with the same methodology used previously is shown. Table 2-39 and

Table 2-40 are results for the 2 large reservoirs TCch1 and TCp4 respectively and therefore comparable with Table 2-38 for many small reservoirs in the current system.

Table 2-39 Parameter λ , percentage harvested area and percentage maximum net return for the different planting criteria (reservoir TCch1)

TCch1	λ	Average harvested area / Max area of rice	% Max net return
ii: Stored water - evaporation	0	87.2%	87.1%
i: Stored water	-	90.1%	89.6%
iii: No failure	0.2	91.4%	90.7%
iv: Maximum net return	0.2	91.4%	90.7%
v: No failure with climate forecast	0.2	91.7%	91.5%
vi: Max. net Return with climate forecast	0.3	93.5%	92.0%

Table 2-40 Parameter λ , percentage harvested area and percentage maximum net return for the different planting criteria (reservoir TCp4)

TCp4	λ	Average harvested area / Max area of rice	% Max Net Return
ii: Stored water - evaporation	0	86.2%	86.2%
i: Stored water	-	89.7%	89.6%
iii: No failure	0.1	86.3%	88.5%
iv: Maximum net return	0.2	90.6%	89.9%
v: No failure with climate forecast	0.2	90.9%	90.7%
vi: Max. net Return with climate forecast	0.3	92.6%	91.3%

The values in Table 2-39 and Table 2-40 are approximately 10 % higher than those in Table 2-38, which reflects a better relationship between the contributing basin and the reservoir capacity. This was taken into account in the design of the alternative system: to have a higher guarantee of water availability to promote the change in the production system to have grassland under irrigation.

Using the same costs and prices to plant and sell rice, the net return is **0.032 US\$ m⁻³** of water used. In the current system with an average efficiency of 79 % it is 0.025 US\$ m⁻³ of reservoir capacity. The alternative system with two large reservoirs has an average effectiveness of 90 % and a water yield of **0,029 US\$ m⁻³** of reservoir capacity, due to its greater efficiency.

In relation to vulnerability assessment, today's livestock industry's high risk as a result of climate variability is eliminated in the alternative production system, with both rice and grasslands under irrigation. It is also verified that water production in the basin, the storage capacity, and the difference in levels for the conduction of water under gravity are enough to eliminate the climate risk of the system.

2.7 WATER BALANCE IN SOUTH AMERICA

2.7.1 Introduction

The South American continent is of particular interest in the global hydrological cycle accounting for 28% of the total world freshwater resource (FAO, 2003). With latitudes ranging between -57.0S and 14.0N and the presence of the Andean chain of mountains that extends almost the entire length of the continent, South America presents a huge diversity in climate and hydrological regime. Patagonian icefields, tropical rainforests of the Amazon and the extensive wetlands of the Pantanal present a challenge for a hydrological model. The continent is also home to some 346 million inhabitants (FAOSTAT) with approximately 75% of the population urbanised. Agriculture is a major source of income for many economies in South America, but most significantly Brazil which in the mid 1990s was the world's main coffee and sugarcane producer and a leading producer of coconut, tobacco and cotton (FAO, 2003). Climate and regime vary spatially but climate variability also has impacts. In recent years, attempts in Argentina to increase energy production using hydropower have been reversed as the region was hit by successive droughts.

In order to understand the complex spatial and temporal relationship between water supply and water demand an integrated modelling approach has been applied to the mainland South American continent. The Global Water Availability Assessment (GWAVA) model (Meigh et al., 1998) enables a consistent modelling approach to be applied across the South American continent using continuous datasets and a consistent methodology. This approach has the advantage of being able to explore the wider spatial patterns of climate change that affect the partner basins.

2.7.2 Global Water Availability Assessment (GWAVA) for South America

2.7.2.1 Introduction

The Global Water Availability Assessment (GWAVA) model (Meigh et al., 1998) combines a detailed hydrological model with the water resources system on a 0.5 degree grid enabling spatially distributed assessments of water availability to be made. The core rainfall-runoff model comprises the probability distributed model (PDM) (Moore, 1985) and two linear reservoirs to route surface and subsurface flow. The PDM conceptualises the basin, or grid cell, as a distribution of soil moisture stores. Upon rainfall the shallowest ones fill and spill first. Evaporation losses from the stores are a function of the soil moisture content. Drainage occurs in the stores whose soil moisture content is above the field capacity. The model parameters defining the size of the soil stores are linked to vegetation cover and soil texture. Remaining parameters include a soil moisture scaling parameter, a soil moisture distribution parameter and surface and subsurface reservoir coefficients and require calibration. Other hydrology sub-models include the snow melt and glacial melt models. A detailed description of the model structure is provided in the WP3 report. At the cell outlet, surface and subsurface flow are summed to provide a 'local' cell runoff. Runoff generated by each cell i.e. the local runoff is accumulated along the gridded river network to simulate the real world drainage network. Calibration of the model has been performed over selected sub-basins by comparing simulated streamflow at cells whose location and basin areas correspond well with the observed areas at gauging stations. (Further information on the sub-basin selection and the calibration process can be found in the WP3 report). The GWAVA model has been applied to the South American continent on a spatial resolution of 0.5 degrees and the model is driven by monthly precipitation, temperature and potential evaporation data. Water demands are computed on a monthly basis and modelled streamflow outputs are also monthly.

Effects of change can be examined through the changes to the simulated streamflow hydrograph available at each cell and through a suite of water availability indices which compare the available freshwater to the demand in that cell.

The model scheme allows the user to apply simple adjustment factors to the driving rainfall or to examine more complex patterns of change obtained from outputs of global climate models (GCMs) and, thus, can be used to examine relationships between precipitation and runoff generation at the cell and basin scale, and the combined effects of changing temperature and precipitation on soil moisture. Building upon this, scenarios of population growth can be used with and without climate change scenarios to understand more fully the relative importance of each effect.

The model spatial resolution of 0.5 degrees imposes a limit on the size of individual basins that can be resolved and studied further.

2.7.2.2 Inputs

Along with climatological data to drive the model, information on land cover, soil texture, mean elevation and drainage direction must be specified per grid cell as well as information on the location and capacity of lakes, wetlands and reservoirs if required. Sub-grid information on elevation bands are computed from a digital elevation model for cells with a mean elevation greater than 2000 m to run the mountain snowmelt sub-model. The annual water demand per cell is estimated from rural and urban populations, livestock numbers and industrial water use all of which are obtained from global datasets. Monthly water demand arising from irrigation is modelled and requires additional inputs of crop location, planting calendar, area and crop types.

To examine climate change impacts, changes in the mean monthly precipitation, potential evaporation and temperature are also required and are typically obtained from global or regional climate model simulations.

2.7.2.3 Results

The two key model outputs are the monthly stream flow series generated at each cell and the water availability indices (WAIs) summarised below in Table 2-41. Other supplementary maps can be produced to examine changes to low flows and standard deviation of flows in cells.

Water availability indices

Comparisons on a cell by cell basis of water yield and demands provide maps showing areas where, for example, water supplies may be insufficient. The comparison can be made in different ways, the simplest (Type 1 index in GWAVA) being to divide the annual volumetric water yield by the annual volumetric demand; however, this does not capture the seasonal or inter-annual variation in water demand and supply. A second method (Type 2) calculates the actual supply available for use, estimated as the driest month in each year which occurs with 90% reliability. This value, termed Qdryav, is also plotted to examine changes to low flows. This is compared to the minimum monthly demand i.e. assumes demands are constant throughout the year. The Type 3 index for surface water is found by calculating the 90% reliable flow for each month of the year separately, rather than calculating a single value based on the driest month in each year. The index is then the minimum (over all months in the year) of this value minus the demand in the same month. This index reflects the critical point in the year whether or not there are variable irrigation demands. The index is expressed as a volume, with positive values indicating an excess of supply over demand and negative values a shortfall. An advantage of this index is that it helps to distinguish areas where demands are large and there is a large shortfall (for instance) from those where both supply and demands are small and, therefore, the shortfall is small. Thus, areas of large-scale water availability problems are picked out from those where the problems are relatively small-scale.

The fourth index (Type 4) was developed so that results could be expressed as a ratio which ranges from -1 (negligible water available to meet demand), though zero (available water meets demand), to 1 (available water exceeds demand).

Examples of these outputs produced for South America are plotted in ArcGIS and shown below in section 2.7.2.4.

Table 2-41 Summary of water availability indices for surface water, groundwater and combined sources as computed in GWAVA

	Index	Definition
Surface water only	SWAI-type 1	Total annual runoff / Total annual demand
	SWAI-type 2	90% reliable driest month runoff / Minimum monthly demand
	SWAI-type 3	Minimum over all months of: (90% reliable monthly runoff – Demand for that month)
	SWAI-type 4	(SWAI-type 3) / (90% reliable monthly runoff + Demand for that month)
Ground water only	GWAI-type 1	Annual groundwater yield / Total annual demand
	GWAI-type 2	Minimum monthly groundwater yield / Minimum monthly demand
	GWAI-type 3	Minimum over all months of: (Monthly groundwater yield – Demand for that month)
	GWAI-type 4	(GWAI-type 3) / (Monthly groundwater yield + Demand for that month)
Com-bined	TWAI-type 1	(Total annual runoff + Annual groundwater yield) / Total annual demand
	TWAI-type 2	(90% reliable driest month runoff + Minimum monthly groundwater yield) / Minimum monthly demand
	TWAI-type 3	Minimum over all months of: (90% reliable monthly runoff + Monthly groundwater yield – Demand for that month)
	TWAI-type 4	(TWAI-type 3) / (90% reliable monthly runoff + Monthly groundwater yield + Demand for that month)

2.7.2.4 Baseline

The model was run for a baseline period of 1961 to 1990. It should be noted, however, that landcover, and all information used to compute the water demands, are assumed to be constant over the baseline period with data used to derive the water demands centred on 1990. Figure 2.118a shows the straightforward Type 1 index as a simple ratio of the annual demand to runoff where 76 cells have an annual deficit of water. As expected the cells with highest runoff volume, i.e. those in the main river channel, have flows considerably in excess of demands annually. In the second plot (Figure 2.118b) the Type 3 index is plotted. The more complex index is Type 4 shown in Figure 2.118c which compares the water availability to the demand such that across most of South America the demand is met. A positive value for the Type 4 index shown as blue on the map indicates a ample supply of water to meet demand whereas a negative value denoted by orange and red indicates cells insufficient water to meet demand i.e. water stress with red indicating a more severe deficit. Overall for the baseline period there are 152 cells experiencing water shortfalls with two main clusters of cells: one in north-east Brazil, a region of intense agriculture, and the second in southern Argentina plus another smaller grouping in Paraguay. Water supply in southern Brazil, Argentina, Uruguay and Paraguay is, of course, supplemented by the use of groundwater pumped from the large regional Guaraní aquifer. In these simulations however, no account has been taken of water supply by groundwater and these maps should be treated as a worst case view if groundwater were to become unusable due to either insufficient recharge or contamination.

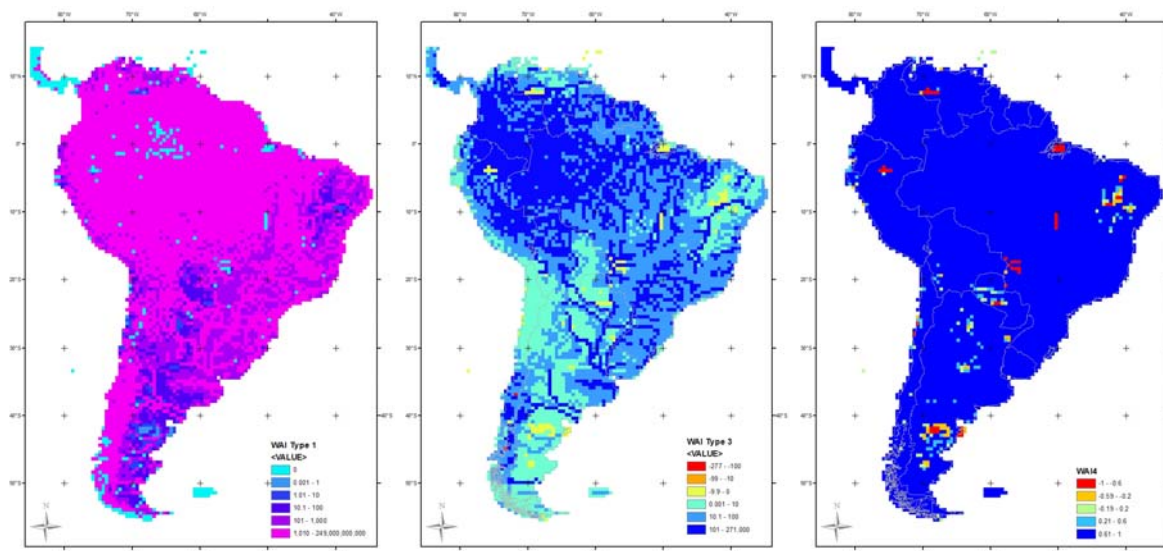


Figure 2.118 Maps illustrating a) WAI Type 1 b) WAI Type 3 and c) WAI Type 4 for South America computed for the baseline period 1961-1990

2.7.3 Scenario Creation and Impact Assessment

2.7.3.1 Climate change

The Fourth Assessment Report on Climate Change (IPCC, 2007) examined results from 24 different Global Circulation Models (GCMs) and four standard emissions scenarios. The IPCC Special Report on Emissions Scenarios (SRES) (IPCC, 2000) defines a standard set of future greenhouse gas concentrations according to storylines which reflect the socio-economic changes in the 21st century. These scenarios are referred to as A2 (a high emissions scenario), A1B (medium emissions scenario) and B1 (a low emissions scenario). The commitment scenario assumes the year 2000 concentrations are held constant i.e. no further increases in the emissions of greenhouse gases after the year 2000.

The range in global warming by the models under these four scenarios shows that the choice of SRES scenario has an increasing influence on global surface warming towards the later half of the 21st century (Figure 2.119).

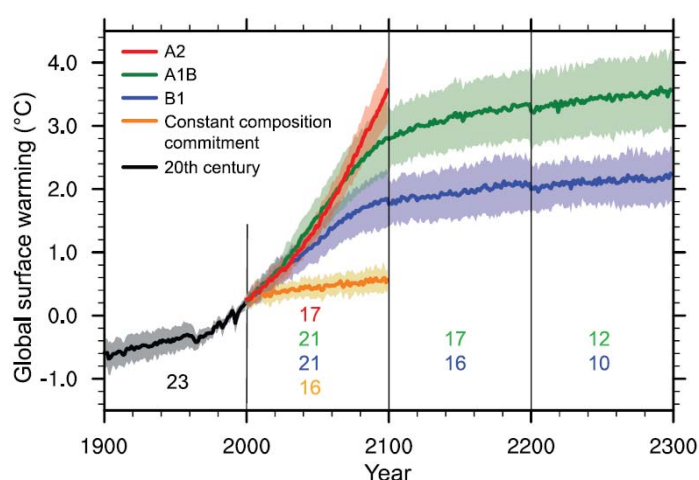


Figure 2.119 Summary plot of the global rise in surface temperatures for the three SRES scenarios. Source: Meehl et al. (2007)

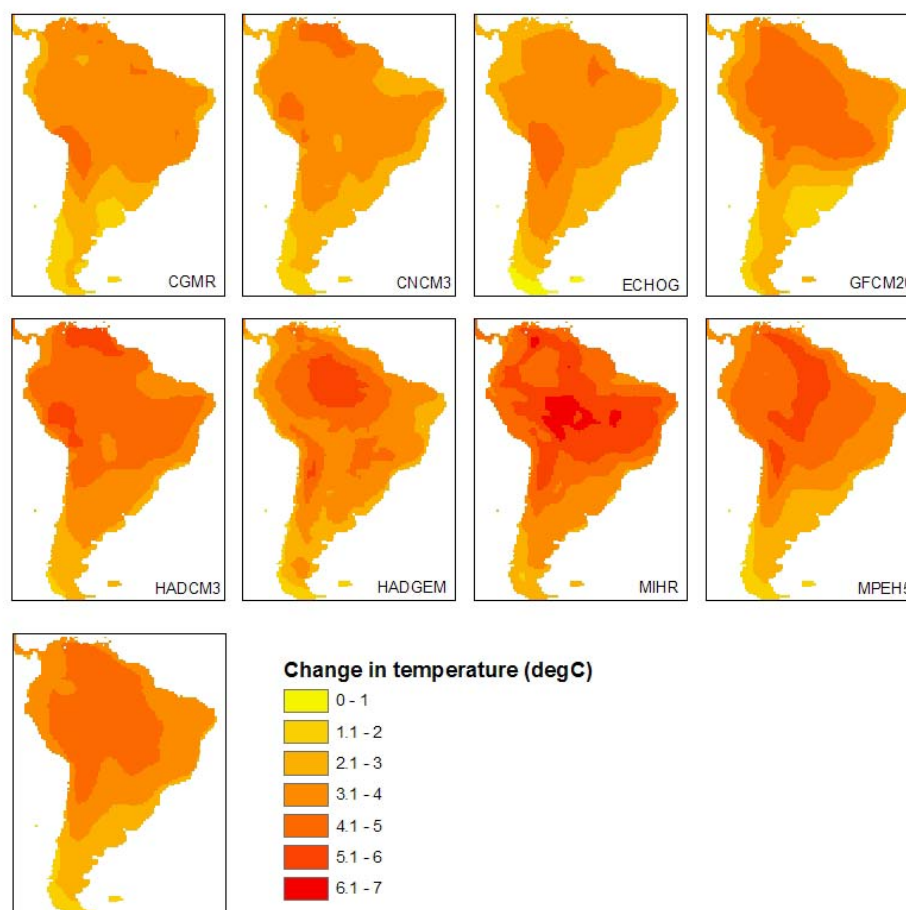


Figure 2.120 Absolute change in annual air temperature for eight GCMs (A1B scenario) and mean change of the eight models (bottom left)

Changes in mean annual temperature (Figure 2.120) and precipitation (Figure 2.121) are plotted for eight GCMs for 2080 and the SRES scenario A1B, to illustrate the variation between models. The pattern of warming is broadly consistent between models with greater warming predicted over the Amazon. The models CNCM3 and ECHOG3 show the least amount of warming annually over the continent, and MIHR the greatest. In contrast, for precipitation, there is little agreement even in the sign of the changes for the Amazon, north-east Brazil and southern Brazil/northern Argentina and northern pacific countries e.g. Columbia, Ecuador and Peru. There is some degree of agreement for a large part of Chile and Patagonia where all models show a decrease in precipitation and for the southernmost reaches of South America which shows an increase in precipitation by 2080. Assuming the model can be given equal weighting the model means indicate little change in annual precipitation over the Amazon but significant decreases in Chile, Argentina and Venezuela.

Precipitation estimates produced by GCMs are still too unreliable to be input directly into a hydrological model. However it is possible to examine the changes in precipitation and compare the models and scenarios accordingly. To this end, a control run and future run are required for each GCM from which to calculate the change. The GWAVA model is set up to take input in the form of percentage changes in the mean monthly precipitation, potential evaporation and absolute change in temperature. These changes are applied to the observed means and a time series reconstructed using the observed anomalies. Sub-monthly data are not readily available so the number of raindays is unchanged from the baseline.

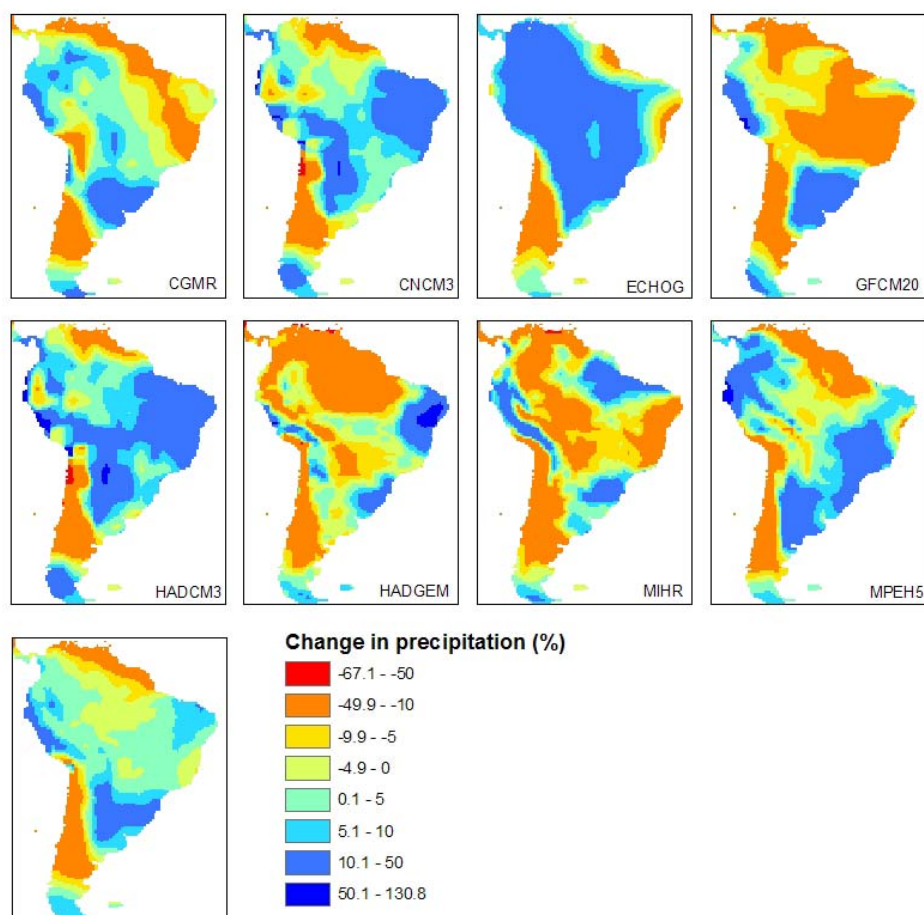


Figure 2.121 Patterns of change in annual precipitation by 2080 for eight GCMs. Blue colours indicate an increase in precipitation, the bottom left figure represents the mean change of the eight models

It was initially hoped that the data from MAGICC/SCENGEN v 4.1 (Hulme et al., 2000) could be used for input into GWAVA in common with the TWINLATIN partners, however this method has three main disadvantages in that :

- they provide data only at 5 degrees which requires greater downscaling than many of the available GCM outputs
- annual changes rather than monthly are provided; and
- the projections do not include the effects of aerosols.

Climate change scenarios have therefore been examined using the results from the more recent set of experiments performed for the IPCC Fourth Assessment report. There are a great many combinations of models and scenarios that could be considered. However the aim of this analysis is to examine as broad a range within a sensible timeframe. With much less variability between models and scenarios in the early 21st century, the 2020 and 2050 scenarios are examined using just one model and the A1B scenarios. Analysis of modelled precipitation over the Amazon (Li et al., 2006) for a range of GCMs showed that the HADCM3 and GISS-ER models were the best models at reproducing the current climate and for this reason the HADCM3 model is used to examine changes in the near future. Unfortunately monthly precipitation was not available for the GISS-ER model and so this model was not included in the comparison. To try and capture the 2080 time horizon and uncertainty, the SRES scenarios will be examined using just the HADCM3 model whilst variability between models will be compared for the A1B emissions scenario. The scenarios/models for which summary control and future precipitation and temperature data are available from the IPCC are summarised by model in the Table 2-42.

Table 2-42 Summary of GCM modelling group/model name and resolution for the eight models examined

Institute(s)/Model Name	Model Acronym	Model resolution*	Scenarios
Canadian Centre for Climate Modelling and Analysis (CCCMA), Canada / CGCM3	CGMR	~2.8° x 2.8°	A1B
Météo-France/ Centre National de Recherches Météorologiques, (CNRM) France /CM3	CNCM3	~1.9° x 1.9°	A1B,A2
Meteorological Institute of the University of Bonn, Meteorological Research Institute of the Korea Meteorological Administration (KMA), and Model and Data Group, Germany/Korea ECHO-G	ECHOG3	~3.9° x 3.9°	A1B,A2
U.S. Department of Commerce/National Oceanic and Atmospheric Administration (NOAA)/Geophysical Fluid Dynamics Laboratory (GFDL), USA /CM2.0	GFCM20	2.0° x 2.5°	A1B, A2
Hadley Centre for Climate Prediction and Research/Met Office, UK HADCM3	HADCM3	2.5° x 3.75°	B1, A1B,A2
Hadley Centre for Climate Prediction and Research/Met Office, UK / HADGEM	HADGEM	~1.3° x 1.9°	A1B
Center for Climate System Research CCSR (University of Tokyo), National Institute for Environmental Studies NIES, and Frontier Research Center for Global Change FRCGC (JAMSTEC),Japan / MIROC3.2_HI	MIHR	~1.1° x 1.1°	B1, A1B,A2
Max Planck Institute for Meteorology(MPI),Germany /ECHAM5	MPEH5	~1.9° x 1.9°	A1B,A2

* Model resolution refers to the GCM atmospheric resolution and is that from which the climatological parameters such as precipitation and air temperature are interpolated.

Data processing

Climate change data were obtained from the IPCC data distribution website (www.ipcc-ddc.org) for all model/scenarios for the control period, 2010-2039, 2040–2069 and 2079–2099 thirty year averages. The data for each model scenario were interpolated to a 0.5 degree grid using the program Xconv (available from British Atmospheric Data Centre (BADC)) which also enables the Netcdf file format to be viewed. The variables available to compute potential evaporation using the Penman based calculation (Penman, 1948) vary from model to model, so to provide consistency across all models the Thornwaite (1948) temperature method was used to calculate potential evaporation for both the GCM control and future runs.

$$PE(mm/month) = 16 \left(\frac{10T}{I} \right)^a$$

where: T is monthly temperature (°C)

The constants I and a are computed from monthly temperature according to:

$$I = \sum_1^{12} \left(\frac{T}{5} \right)^{1.514}$$

$$a = 67.5e-8 I^3 - 77.1e-6 I^2 + 0.01791I + 0.492$$

This change is applied to the calculated baseline potential evaporation.

The three sets of experiments were carried out to understand the likely trend in changes that will affect South America. These involved running GWAVA with the changes in precipitation, potential evaporation and temperature with baseline demands isolating the climate impact. The impacts are considered in terms of changes to average flows, an index low flow and also in terms of the Water Availability Index Type 4.

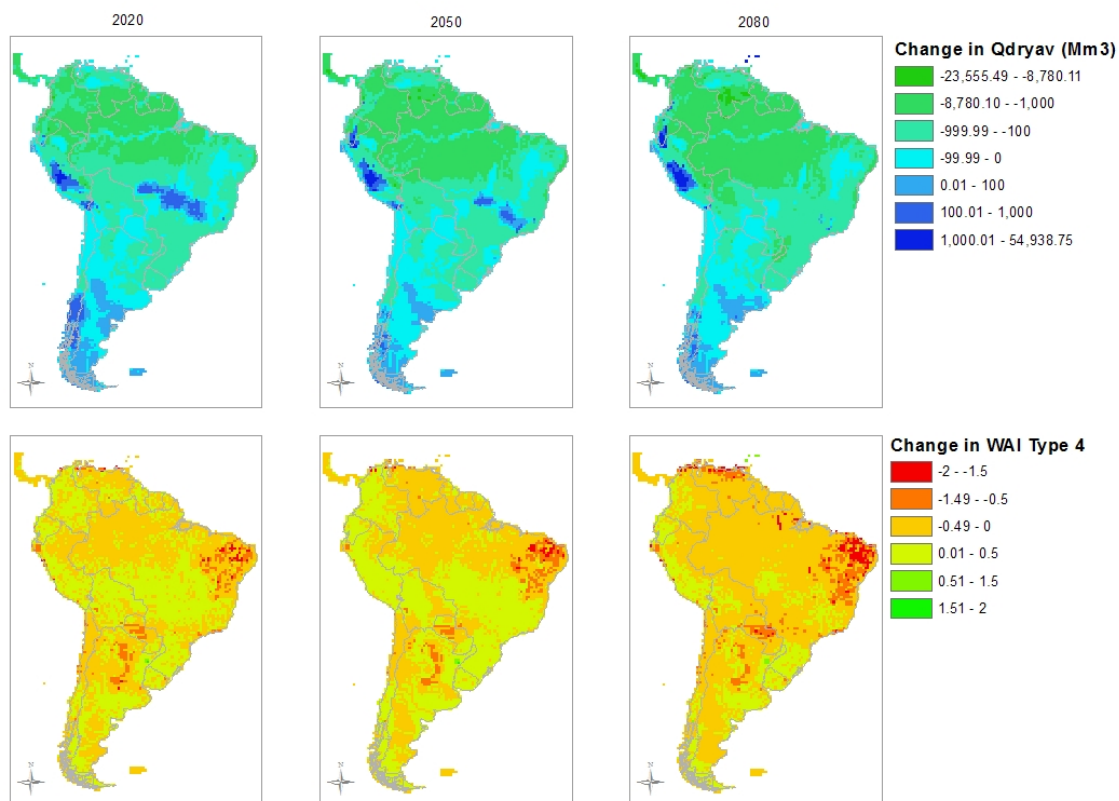


Figure 2.122 Changes in the low flow index (above) and WAI 4 (below) for 2020, 2050 and 2080.

Comparison of the HADCM3 A1B future climates for 2020, 2050 and 2080 with the 1961–1990 baseline show increases in the average continental temperatures of 1.36 °C, 2.72 °C and 4.22 °C, respectively, and very modest increases in precipitation of 1.44%, 3.13% and 3.57%, respectively, yet impacts on the index low flow volumes are greatly affected with respective decreases of 21%, 34% and 54%. These dramatic reductions are due in part to the reduction in winter precipitation and to increasing temperatures and soil moisture deficits in the summer months. The plots in Figure 2.122 show the distribution of changes in the low flow index (Qdryav) with dark blues indicating an increase in flows and greens a decrease. The plots of changes in Figure 2.122 show the change water availability index from the baseline with orange and reds indicating a reduction in the Type 4 index i.e. moving towards or becoming increasingly water stressed, whereas greens indicate cells becoming less water stressed. The total number of cells experiencing insufficient water to meet demand are summarised in Figure 2.123. In terms of the Type 4 index there are a larger number of cells more severely affected between 2050 and 2080 than for the first half of the 21st century although the average Type 4 index of all cells in a water scarce situation is largely unchanged. The cells most affected are located in the northern Venezuela, north east Brazil, Paraguay and northern Argentina.

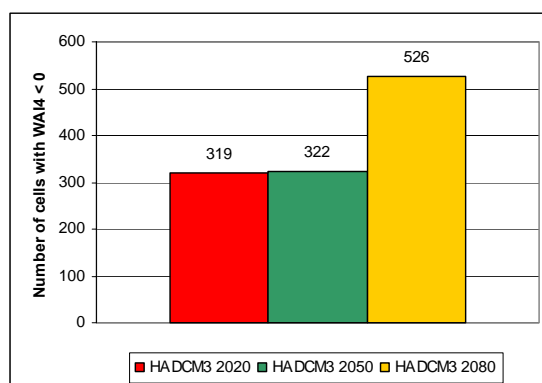


Figure 2.123 Summary plot of the number of cells experiencing water stress under one GCM (HADCM3) for three timeslices: 2020, 2050 and 2080.

To understand how much the above results are affected by the choice of model statistics focussing on water resources for eight GCMs for the year 2080 and the A1B emissions scenario are compared to the baseline values in Table 2-43. The value of mean flow represents the annual average flow as an average of all cells and shows a wide degree variation between models with the model ECHOG actually showing an increase in both the mean annual flow and the low flow index. The index low flow show a similar level of change again with the ECHOG model showing increases while HADGEM shows the largest decline. Figure 2.124 shows how this translates to the number of cells that are water stressed and shows that the HADCM3 and MIHR models yield the most water stressed cells and, despite increases in annual flows the ECHOG model indicates an increase in the number of water stressed cells.

In terms of the Type 4 index all models show a worsening situation by 2080. In a comparison of the three emissions scenarios using the Type 4 index, although the A2 scenario leads to greater warming and lower mean flows, the index indicates a slightly larger area being affected by deficits in water supply for the A1B scenario.

Table 2-43 Comparison of flow statistics and water availability indices for eight climate scenarios in 2080

GCM	Mean annual flow (Mm ³)	Qdryav (Mm ³)
Baseline	62529	2784
CGMR	44355	2224
CNCM3	43766	2141
ECHOG	62643	3158
GFCM20	37656	1629
HADCM3	26494	1266
HADGEM	19912	1028
MIHR	32160	1712
MPEH5	41399	1859

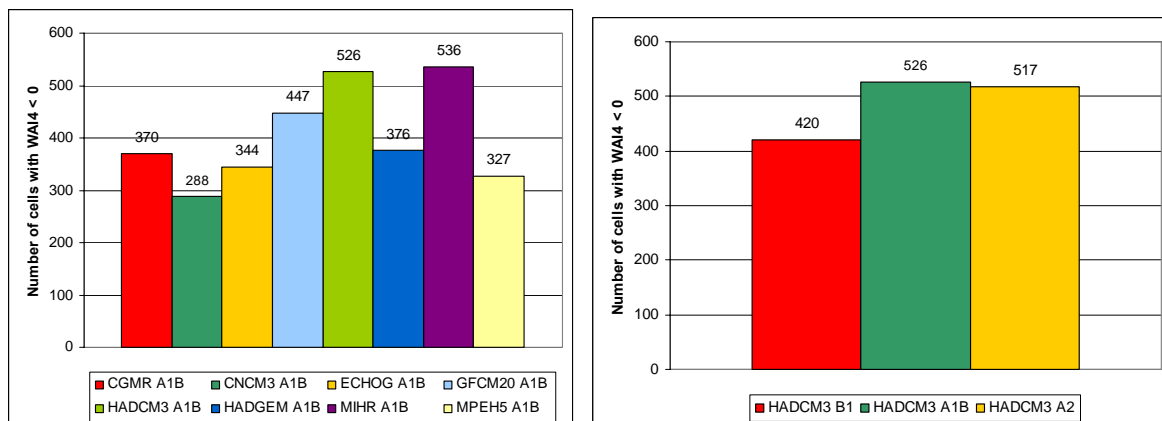


Figure 2.124 Summary plots comparing the number of cells in a water stressed state for eight GCMS (left) and the three SRES scenarios (right).

2.7.3.2 Land use change

Although land use changes were examined by some of the partner groups, the level of detail was greater than could be adequately represented within the 0.5 degree resolution of this model.

2.7.3.3 Changes in water demands

The water demand scenarios considered under human development relate to the water demand from the domestic sector encompassing water for drinking, subsistence farming, municipal services such as hospitals, etc. The rising trend in domestic water demand is driven upwards, primarily by the increasing population exerting a larger demand for drinking water, as well as, increasing standards of living, particularly in growing economies where there are improvements in access to reliable water supply and ownership of devices such as washing machines. Trends of increasing per capita water consumption with growing economic activity as indicated by economic measures such as Gross Domestic Product (GDP) are well known. Migration of populations from rural to urban dwellings also contributes to increases in water demand in cities.

This scenario does not include other indirect impacts such as increased irrigation to provide food for growing populations.

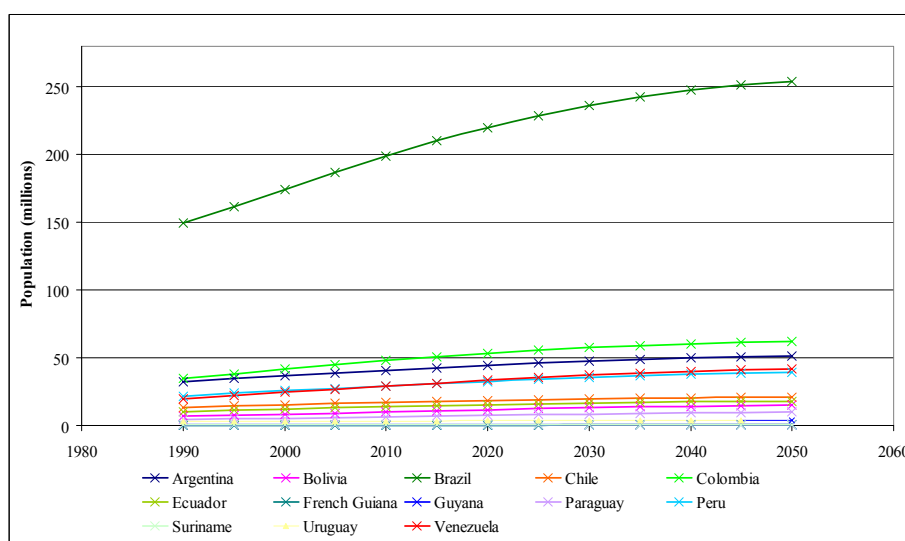


Figure 2.125 Population projections (medium variant) for South American nations to the year 2050

Human populations are, in general, expected to continue rising with growth rates plateauing towards the latter half of the 21st century (UN, 2004). The UN World Population Projections (WPP) (UN, 2006) produce low, medium and high variant estimates of future populations for each country based on modelling fertility, birth and death rates. Projected population (medium variant) for South American countries up to 2050 (Figure 2.125) indicate a steady increase. Projections of the rural/urban population split (UNPD, 2006) shown in

Table 2-44 are available up to year 2030 and generally confirm that rural populations will continue to reduce as growth rates reduce and people migrate to cities. Overall, total continental population under the medium variant projection as applied to the GWAVA baseline will increase from 297 million, to 442 million in 2020 with over 86% of the population living in cities. Although the percentage urban populations are assumed to be constant after 2030, the estimated total population for South America is 523 million for 2050.

Table 2-44 Projected urban and rural populations (thousands) and percentage urban population for South America by country for 2020 and 2030

	1990			2020			2030		
	Population ('000s)		% Urban	Population		% Urban	Population		% Urban
	Urban	Rural		Urban	Rural		Urban	Rural	
Argentina	28345	4236	87	41016	3470	92.2	44302	3232	93.2
Bolivia	3708	2961	55.6	8263	3375	71	9802	3232	75.2
Brazil	111842	37680	74.8	196893	23099	89.5	215433	21047	91.1
Chile	10978	2201	83.3	16961	1678	91	18255	1523	92.3
Colombia	23959	10916	68.7	41153	12085	77.3	46234	11343	80.3
Ecuador	5660	4612	55.1	10748	4628	69.9	12376	4303	74.2
French	86	30	74.5	210	57	78.6	260	59	81.4
Guyana	216	515	29.5	218	482	31.2	244	416	37
Paraguay	2069	2179	48.7	5055	2478	67.1	6099	2384	71.9
Peru	14994	6768	68.9	24828	7712	76.3	28202	7362	79.3
Suriname	275	127	68.3	379	101	79	394	87	82
Uruguay	2764	342	89	3268	227	93.5	3385	205	94.3
Venezuela	16574	3157	84	32245	1170	96.5	36072	1077	97.1

Method

The changes in population were mapped using the 1990 spatial distribution of population derived from the Gridded Population of the World (CIESIN et al., 2005) dataset and an urban fraction derived from the Global Rural-Urban Mapping Project (GRUMP) (CIESIN et al., 2004). The future population scenarios were applied as percentage changes from 1990 values at the data resolution of 0.083333 degrees for urban populations and rural population applied to the remaining pixels before being upscaled to 0.5 degrees.

There are few very accurate data on per capita water use either for the baseline or for future projections or urban or rural populations. More easily obtainable are estimates of per capita water resource availability which are simply an estimate of the total freshwater resources divided by the country's population. However this is a rather different quantity that does not reflect the water people actually consume or take account of network losses and returns. An estimate applied in an earlier study in Southern Africa (Meigh et al., 1998) and given by the World Health Organisation as a minimum water requirement for human consumption of 23 l/capita/day (but rounded to 25 l/capita/day) is used as a baseline value for rural populations. This value is likely to be lower than that

actually used in many parts of South America particularly as access to water (90% of the population) is significantly higher than that in Sub-Saharan Africa (56% of total population) (WHO and UNICEF, 2006). However, the inability to meet this minimum requirement indicates a genuine water scarcity. The future estimates used here are best estimates as provided in the methodology by Meigh et al. (1998) and it is therefore assumed that per capita consumption across Latin America will continue to grow. The values shown in Table 2-45 are applied to all countries.

Table 2-45 Values of per capita water use estimated for baseline and two future scenarios

	Rural (l/capita/day)	Urban (l/capita/day)	Special/Large Urban (l/capita/day)
1990	25.0	50.	140.
2020	50.0	140.	160.
2050	50.0	140.	160.

The plots (Figure 2.126) of the Type 4 index highlight the cells facing increasing water stress for 2020 and 2050. As for the baseline the cell experiencing water stress fall into two distinct clusters: one in north-east Brazil and the other in Southern Argentina with some smaller areas in Paraguay. It is quite difficult to distinguish major differences between the two plots in terms of the scale of the deficits as indicated by the Type 4 index. There is a significant increase in the number of cells experiencing a deficit from the baseline, 152 compared with 204 and 215 for 2020 and 2050 respectively, which can be attributed to the much larger increases in urban water demand which are fairly localised compared with the more extensive rural water demands.

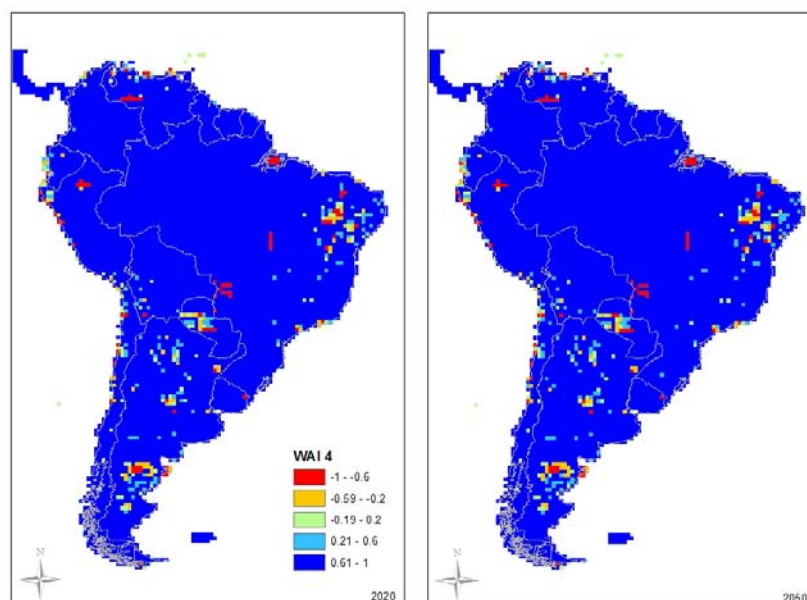


Figure 2.126 Mapping the Type 4 Water availability index for South America for two water demand scenarios of population growth for the years a) 2020 and b) 2050

2.7.3.4 Combined effects

The climate change scenarios do of course have implied assumptions about the future global populations and in this section the effects of a combination of climate change and growing demand for

water due to population growth are considered. Three combined scenarios have been examined to provide ‘realistic’ snapshots of water availability for the years 2020, 2050 and 2080 as set out in Table 2-46. As medium variant population estimates show a levelling off of population growth after 2050, the 2050s population grids have used for the 2080 simulation.

Table 2-46 Summary of the three combined scenarios performed and the driving data for each

Scenario	Human Development	Climate change
Combined 2020	2020 population (medium variant)	HADCM3 A1B – 2020
Combined 2050	2050 population (medium variant)	HADCM3 A1B - 2050
Combined 2080	2050 population (medium variant)	HADCM3 A1B – 2080

The results of these three scenarios are shown as maps of the Type 4 index (Figure 2.127) with blue areas indicating supply meets demand at all times whereas orange and red cells are those whose water supply fails to meet demands. It is very clear from the maps that there is an intensification of deficits in cells experiencing water stress moving from 2020 to 2050 as well as an extension of the area that is affected in particular by 2080. It is very clear from Figure 2.128 that the combined effect is much greater than for either climate or demand changes alone.

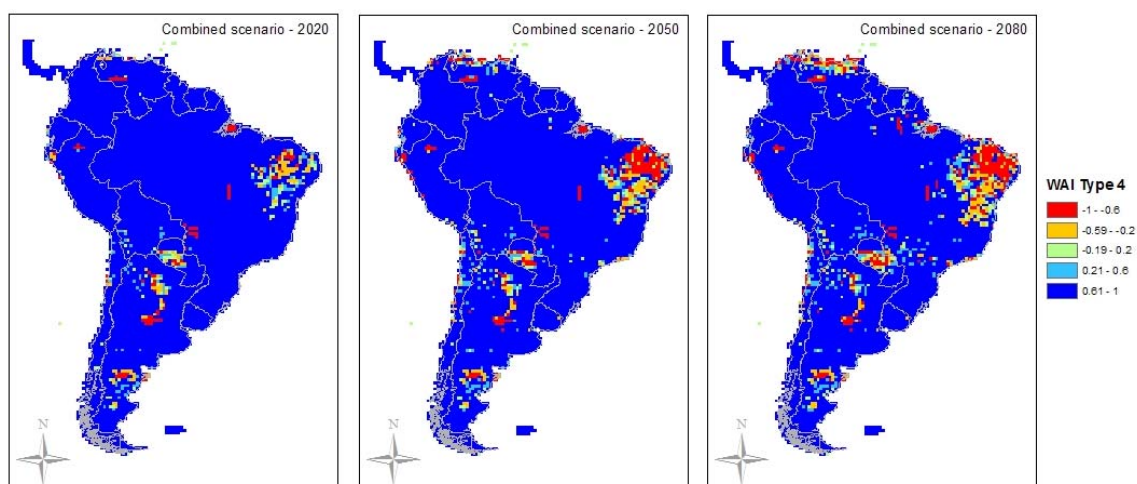


Figure 2.127 Plots of the Type 4 index for South America for the three combined scenarios

The combination of climate change and increasing water demands due to population growth and development show very clearly the worsening situation that both effects will have, with a higher number of cells, 371 compared to 319 under climate change alone, by 2020 are water stressed.

2.7.4 Vulnerability assessment

The key model outputs from GWAVA can be used to inform water planners and policy makers of the potential scale of water deficits or surpluses and areas of concerns. In addition, time series of flows can be examined for particular river basins or, in the case of this study, particular flow statistics may be mapped both for the baseline and the future. However, issues such as sensitivity to change and vulnerability cannot be addressed directly by modelling alone but require alternate approaches such as

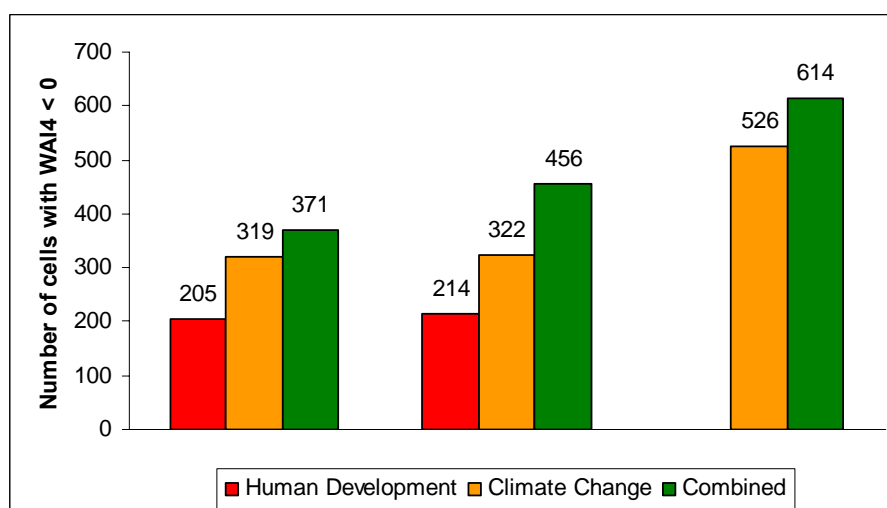


Figure 2.128 Summary plot comparing the number of cells experiencing deficits for single and combined scenarios

the Climate Vulnerability Index (CVI) (Sullivan and Meigh, 2005; Meigh et al., 2005) which considers socio-economic factors such as access to, and effective management of water, as well as physical factors such as availability of resource and climate. The GWAVA model may be used to examine the effect of some mitigating strategies such as improvement to irrigation efficiency and can help stakeholders, planners and managers understand more fully the consequence of certain changes be they in the climate or to the demands.

In a simplistic approach it is possible to use to results from GWAVA to determine, for example, some measure of vulnerability on a broad scale by expressing the impacts rather than as a water stress index but in terms of total populations or total irrigated land experiencing water deficits across South America region. An example is given in Table 2-47 in which populations are summed across all the cells which are classed as water stressed according to the Type 4 index.

Table 2-47 Comparison of the WAI4 Index and the total population at risk of water deficits

Scenario	Number of cells with a Type 4 index < 0	Total population (millions)
Baseline	157	1.8
2020 combined	371	10.0
2050 combined	456	72.1
2080 combined	614	88.8

In Table 2-47 the total populations deemed to be vulnerable are compared for the baseline and the three combined scenarios and highlight a dramatic increase in the numbers of people at risk by 2050 as highly populated areas experience deficits.

2.7.5 Summary

A macro-scale hydrological model, GWAVA has been applied to mainland South America encompassing four TWINLATIN basins: Baker, Catamayo-Chira, Cauca and Cuareim/Quaraí, three of which are transboundary basins. The model was calibrated against observed streamflow data and replicated flows for much of the continent, the main exceptions are the very small catchments on the Pacific side of the Andes for which the grid resolution was too coarse to extract single basins and for which there are generally insufficient observed data against which to compare the model.

The model was run for a baseline period of 1961 to 1990 against which all scenarios are compared. The changes have been examined in terms of changes to the index low flow and the water availability indices, in particular the Type 4 index. Under baseline conditions 152 cells experience water deficits i.e. are water stressed appearing in two main regions: north east Brazil and southern Argentina.

Scenarios are a useful tool in understanding the possible outcomes of change and in the context of this study enables consideration of the effects of climate change combined with water demand changes. Scenarios are essentially a means to examine the response of a system to 'natural' patterns of change rather than simple sensitivity tests and there are, of course, numerous uncertainties associated with these types of scenarios which are discussed below. These scenarios therefore provide indications of response that may be experienced and should not be taken as absolute predictors of change.

Climate change scenarios have been examined through the use of information derived from the outputs of Global Circulation Models, applying changes in mean monthly temperature, precipitation and potential evaporation to baseline means. The climate scenarios in general show increased annual warming and hence potential evaporation across South America and all models indicate small increases in annual precipitation. The pattern of change in precipitation is particularly mixed around approximately the line of 30 degrees latitude however, precipitation is likely to decrease in Venezuela, and Chile, whilst there may be modest increases in the southern parts of South America.

Scenarios of increasing water demand due to population growth have also been considered. Changes to human populations are more certain in terms of patterns and direction of change, but exact future water demand estimates are still imprecise. Much of the increase in population and therefore water demand will occur in existing urbanised areas and the effects of water shortages are therefore very localised, with relatively few additional cells moving into water stressed states. Examination of the populations in cells that are classed as water stressed in some ways confirms this results and reveals the vulnerability of large conurbations to climate change.

One important conclusion is the need to take the effects of climate change in combination with demand changes and, crucially, that these should take account of the seasonal changes which impact on both the supply of water and the water demand. The results of the combined scenarios show that areas most at risk are Venezuela, north east Brazil, much of Paraguay and two regions in Argentina.

Uncertainties in the water availability estimates arise from both estimation of the hydrological cycle and the water demand itself. Another approach is to think broadly of uncertainties in data, model structure or the processes represented by the model. Data uncertainties arise from not knowing the true value of the water demands per cell for every month of the simulation. To reduce these uncertainties data from as many sources as possible are used to validate model inputs however some errors will remain. Model uncertainties arise from the ability of the model to capture to processes being modelled. In examining climate change scenarios uncertainties in the hydrological model are compounded by the uncertainties and approximations made associated with the GCMs themselves. It is clear that are considerable uncertainties in the predicted future climates, with models showing both positive and negative trends in future rainfall patterns across South America. Finally there are uncertainties introduced by use of a simplistic method used to examine climate change and which very likely leads to an underestimation as to the true variability of the future climate and this in turn would lead to an underestimate of the extreme events of droughts and floods. Unfortunately this last point is one that is still to be addressed by the improvement of rainfall generating processes in climate models; downscaling techniques such as the use of regional climate have shown some promise but there are currently no simulations that cover the whole South American continent.

Recommendations for the future include representation of groundwater sources to provide a fuller picture of water use and water stress particularly in southern Brazil and Argentina. It is also important to understand impacts not only on human beings but on environmental impacts and such a model may also be used identify area at risk e.g. from a reduction in environmental flows. In order to more accurately examine impacts of climate change a new method to understand and incorporate changes in variability is required which would in turn lead to better estimates of future extremes and assessment of water resources.

3 CONCLUSIONS AND RECOMMENDATIONS

The main objective of Work Package 8 “Change effects and Vulnerability assessment” was to estimate the effects of future climate change, land use change and water resources developments on the hydrological regime, on water availability and water quality, and its ecological, societal and economical consequences.

In this report, the analysis of change effects and vulnerability assessment of 5 Latin American basins and the South American continent was described. The study areas show large variations in geography, climate, hydroecology and natural resources, as well as important differences in socio-political systems, economic development, cultures and traditions.

In the first phase, future scenarios were created. The scenarios concern climate change, land use change and water resources development (rural and urban development, hydropower projects, etc.). In case of the *climate change* scenarios, all basins agreed to use the MAGICC/SCENGEN model to investigate future climate change and its uncertainties. An adapted manual for the use of MAGICC/SCENGEN was prepared (see Annex 1, in Spanish). In some cases, additional expert judgement change scenarios were formulated, mainly to test the vulnerability of the basin characteristics to change. For the continental modelling, scenarios from the IPCC Fourth assessment Report were used directly. *Land use change* scenarios were created principally by expert judgement. The main reason was limited data availability and quality that would have been necessary for land use/land cover change modelling. Scenarios concerning *water resources developments and changes in water demand* focussed on hydropower development (Baker), reservoir structures for irrigation (Quaraí/Cuareim) and changes in water demand related to agriculture (Cuareim) and population growth, agriculture and industry (Cauca). The continental modelling focused on population growth.

After change scenarios were created, the impact of these scenarios was estimated using calibrated and validated models. For that reason, input from mainly Work Packages 3 (“Hydrological modelling, flooding, erosion, water scarcity and water abstraction”) and 6 (“Pollution pressure and impact analysis”) was needed.

The main outcomes of scenario impact assessment analyses are summarised in the following tables:

Basin	Scenario	Impact of Climate Change
Baker	Perturbations of time series with change signals for temperature and precipitation	Hydrology is highly sensitive to changes: % reduction in discharge is higher than the corresponding % change in annual precipitation. Effect is less pronounced in upper basin; here, the snow season will shorten, with more rain than snowfall during winter months and an earlier snowmelt discharge peak.
Catamayo-Chira	2 climate change scenarios based on A1 and B2 and 4 GCMs	A decrease in mean annual precipitation results in decreasing water yields and decrease of sediment yield.
Cauca	Perturbations of time series with change signals for temperature and precipitation	Flows tend to increase (+ 3 %) with increasing rainfall (+ 2 %). Impact is larger on high flows.
Lago de Nicaragua	Perturbations of time series with change signals for temperature and precipitation	High uncertainty persist with respect to the intensity and even direction of climate change variables. If higher temperatures occur in combination with lower precipitation rates, the water balance might be seriously affected.
Quaraí	Hypothetical changes in annual mean	The Quaraí river basin is sensitive to changes

Basin	Scenario	Impact of Climate Change
	precipitation and temperature for sensitivity analysis	in precipitation: 10% change in rainfall results in 18.5% change in medium stream flow. Low flows are less susceptible to changes in rainfall. A 2°C increase in temperature results in a 4% decrease in medium stream flow. Low flows are more sensitive to temperature change.
	Monthly changes in temperature and precipitation from climatic models using MAGICC/SCENGEN (2050)	On average, expected changes are higher for median to high flows. Median flows are expected to increase (+ 10%). Low flows might increase, but less significantly (+ 5%). This slight increase is expected to be most important during the summer months.
Cuareim	Extrapolation of frequency of ENSO events an non-linear tendency	Higher precipitation generates higher runoff, slightly higher percentages of harvested area and slightly higher net returns
South America	8 Global Climate Models with one SRES scenario A1B, and HADCM3 with three SRES scenarios A1B, A2 and B1, for time horizons 2020, 2050 and 2080.	7 out of 8 models show a worsening situation by 2080 with lower mean flows and lower dry season flows. Using HADCM3 A1B, the number of grid cells experiencing water stress (i.e. demand > supply) doubles by 2020 and 2050, and quadruples by 2080.

Table 3-1 Summary impact assessment climate change scenarios

Basin	Scenario	Impact of Land Use Change
Baker	none	
Catamayo-Chira	1. Development based on actual trends	SWAT predicts higher runoff values (+ 7 %), but lower base flows (- 10 % up to - 34 %). In general, water yields will be higher (+ 4 %). Sediment yields are estimated to be higher (+ 28 %, SWAT) or show no change (WaTEM/SEDEM). SWAT shows more erosion in the centre of the basin; WaTEM/SEDEM shows more soil loss in microbasins with conversions from forest to crops.
	2. Sustainable development scenario	SWAT predicts higher runoff values (+ 12 %) with higher base flows (+ 15 %). Water yields will be higher (+ 4 %). Both SWAT and WaTEM/SEDEM estimate annual soil losses and sediment yield to be lower (- 21 %).
Cauca	Changes of cropland area	Impact on water demand (see Table 3-3)
	De/afforestation (25 – 35 – 40 % of the basin covered by forest)	Stream flow seems not sensitive to changes in forest coverage.
Lago de Nicaragua	none	
Quaraí	10% of the land covered with pasture changes into Eucalyptus plantations (1. without contact to groundwater / 2. with moderate access to groundwater / 3.	Reduction of average stream flow: impact will be relatively low if the forests are planted and managed in order to avoid access to shallow unconfined aquifers. Eucalyptus forests

Basin	Scenario	Impact of Land Use Change
	with facilitated access to groundwater)	planted in areas of shallow groundwater will have clear impact on low flows, which are already very low in the region.
Cuareim	Soils suitable for summer crops will change from pasture into rice	(no results)
South America	none	

Table 3-2 Summary impact assessment of land use change scenarios

Basin	Scenario	Impact of Water Resources Development and Changes in Water Demand
Baker	none (refer to WP 9)	
Catamayo-Chira	none	
Cauca	Changes in water demand related to population growth, bovine industry, agriculture and industry	Net water availability increases, water deficits in the months July-August tend to decrease.
Lago de Nicaragua	none	
Quaraí	Scenarios related to the presence or absence of water resources structures related to irrigation:	The impact of the use of the water of the small reservoirs seems to be relatively small; however not negligible. The most important impact related to water resources use in the Quaraí river basin is the direct withdrawals of the rivers, which are causing the river to dry out sometimes. The model results confirm the presence of conflicts among different water users (farmers and public supply) and between the users of the two involved countries. Water is the most important limiting factor to rice growing activity in the basin.
Cuareim	Water demand increases due to conversion from pasture into rice, and because of irrigation of grasslands Two large reservoirs in the upper basin	Higher percentages of harvested area and maximum net return Risks related to climate variability are eliminated
South America	Changes in water demand related to population growth for time horizons 2020 and 2050	The number of grid cells experiencing water stress (i.e. demand > supply) increases by 34% in 2020 and by 41% in 2050. These are largely caused by localised increases in urban water demands. These significantly worse when combined with the climate change scenarios.

Table 3-3 Summary impact assessment of water resources development and changes in water demand scenarios

In a third phase, the vulnerability of water bodies was assessed based on the modelled impacts of future scenarios. Vulnerability is defined as the extent to which a natural or social system is susceptible to sustaining damage from climate change and changes in pressure due to human activities. From the previous analysis, we can conclude that the probability of exposure to changed future conditions of water availability and/or quality in most basins is high.

Variations in water flows and groundwater recharge, whether of climatic origin or due to land mismanagement, can add to drought and flood events, which can have catastrophic effects in terms of large scale loss of human life and damage to economic, social and environmental systems. Water pollution creates another set of risks, affecting human health, economic development and ecosystem functions. Economic risks are also important in water resources management and development due to the often large-scale and long-term character of the investments required. Political instability and change represents yet another important risk factor for integrated water resources management. To date, relatively little attention has been paid to the systematic assessment of risk mitigation costs and benefits across the water use sectors and to the consequent evaluation of various risk trade-off options.

Additionally, an integrated approach to water resources management entails identification of conflicts of interest between upstream and downstream stakeholders. The consumptive “losses” upstream will reduce river flows. The pollution loads discharged upstream will degrade river water quality. Land use changes upstream may alter groundwater recharge and river flow seasonality. Flood control measures upstream may threaten flood-dependent livelihoods downstream. Such conflicts of interest must be considered with full acknowledgement of the range of physical and social linkages that exist in complex systems. Recognition of downstream vulnerability to upstream activities is imperative. Once again management involves both natural and human systems.

Reducing people’s vulnerability to environmental and socio-economic changes can involve strengthening local rights by, for example, developing institutional forms that are more inclusive of local concerns or strengthening resource tenure to give people secure access to their livelihood assets and increased control over how local resources are used. Reducing vulnerability includes access to better financial and technical support and information, and investing in the capacity to cope with natural disasters and adapt to climate change.

However, an important remark on the accuracy of and the uncertainty in results should be made. On the one hand, a certain degree of uncertainty is linked to the use of hydrologic models to assess the impact of change scenarios. The degree of accuracy that can be reached with hydrological modelling is highly dependent on the quantity and quality of the input data. This problematic is described in more detail in the reports of Work Packages 3 and 6. On the other hand, it is very difficult to assess the accuracy of future change scenarios formulated in this work package, but we should bear in mind uncertainty is most probably high. In particular, the climate change scenarios are highly uncertain. In most cases here studied, large differences exist between models and SRES scenarios. The difference between the values of different models (for the same emissions scenario) is in many cases much larger than the difference in the predictions of a single model, considering different emissions scenarios.

A first recommendation for the future is to use the new version of MAGICC/SCENGEN (version 5.3.v2, released December 2008). This new version further extends the possibilities of the version that was used under TWINLATIN, and also includes important improvements: e.g. updated confidence intervals for climate sensitivity, improved model for calculating the sea level rise, improved resolution of output grid (2.5° x 2.5°), addition of mean sea level pressure data, etc.

Secondly, the assessment of water resources availability and quality, and their possible long-term changes through consumptive water use, climate or land use change, are highly dependent on reliable data from monitoring and gauging systems. In almost all TWINLATIN study basins, the currently existing hydrometeorological network and available time series were indicated to limit the possibilities for hydrological modelling and impact assessment in an important way. This emphasises the need for resources to be allocated for the investment, operation and maintenance of this aspect of water infrastructure. For future high quality hydrological modelling efforts investments should therefore be made in (i) improving and extending the existing monitoring networks, and (ii) combining traditional means of monitoring with additional research on the use (and usefulness) of alternative ways for monitoring hydrometeorological variables, such as remote sensing techniques. In this context also the importance of metadata storage to facilitate sharing of data among communities, minimizing duplication, reducing costs and facilitating efficient analysis and decision making and systematic quality control of hydrometeorological data should be pointed out. In case of binational river basins (e.g. Cocibolca Lake Basin, Catamayo-Chira Basin) there is an imperative need for trouble-free data

interchange, agreements on uniform classification systems (e.g. land use maps, soil maps) and (meta)data storage etc.

Finally, public awareness is needed in order to mobilize effective support for sustainable water management and induce the changes in behaviour and action required to achieve this. Additionally, public awareness and subsequent pressure for action may be vital in fostering the political will to act. In this context, governments at national, regional and local levels have the responsibility for making participation possible. This involves the creation of mechanisms for stakeholder consultation at all spatial scales; such as national, basin or aquifer, catchment and community levels. The principle of stakeholder participation in water resources management requires a serious effort of raising awareness among politicians, decision-makers in the water sector, professionals, interest groups and the public at large. In any attempt to attract attention and support for water management from these groups, success will depend upon the mechanisms of communication and the quality and relevance of available information.

REFERENCES

- Abu El-Nasr, A., Arnold, J., Feyen, J. and Berlamont, J., 2005. Modelling the hydrology of a catchment using a distributed and a semi-distributed model. *Hydrological Processes*, 19(3): 573-587.
- Andersson, L. et al., 2006. Impact of climate change and development scenarios on flow patterns in the Okavango River. *Journal of Hydrology*, 331(1-2): 43-57.
- Andréassian, V., 2004. Waters and forests: from historical controversy to scientific debate. *Journal of Hydrology*, 291(1-2): 1-27.
- Arnold, J., Srinivasan, R., Muttiah, R. and Williams, J., 1998. Large area hydrologic modeling and assessment - Part 1: Model development. *Journal of the American Water Resources Association*, 34(1): 73-89.
- Arnold, J. et al., 2009. *Soil and Water Assessment Tool (SWAT): Global Applications*, World Association of Soil and Water Conservation.
- Beven, K., 2001. *Rainfall-Runoff Modelling: The Primer*. John Wiley and Sons.
- Bosch, J. and Hewlett, J., 1982. A review of catchment experiments to determine the effect of vegetation changes on water yield and evapotranspiration. *Journal of Hydrology*, 55(1-4): 3-23.
- Box, G. and Jenkins, G., 1976. *Time series analysis: forecasting and control*. Oakland, California, Holden-Day, 575 pp.
- Calder, I., 2002. Eucalyptus, water and the environment. In: J. Coppen (Editor), *Eucalyptus: the genus Eucalyptus*. CRC Press, pp. 450.
- Cao, W., Bowden, W., Davie, T. and Fenemor, A., 2006. Multi-variable and multi-site calibration and validation of SWAT in a large mountainous catchment with high spatial variability. *Hydrological Processes*, 20(5): 1057-1073.
- Chalecki, E. and Gleick, P., 1999. A framework of ordered climate effects on water resources: a comprehensive bibliography. *Journal of the American Water Resources Association*, 35(6): 1657-1665.
- Chaplot, V., 2007. Water and soil resources response to rising levels of atmospheric CO₂ concentration and to changes in precipitation and air temperature. *Journal of Hydrology*, 337(1-2): 159-171.
- Chiew, F., 2006. Estimation of rainfall elasticity of streamflow in Australia. *Hydrological Sciences Journal*, 51(4): 613-625.
- Chiew, F. and McMahon, T., 2002. Modelling the impacts of climate change on Australian streamflow. *Hydrological Processes*, 16(6): 1235-1245.
- CIESIN (Center for International Earth Science Information Network), Columbia University; and Centro Internacional de Agricultura Tropical (CIAT) 2005. *Gridded Population of the World Version 3 (GPWv3): Population Grids*. Palisades, NY: Socioeconomic Data and Applications Center (SEDAC), Columbia University. Available at <http://sedac.ciesin.columbia.edu/gpw/>. (date of download).
- CIESIN (Center for International Earth Science Information Network), Columbia University; The International Food Policy Research Institute (IFPRI); The World Bank; and The International Center for Tropical Agriculture (CIAT) 2004. *Global Rural-Urban Mapping Project (GRUMP): Urban Mask* Downloaded from: <http://beta.sedac.ciesin.columbia.edu/gpw/>
- Collischonn, W., 2001. *Simulação hidrológica de grandes bacias*, Universidade Federal do Rio Grande do Sul, Porto Alegre, Brasil.

- Collischonn, W., Allasia, D., Da Silva, B. and Tucci, C., 2007. The MGB-IPH model for large-scale rainfall-runoff modelling. *Hydrological Sciences Journal*, 52(5): 878-895.
- CONAMA-DGF, 2006. Estudio de la variabilidad climática en Chile para el siglo XXI, Comisión Nacional del Medio Ambiente. Departamento de Geofísica. Facultad de Ciencias - Físicas y Matemáticas. Universidad de Chile.
- Consorcio ATA-UNP-UNL, 2003. Caracterización Hídrica y Adecuación entre la Oferta y la Demanda en el Ámbito de la Cuenca Binacional Catamayo Chira. Volumen I Resumen Ejecutivo, Loja - Piura.
- Consorcio ATA-UNP-UNL, 2003. Caracterización Hídrica y Adecuación entre la Oferta y la Demanda en el Ámbito de la Cuenca Binacional Catamayo Chira. Volumen III Estudios Basicos - Tomo 3.2 Estudio Climático, Loja - Piura.
- Consorcio ATA-UNP-UNL, 2003. Caracterización territorial y documentación básica en el ámbito de la cuenca binacional Catamayo-Chira, Loja - Piura.
- Consorcio ATA-UNP-UNL, 2003. Caracterización territorial y documentación básica en el ámbito de la cuenca binacional Catamayo-Chira. Volumen I Informe Principal, Loja - Piura.
- Consultores ZEE, 2006. Proyecto Binacional de Ordenamiento, Manejo y Desarrollo de la Cuenca Catamayo-Chira, Zonificación Ecológica Económica, Loja - Piura.
- Cornish, P. and Vertessy, R., 2001. Forest age-induced changes in evapotranspiration and water yield in a eucalypt forest. *Journal of Hydrology*, 242(1-2): 43-63.
- Crisci, M., Fernández, M. and Trambauer, P., 2007. Economic and environmental viability of a regional irrigation system by gravity in the cuarei River Basin for the production of rice-grassland, Thesis - Facultad de Ingeniería - Universidad de la República, Uruguay.
- CVC, 1995. Proyección de la Población y la Demanda de Agua para el Consumo Humano en la Cuenca del Río Cauca del Departamento del Valle del Cauca 1995-2020, División de Proyectos Técnicos. Grupo de Recursos Hídricos.
- CVC, 2000. Balance Oferta-Demanda de Agua Cuencas de los Ríos Nima, Amaime, Guadalajara, San Pedro y Bugalagrande, Subdirección de Gestión Ambiental. Grupo de Recursos Hídricos.
- CVC and Universidad del Valle, 2007. Análisis de los determinantes socioeconómicos de la demanda de agua, Santiago de Cali, Colombia - Convenio 110 (2007).
- Debels, P. et al., 2007. Hydrological modelling, economic evaluation and public participation in the context of a twinning project: results from a case study on the Biobío Basin, Chile, Expert meeting on Regional Impacts, Adaptation, Vulnerability and Mitigation - Integrating Analysis of Regional Climate Change and Response Options, IPCC TGICA Workshop, START & PACE/USP, Nadi, Fiji.
- Debels, P. et al., 2008. IUPA: a tool for the evaluation of the general usefulness of practices for adaptation to climate change and variability. *Natural Hazards*.
- Dent, D. and Young, A., 1981. Soil survey and land evaluation. George allen and Unwid., London, 278 pp.
- Di Luzio, M., Srinivasan, R., Arnold, J. and Neitsch, S., 2002. ArcView interface for SWAT 2000 - User's Guide, Texas Water Resources Institute, College Station, USA.
- Eckhardt, K., Fohrer, N. and Frede, H., 2005. Automatic model calibration. *Hydrological Processes*, 19(3): 651-658.
- Engel, V., Jobbagy, E., Stieglitz, M., Williams, M. and Jackson, R., 2005. Hydrological consequences of eucalyptus afforestation in the argentine pampas. *Water Resources Research*, 41(10).
- FAO (Food and Agriculture Organisation), 2003. Review of world water resources by country. FAO Water Report 23. FAO, Rome, 71 pp.

- Feijó Uday, F. and Chalán Briceño, L., 2008. Análisis multitemporal de la cobertura vegetal de la cuenca Catamayo, Universidad Nacional de Loja.
- Fu, G., Charles, S. and Chiew, F., 2007. A two-parameter climate elasticity of streamflow index to assess climate change effects on annual streamflow. *Water Resources Research*, 43(11).
- Fung, C., Farquharson, F. and Chowdhury, J., 2006. Exploring the impacts of climate change on water resources - Regional impacts at a regional scale: Bangladesh, *Climate Variability and Change - Hydrological Impacts*, Proceedings of the Fifth FRIEND World Conference held at Havana, Cuba, November 2006, IAHS Publication 308.
- Gassman, P., Reyes, M., Green, C. and Arnold, J., 2007. The soil and water assessment tool: Historical development, applications, and future research directions. *Transactions of the ASABE*, 50(4): 1211-1250.
- Gellens, D. and Roulin, E., 1998. Streamflow response of Belgian catchments to IPCC climate change scenarios. *Journal of Hydrology*, 210(1-4): 242-258.
- Gleick, P., 1986. Methods for evaluating the regional hydrologic impacts of global climatic changes. *Journal of Hydrology*, 88(1-2): 97-116.
- Gobernación del Valle del Cauca, 1996-2006. Evaluaciones Agrícolas, Ministerio de Agricultura y Desarrollo rural, Unidad de Planificación Agropecuaria.
- Gobernación del Valle del Cauca, 2006-2007. Evaluaciones Agrícolas, Ministerio de Agricultura y Desarrollo rural, Unidad de Planificación Agropecuaria.
- Gosain, A., Rao, S., Srinivasan, R. and Reddy, N., 2005. Return-flow assessment for irrigation command in the Palleru river basin using SWAT model. *Hydrological Processes*, 19(3): 673-682.
- Govender, M. and Everson, C., 2005. Modelling streamflow from two small South African experimental catchments using the SWAT model. *Hydrological Processes*, 19(3): 683-692.
- Gruber, P., 2008. Analisis and Modeling of Land Use Changes in the Río Quiroz river catchment, Peru, Hochschule für Forstwirtschaft Rottenburg, Rottenburg am Neckar.
- Hulme, M., Raper, S. and Wigley, T., 1995. An integrated framework to address climate-change (ESCAPE) and further developments of the global and regional climate modules (MAGICC). *Energy Policy*, 23(4-5): 347-355.
- Hulme, M., Wigley, T.M.L., Barrow, E.M., Raper, S.C.B., Centella, A., Smith, S.J. and Chipanshi, A.C., 2000. Using a Climate Scenario Generator for Vulnerability and Adaptation Assessments: MAGICC and SCENGEN Version 2.4 Workbook. Climatic Research Unit, UEA, Norwich, UK, 52 pp.
- INADE, 1994. Estudio - Plan de Manejo de las Cuencas del Reservorio Poechos, Lima.
- INCOL S.A., Gómez Cajiao y Asociados Cia. Ltda., Silva Carreño y Asociados Ltda. and CVC, 1993. Plan del Agua: Margen derecha del Río Cauca entre los ríos Ovejas y Amaime - Fase I: Reconocimiento e Inventario, Santiago de Cali, Colombia.
- IPCC, 1997. An introduction to simple climate models used in the IPCC Second Assessment Report - IPCC Technical Paper II, Intergovernmental Panel on Climate Change, Geneva, Switzerland.
- IPCC, 2000. IPCC Special Report - Emissions Scenarios - Summary for Policymakers. Nakicenovic, N. and Swart, R. (eds.). Intergovernmental Panel on Climate Change, Geneva, Switzerland. Cambridge University Press, UK, 570 pp.
- IPCC, 2001. Climate Change 2001: Impacts, Adaptation and Vulnerability - Contribution of Working Group II to the Third Assessment Report of the Intergovernmental Panel on Climate Change. Cambridge University Press, 976 pp.

- IPCC, 2001. *Climate Change 2001: The scientific basis. Contribution of Working Group I to the Third Assessment Report of the Intergovernmental Panel on Climate Change*. Cambridge University Press, Cambridge and New York.
- IPCC, 2007. *Climate Change 2007: The Physical Science Basis - Contribution of Working Group I to the Fourth Assessment Report of the Intergovernmental Panel on Climate Change*. Solomon, S., Qin, D., Manning, M., Chen, Z., Marquis, M., Averyt, K.B., Tignor M. and Miller, H.L. (eds.). Cambridge University Press, Cambridge, United Kingdom and New York, NY, USA, 996 pp.
- IPCC, 2007. *Climate Change 2007: Mitigation - Contribution of Working Group III to the Fourth Assessment Report of the Intergovernmental Panel on Climate Change*. Working Group II, Intergovernmental Panel on Climate Change, Martin Parry, Osvaldo Canziani, Intergovernmental Panel on Climate Change Working Group II., Jean Palutikof. Cambridge University Press, 851 pp.
- IPCC, 2007. *Climate Change 2007: Synthesis Report - Contribution of Working Groups I, II and III to the Fourth Assessment Report of the Intergovernmental Panel on Climate Change*, Geneva, Switzerland.
- IUCN, 2000. *Vision for Water and Nature - A world strategy for conservation and sustainable management of water resources in the 21st century*, IUCN - The World Conservation Union.
- Kelliher, F., Leuning, R., Raupach, M. and Schulze, E., 1995. Maximum conductances for evaporation from global vegetation types. *Agricultural and Forest Meteorology*, 73(1-2): 1-16.
- Kilsby, C. et al., 2007. A daily weather generator for use in climate change studies. *Environmental Modelling & Software*, 22(12): 1705-1719.
- Kouwen, N., Soulis, E., Pietroniro, A., Donald, J. and Harrington, R., 1993. Grouping response units for distributed hydrologic modelling. *Journal of Water Resources Management and Planning*, 119(3): 289-305.
- Lambin, E., Geist, H. and Lepers, E., 2003. Dynamics of land-use and land-cover change in tropical regions. *Annual Review of Environment and Resources*, 28: 205-241.
- Lambin, E., Rounsevell, M. and Geist, H., 2000. Are agricultural land-use models able to predict changes in land-use intensity? *Agriculture Ecosystems & Environment*, 82(1-3): 321-331.
- Li W., Fu R. and Dickinson R., 2006. Rainfall and its seasonality over the Amazon in the 21st century as assessed by coupled models for the IPCC AR4. *Journal of Geophysical Research* VOL. 111, D02111, doi:10.1029/2005JD006355, 2006.
- Liang, X., Lettenmaier, D., Wood, E. and Burges, S., 1994. A simple hydrologically based model of land-surface water and energy fluxes for general-circulation models. *Journal of Geophysical Research-Atmospheres*, 99(D7): 14415-14428.
- Lopez-Moreno, J. and Nogues-Bravo, D., 2005. A generalized additive model for the spatial distribution of snowpack in the Spanish Pyrenees. *Hydrological Processes*, 19(16): 3167-3176.
- Meehl, G.A., Stocker, T.F., Collins, W.D., Friedlingstein, P., Gaye, A.T., Gregory, J.M., Kitoh, A., Knutti, R., Murphy, J.M., Noda, A., Raper, S.C.B., Watterson, I.G., Weaver A.J. and Zhao, Z.-C., 2007. *Global Climate Projections*. In: Solomon, S., Qin, D., Manning, M., Chen, Z., Marquis, M., Averyt, K.B., Tignor M. and Miller, H.L. (eds.) *Climate Change 2007: The Physical Science Basis. Contribution of Working Group I to the Fourth Assessment Report of the Intergovernmental Panel on Climate Change*. Cambridge University Press, Cambridge, United Kingdom and New York, NY, USA, 996pp.
- Meigh J.R., McKenzie A.A., Austin B., Bradford R. and Reynard N.S., 1998. *Assessment of global water resources – phase 2: Estimates of present and future water availability for Eastern and Southern Africa*. Report to DFID 94/8.

- Meigh J.R., McKenzie A.A. and Sene K.J., 1999. A grid-based approach to water scarcity estimates for eastern and southern Africa. *Water Resources Management*, 13: 85-115.
- Meigh, J.R., Folwell, S.S. and Sullivan, C.A. 2005. Linking water resources and global change in West Africa: options for assessment VIIth IAHS Scientific Assembly, Foz do Iguaçu, Brazil, 3-9 April 2005.
- Mielke, M. et al., 1999. Stomatal control of transpiration in the canopy of a clonal *Eucalyptus grandis* plantation. *Trees - Structure and Function*, 13(3): 152-160.
- Molfino, J., Morelli, C., Califra, A., Clerici, C. and Petraglia, C., 2000. Zonificación de tierras de la cuenca del Río Cuareim - Evaluación de dos sistemas de producción bajo riego - Aportes a su regulación hídrica, Proyecto FAO GCP/RLA126/JPN.
- Moore, R.J., 1985. The probability-distributed principle and runoff production at point and basin scales. *Hydrological Sciences Journal* 30(2): 273-297.
- Nakicenovic, N. and Swart, R., 2000. Special Report on Emissions Scenarios - A Special Report of IPCC Working Group III of the Intergovernmental Panel on Climate Change. Cambridge University Press, London.
- Neitsch, S., Arnold, J., Kiniry, J., Williams, J. and King, K., 2002. Soil and Water Assessment Tool Theoretical Documentation. Version 2000, Texas Water Resources Institute, College Station, USA.
- Nijssen, B., Lettenmaier, D., Liang, X., Wetzel, S. and Wood, E., 1997. Streamflow simulation for continental-scale river basins. *Water Resources Research*, 33(4): 711-724.
- Oñate-Valdivieso, F., 2008. Régimen hidrológico, influencia de los cambios climáticos. Universidad Técnica Particular de Loja.
- Penman, H.L., 1948. Natural evaporation from open water, bare soil and grass. *Proceedings of the Royal Society of London*, A193: 120-146.
- Pisciottano, G., Diaz, A., Cazes, G. and Mechoso, C., 1994. El Niño Southern Oscillation impact on rainfall in Uruguay. *Journal of Climate*, 7(8): 1286-1302.
- Podwojewski, P. and Poulenard, J., 2000. Los suelos de los páramos del Ecuador. In: P. Mena, C. Josse and G. Medina (Editors), *Los Suelos del Páramo. Serie Páramo*, vol.5. Grupo de Trabajo en Páramos del Ecuador/Abya Yala, Quito, Ecuador, pp. 1-26.
- Renard, K., Foster, G., Weesies, G., McCool, D. and Yoder, D., 1997. Predicting soil erosion by water: a guide to conservation planning with the Revised Universal Soil Loss Equation (RUSLE). *USDA Agricultural Handbook*, 703.
- Richardson, C., 1981. Stochastic simulation of daily precipitation, temperature, and solar-radiation. *Water Resources Research*, 17(1): 182-190.
- Roel, A. and Baethgen, W., 2005. Asociación entre las fases de El Niño y la producción arrocerá del Uruguay. *INIA Serie Técnica*, 148: 19.
- Sankarasubramanian, A., Vogel, R. and Limbrunner, J., 2001. Climate elasticity of streamflow in the United States. *Water Resources Research*, 37(6): 1771-1781.
- Scott, D. and Lesch, W., 1997. Streamflow responses to afforestation with *Eucalyptus grandis* and *Pinus patula* and to felling in the Mokobulaan experimental catchments, South Africa. *Journal of Hydrology*, 199(3-4): 360-377.
- Semenov, M. and Barrow, E., 1997. Use of a stochastic weather generator in the development of climate change scenarios. *Climatic Change*, 35(4): 397-414.
- Sharpley, A.N. and Williams, J., 1990. EPIC, Erosion/Productivity Impact Calculator, U.S. Dept. of Agriculture, Agricultural Research Service, Technical Bulletin, Washington, D.C.

- Shiklomanov, I., 1999. World Water Resources: Modern Assessment and Outlook for the 21st Century, Federal Service of Russia for Hydrometeorology and Environment Monitoring: State Hydrological Institute, IHP-UNESCO.
- Shuttleworth, W., 1993. Evaporation. In: D. Maidment (Editor), Handbook of hydrology. McGraw-Hill, New York.
- Sikka, A., Samra, J., Sharda, V., Samraj, P. and Lakshmanan, V., 2003. Low flow and high flow responses to converting natural grassland into bluegum (*Eucalyptus globulus*) in Nilgiris watersheds of South India. *Journal of Hydrology*, 270(1-2): 12-26.
- Soares, J. and Almeida, A., 2001. Modeling the water balance and soil water fluxes in a fast growing *Eucalyptus* plantation in Brazil. *Journal of Hydrology*, 253(1-4): 130-147.
- Soulis, E., Seglenieks, F., Bastien, J., Davidson, B. and Cai, C., 2004. Scaling hydrological processes in WATCLASS 3.0, *Eos Trans. AGU*, 85 (17), Jt. Assem. Suppl., Abstract H43C-02.
- Stape, J., Binkley, D. and Ryan, M., 2004. *Eucalyptus* production and the supply, use and efficiency of use of water, light and nitrogen across a geographic gradient in Brazil. *Forest Ecology and Management*, 193(1-2): 17-31.
- Stehr, A., Debels, P., Romero, F. and Alcayaga, H., 2008. Hydrological modelling with SWAT under conditions of limited data availability: evaluation of results from a Chilean case study. *Hydrological Sciences Journal-Journal des Sciences Hydrologiques*, 53(3): 588-601.
- Sullivan, C.A. and Meigh, J.R., 2005. Targeting attention on local vulnerabilities using an integrated indicator approach: the example of the Climate Vulnerability Index. *Water Science and Technology*, Special Issue on Climate Change, 51(5): 69-78.
- Thodsen, H., 2007. The influence of climate change on stream flow in Danish rivers. *Journal of Hydrology*, 333(2-4): 226-238.
- Thornwaite C.W., 1948. An approach towards a rational classification of climate; *Geographical Review* 38: 55-94.
- Tripathi, M., Raghuwanshi, N. and Rao, G., 2006. Effect of watershed subdivision on simulation of water balance components. *Hydrological Processes*, 20(5): 1137-1156.
- Tripathi, S., Srinivas, V. and Nanjundiah, R., 2006. Downscaling of precipitation for climate change scenarios: A support vector machine approach. *Journal of Hydrology*, 330(3-4): 621-640.
- UN, 1992. United Nations framework convention on climate change, UNFCCC Secretariat, Germany.
- UN, 2004. World population to 2300. New York. 240 pp.
- UN, 2006. World Population Prospects: The 2006 Revision. New York.
- UNEP, 1999. Global Environment Outlook, United Nations Environment Programme/Oxford University Press.
- UNFCCC, 2002. Delhi ministerial declaration on climate change and sustainable development, In: Eighth conference of the parties to the UNFCCC, New Delhi, Oct, Nov 2002.
- USDA, 1999. Soil taxonomy: a basic system of soil classification for making and interpreting soil surveys. Agriculture Handbook No. 436. Soil Conservation Service, U.S. Department of Agriculture, Washington.
- Van Dessel, W., Van Rompaey, A., Szilassi, P., Jordan, G. and Csillag, G., in prep. Sensitivity analysis of logistic regression parameterization for land use and land cover probability prediction. *International Journal of Geographical Information Science*.
- van Griensven, A. and Bauwens, W., 2003. Multiobjective autocalibration for semidistributed water quality models. *Water Resources Research*, 39(12): 1348.

- van Griensven, A. et al., 2006. A global sensitivity analysis tool for the parameters of multi-variable catchment models. *Journal of Hydrology*, 324(1-4): 10-23.
- Van Oost, K., Govers, G. and Desmet, P., 2000. Evaluating the effects of changes in landscape structure on soil erosion by water and tillage. *Landscape Ecology*, 15(6): 577-589.
- Van Rompaey, A., Verstraeten, G., Van Oost, K., Govers, G. and Poesen, J., 2001. Modelling mean annual sediment yield using a distributed approach. *Earth Surface Processes and Landforms*, 26(11): 1221-1236.
- Vitousek, P., Mooney, H., Lubchenco, J. and Melillo, J., 2007. Human domination of Earth's ecosystems. *Science*, 277(5325): 494-499.
- Wagener, T. and Franks, S., 2005. Regional hydrological impacts of climate change - impact assessment and decision making. In: T. Wagener and S. Franks (Editors), *Regional hydrological impacts of climate change*. International Association of Hydrological Sciences.
- Wigley, T., 2003. *MAGICC/SCENGEN 4.1: technical manual*, National Center for Atmospheric Research, Colorado, USA.
- Wigley, T., 2003. *MAGICC/SCENGEN 4.1: user manual*, National Center for Atmospheric Research, Colorado, USA.
- Wigley, T., Raper, S., Hulme, M. and Smith, S., 2000. *The MAGICC/SCENGEN Climate Scenario Generator: Version 2.4, Technical Manual*, Climatic Research Unit, UEA, Norwich, UK.
- WHO (World Health Organization) and UNICEF (United Nation's Children's Fund), 2006. *Meeting the MDG Drinking Water and Sanitation Target: The Urban and Rural Challenge of the Decade*. Geneva: WHO and New York: UNICEF. Available online at http://www.wssinfo.org/pdf/JMP_06.pdf.
- WMO (World Meteorological Organization), 2004. *WMO statement on the status of global climate in 2003*, WMO Publ. no. 996, WMO, Geneva, Switzerland.
- Wood, E., Lettenmaier, D. and Zartarian, V., 1992. A land-surface hydrology parameterization with subgrid variability for general-circulation models. *Journal of Geophysical Research-Atmospheres*, 97(D3): 2717-2728.
- WRI, 1998. *A guide to the Global Environment*, World Resource Institute/Oxford University Press.
- Xu, C., 1999. Climate change and hydrologic models: A review of existing gaps and recent research developments. *Water Resources Management*, 13(5): 369-382.
- Xu, C., 1999. From GCMs to river flow: a review of downscaling methods and hydrologic modelling approaches. *Progress in Physical Geography*, 23(2): 229-249.
- Xu, C. and Singh, V., 2004. Review on regional water resources assessment models under stationary and changing climate. *Water Resources Management*, 18(6): 591-612.
- Xu, C., Widen, E. and Halldin, S., 2005. Modelling Hydrological Consequences of Climate Change—Progress and Challenges. *Advances in Atmospheric Sciences*, 22(6): 789-797.
- Yu, Z., Pollard, D. and Cheng, L., 2006. On continental-scale hydrologic simulations with a coupled hydrologic model. *Journal of Hydrology*, 331(1-2): 110-124.

ANNEX 1

ANÁLISIS DE LA (VARIABILIDAD¹ EN LA) DIRECCIÓN Y MAGNITUD DE SEÑALES DE CAMBIO CLIMÁTICO PARA LAS ÁREAS DE ESTUDIO DEL PROYECTO TWINLATIN

**USO DEL SOFTWARE “MAGICC-SCENGEN v.4.1”
PARA OBTENER Y ANALIZAR
LA MAGNITUD Y DIRECCIÓN DEL CAMBIO REGIONALIZADO
PARA LAS CUENCAS DEL PROYECTO TWINLATIN,
PARA DIFERENTES ESCENARIOS DE CAMBIO CLIMÁTICO GLOBAL**

elaborado por P. Debels (EULA/CIEMA - pdebels@gmail.com)
como documento guía para la implementación armonizada de las actividades específicas relacionadas al
Paquete de Trabajo # 8 del proyecto TWINLATIN (CE 6PM)

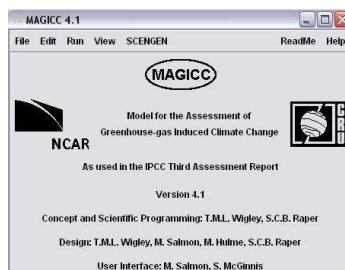
Tutorial con los pasos a seguir para obtener, mediante el software MAGICC-SCENGEN, para las distintas cuencas del Twinlatin, valores de cambio en temperatura y precipitaciones (con respecto al clima del período de referencia 1961-1990) para diferentes periodos del futuro, para diferentes escenarios de emisiones de gases invernaderos, calculados en base a diferentes Modelos de Circulación General.

El resultado de la aplicación de los pasos indicados en el manual consistirá de una tabla de datos que dará una indicación de (*la variabilidad existente entre las simulaciones de*) la dirección y magnitud de los cambios de temperatura y precipitaciones para las áreas bajo consideración. Estos valores posteriormente pueden ser utilizados para perturbar datos meteorológicos de referencia (series de tiempo de datos observados, que representan el clima actual), y así generar plausibles escenarios de condiciones climáticas futuras para las cuencas del Twinlatin.

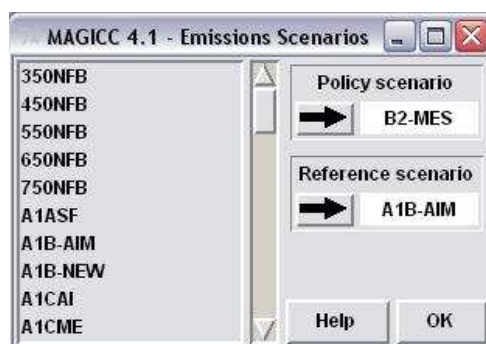
Nota: para un adecuado funcionamiento, el software MAGICC-SCENGEN SE DEBE instalar en el directorio C:\SG41

¹ Concordancias/discrepancias en los resultados de cambio generados mediante los diferentes Modelos de Circulación General (GCMs), desarrollados en distintos centros “expertos” mundiales, y mediante la aplicación de diferentes escenarios hipotéticos para las futuras emisiones de gases invernaderos

Paso 1: Para comenzar el análisis de las señales de cambio regionalizados, nos dirigimos a **C:\SG41\SCEN-41\magicc** e iniciamos la aplicación **magicc.exe** (*se puede generar un acceso directo en el escritorio para facilitar el futuro acceso al programa*). Mediante **MAGICC**, generaremos la señal de **cambio en la temperatura promedio mundial**, para un determinado momento en el siglo XXI, en función de un determinado escenario de emisión de gases invernaderos. Aparecerá la siguiente ventana:



Paso 2: Trabajaremos recorriendo los menús desde izquierda hacia derecha, comenzando por el menú “**Edit**”. Bajo el menú “**Edit**”, seleccionamos la opción “**Emission Scenarios**”. Se nos abre la siguiente ventana:



Vamos a analizar las señales de cambio climático global en función de 6 diferentes, plausibles escenarios de emisiones de gases invernaderos: estos son los 6 (4 +2) escenarios llamados “**marker scenarios**” del **SRES** (“*Special Report on Emission Scenarios*” elaborado por el **IPCC**).

Estos son:

SRES marker scenario	Modelo	nombre en MAGICC
A1FI (A1G)	MINICAM	A1FI-MI
A1T	MESSAGE	A1T-MES
A1B	AIM	A1B-AIM
A2	ASF	A2-ASF
B2	MESSAGE	B2-MES
B1	IMAGE	B1-IMA

Algunas referencias y un poco más de información sobre este informe y los escenarios de emisiones se encuentra en la sección final de este documento

Paso 3: Para cada corrida de la herramienta MAGICC, es posible analizar los resultados (*cambios en la temperatura global*) para 2 de estos escenarios a la vez. Después de cada corrida de MAGICC, estos 2 resultados pueden ser utilizados por **SCENGEN**, para ver el **impacto** de cada uno de estos **escenarios a nivel regional**.

Para efectos de nuestro ejercicio, podemos empezar analizando, por ejemplo, el **A1FI-MI** y el **B1-IMA**. Después de terminar nuestro primer ejercicio, tendremos que repetir los mismos pasos para los 4 demás escenarios de emisiones:

Se selecciona desde la columna izquierda **A1FI-MI**, para luego hacer clic en la flecha que acompaña el texto “**Policy Scenario**”. Luego seleccionamos **B1-IMA** y haremos clic donde dice “**Reference Scenario**”. Luego clic en **OK**.

Paso 4: Para nuestro ejercicio, utilizaremos los valores de parámetros predeterminados de la herramienta MAGICC, por lo que podemos dirigirnos directamente hacia el menú “**Run**” > “**Run Model**” (*para mayor información sobre los diferentes parámetros de la herramienta MAGICC, hacemos referencia a su manual de usuario*).

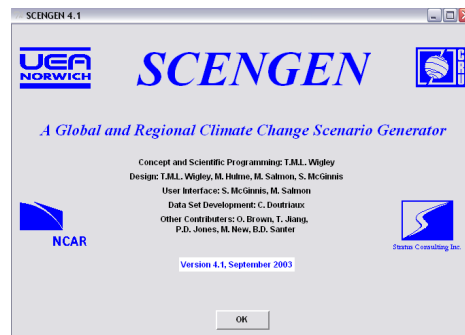
MAGICC ahora calcula - entre otros resultados - los cambios en la temperatura promedio global entre 1990 y 2100 (utilizando como referencia la temperatura global de 1990). Es este el resultado de MAGICC que será utilizado por el segundo modulo del software (SCENGEN), para producir los cambios “regionalizados”, que son aquellos que vamos a utilizar para nuestros estudios de impacto en las cuencas del Twinlatin.

Para el cálculo del cambio en la temperatura promedio global en nuestro ejercicio, nosotros utilizamos la opción estándar (“*Model: User*”) de MAGICC. La señal de cambio en la temperatura promedio global obtenida de esta manera luego es llevada a SCENGEN, donde es utilizada como base para definir los patrones espaciales de cambio para nuestros “*sitios de interés*”. SCENGEN nos permitirá comparar los efectos regionales (y analizar sus diferencias) para diferentes modelos GCM y para diferentes escenarios de emisión, **para un mismo cambio en el valor de la temperatura promedio global**.

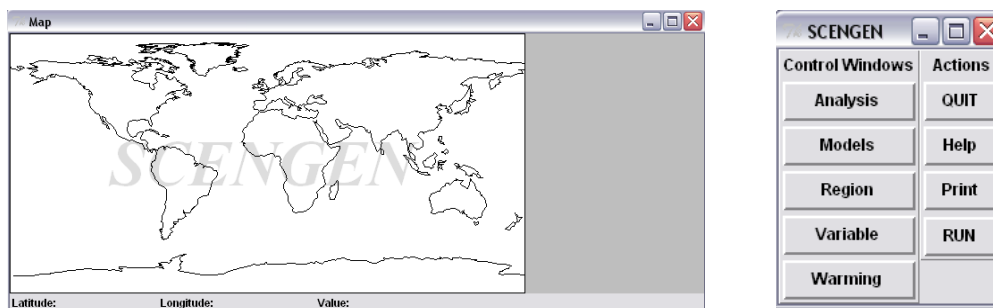
Observación: Mediante MAGICC, el usuario también puede evaluar la sensibilidad de las simulaciones de cambio (en la temperatura promedio) global frente a la selección de un GCM particular, u frente a diferentes valores para los parámetros del modelo (este último aspecto es algo que este “*ejercicio Twinlatin*” no contempla, sin embargo el usuario está libre de hacer este ejercicio en caso de estar interesado en tal evaluación). Aun cuando en nuestro ejercicio, por ahora, nosotros estamos utilizando la opción estándar (“*Model: User*”), **una corrida opcional de MAGICC que contempla la selección de un GCM particular en el paso 4 es sugerida para aquellas cuencas donde se va a querer comparar resultados obtenidos mediante MAGICC-SCENGEN con resultados provenientes de la corrida de un Modelo Regional de Circulación (RCM). Por ejemplo, si el RCM está basado en el GCM HadCM3, entonces el usuario puede hacer una corrida adicional de MAGICC con la opción: [Model: HadCM3] bajo el menú [Edit] > [Model Parameters], para así poder hacer una comparación más directa de los resultados.** La opción de simular un Modelo de Circulación General (GCM) particular existe en MAGICC para los siguiente 7 GCMs: GFDL, CSIRO, HadCM3, HadCM2, ECH4-OPIC, PCM y CSM.

En el Tercer Informe de Evaluación (*Third Assessment Report, TAR*) del Panel Intergubernamental sobre el Cambio Climático (**IPCC**), las incertidumbres sobre los cambios que se producir(í)an en la temperatura promedio global fueron determinadas mediante la simulación, por separado, con cada uno de los 7 GCMs anteriormente mencionados.

Paso 5: Después de correr el modelo MAGICC, iniciaremos la herramienta “SCENGEN” > “Run SCENGEN”. Se abre una nueva ventana:

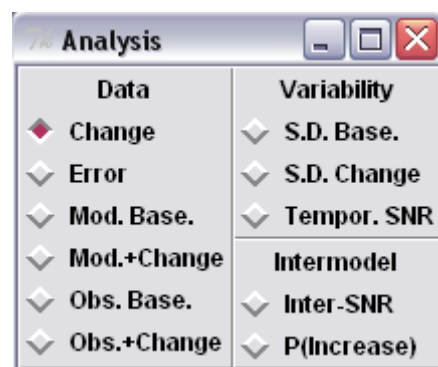


Después de hacer clic en “OK”, se visualizará un mapa del mundo en una ventana, y un menú de comandos en otra:



Empezaremos trabajando los menús de SCENGEN desde arriba hacia abajo:

Paso 6: Mediante la nueva ventana “Analysis” (para abrirla, hacer clic en la opción “Analysis” dentro de la ventana “SCENGEN”), seleccionamos el tipo de análisis que queremos ejecutar:




En esta fase, queremos analizar las señales de cambio climático, por lo que seleccionamos la opción “Change”.

Los valores de cambio que SCENGEN nos entregará serán: cambios (modelados) del clima (para una ventana de tiempo de 30 años) en el futuro, con respecto al clima (modelado) del período de referencia 1961-1990.

Estos valores de cambio luego pueden ser usados por el usuario para perturbar series de tiempo de datos observados localmente (la cuenca de estudio), para el mismo período de referencia (1961-1990).

En caso de que el usuario no disponga de buenas series de tiempo de datos observados (precipitación, temperatura,...) para el periodo de referencia mencionado, contactarse con pdebels@udec.cl para ver si es posible desarrollar una estrategia alternativa.

Luego de haber seleccionado la opción “**Change**”, cerramos la ventana haciendo clic en el botón , y nos dirigimos nuevamente a la ventana principal de **SCENGEN**.

Paso 7: El próximo paso consiste en seleccionar los modelos **GCM** de los cuales queremos visualizar los resultados de ‘cambio’ regionalizado. Desde la ventana “**SCENGEN**”, seleccionamos “**Models**”.

Como los diferentes Modelos de Circulación General (**GCM**, por sus siglas en inglés) generados por diferentes “centros expertos” mundiales pueden y suelen producir, para un mismo cambio de la temperatura global, significativas diferencias entre sus proyecciones de cambio climático regional, vamos a analizar estas señales de cambio no sólo para 1 GCM, sino para varios de estos GCM, para así obtener una idea de que tan grandes son estas diferencias en las proyecciones de los diferentes modelos para nuestras respectivas áreas de estudio. En el contexto del TWINLATIN y de modo de homogeneizar el trabajo entre los diferentes miembros de nuestro Consorcio, se sugiere analizar los resultados ‘producidos’ mediante los **siguientes 9 GCM**:

nombre GCM	CCCMa	CCSR/NIES	CSIRO	ECHAM4.5	GFDL	HADCM2	HADCM3	NCAR/PCM	CSM
nombre en SCENGEN	CCC199	CCSR96	CSI296	ECH498	GFDL90	HAD295	HAD300	PCM	CSM98
country	Canada	Japan	Australia	Germany	USA	UK	UK	USA	USA

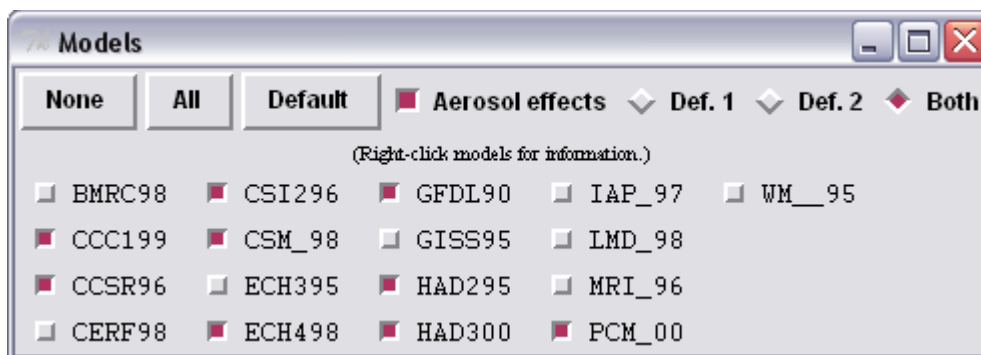
Para un mismo escenario de emisiones (ej. el A1FI-MI, uno de los 2 escenarios seleccionados en el paso 3), los diferentes modelos GCM producen diferentes cambios en la temperatura promedio global. Por encima de estas diferencias, los diferentes GCM también producirán diferentes patrones espaciales del cambio climático regional y/o “local”, inclusive para un mismo cambio en la temperatura promedio global (lo que se puede observar al, por ejemplo, normalizar el cambio en la temperatura promedio global).


En el contexto de TWINLATIN, lo que nosotros analizaremos mediante nuestro ejercicio SCENGEN son estas últimas diferencias, es decir los diferentes patrones espaciales de cambio para una misma proyección de cambio de la temperatura global. Por esto, utilizamos como base para nuestro análisis, el cambio global producido mediante MAGICC.

Aparte de los 7 GCMs utilizados en el TAR, nosotros también incluimos en nuestro análisis los siguientes GCM: CCSR/NIES y CCCMa

En la nueva ventana que se abre, seleccionaremos los 9 modelos (mencionados en la tabla superior) de los cuales queremos analizar la respuesta (*es decir, la señal de cambio climático*) frente al forzamiento climatológico producido por los 2 escenarios de emisiones seleccionados mediante MAGICC en el paso 3.

En la ventana “models”, se seleccionan los 9 modelos tal como está indicado en la figura dada aquí abajo. Al mismo tiempo, especificamos que queremos incluir el efecto de Aerosoles (“**Aerosol effects**”), y que queremos que los análisis se realicen tanto para Definición 1 como para Definición 2 (seleccionar “**Both**”) (*para mayor explicación sobre el significado de Definición 1 y 2 referimos al manual de MAGICC-SCENGEN*).



Nuevamente, para avanzar cerramos esta ventana mediante el botón  y volvemos a la ventana principal “SCENGEN”.

Paso 8: Ahora, mediante el menú “**Region**”, podemos seleccionar el área geográfica para el cual queremos visualizar las salidas de los modelos GCM seleccionados en el paso 7. Antes de proceder, conviene anotar en una hoja la posición geográfica de nuestro área de estudio (coordenadas **LATITUD** y **LONGITUD**).

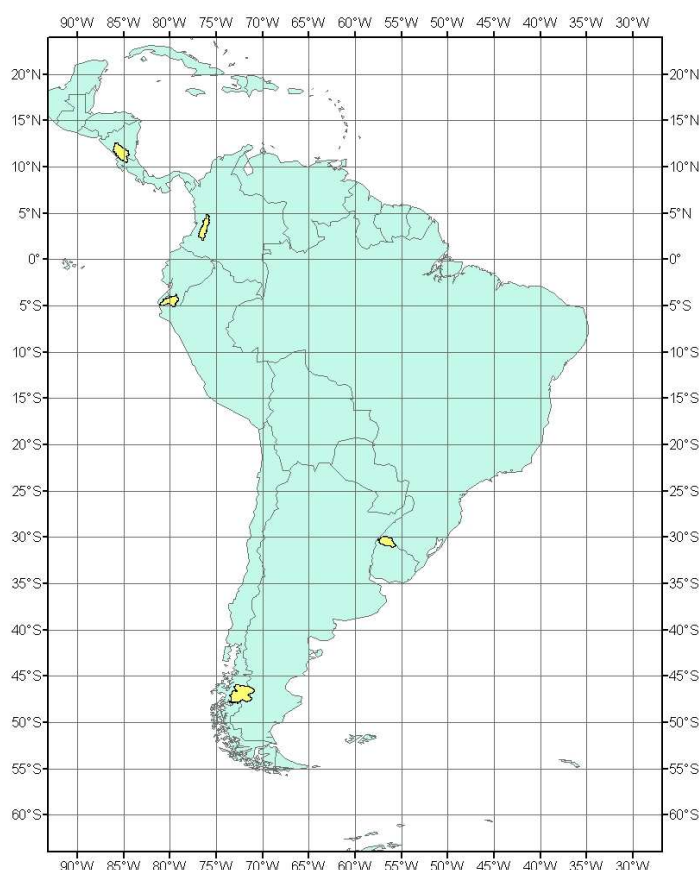
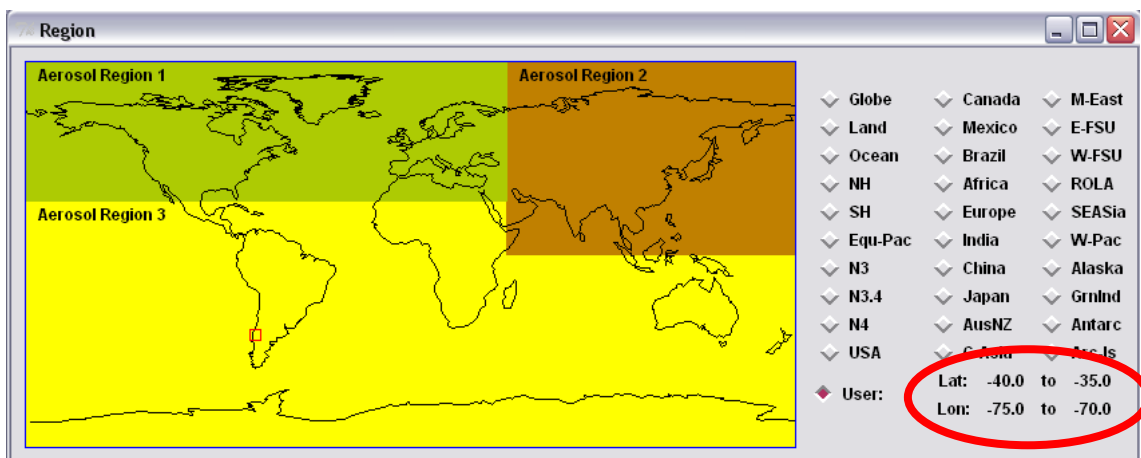


Figura: Mapa de LatinoAmerica con las cuencas del Twinlatin visualizadas. El mapa incluye una visualización de la malla (píxeles de 5° x 5°) con la cual SCENGEN almacena sus resultados.


Con el mouse, en la ventana “**Region**” haremos clic en el pixel que corresponde a nuestra área de interés. Automáticamente, se activará la opción “**User**” en la parte derecha de la ventana, y aparecerán las coordenadas geográficas que corresponden al área seleccionado.



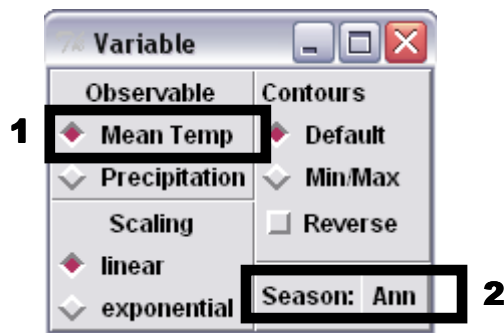
En la figura superior, hemos hecho clic con el mouse en el pixel que comprende a la **Cuenca del Río Biobío en Chile**. El pixel seleccionado queda marcado en el mapa con un cuadrado rojo. En la parte derecha de la figura, aparecen las coordenadas que nos permiten verificar que el pixel seleccionado corresponde bien con el área deseado.

Algunas cuencas del Twinlatin abarcan más de un pixel de la malla de SCENGEN: en estos casos, el análisis mediante SCENGEN se debería repetir separadamente para cada pixel. En caso de querer obtener valores promedios mediante la selección de un área compuesto por varios pixeles, esto se logra al mantener apretado el botón izquierda del ratón hasta tener seleccionado el área completo (“clic and drag”).

En este punto, conviene hacer una observación con respecto a lo que se llama la “skillfull resolution” de los GCM, es decir, la resolución espacial para la cual se asume que los GCM producen resultados “realistas”. Es generalmente sugerido que la capacidad de los GCM para producir resultados realistas es mayor a medida que el nivel de tanto la escala espacial como temporal aumenten (vea por ejemplo: Hewitson, B., 2003²). Por el otro lado, para aplicaciones al nivel de la cuenca hidrográfica individual (como en nuestros casos), la variación espacial que tienen los climas en la región Latinoamericana, y sobre todo en CentroAmerica y la zona de los Andes, no justifica el uso de valores de cambio que hayan sido “promediados” (tal como está sugerido en la publicación de Hewitson) u contruidos a partir de un conjunto de pixeles colindantes. Ambas consideraciones anteriores deben ser tomadas en cuenta al utilizar los resultados generados por SCENGEN al nivel de pixeles individuales.

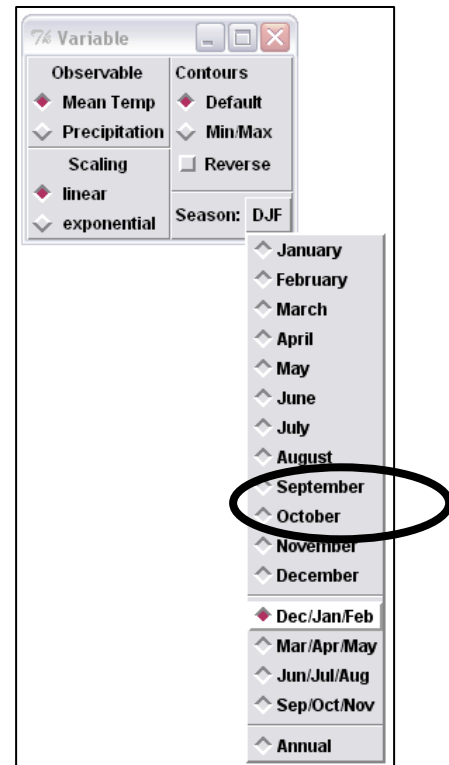
Paso 9: Para dar el próximo paso, se cierre la ventana “**Region**” con , se vuelve a la ventana “**SCENGEN**” y se selecciona la opción “**Variable**”.

² Hewitson, B. (2003). Developing Perturbations for Climate Change Impact Assessments. AIACC Working Paper N° 3. An electronic publication of the AIACC project available at: www.aiaccproject.org

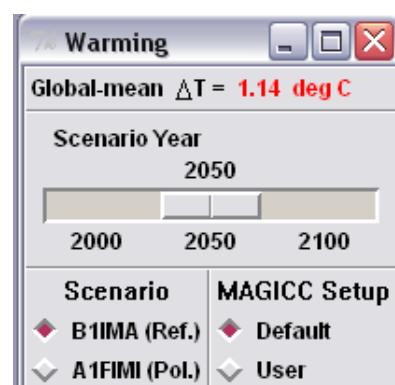


En esta nueva ventana, ahora se procede a (1) seleccionar la variable para la cual se quiere analizar la señal de cambio. Además (2), se indica a que escala temporal se quiere que la señal de cambio sea analizada/visualizada (*es decir, en este caso -en función del ejemplo indicado en la figura arriba- los cambios que serán analizados son los cambios en la temperatura promedio anual*).

Entonces, el primer ejercicio lo haremos para **temperatura promedio**, analizando los cambios en sus **valores promedio anuales**. Para estos efectos, la selección de opciones se efectúa tal como indicado en la figura superior. Luego, se procede a cerrar la ventana (✖), y se vuelve al menú principal (ventana “SCENGEN”).

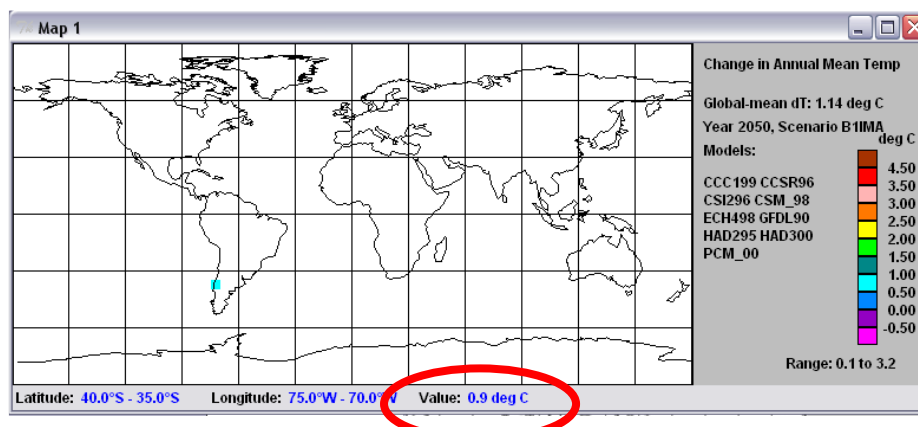


Paso 10: Ahora activaremos la opción “Warming” para (1) seleccionar la **ventana de tiempo** para la cual queremos realizar el análisis, y para (2) especificar para cual de los 2 **escenarios de emisiones** seleccionados mediante MAGICC en el paso 3 queremos visualizar los resultados primero (la ventana nos entrega ambas opciones; solo se puede seleccionar una opción a la vez). Seleccionamos 2050 como año central de la ventana de tiempo de 30 años para la cual queremos analizar los cambios (con respecto a 1961-1990). Empezamos analizando los cambios bajo el escenario de emisiones B1IMA. Cerrar ventana con ✖. (En este ejercicio, hemos utilizado el modo estándar en MAGICC, por lo que no es necesario cambiar la opción preseleccionada bajo “MAGICC Setup”. En otros casos, puede ser necesario seleccionar la opción “User”).



Mediante las ventanas anteriores (incluyendo la ventana indicada aquí arriba), se tomó la decisión de visualizar los resultados del cambio (a) en la **temperatura promedio anual** (según la selección realizada en el paso 9), para (b) cada uno de los **9 modelos de circulación general** (GCMs) seleccionados en el paso 7, para (c) el área comprendida entre las coordenadas **LATITUD -40 a -35**, y **LONGITUD -75 a -70** (lo cual fue definido en el paso 8), para (d) una ventana de tiempo de **30 años** (~cambio “climático”) centrada en el año **2050** (lo que se define en la ventana “Warming”, paso 10 – solo se define el año central³), para (e) el escenario de emisiones **B1-IMA** (también definido en este paso). El valor de cambio que se obtendrá es con respecto a la temperatura promedio anual simulada para el área de estudio (pixel seleccionado), para el **período de referencia 1961-1990**.

Paso 11: Ahora que se encuentren especificadas todas las opciones, podemos correr el modelo SCENGEN (ventana “SCENGEN” > “Actions” > “Run”. SCENGEN visualizará el siguiente mapa:



En el mapa, aparecen nombrados los diferentes GCMs que han sido seleccionados para esta corrida del modelo. Además, se hace mención del escenario de emisiones utilizado, así como del año central de la ventana de tiempo para la cual aplica la modelación. Al apuntar con el mouse el pixel que corresponde a nuestro área de estudio, aparecerá en la parte inferior de la figura la expresión numérica del cambio climático regionalizado para la variable seleccionada (en conjunto con las coordenadas de la localización), siendo este valor el **promedio** de los cambios generados para los **9 GCMs** seleccionados. En este caso, mediante MAGICC-SCENGEN, utilizando las salidas de los 9 modelos seleccionados en el paso 7, para el escenario de emisiones **B1** (modelo IMAGE), se proyectó un cambio “*regionalizado*”⁴ de la temperatura promedio anual para el periodo de **30 años** centrado en el año **2050** de **+0,9 grados Celsius** (en comparación con la temperatura promedio anual modelada para el pixel durante el **período de referencia** - el cual en el caso de SCENGEN corresponde a 1961-1990).

Paso 12: Los resultados detallados (entre los cuales se encuentran los cambios para cada uno de los modelos) ahora pueden ser leídos del archivo de salida de SCENGEN “AREAAVES.OUT”, generado y almacenado en el siguiente directorio:

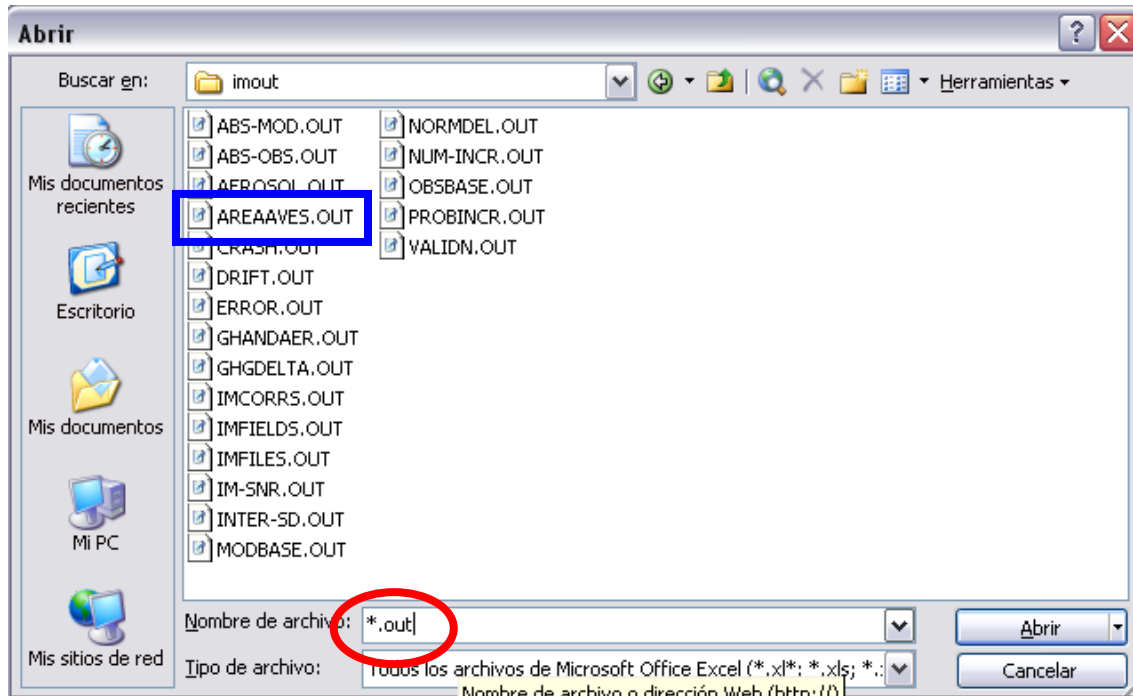
C:\SG41\SCEN-41\engine\imout

³ El tamaño de la ventana de tiempo, es decir 30 años, es un valor predeterminado de SCENGEN y no puede ser alterado por el usuario

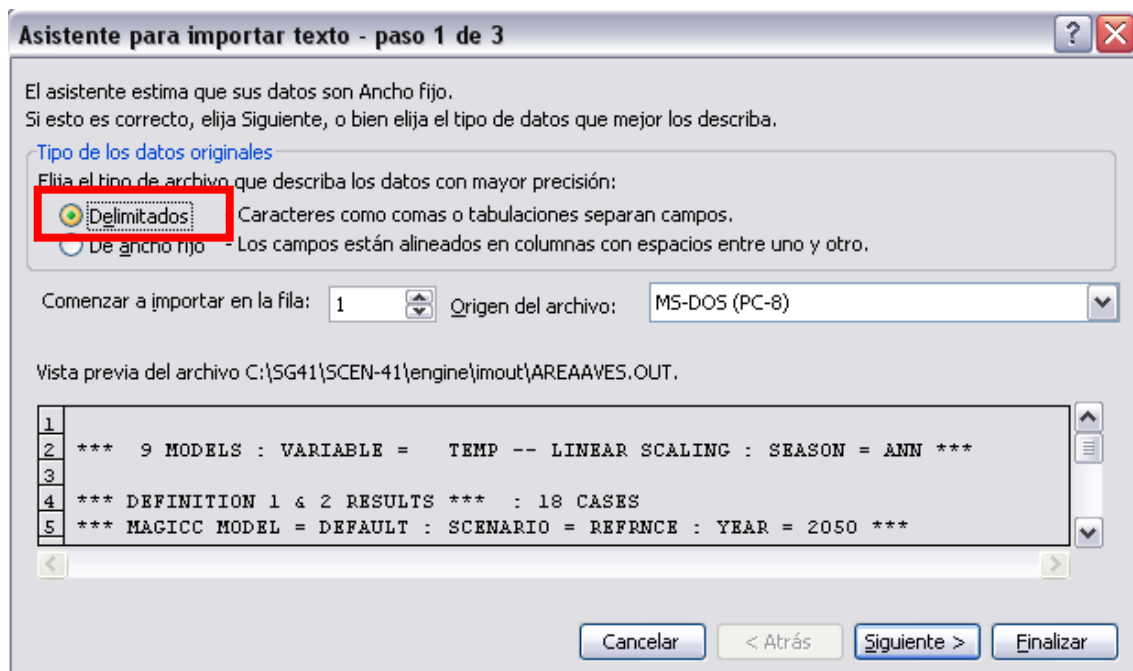
⁴ La regionalización en SCENGEN se produce mediante un proceso de “pattern scaling”. Para entender mejor el concepto de “pattern scaling” y sus limitaciones, referimos al manual de MAGICC-SCENGEN, y a las referencias bibliográficas hechas en él.

Podemos abrir el archivo mediante EXCEL, para analizar su contenido. En EXCEL, vamos a:

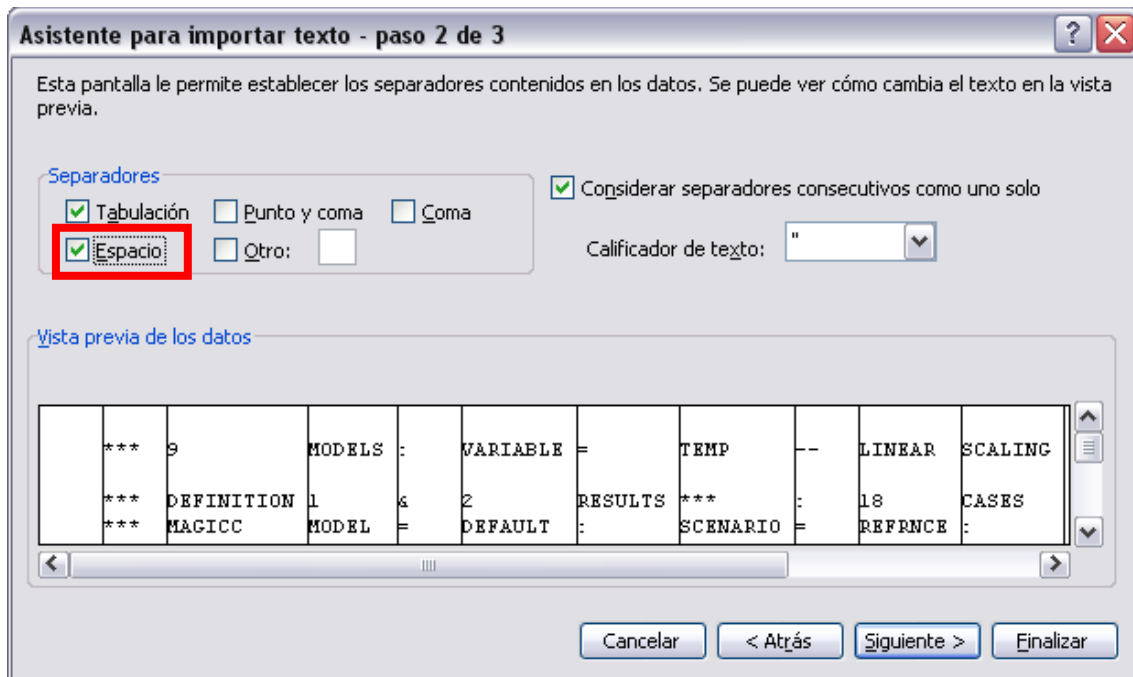
“**Archivo**” > “**Abrir**” y seleccionamos el archivo “**AREAAVES.OUT**”. Luego hacer clic en el botón “**Abrir**”.



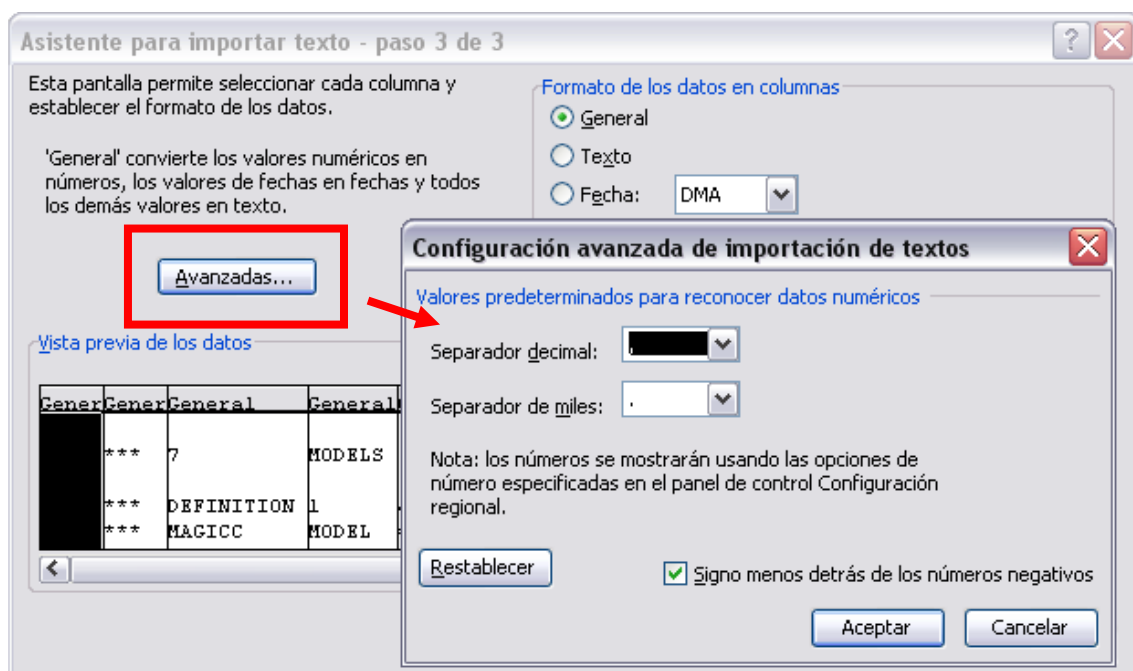
Luego seleccionamos la opción “**Delimitados**” + clic en “**Siguiente**”



Luego activemos la opción de separadores “**espacio**” seguido nuevamente por clic en “**Siguiente**”:



Dependiendo de la configuración de su máquina, puede ser necesario modificar el uso estándar de “punto” y “coma” como separadores de miles/decimales, lo cual se puede realizar mediante la opción “**Avanzadas**” de la siguiente ventana (especificar uso de . u , en la ventana “**Configuración avanzada de importación de textos**”):



Finalmente, hacer clic en “**Aceptar**” y luego “**Finalizar**” para realizar la importación de datos en EXCEL.

Aun cuando el archivo contiene mucha información relevante, por ahora nuestro principal interés está en los resultados contenidos en el rectángulo rojo indicado en la siguiente figura (entre las **celdas B72 y J89**):

	A	B	C	D	E	F	G	H	I	J	K
64		GHG	ONLY	:	AREA	AVERAGE	=	0,925	degC	(FOR	SCALE
65		AEROSOL	ONLY	:	AREA	AVERAGE	=	-0,021	degC	(FOR	SCALE
66		GHG	AND	AEROSOL	:	AREA	AVERAGE	=	0,905	degC	(FOR
67											
68											
69		***	SCALED	AREA	AVERAGE	RESULTS	FOR	INDIVIDUAL	MODELS	***	
70		(AEROSOLS	INCLUDED)								
71											
72		MODEL	=	CCC1D1	:	AREA	AVE	=	0,978	(degC)	
73		MODEL	=	CCSRD1	:	AREA	AVE	=	1,081	(degC)	
74		MODEL	=	CSI2D1	:	AREA	AVE	=	0,748	(degC)	
75		MODEL	=	CSM_D1	:	AREA	AVE	=	1,093	(degC)	
76		MODEL	=	ECH4D1	:	AREA	AVE	=	0,611	(degC)	
77		MODEL	=	GFDLD1	:	AREA	AVE	=	1,208	(degC)	
78		MODEL	=	HAD2D1	:	AREA	AVE	=	0,68	(degC)	
79		MODEL	=	HAD3D1	:	AREA	AVE	=	0,714	(degC)	
80		MODEL	=	PCM_D1	:	AREA	AVE	=	1,104	(degC)	
81		MODEL	=	CCC1D2	:	AREA	AVE	=	1,047	(degC)	
82		MODEL	=	CCSRD2	:	AREA	AVE	=	0,886	(degC)	
83		MODEL	=	CSI2D2	:	AREA	AVE	=	0,829	(degC)	
84		MODEL	=	CSM_D2	:	AREA	AVE	=	0,955	(degC)	
85		MODEL	=	ECH4D2	:	AREA	AVE	=	0,817	(degC)	
86		MODEL	=	GFDLD2	:	AREA	AVE	=	1,104	(degC)	
87		MODEL	=	HAD2D2	:	AREA	AVE	=	0,668	(degC)	
88		MODEL	=	HAD3D2	:	AREA	AVE	=	0,875	(degC)	
89		MODEL	=	PCM_D2	:	AREA	AVE	=	0,886	(degC)	
90		MODEL	=	MODBAR	:	AREA	AVE	=	0,905	(degC)	
91											

Los primeros 9 datos contienen los resultados del cambio climático regionalizado (promedio del área seleccionado en el paso 8) –en términos de cambios absolutos en la temperatura promedio anual- para los 9 GCMs seleccionados, para la opción “Def 1”. Los siguientes 9 datos son los resultados correspondientes a la opción “Def 2”. **Los resultados que utilizaremos para nuestro análisis de cambio climático en Twinlatin son aquellos correspondientes a la “Def 2”.**

Ahora podemos copiar la información contenida en las celdas **I72–I80** (para “Def 1”) (rectángulo azul en la figura superior) y en las celdas **I81–I89** (para “Def 2”) (rectángulo verde en la figura superior) a nuestra tabla de resumen en la hoja de cálculo “temp2050” la cual se encuentra ya preparada en el libro de cálculo EXCEL llamado “changes_scengen_[nombre cuenca].xls”. Este libro de cálculo ha sido enviado en conjunto con el material de documentación (“copiar” > edición > “pegado especial” > opción “transponer”; verificar si la numeración de celdas mencionada aquí arriba corresponde a la numeración en su hoja Excel):

		GHG + AS		CHANGE AT_YEAR 2050										
DEF-1		GHG + AS		CCCma	CCSRMIES	CSIRO	ECHAM4.5	GFDL	HADCM2	HADCM3	NCAR/PCM	CSM	CCCma	CCSI
GCM →		ΔT ↓		LINEAR SCALING										
SRES marker scenario ↓		ΔT ↓		LINEAR SCALING										
study area grid cell	A1FI (A1G)			0,978	1,081	0,748	1,093	0,611	1,208	0,68	0,714	1,104		
	A1T													
	A1B													
	A2													
	B2													
	B1													
USE THIS SET FOR IMPACT ASSESSMENT														
DEF-2 (drift)		GHG + AS		CHANGE AT_YEAR 2050										
GCM →		ΔT ↓		CCCma	CCSRMIES	CSIRO	ECHAM4.5	GFDL	HADCM2	HADCM3	NCAR/PCM	CSM	CCCma	CCSI
SRES marker scenario ↓		ΔT ↓		LINEAR SCALING										
study area grid cell	A1FI (A1G)			1,047	0,886	0,829	0,955	0,817	1,104	0,668	0,875	0,886		
	A1T													
	A1B													
	A2													
	B2													
	B1													

El dato de **cambio de la temperatura global** (con respecto a 1990) proporcionado por MAGICC también está contenido en el archivo “AREAAVES.OUT” (vea el *círculo negro* en la siguiente figura). Copiamos este valor hacia la celda C52 y C63 de nuestra hoja de cálculo Excel “temp2050” (libro EXCEL: “changes_scengen_[nombre_cuenca].xls”).

1	A	B	C	D	E	F	G	H	I	J	K
2		***		9 MODELS	:	VARIABLE	=	TEMP	--	LINEAR	SCALING
3											
4		***	DEFINITION	1 &	2 RESULTS	***	SCENARIO	=	18 CASES		
5		***	MAGICC	MODEL	=	DEFAULT	:	SCENARIO	=	REFRNC	YE
6		***	GLOBAL-ME	Delta-T	USED	FOR	SCALING	=	1,148	degC	
7		***	TOTAL	GLOBAL-ME	Delta-T	=	1,143	degC			
8											
9	GRID	BOX	CENTRAL	POINTS	(5deg	by	GRID)				
10	LATITUDE	RANGE	=	-37,5	TO	-37,5	degreesN	INCLUSIVE			
11	LONGITUDE	RANGE	=	-72,5	TO	-72,5	degreesE	INCLUSIVE			
12											
13	LATITUDE	GRID	RANGE	26,26	:	LONGITUDE	GRID	RANGE	22,22	INCLUSIVE	
14											
15											
16	***	AREA	AVERAGE	RESULTS	FOR	NORMALIZE	(GHG	CHANGES	***		
17											

Otra información de interés contenido en este archivo (y que queremos copiar a “changes_scengen_[nombre_cuenca].xls” es:

1. **“OVERALL MEAN”**: el **promedio** (*i.e. de los 9 modelos*) de las **señales de cambio regionalizados** (*i.e. para nuestro pixel de interés*) y **normalizados** (*i.e. para un cambio de la temperatura global de 1°C*) (calculado solo considerando el efecto de gases invernaderos y no de aerosoles)

	A	B	C	D	E	F	G	H	I	J
16		***	AREA	AVERAGE	RESULTS	FOR	NORMALIZE	GHG	CHANGES	***
17		MODEL	=	CCC1D1	:	AREA	AVE	=	0,87	:
18		MODEL	=	CCSRD1	:	AREA	AVE	=	0,96	:
19		MODEL	=	CSI2D1	:	AREA	AVE	=	0,67	:
20		MODEL	=	CSM_D1	:	AREA	AVE	=	0,97	:
21		MODEL	=	ECH4D1	:	AREA	AVE	=	0,55	:
22		MODEL	=	GFDL1	:	AREA	AVE	=	1,07	:
23		MODEL	=	HAD2D1	:	AREA	AVE	=	0,61	:
24		MODEL	=	HAD3D1	:	AREA	AVE	=	0,64	:
25		MODEL	=	PCM_D1	:	AREA	AVE	=	0,98	:
26		MODEL	=	CCC1D2	:	AREA	AVE	=	0,93	:
27		MODEL	=	CCSRD2	:	AREA	AVE	=	0,79	:
28		MODEL	=	CSI2D2	:	AREA	AVE	=	0,74	:
29		MODEL	=	CSM_D2	:	AREA	AVE	=	0,85	:
30		MODEL	=	ECH4D2	:	AREA	AVE	=	0,73	:
31		MODEL	=	GFDL2	:	AREA	AVE	=	0,98	:
32		MODEL	=	HAD2D2	:	AREA	AVE	=	0,6	:
33		MODEL	=	HAD3D2	:	AREA	AVE	=	0,78	:
34		MODEL	=	PCM_D2	:	AREA	AVE	=	0,79	:
35		MODEL	=	MODBAR	:	AREA	AVE	=	0,806	:
36										
37										
38		OVERALL	MEAN	=	0,806	degC/degC				
39		INTER-MODES	S.D.	=	0,15	degC/degC	(FOR	NORMALIZE	GHG	DATA)
40		HERE,	INTER-MODES	S.D.	IS	THE	S.D.	OF	THE	AREA
41										

2. “**INTER-MOD S.D.**”: la **desviación estándar** (*i.e. de los 9 modelos*) entre los cambios promedios anuales regionalizados y normalizados (*calculado solo considerando el efecto de gases invernaderos y no de aerosoles*)
3. “**INTER-MOD SNR**”: la **razón señal/ruido**, es decir la relación entre la magnitud de la señal promedio de cambio (obtenido en 1) y la desviación estándar INTER-MOD S.D. (obtenido en 2) (*calculado solo considerando el efecto de gases invernaderos y no de aerosoles*)
4. la **probabilidad de incremento** (“**PROB OF INCREASE**”), la cual es calculada en función del número de modelos que predicen un aumento en la temperatura (asignando un mismo nivel de confianza a cada uno de los 9 modelos) (*valor máximo es 1, indicando que todos los modelos predicen un aumento; valores cercanos a 1 indican alto grado de concordancia entre los modelos en la predicción de un aumento; valores cercanos a 0 indican alto grado de concordancia entre los modelos en la predicción de una disminución*) (*calculado solo considerando el efecto de gases invernaderos y no de aerosoles*)

	A	B	C	D	E	F	G	H	I	J	K	L
55												
56												
57		***	AREA	AVERAGE	RESULTS	FOR	MODEL-MEA	***				
58		HERE,	INTER-MOD	S.D.	IS	THE	AREA	AVE	OF	THE	INDIVIDUAL	GRIDPOINT
59		(AEROSOLS	SHOULD	ALWAYS	BE	INCLUDED	IN	FURTHER	ANALYSES)			
60												
61		INTER-MOD	S.D.	:	AREA	AVERAGE	=	0,15	degC	(FOR	NORMALIZE	(GHG
62		INTER-MOD	SNR	:	AREA	AVERAGE	=	5,367	(FOR	NORMALIZE	(GHG	DATA)
63		PROB	OF	INCREASE	:	AREA	AVERAGE	=	1	(FOR	NORMALIZE	(GHG
64		GHG	ONLY	:	AREA	AVERAGE	=	0,925	degC	(FOR	SCALED	DATA)
65		AEROSOL	ONLY	:	AREA	AVERAGE	=	-0,021	degC	(FOR	SCALED	DATA)
66		GHG	AND	AEROSOL	:	AREA	AVERAGE	=	0,905	degC	(FOR	SCALED
67												
68		***	SCALED	AREA	AVERAGE	RESULTS	FOR	INDIVIDUAL	MODELS	***		
69		(AEROSOLS	INCLUDED)									
70												
71												
72		MODEL	=	CCC1D1	:	AREA	AVE	=	0,978	(degC)		
73		MODEL	=	CCSRD1	:	AREA	AVE	=	1,081	(degC)		
74		MODEL	=	CSI2D1	:	AREA	AVE	=	0,748	(degC)		
75		MODEL	=	CSM_D1	:	AREA	AVE	=	1,093	(degC)		
76		MODEL	=	ECH4D1	:	AREA	AVE	=	0,611	(degC)		
77		MODEL	=	GFDL1	:	AREA	AVE	=	1,208	(degC)		
78		MODEL	=	HAD2D1	:	AREA	AVE	=	0,68	(degC)		
79		MODEL	=	HAD3D1	:	AREA	AVE	=	0,714	(degC)		
80		MODEL	=	PCM_D1	:	AREA	AVE	=	1,104	(degC)		
81		MODEL	=	CCC1D2	:	AREA	AVE	=	1,047	(degC)		
82		MODEL	=	CCSRD2	:	AREA	AVE	=	0,886	(degC)		
83		MODEL	=	CSI2D2	:	AREA	AVE	=	0,829	(degC)		

	A	B	C	D	E	F
84						
85			GLOBAL			
86		SRES marker scenario	MAGICC mean ΔT (default model selection)	MEAN CHANGE	INTER-MODEL SD	INTER-MODEL SNR
87						PROB OF INCREASE
88				all 4 for normalized GHG data only		
89				degC/degC	degC/degC	degC/degC
90		A1FI (A1G)	1,67			
91		A1T	1,60	0,81	0,15	5,37
92		A1B	1,48			1,00
93		A2	1,30			
94		B2	1,33			
95		B1	1,14			
96						
97						

El cambio promedio es normalizado (i.e. cambio por grado de aumento de la temperatura global; valor en el rectángulo verde), por lo que da una indicación de si el cambio para la zona de interés se proyecta como más o menos fuerte que el cambio de la temperatura global.

Un alto valor del SNR indica que la señal “promedio” de cambio es fuerte en comparación con las diferencias observadas entre las predicciones de cambio obtenidas mediante los diferentes modelos (SNR = promedio de los cambios/desviación estándar de los cambios).

Paso 13: [OPCIONAL] Este paso consiste en leer la “representación” (modelada) del clima actual mediante los diferentes GCM. Nuevamente desde el archivo

“AREAAVES.OUT”, copiamos la siguiente sección (ver figura) a “changes_scengen_[nombre_cuenca].xls”:

***	AREA	AVERAGE	RESULTS	FOR	BASELINE	CLIMATE	***
MODEL =	CCC1	:	AREA	AVE	=		11,74
MODEL =	CCSR	:	AREA	AVE	=		10,54
MODEL =	CSI2	:	AREA	AVE	=		10,69
MODEL =	CSM	:	AREA	AVE	=		11,04
MODEL =	ECH4	:	AREA	AVE	=		12,98
MODEL =	GFDL	:	AREA	AVE	=		11,44
MODEL =	HAD2	:	AREA	AVE	=		10,24
MODEL =	HAD3	:	AREA	AVE	=		10,04
MODEL =	PCM	:	AREA	AVE	=		10,51
MODEL =	MBAR	:	AREA	AVE	=		11,024

SRES marker		modelo	nombre en MAGICC
A1F1 (A1G)	MINICAM	A1F1-MI	
A1T	MESSAGE	A1T-MES	
A1B	AIM	A1B-AIM	
A2	ASF	A2-ASF	
B2	MESSAGE	B2-MES	
B1	IMAGE	B1-IMA	

simulated GCM		CCCma	CCSR/MES	CSIRO	ECHAM4.5	GFDL	HADCM2	HADCM3	NCAR/PCM	CSM
study area	modeled baseline [%]	11,74	10,54	10,69	11,04	12,98	11,44	10,24	10,04	10,51
grid cell	"observed" baseline [%]									
	baseline model "error" [%]									
1x3 N-S window	S.D. model "error" [%]									
3x3 N-S-E-W window	S.D. model "error" [%]									

Paso 14: [OPCIONAL] Para ver como la representación –mediante SCENGEN- de los patrones regionales de los diferentes modelos GCM se relaciona con los climas regionales “observados” (es decir, medido por estaciones meteorológicas u otras técnicas), llenaremos la siguiente columna de nuestra tabla en el archivo “changes_scengen_[nombre_cuenca].xls” con el valor “observado” que se encuentra almacenado en la base de datos de SCENGEN para el área de interés. (Este paso, para temperatura anual lo debemos hacer 1 sola vez: al volver a hacer el ejercicio MAGICC-SCENGEN para otros escenarios SRES, no será necesario repetir este paso.)

Para ello, abriremos mediante EXCEL el siguiente archivo “OBSBASE.OUT”, siguiendo un procedimiento similar a aquel utilizado para leer “AREAAVES.OUT”. Este archivo contiene una matriz con los valores del clima observado para cada una de las celdas de 5° x 5° que SCENGEN utiliza para cubrir la superficie mundial. Utilizando las coordenadas Latitud / Longitud de nuestra área de estudio (por ejemplo: -70°a -75°

E; - 35°a -40° N en el caso de la Cuenca del Biobío), podemos ubicar, dentro de la matriz, la celda de nuestro interés (buscar las coordenadas correspondientes al centro de nuestro pixel de interés, en este caso: -72.5 y 37.5):

	A	B	C	D	E	F	G	V	W	X	Y
4			OBSERVED	BASELINE	CLIMATE	(degC)					
5		degN/degE									
6			-177,5	-172,5	-167,5	-162,5	-157,5	-82,5	-77,5	-72,5	-67,5
7		87,5	-16,96	-16,99	-17,11	-17,18	-17,16	-17,85	-17,65	-17,65	-17,61
8		82,5	-16,07	-16,04	-16,04	-16,03	-16,02	-21,79	-22,07	-20,47	-18,41
9		77,5	-14,17	-14,14	-14,2	-14,32	-14,51	-19,56	-17,28	-14,54	-14,41
10		72,5	-12,54	-12,42	-12,63	-12,51	-12,67	-15,38	-15,51	-14,18	-12,87
11		67,5	-9,53	-8,62	-8,76	-7,71	-8,94	-13,49	-12,25	-11,6	-11,94
12		62,5	-3,78	-2,98	-3,01	-2,85	-3,66	-11,24	-9,51	-9,35	-9,18
13		57,5	2,36	2,81	3,17	3,01	2,42	-7,65	-6,64	-6,65	-6,01
14		52,5	4,54	4,96	5,3	5,71	6,25	-2,83	-2,84	-3,47	-3,04
15		47,5	6,66	6,99	7,29	7,64	7,96	2,37	2,15	2,06	3,15
16		42,5	10,4	10,65	10,75	11,08	11,36	8	7,83	8,23	9,32
17		37,5	15,34	15,24	15,42	15,6	15,62	12,24	13,89	16,34	17,46
18		32,5	19,09	18,99	19,12	19,1	19,09	18,15	20,47	20,96	21,2
19		27,5	22,14	22,02	21,94	21,79	21,55	23,16	23,72	23,57	23,37
20		22,5	24,3	24,16	23,93	23,77	23,31	25,51	25,38	25,51	25,28
21		17,5	25,42	25,39	25,42	25,12	24,44	26,62	26,41	26,07	26,16
22		12,5	26,51	26,49	26,21	25,73	25,65	26,09	26,86	26,42	26,44
23		7,5	27,16	27,15	26,81	26,36	26,35	26,88	26,25	23,95	26,25
24		2,5	27,5	27,28	26,93	26,45	26,38	24,81	22,7	24,95	25,69
25		-2,5	27,67	27,41	26,98	26,74	26,48	22,58	22,61	26,31	26,07
26		-7,5	27,86	27,62	27,29	27,32	27,32	21,37	20,01	26,3	26,39
27		-12,5	27,22	27,14	26,88	27,04	27,18	20,41	16,41	17	24,98
28		-17,5	25,74	25,63	25,66	25,76	25,75	19,51	18,98	15,85	13,02
29		-22,5	23,29	23,18	23,27	23,2	23,43	18,66	18,13	17,64	8,9
30		-27,5	20,65	20,54	20,36	20,49	20,5	18,14	17,31	15,5	10,16
31		-32,5	18,05	17,85	17,62	17,46	17,47	16,61	16,19	14,55	14,95
32		-37,5	15,82	15,31	14,97	14,74	14,64	14,41	14,18	11,42	13,99
33		-42,5	13,27	13,11	12,66	12,34	12,11	12,01	12,01	11,71	11,16
34		-47,5	10,09	10,45	10,33	10,06	9,7	9,3	9,47	6,47	9,79
35		-52,5	7,49	7,61	7,39	7,28	6,98	6,93	6,86	6,09	6,99

El valor correspondiente lo copiamos a nuestro libro de cálculo EXCEL, y procedemos a calcular el “error”⁵ en la modelación del “clima base”, para cada GCM utilizado.

VARIABLE:	TEMPERATURE	SRES marker	modelo	nombre en MAGICC
CHANGE:	ABSOLUTE VALUE	A1F1 (A1G)	MIRCAM	A1F1.M
SEASON:	ANNUAL	A1T	MESSAGE	A1T.MES
MAGICC:	DEFAULT	A1B	AM	A1B-AM
LATITUDE:	-35 -0	A2	ASF	A2.ASF
LONGITUDE:	-78 -75	B2	MESSAGE	B2.MES
DEF YEAR:	1990	B1	IMAGE	B1-MA

		MODEL ERROR - ANNUAL MEAN TEMPERATURE								
		CCCMa	CCSRMES	CSIRO	ECHAM5	GFDL	HADCM2	HADCM3	INCARPCM	CSM
study area	modeted baseline [°C]	11,74	10,54	10,69	11,04	12,88	11,44	10,24	10,04	10,51
grid cell	"observed" baseline [°C]					11,42				
	baseline model "error" [ΔT]	0,32	-0,86	-0,73	-0,38	1,56	0,02	-1,18	-1,38	-0,91
1x3 N-S window	baseline model "error" [%]									
	S.D. model "error"									
3x3 N-S-E-W window	baseline model "error" [%]									
	S.D. model "error"									

⁵ Es muy importante tener cuidado al interpretar el valor del error calculado: el “clima base observado” en SCENGEN está construido a partir de una base de datos mundial la cual incluye un número muy limitado de estaciones meteorológicas; en este sentido es posible (probable) que para un área de estudio en particular, la representación del “clima base” mediante SCENGEN es imperfecto o inclusive deficiente, sobre todo cuando el número de estaciones meteorológicas que han sido utilizados para calcular el “clima base” de un determinado pixel (5°x5°) es reducido y por ende insuficiente para representar adecuadamente el “clima promedio” del pixel bajo consideración (error en la representación del clima base real mediante SCENGEN). Más información sobre cómo esta representación del “clima base” incluida en SCENGEN ha sido construido se puede encontrar al final de este documento. Además de la comparación del “clima base” modelado con el clima base “observado” de SCENGEN, **recomendamos que el usuario se base en su propio conocimiento del área de estudio para hacer una evaluación aproximada de la calidad de la representación climática obtenida por medio de SCENGEN.**

OTRAS ACTIVIDADES OPCIONALES: Es posible mediante SCENGEN calcular la razón señal-ruido temporal (“Temporal signal to Boise ratio”), además de los cambios en la desviación estándar de las series de tiempo meteorológicas. Para aquellos usuarios interesados en estos aspectos de SCENGEN, se refiere al manual del software (o me pueden contactar por correo electrónico – pdebels@udec.cl).

*Hasta aquí, hemos obtenido mediante el modelo SCENGEN los resultados para **cambios absolutos en temperatura promedio anual para 9 GCMs para 1 solo escenario de emisiones, para una ventana de tiempo (30 años) en el futuro centrada alrededor del año 2050, con respecto al periodo de referencia 1961-1990** (y en función de un cambio global único (obtenido mediante el modelo MAGICC) de la temperatura promedio anual de **1.14°C** con respecto a la temperatura global del año 1990).*

Ahora necesitaremos repetir el ejercicio para: (i) cambios en precipitación; (ii) los otros 5 escenarios de emisiones; (iii) otras ventanas de tiempo, y (iv) cambios a nivel mensual y/o estacional.

Paso 15: El próximo paso consiste en calcular el **cambio porcentual** en la **precipitación promedio anual**, dejando todos los demás parámetros sin cambiar. Para ello, **cerramos** el libro de cálculo “**AREAAVES.OUT**” (y, en caso de aplicar, “**OBSBASE.OUT**”) y volvemos a la ventana “**SCENGEN**”. Abrimos el menú “**Variable**”. Cambiamos la variable seleccionada a “**Precipitation**” y (*¡importante! – ¡este paso se debe repetir cada vez!*) mediante el menú “**Region**” volvemos a seleccionar la celda correspondiente a nuestra área de interés, tal como lo hicimos en el paso 8. Volvemos a correr el modelo (“**RUN**”).

Volvemos a leer el archivo de salida de SCENGEN “**AREAAVES.OUT**”, tal como lo hicimos en el paso 12. La información contenida en el archivo de salida ahora corresponde a los cambios porcentuales en precipitación promedio anual, con respecto a los valores modelados para el periodo de referencia 1961-1990. De similar forma como lo hicimos en el caso de temperatura, copiamos la información de salida de la modelación a la hoja de cálculo “**prec2050**” de nuestro libro de cálculo “**changes_scengen_[nombre cuenca].xls**”.

*¡Es importante indicar que los resultados que SCENGEN nos entrega corresponden al **cambio relativo** en la **precipitación promedio anual**, expresando este cambio como un porcentaje **del valor promedio modelado** de la precipitación anual para el período de **referencia de 1961-1990**. Sin embargo, el **período de referencia** con valores **observados** de precipitación contenidos en SCENGEN corresponde a **1981-2000!** (la diferencia en los períodos de referencia para datos observados de precipitación y temperatura se debe a la disponibilidad diferenciada de series de tiempo históricas de precipitación y temperatura; son estas las series de tiempo que han constituido la base para el clima de referencia utilizada en SCENGEN– un poco mas de información sobre este aspecto está incluido en la sección final de este documento WORD).*

DEF-1		GHG + AS	%CHANGE_PP_YEAR 2050									
GCM →			CCCMa	CCSRNIES	CSIRO	ECHAM4.5	GFDL	HADCM2	HADCM3	NCARPCM	CSM	CCCMa
SRES marker scenario ↓		ΔT ↓	LINEAR SCALING									
study area grid cell	A1FI (A1G)											
	A1T											
	A1B											
	A2											
	B2											
	B1	1,14	-7,70	-9,33	-1,12	-2,55	-20,75	-0,17	-11,53	-11,13	-3,20	
USE THIS SET FOR IMPACT ASSESSMENT												
DEF-2 (drift)		GHG + AS	%CHANGE_PP_YEAR 2050									
GCM →			CCCMa	CCSRNIES	CSIRO	ECHAM4.5	GFDL	HADCM2	HADCM3	NCARPCM	CSM	CCCMa
SRES marker scenario ↓		ΔT ↓	LINEAR SCALING									
study area grid cell	A1FI (A1G)											
	A1T											
	A1B											
	A2											
	B2											
	B1	1,14	-5,32	-8,17	2,62	-5,21	-19,74	-3,50	-18,47	-8,40	-2,14	

Tal como lo hicimos en paso 12, ahora podemos leer desde el archivo “AREAAVES.OUT” los siguientes valores, esta vez para precipitación anual:

“OVERAL MEAN”
 ”INTER-MOD SD”
 ”INTER-MOD SNR”
 ”PROB OF INCREASE”
 etc.

Llenamos los valores en las correspondientes celdas de nuestra hoja de cálculo “prec2050”:

SRES marker scenario	GLOBAL					
	MAGICC mean ΔT (default model selection)	MEAN CHANGE	INTER-MODEL SD	INTER-MODEL SNR	PROB OF INCREASE	
		all 4 for normalized GHG data only				
		%/degC	%/degC			
A1FI (A1G)	1,67					
A1T	1,60					
A1B	1,48	-6,49	5,71	-1,14	0,13	
A2	1,30					
B2	1,33					
B1	1,14					

Cerramos “AREAAVES.OUT”.

Paso 16: Ahora retomaremos a partir del *paso 10*, pero esta vez especificamos como escenario de emisiones “A1FIMI”: abrimos la ventana **Warming** y cambiamos nuestra selección de escenarios de emisión a “A1FIMI”. Cerramos la ventana, volvemos a especificar nuestra área geográfica de interés bajo **Region** (tal como lo

hicimos en el **paso 8**) y volvemos a correr la herramienta. Abrimos el archivo de salida “AREAAVES.OUT” y copiamos los resultados a nuestro libro de cálculo EXCEL, tal como lo hemos hecho en los pasos anteriores.

(no será necesario repetir todos los pasos, ya que –como verán- algunos resultados son independientes del escenario SRES seleccionado)

Repetimos el mismo proceso, esta vez volviendo a seleccionar como variable a modelar “**Temperature**” en la ventana “**Variable**” (*¡Es importante volver a especificar el área de interés en el menú “Region” cada vez que se corre SCENGEN!*).

Los resultados obtenidos hasta ahora están contenidos en las siguientes tablas:

para temperatura:

DEF-1		GHG + AS	CHANGE_ΔT_YEAR 2050									
GCM →		ΔT ↓	CCCma	CCSRNIES	CSIRO	CSM	ECHAM4.5	GFDL	HADCM2	HADCM3	NCAR/PCM	CCCma
SRES marker escenario ↓			LINEAR SCALING									
study area grid cell	A1FI (A1G)	1,67	1,263	1,421	0,912	1,439	0,701	1,615	0,806	0,859	1,456	
	A1T											
	A1B											
	A2											
	B1	1,14	0,978	1,081	0,748	1,093	0,611	1,208	0,68	0,714	1,104	
DEF-2 (drift)		GHG + AS	CHANGE_ΔT_YEAR 2050									
GCM →		ΔT ↓	CCCma	CCSRNIES	CSIRO	CSM	ECHAM4.5	GFDL	HADCM2	HADCM3	NCAR/PCM	CCCma
SRES marker escenario ↓			LINEAR SCALING									
study area grid cell	A1FI (A1G)	1,67	1,368	1,122	1,035	1,228	1,017	1,456	0,789	1,105	1,122	
	A1T											
	A1B											
	A2											
	B1	1,14	1,047	0,886	0,829	0,955	0,817	1,104	0,668	0,875	0,886	

para precipitación:

DEF-1		GHG + AS	%CHANGE_PP_YEAR 2050									
GCM →		ΔT ↓	CCCma	CCSRNIES	CSIRO	CSM	ECHAM4.5	GFDL	HADCM2	HADCM3	NCAR/PCM	CCCma
SRES marker escenario ↓			LINEAR SCALING									
study area grid cell	A1FI (A1G)		-10,37	-12,87	-0,30	-2,50	-30,36	1,16	-16,24	-15,63	-3,48	
	A1T											
	A1B											
	A2											
	B1	1,14	-7,70	-9,33	-1,12	-2,55	-20,75	-0,17	-11,53	-11,13	-3,20	
DEF-2 (drift)		GHG + AS	%CHANGE_PP_YEAR 2050									
GCM →		ΔT ↓	CCCma	CCSRNIES	CSIRO	CSM	ECHAM4.5	GFDL	HADCM2	HADCM3	NCAR/PCM	CCCma
SRES marker escenario ↓			LINEAR SCALING									
study area grid cell	A1FI (A1G)		-6,74	-11,09	5,43	-6,56	-28,81	-3,94	-26,88	-11,45	-1,87	
	A1T											
	A1B											
	A2											
	B1	1,14	-5,32	-8,17	2,62	-5,21	-19,74	-3,50	-18,47	-8,40	-2,14	

Mientras permanecemos en SCENGEN, podemos comple(men)tar el análisis (*para los 2 escenarios de emisiones actualmente modelados con MAGICC*) para otras ventanas de tiempo del siglo XXI. Para efectos de **twinning**, quisiéramos recomendar -de forma preliminar (*ver nota en azul aquí abajo*)-considerar la **aplicación de SCENGEN para 3 ventanas de tiempo**, centradas alrededor de respectivamente, los años: **2020, 2050 y 2085**. Sin embargo, lo mínimo (para efectos de twinning) sería que todos los partners de Twinlatin apliquen el SCENGEN para la ventana de tiempo centrada en “**2050**”.

*La decisión final sobre las ventanas de tiempo que se van a modelar con MAGICC-SCENGEN debiera ser inspirada en el uso posterior que se le va a dar a dicha información. Si consideran utilizar otras proyecciones de cambio climático en el contexto de TWINLATIN aparte de aquellas generadas mediante MAGICC-SCENGEN (por ejemplo, salidas de corridas de Modelos Regionales de Circulación – los llamados RCM), puede ser muy útil asegurarse que las ventanas de tiempo seleccionadas para los análisis mediante MAGICC-SCENGEN correspondan con el espacio temporal para el cual tendrán disponibles las proyecciones alternativas, de modo de permitir una comparación (también fijarse en cual ha sido el periodo de referencia utilizado en el RCM). En caso de querer hacer **modelación de impacto combinado de cambios en el uso del suelo con cambio climático**, puede ser importante asegurar que la periodicidad de los escenarios de cambio en el uso del suelo corresponde con las ventanas de tiempo elegidas para analizar la señal de cambio climático*

También quisiéramos recomendar realizar el análisis no sólo para las condiciones de los promedios anuales, sino también al nivel de una escala temporal más fina: por ejemplo a **nivel estacional** (las opciones **Dec/Jan/Feb; Mar/Abr/May; Jun/Jul/Aug y Sep/Oct/Nov** pueden ser definidas en el paso 9) u inclusive a **nivel mensual** (también a definir en el paso 9).

La decisión sobre la resolución temporal mínima que se va a considerar en el ejercicio con MAGICC-SCENGEN debiera ser inspirada en el uso posterior que se le va a dar a dicha información⁶, pero se sugiere que todos los partners realicen al menos el análisis completo (9 GCM, 6 marker scenarios) a nivel anual, para 3 ventanas de tiempo, una a principios, mitad (2050) y fines del siglo XXI respectivamente.

Paso 17: Necesitamos llenar la tabla para los restantes escenarios de emisiones **A1T, A1B, A2 y B2**. Para ello, vamos a necesitar repetir todos los pasos anteriores, desde del **paso 1 hasta el paso 16**.

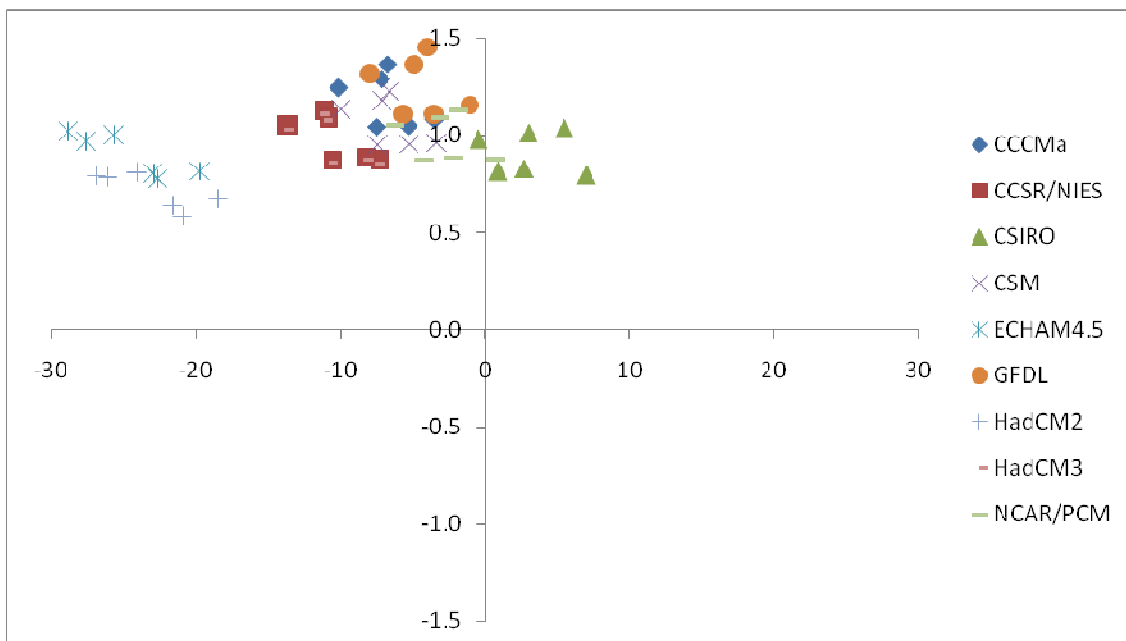
La idea de lo anterior es ver que tan diferentes son las respuestas (*señales de cambio en precipitaciones y en temperatura*) obtenidas para nuestros áreas de estudio, para los diferentes escenarios de emisiones (*analizando los 6 SRES marker scenarios mencionados más arriba*) y para distintos Modelos de Circulación General (*los 9 GCM mencionados más arriba*).

En el libro de calculo de EXCEL, se puede apreciar que el ejercicio también se podría realizar para la opción “Exponential” scaling del menú “Variable” de SCENGEN. Sin embargo, es de esperar que las diferencias obtenidas mediante las opciones “Linear” y “Exponential” sean relativamente pequeñas. Para efectos del twinning en Twinlatin, creemos es suficiente hacer el ejercicio sólo con la opción “Linear” scaling, pero en caso de estar interesados los partners pueden también analizar la sensibilidad de los resultados frente a ambas opciones de scaling ofrecidos por el software SCENGEN.

Al terminar el ejercicio anterior, para cada combinación [GCM] X [escenario SRES], hemos obtenido un valor de cambio “regionalizado” en temperatura (ΔT) y un valor de cambio “regionalizado” en precipitación ($\% \Delta P$), en función de un cambio en la temperatura promedio global con respecto al año 1990. Estos valores (cambio en temperatura y cambio en precipitación) ahora pueden ser graficados mediante puntos

⁶ Por ejemplo, a muchas veces las señales de cambio porcentual de precipitaciones (o absoluto de temperatura) pueden ser muy diferentes para las diferentes estaciones/meses del año (ej. *cambio más pronunciado en la estación lluviosa que en la estación seca, etc.*). En estos casos, para efectos de modelación hidrológica y/o de erosión, puede ser interesante generar las series de tiempo futuras (que servirán de input para modelar el efecto del cambio climático sobre hidrología, erosión, etc.) al perturbar los climas de referencia a nivel estacional o mensual, en vez de usar un solo valor de cambio (en el promedio anual) para generar las futuras series de tiempo.

(X;Y) en un sistema de ejes cartesianos, tal como se indica en la siguiente figura (en este caso: (ΔT ; $\% \Delta P$)):



En la figura superior, los 2 ejes de nuestro sistema cartesiano dividen nuestro espacio de puntos en 4 cuadrantes. El eje X representa cambios porcentuales en la precipitación promedio anual, mientras que el eje Y representa cambios absolutos en la temperatura promedio anual. **Todos estos valores están en función de un cambio en la temperatura promedio global modelado mediante MAGICC, el cual es único para un determinado escenario de emisiones, y el cual toma como referencia la temperatura global del año 1990.** Si los puntos en nuestro gráfico están distribuidos en más de uno de los cuadrantes, significa que no hay consenso en la dirección de los cambios simulados para los diferentes GCMs y los diferentes escenarios de emisiones mediante SCENGEN. En la aplicación superior para el Biobío (ventana de 30 años centrado en el 2050), todos los modelos predicen para todos los escenarios de emisiones un aumento en la temperatura; para la gran mayoría de los casos, estos cambios van asociados a una disminución de las precipitaciones. Aún así, existen importantes diferencias en la magnitud de los cambios simulados. Un análisis de sensibilidad de un modelo hidrológico que considera perturbaciones (incrementales) en las series de entrada de temperatura y precipitaciones de entre $+0.5^{\circ}\text{C}$ y $+1.5^{\circ}\text{C}$ / $+10\%$ y -30% , respectivamente, abarcaría el campo completo de magnitudes de cambios obtenidos mediante nuestro ejercicio en MAGICC-SCENGEN

USO DE LOS RESULTADOS OBTENIDOS MEDIANTE MAGICC-SCENGEN

Los resultados obtenidos mediante MAGICC-SCENGEN ahora pueden ser utilizados en combinación con las herramientas desarrolladas y/o utilizadas en otros paquetes de trabajo tales como:

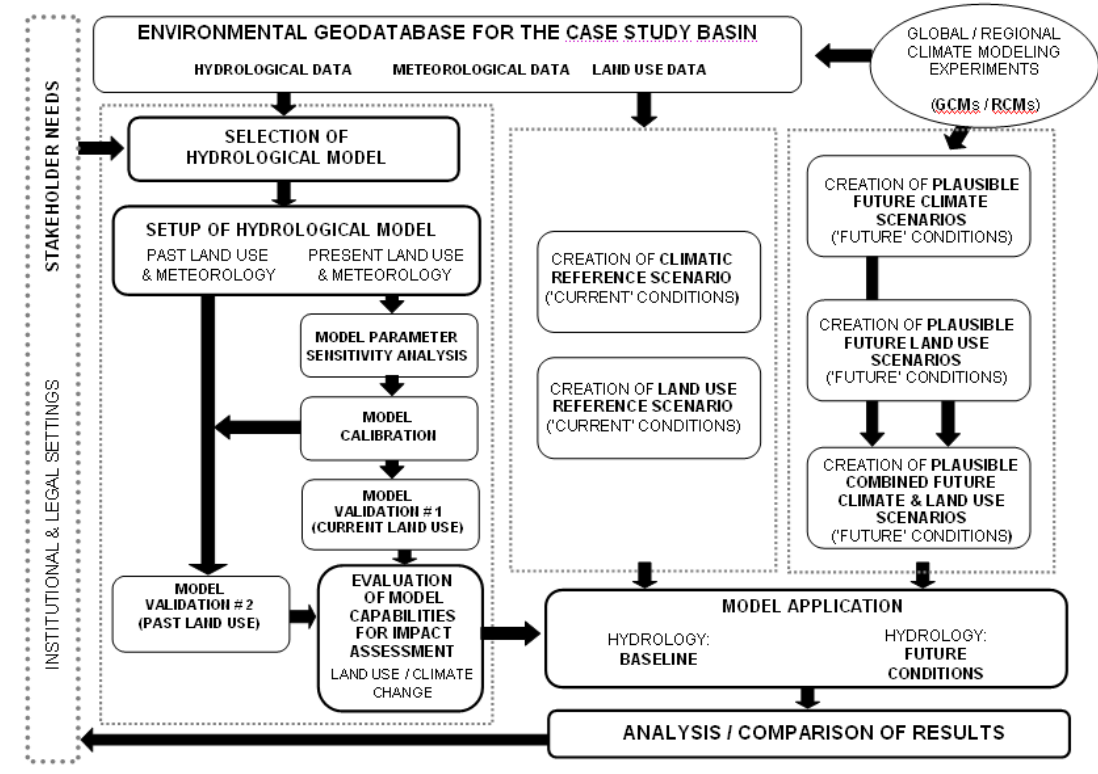
- WP03: Hydrological Modelling
- WP06: Pressures & Impacts

Al combinar las herramientas de dichos paquetes con los resultados de MAGICC-SCENGEN, es posible hacer una primera evaluación de los posibles impactos del cambio climático sobre, por ejemplo, los caudales, la erosión, niveles de contaminantes etc. Posteriormente, esta información nuevamente puede ser combinada con, por ejemplo, resultados u herramientas del paquete WP08, para hacer las correspondientes evaluaciones económicas.

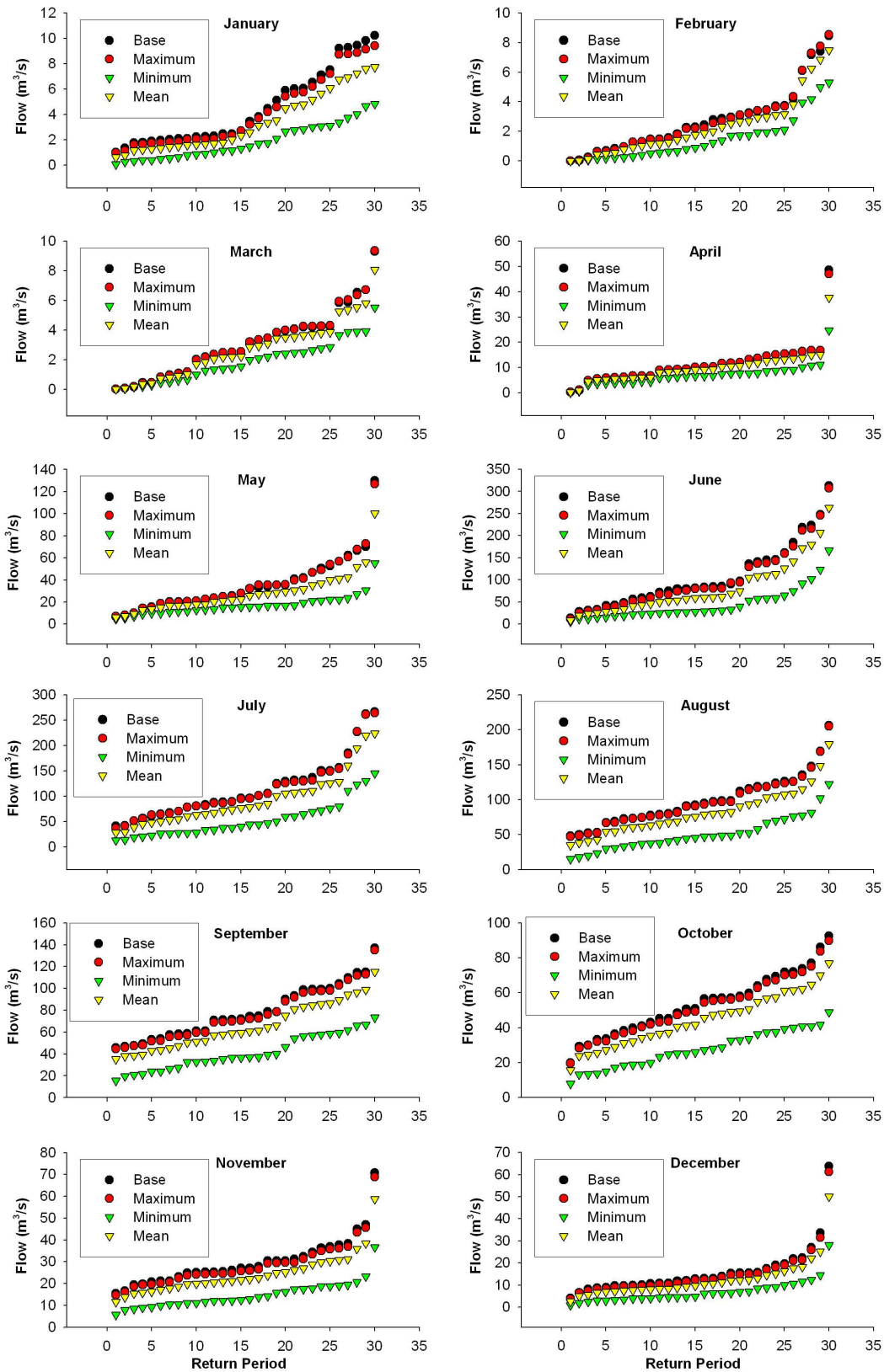
Es importante indicar que los “análisis de impacto” realizados en base a los resultados de MAGICC-SCENGEN se deben interpretar más bien como “análisis de sensibilidad” de los modelos/herramientas utilizados (y de los sistemas/procesos que representan, por ej. el ciclo hidrológico, la erosión) frente a plausibles escenarios de cambio, y no como un pronóstico real de cuáles serán las futuras condiciones. Esto se debe a los numerosos niveles de incertidumbre asociados a la generación de escenarios de futuros cambios climáticos, lo cual quedo reflejado en el ejercicio anterior – y que se observa fácilmente- en la heterogeneidad de las respuestas obtenidas mediante los distintos modelos, y para los varios escenarios de emisión. También se podría, para efectos del análisis de sensibilidad de un modelo hidrológico (u otro), perturbar las series de tiempo de entrada (precipitaciones, temperatura) en forma sistemática (ej. multiplicar series observadas de precipitación con 0.6, 0.8, 0.9, 1.10, 1.2 y 1.4) y luego indicar donde se encuentran los valores de cambio obtenidos con MAGICC-SCENGEN dentro del rango total de perturbaciones (de -40% a +40% en el ejemplo anterior) aplicadas.

A continuación, se describe brevemente cómo los resultados de MAGICC-SCENGEN para el Biobío han sido utilizados para evaluar la sensibilidad de los caudales en la subcuenca del Vergara (para determinados períodos de retorno) frente a diferentes perturbaciones del clima de referencia:

- Series de tiempo de precipitación observada para 5 estaciones de la Cuenca del Vergara fueron perturbadas en función de las señales de cambio obtenidos mediante MAGICC-SCENGEN
- El modelo hidrológico fue aplicado utilizando la serie de tiempo de referencia (calibración y validación)
- El modelo hidrológico fue aplicado utilizando las series de tiempo perturbadas
- Todos los resultados fueron analizados y graficados, de modo de indicar la sensibilidad de los caudales promedios mensuales frente a las diferentes magnitudes de cambio obtenidos mediante MAGICC-SCENGEN (ver figura)



La figura siguiente permite comparar el impacto en la hidrología de una cuenca obtenido mediante la simulación de 42 (7 GCMs x 6 escenarios de emisiones) escenarios de cambio climático versus una simulación del clima actual (“Base”). Los escenarios de cambio climático han sido generados al perturbar el clima de referencia para la cuenca en función de los valores de cambio obtenidos mediante MAGICC-SCENGEN. Aparte de la línea base, la figura muestra el máximo, mínimo y promedio de los valores obtenidos mediante las 42 simulaciones. El eje X indica el periodo de retorno. El usuario puede interpretar los resultados de la siguiente manera (ejemplo): el valor de flujo [leer eje Y] correspondiente a X=10 significa que estadísticamente hablando 10 veces en un periodo de 30 años el valor del caudal promedio para el mes bajo consideración será inferior o igual al valor que se lee para el punto correspondiente en el gráfico. De este modo, se puede observar que la frecuencia de caudales promedios mensuales altos podría bajar considerablemente bajo distintos escenarios de cambio climático, donde la magnitud del cambio es fuertemente dependiente del escenario de cambio utilizado.



**TWINLATIN WORK PACKAGE ON CHANGE EFFECTS &
VULNERABILITY**

SOME BACKGROUND INFORMATION...

(additional reading on the topic recommended)

On MAGICC-SCENGEN...

(from “*Generación de Escenarios Regionalizados de Cambio Climático para España, Primera Fase, Febrero 2007 – Ministerio de Medio Ambiente / Instituto Nacional de Meteorología*)

5.2. Utilización de la herramienta MAGICC-SCENGEN. Validación de modelos globales.

El método de escalado de patrones (*pattern-scaling*) se desarrolló a finales de los años 80 (Santer *et al.*, 1990) y se basa en el hecho de que los patrones de cambio climático futuro permanecen bastante similares independientemente de la magnitud total (media global) del cambio, al menos por lo que respecta a los Gases de Efecto Invernadero (GEI). La situación es bastante más compleja cuando se incluyen los efectos de los aerosoles. Lo que esto implica es que se puede tomar el patrón de cambio generado para un momento futuro y con un cierto AOGCM y correspondiente a un calentamiento global medio de ΔT_e y simplemente escalar e $\Delta T / \Delta T_e$ para obtener el patrón de cambio correspondiente a un mayor o menor calentamiento global (ΔT). El método de escalado de patrones puede expresarse como $\Delta X_i(t) = \Delta X_{e,i} (\Delta T(t) / \Delta T_e)$. Donde X se refiere a cualquier variable climática (temperatura, precipitación, etc), el subíndice i se refiere a un punto de rejilla particular, y Δ representa el cambio relativo a un periodo de referencia (que con frecuencia es 1961-90). En la práctica, los datos de los AOGCMs se almacenan en forma “normalizada”, es decir patrones de cambio por unidad (1°C) de calentamiento global.

El generador de escenarios climáticos (GEC) más ampliamente utilizado es el MAGICC/SCENGEN acrónimo que corresponde a “Model for the Assessment of Greenhouse-gas Induce Climate Change/SCENario GENerator”. La versión 2.4 de MAGICC/SCENGEN (Wigley *et al.*, 2000; Hulme *et al.* 2000) ha sido ampliamente utilizada en el tercer informe de evaluación del IPCC (2001). La más reciente versión 4.1 (Wigley, 2003a, 2003b) actualiza la versión de MAGICC utilizada por el tercer informe de evaluación y utiliza todos los escenarios de emisión SRES y entre otras mejoras permite investigar los cambios en variabilidad y hacer proyecciones probabilísticas. Otros GEC tales como COSMIC2 (“Country Specific Model for Intertemporal Climate”, Version 2) (Schlesinger y Williams, 1997) han sido también muy utilizados en estudios de impacto y proporcionan estimaciones por países del cambio en temperatura y precipitación media mensual con datos de 14 AOGCM y 28 escenarios de emisión.

La utilización de GEC permite una evaluación tangible de las incertidumbres inherentes a la predicción del clima futuro. Muy pocos países tienen la capacidad, los recursos o el tiempo para realizar experimentos utilizando modelos globales o regionales dedicados a la producción de escenarios nacionales o regionales. La utilización de tales modelos, cuando es factible, sólo permite explorar una pequeña parte del amplio rango de posibilidades que se abren cuando se considera un gran número de escenarios de emisión, de modelos climáticos, etc. La utilidad de los GEC reside en que: (i) pueden emular el comportamiento de modelos más complejos; (ii) son rápidos y eficientes para explorar las incertidumbres de la predicción climática; y (iii) pueden utilizarse en muchas regiones.

La principal característica de los resultados alcanzados relativos a futuros escenarios climáticos utilizando diferentes GEC es, en primer lugar, la robustez de los mismos, ya que las proyecciones permiten utilizar una gran mayoría de las simulaciones globales realizadas hasta

la fecha. Asimismo, el uso de los GEC permite estimar la cascada de incertidumbres asociadas a todo el proceso de generación de escenarios climáticos.

Los modelos, como MAGICC-SCENGEN, que se basan en el escalado de patrones constan de dos módulos diferenciados. El primero (**MAGICC**) consta de un modelo climático simple (véase (Harvey *et al.*, 1997) para una definición de estos modelos) que emula el comportamiento de los modelos 3D. Estos modelos producen valores de temperatura media global en superficie y del nivel medio de la superficie del mar para unas ciertas emisiones de gases de efecto invernadero y de dióxido de azufre. Los usuarios pueden utilizar diferentes escenarios de emisiones y ciertos parámetros del modelo para explorar las incertidumbres. El segundo módulo (**SCENGEN**) es fundamentalmente una base de datos que contiene los resultados de un gran número de experimentos con AOGCM, así como datos correspondientes al clima en un periodo de referencia para poder expresar las proyecciones climáticas en forma de cambios con respecto al periodo de referencia. Los diferentes campos en la base de datos esencialmente almacenan patrones normalizados que se modifican con los valores globales del modelo climático simple. El modelo climático simple en el caso de MAGICC se trata de un modelo acoplado de ciclo de gases, temperatura global media y nivel del mar global medio. El modelo es del tipo difusión hacia arriba-balance de energía (*upwelling difusión-energy balance* (UD/EB)) dividido en dos hemisferios y éstos a su vez divididos en una “caja” de tierra y otra de océano. En el IPCC-TAR (2001) (Ap. 9.1) puede verse una detallada descripción de cómo sintonizar un modelo simple como el MAGICC a los resultados obtenidos con AOGCMs. Una vez sintonizado MAGICC puede utilizarse para emular y extender sus resultados. Los modelos simples permiten comparar diferencias entre escenarios sin los efectos enmascaradores de la variabilidad natural, o de la similar variabilidad que tiene lugar en los AOGCMs (Harvey *et al.*, 1997). Por otra parte, los modelos sencillos permiten explorar el efecto de las incertidumbres provenientes de la sensibilidad del clima y de la captura de calor del océano. Un GEC como MAGICC-SCENGEN permite explorar fácilmente el grado de incertidumbre asociado con las proyecciones realizadas con una variedad de modelos globales. Dependiendo de las variables que se consideren los modelos muestran un grado mayor o menor de acuerdo y en consecuencia una mayor o menor robustez de las conclusiones. La figura 5.4 muestra la gran dispersión que se observa para la variable precipitación entre las simulaciones realizadas con los 16 modelos globales incluidos en MAGICC-SCENGEN.

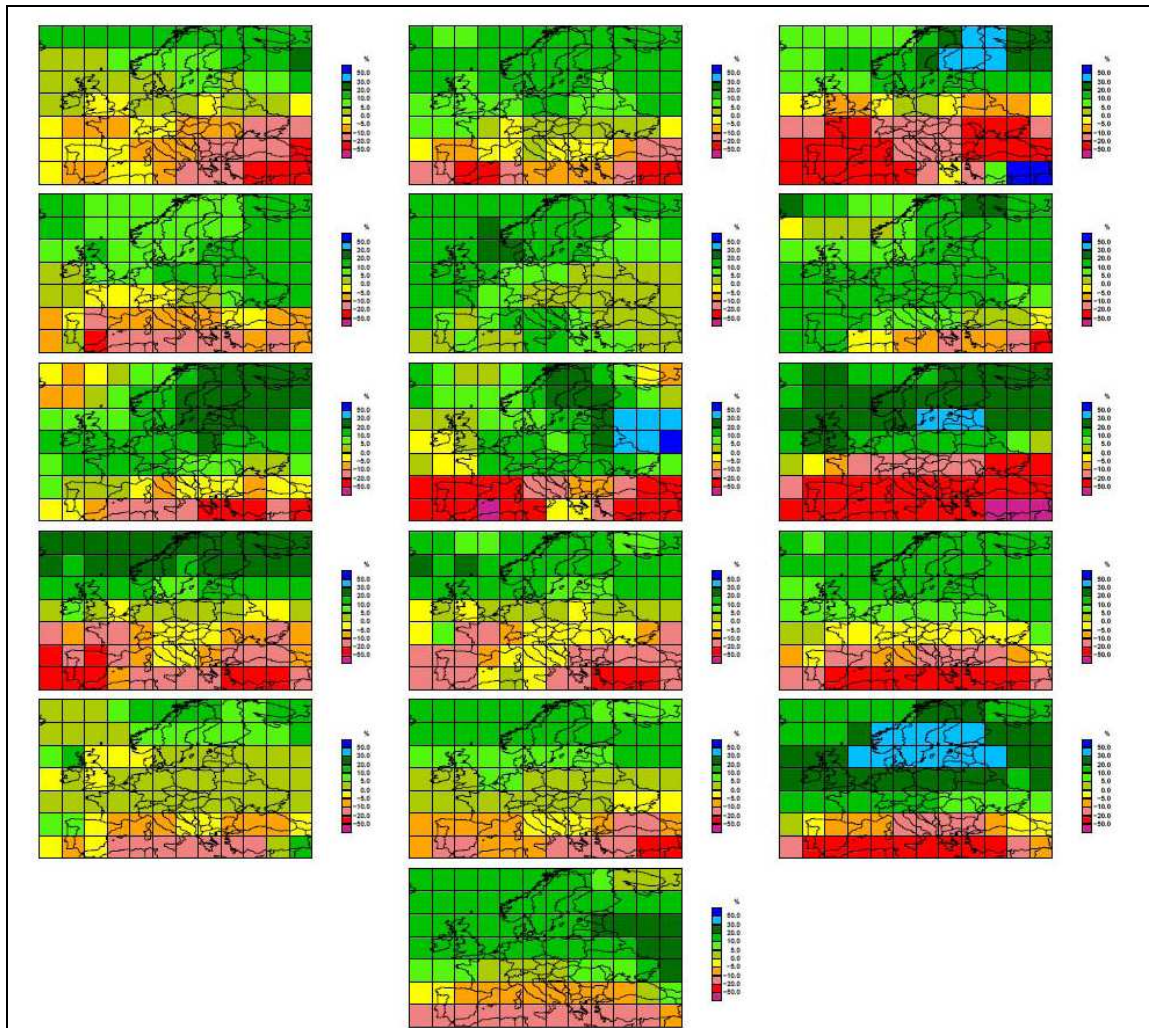


Figura 5. 4.- Cambio de precipitación anual bajo el escenario de emisión SRES A2 para el periodo (2086-2115) con respecto al periodo de referencia (1961-1990) obtenido con 16 AOGCMs. Producido con MAGICC/SCENGEN (versión 2.4) con la opción de sensibilidad climática media y los parámetros de MAGICC por defecto que producen un promedio global de incremento de temperatura (incluyendo GEI y SO₄) de 3.04°C.

Para una mejor interpretación de los resultados se pueden aplicar algunas técnicas ya utilizadas operativamente en las predicciones a medio y corto plazo. En particular, se pueden agrupar las distintas predicciones mediante técnicas de análisis cluster, se pueden promediar, se pueden presentar horquillas de valores máximos y mínimos en una región de referencia, etc. El promediado de todos los miembros del conjunto de predicciones realizadas con distintos modelos puede proporcionar un resultado más robusto y plausible por la tendencia a la compensación de errores sistemáticos de los distintos modelos. Este hecho ya ha sido ampliamente demostrado en los plazos de predicción cortos, medios y estacionales. Sin embargo no debe olvidarse que el promediado puede enmascarar comportamientos extremos en el caso de variables que presenten signos positivos y negativos.

La fig. 5.5 muestra un promediado sobre los 16 modelos para un escenario de emisión particular (SRES A2) y diferenciado por estaciones para precipitación y temperatura media. La precipitación muestra sobre la península Ibérica una clara tendencia a la reducción anual de la precipitación y una tendencia a la disminución en los meses de verano. Esta disminución en términos porcentuales puede ser insignificante en términos absolutos debido a la poca precipitación estival sobre todo en la mitad meridional de la península. El promedio anual de los 16 modelos muestra una reducción de la precipitación entre el 10 y 20% para la mitad meridional de la península y entre 5 y 10%

en los cuadrantes NO y NE de la Península Ibérica. Por estaciones se observa una disminución de precipitación salvo en la mitad norte y en la estación invernal donde se estima un aumento de la precipitación. La temperatura media, muestra también incrementos mayores en los meses veraniegos (superiores a 4.5°C en la mitad oriental de la península), consistente con los resultados obtenidos en la sección anterior. Los promedios correspondientes a otras variables (no mostrados aquí) dan resultados consistentes en términos de tensión de vapor y de nubosidad. Cabe destacar que el promedio para la nubosidad muestra un ligero aumento de la misma en los meses invernales, frente a la reducción en el resto del año y en el promedio anual. Este aumento invernal es consistente con el ligero aumento invernal del promedio del cambio de precipitación. En términos del módulo de la velocidad, se nota una tendencia a la disminución porcentual en todas las estaciones salvo en el verano. De nuevo, hay que ser cautos a la hora de interpretar este aumento veraniego en una estación en la que predominan las situaciones con poco flujo debido a la circulación general. Cuando se plantea el problema de qué modelo global elegir entre los muchos disponibles para preparar escenarios regionalizados y los posteriores estudios de impacto, hay una serie de criterios normalmente admitidos (Smith y Hulme, 1998). Entre estos criterios se pueden mencionar: (i) la menor antigüedad del modelo; (ii) la mejor representación del clima actual y de los paleoclimas; (iii) la mayor resolución; y (iv) la representatividad de los modelos para representar un amplio abanico de posibles climas futuros utilizando solamente dos o tres modelos. La validación del modelo frente al clima actual es un criterio muy sólido y objetivo, pero debe tenerse siempre presente que una buena representación del clima actual no tiene por qué representar una garantía de buena simulación del clima futuro. Las tablas 5.1 y 5.2 muestran diferentes índices de verificación de la temperatura media anual y de precipitación media diaria de 17 modelos para un área que abarca desde los 27.5° a los 52.5° de latitud norte y desde los 22.5°E a 12.5°O en longitud. La comparación se ha realizado con la climatología CRU (Climate Research Unit, (New *et al.*, 1999)) Los valores de los índices de verificación pueden utilizarse bien para seleccionar los modelos o para ponderarlos cuando se calculan promedios.

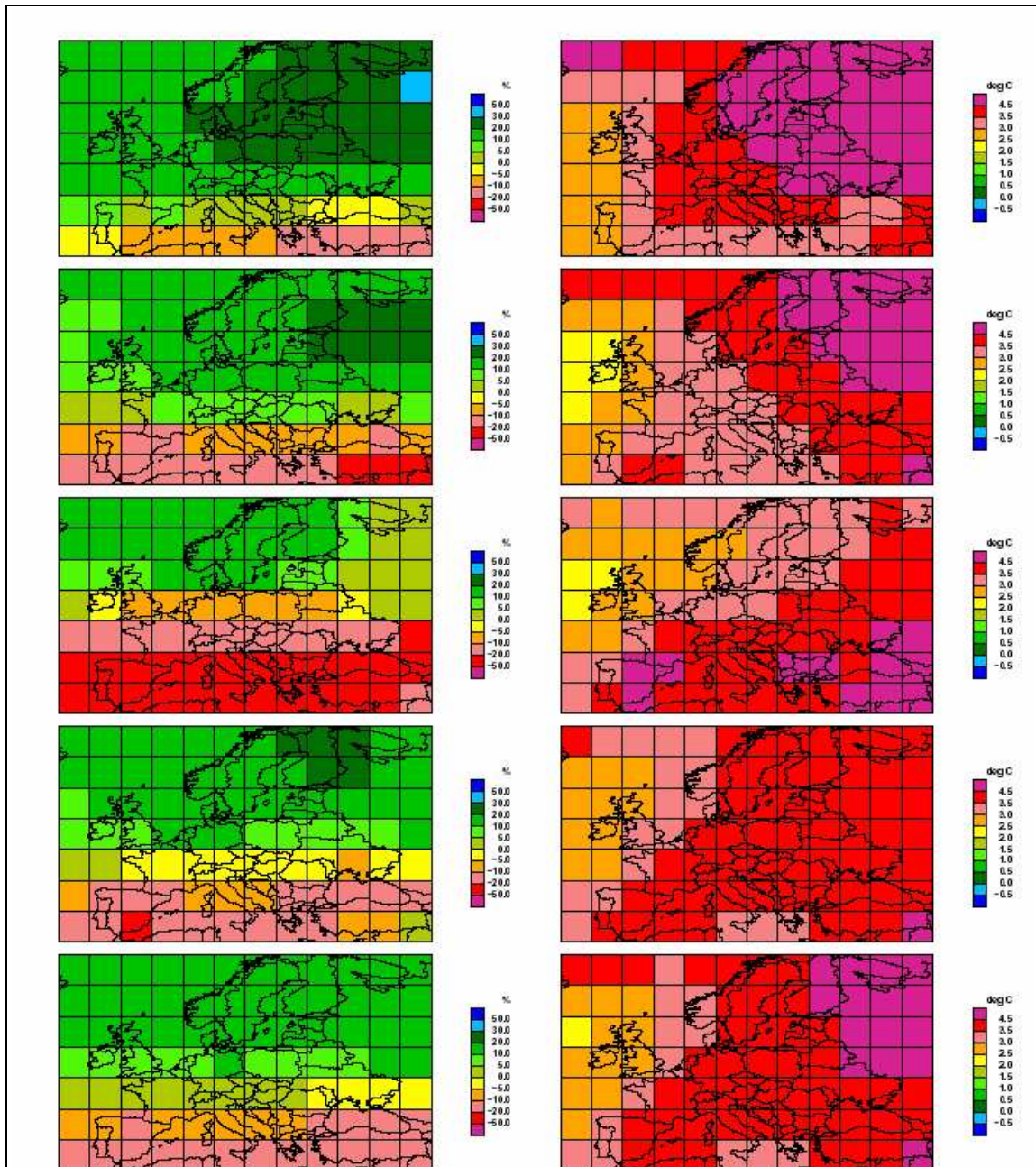


Figura 5.5.- Cambio de precipitación (izquierda) y temperatura media (derecha) bajo el escenario de emisión SRES A2 para el período (2086-2015) con respecto al período de referencia (1961-1990) basado en el promedio de 16 AOCGM para invierno (fila 1^a), primavera (fila 2^a), verano (fila 3^a), otoño (fila 4^a) y para el promedio anual (fila 5^a). Producido con MAGICC-SCENGEN (version 2.4) con la opción de sensibilidad climática media y los parámetros de MAGICC por defecto

MODELO CORREL RMSE BIAS
 BMRCTR .968 2.242 -1.357
 CCC1TR .901 2.182 -.391
 CCSRTR .933 3.136 -2.536
 CERFTR .929 2.351 -1.576
 CSI2TR .979 1.171 .177
 CSM_TR .855 2.797 1.481
 ECH3TR .955 1.455 -.562
 ECH4TR .988 .832 -.449
 GFDLTR .962 3.237 2.959

GISSTR	.947	2.452	.044
HAD2TR	.987	1.076	.769
HAD3TR	.987	1.052	.739
IAP_TR	.926	2.085	.622
LMD_TR	.932	1.659	-.132
MRI_TR	.956	2.765	-2.293
PCM_TR	.865	3.236	2.277
W&M_TR	.896	5.361	-4.967

Tabla 5.1.- Índices de verificación (correlación, error cuadrático medio, error medio) para los modelos listados en la columna de la izquierda y para la temperatura media en el periodo de referencia. (Producido con MAGICC-SCENGEN, version 4.1). Unidades: °C

MODELO CORREL RMSE BIAS

BMRCTR	.894	1.021	-.275
CCC1TR	.930	.410	-.109
CCSRTR	.908	.603	-.105
CERFTR	.938	.707	-.372
CSI2TR	.954	.481	-.274
CSM_TR	.958	.530	-.321
ECH3TR	.938	.417	.057
ECH4TR	.972	.253	-.116
GFDLTR	.929	.435	-.280
GISSTR	.956	.552	-.260
HAD2TR	.958	.438	-.222
HAD3TR	.980	.332	-.251
IAP_TR	.915	.496	.334
LMD_TR	.798	.764	-.483
MRI_TR	.938	.420	-.166
PCM_TR	.951	.469	-.169
W&M_TR	.908	1.038	-.716
MODBAR	.967	.393	-.219

Tabla 5.2.- Índices de verificación (correlación, error cuadrático medio, error medio) para los modelos listados en la columna de la izquierda y para precipitación en el periodo de referencia. (Producido con MAGICC-SCENGEN, version 4.1). Unidades: mm/día

On MAGICC-SCENGEN...

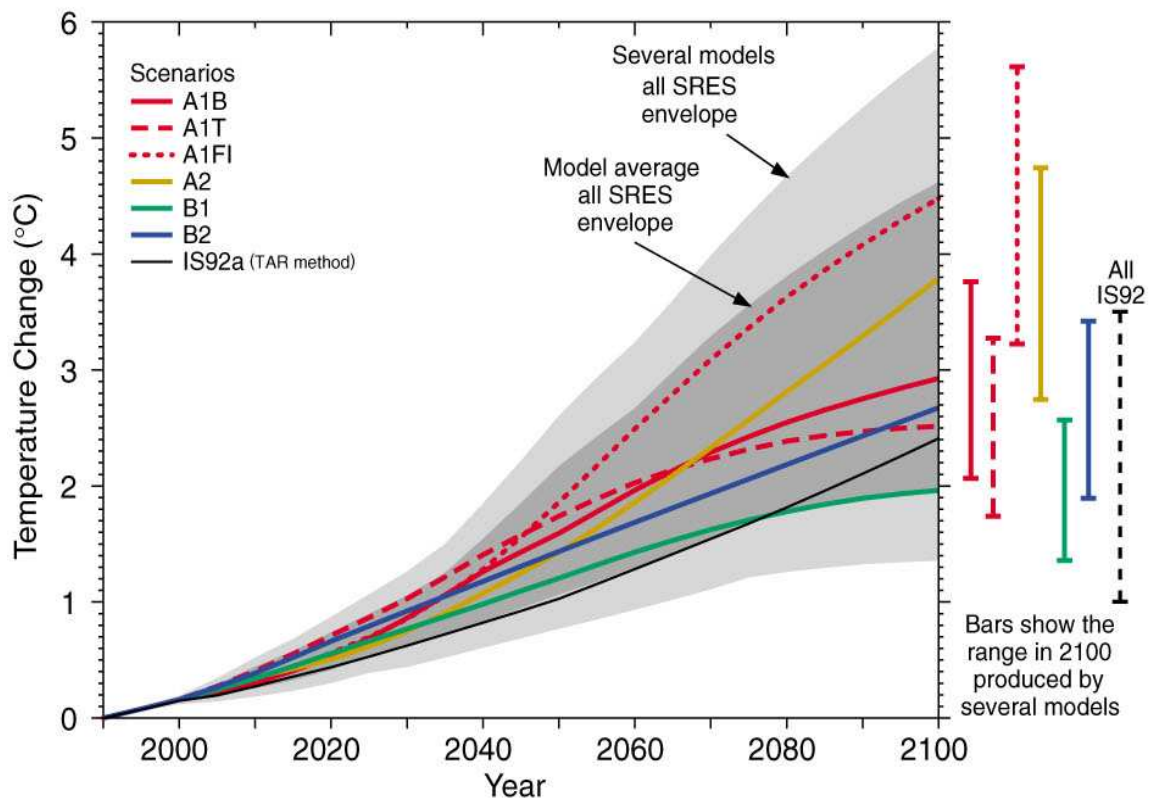
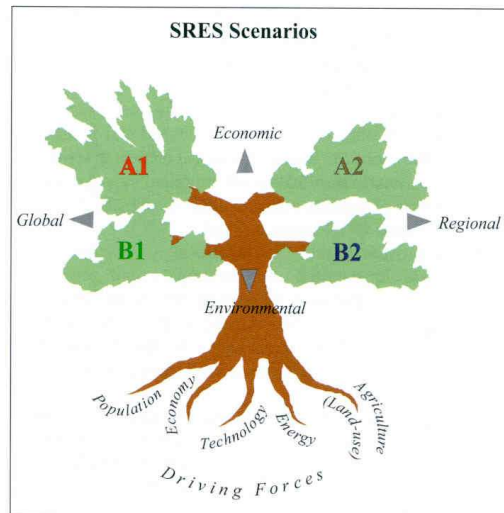
(from “*Using a Climate Scenario Generator for Vulnerability and Adaptation Assessments: MAGICC and SCENGEN version 2.4 workbook*)

The **default reference year** in MAGICC is **1990**. This follows the IPCC convention adopted in the First (1990), Second (1996), and Third (2001) Assessment Reports. **Other reference years can, however, be chosen.** For example, to view changes in climate with respect to the pre-industrial era, the **year 1765** could be chosen. This is the **initialisation year for MAGICC**. Alternatively, the **reference period 1961-90 may be preferred since many observed climate normals and gridded climate data sets describe present climate as the average of 1961-90. In this case, 1976 should be chosen as the reference year for MAGICC** since this is the approximate mid-point of the period 1961-90. Whatever reference year is selected, it is **important that you document your choice** in reports or analyses that use MAGICC results. Your choice of reference year in MAGICC does not affect your choice of reference year in SCENGEN (cf. Box 2.5, p.17).

From IPCC TAR

Escenarios de emisiones de gases invernaderos para el siglo XXI: 4 grandes grupos u familias: A1, A2, B1 y B2 en función de un previsto desarrollo económico mundial: más globalizado versus más regionalizado // con énfasis netamente en el desarrollo económico versus con mayor énfasis en protección del ambiente.

La segunda figura muestra para los diferentes escenarios su estimado impacto en la temperatura promedio global durante el siglo XXI.



From the IPCC Special Report on Emission Scenarios⁷:
<http://www.grida.no/climate/ipcc/emission/137.htm>

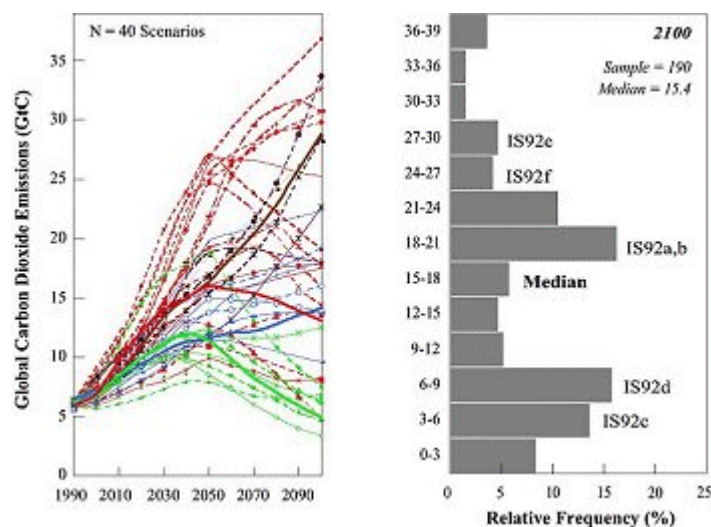


Figure 6-5: Global energy-related and industrial CO₂ emissions for the 40 SRES scenarios. The individual scenarios are shown grouped into **four scenario families**. **Marker scenarios** are shown as **bold continuous lines** and the other 36 scenarios as dashed lines. The emissions profiles are dynamic, ranging from continuous increases to those that curve through a maximum and then decline. **The relative positions of the scenarios change in time**, with numerous cross-overs among the individual emissions trajectories. The histogram on the right shows, for comparison, the frequency distribution of energy-related and industrial CO₂ emissions based on the scenario database. The histogram indicates the relative position of the four marker scenarios and the six IS92 scenarios compared to the emissions in the literature. **Jointly, the SRES scenarios span most of the range of scenarios in the literature.**

Figure 6-5 shows that the marker scenarios by themselves cover a large portion of the overall scenario distribution. This is one reason why the SRES writing team **recommends the use of at least the four marker scenarios.** Together, they cover a large range of future emissions, both with respect to the scenarios in the literature and the full SRES scenario set.

Box 6-3 Main Findings and Implications of SRES Scenarios

- The four scenario families each have a narrative storyline and consist of 40 scenarios developed by six modeling groups.
- The 40 scenarios cover the full range of GHGs and SO₂ emissions consistent with the underlying range of driving forces from scenario literature.

⁷ Actualmente, el AR4 o Cuarto Informe del IPCC ha sido publicado. Sin embargo, herramientas tales como el MAGICC-SCENGEN aún no están disponibles para realizar los análisis propuestos en función de los contenidos de este nuevo informe. Por el momento sugerimos en el contexto del TWINLATIN el uso de MAGICC-SCENGEN con los “marker escenarios” del SRES aplicados mediante los GCM que han sido utilizados para el Third Assessment Report TAR.

- The 40 SRES scenarios fall into different groups - the three scenario families A2, B1, and B2, plus four groups within the A1 scenario family, two of which (A1C and A1G) have been combined into one fossil-intensive group A1FI in the Summary for Policymakers. The four A1 groups are distinguished by their technological emphasis - on coal (A1C), oil and gas (A1G), non-fossil energy sources (A1T), or a balance across all sources (A1).
- The scenarios are grouped into four categories of cumulative CO₂ emissions, which indicate that scenarios with different driving forces can lead to similar cumulative emissions and those with similar driving forces can branch out into different categories of cumulative emissions.
- **Four from 40 scenarios are designated as marker scenarios that are characteristic of the four scenarios families. Together with the two additional illustrative scenarios selected from the scenario groups in the A1 family, they capture most of the emissions and driving forces spanned by the full set of the scenarios.**
- **There is no single central or "best guess" scenario, and probabilities or likelihood are not assigned to individual scenarios. Instead, the writing team recommends that the smallest set of scenarios used should include the four designated marker scenarios and the two additional illustrative scenarios selected from the scenario groups in the A1 family.**
- (...)

Box 6-4: Recommendations for Consideration by the User Communities

- (...)
- *Concerning large-scale climate models, the writing team recommends that the minimum set of SRES scenarios should include the four designated marker scenarios and the two additional illustrative scenarios selected from the scenario groups in the A1 family. (...)*
- (...)

Scenarios are essentially educational tools to help:

- see ranges of potential climate change
- provide tools for better understanding
- sensitivities of systems (e.g. hydrology: by modeling a series of plausible climate change signals and seeing their impacts on model (hydrology) results)

Some information on the different climate models:

http://www-pcmdi.llnl.gov/ipcc/model_documentation/ipcc_model_documentation.php

CPC Merged Analysis of Precipitation (CMAP)

Merged Satellite/Gauge/NWP Dataset

SCENGEN's displayable **baseline climatologies** are based on the **globally-complete CMAP (Xie and Arkin, 1997 – updated) precipitation** and CRU (New et al., 1999) temperature climatologies. The **precipitation climatology** is the **mean over 1981-2000**, while the temperature climatology is for 1961-90.

For more information, check:

- Xie, P. and P. A. Arkin, 1997: Global precipitation: A 17-year monthly analysis based on gauge observations, satellite estimates, and numerical model outputs *Bull. Amer. Meteor. Soc.*, **78**, 2539-2558.
- Xie, P., and P. A. Arkin, 1995: An intercomparison of gauge observations and satellite estimates of monthly precipitation. *J. Appl. Meteor.*, **34**, 1143–1160.
- http://rain.atmos.colostate.edu/CRDC/datasets/CMAP_NWP.html
- <http://www.cgd.ucar.edu/cas/guide/Data/xiearkin.html>
- http://www.cpc.ncep.noaa.gov/products/global_precip/html/wpage.cmap.html
- <http://www.cgd.ucar.edu/cas/guide/Data/xiearkin.html>
- <http://daac.gsfc.nasa.gov/interdisc/readmes/gpcc.shtml>

Crucial points to be kept in mind by potential users of CMAP data sets:

1. The quality of the analysis is highly dependent on the quality and amount of input data used. **Areas with sparse or no gauges**, or areas where the satellite estimates have large errors or poor sampling, are **likely to exhibit larger errors**
2. In general, the data set is **best suited** to identifying and quantifying in a relative manner the **spatial and temporal variability of precipitation in the tropics**. Variability in mid-latitudes is characterized less well, but still usefully. Great care is required in using the data at latitudes poleward of 60 degrees.
3. The **absolute values** given are generally **less worthy** of confidence **than the variability**. Global averages appear to be accurate to within 5-10%, but **individual grid area values probably have much greater uncertainties**.

CMAP data sources

Global monthly precipitation analyses with complete coverage and improved quality are produced by merging several kinds of individual data sources with different characteristics. In Xie & Arkin (1997), reference is made to the gauge-based monthly analysis produced by the Global Precipitation Climatology Centre (GPCC; Rudolf et al. 1994), the IR-based GPI (Arkin and Meisner 1987), the OLR-based OPI (Xie and Arkin 1997), the MSU-based Spencer (Spencer 1993), the SSM/I-scattering-based NOAA/NESDIS (Grody 1991; Ferraro et al. 1994), the SSM/I-emission-based Chang (Wilheit et al. 1991), and the precipitation distributions from the NCEP–NCAR reanalysis (Kalnay et al. 1996).

CMAP gauge-based data: combination of GPCC and Xie et al. (1996)

The gauge-based monthly analysis produced by the Global Precipitation Climatology Centre (GPCC; Rudolf et al. 1994) is constructed by interpolating quality-controlled observations from over 6700 stations globally using the spherical version of the Shepard (1968) scheme (Rudolf et al. 1994). The GPCC collects monthly precipitation totals received from CLIMAT and SYNOP reports via the World Weather Watch GTS (Global Telecommunication System) of the World Meteorological Organization (WMO). The GPCC also acquires monthly precipitation data from international/national meteorological and hydrological services/institutions. An interim database of about 6700 meteorological stations is defined. Surface rain-gauge based monthly precipitation data from these stations are analyzed over land areas and a gridded dataset is created (Rudolf, 1996; Rudolf et. al. 1994; and Rudolf, 1993), using a spatial objective analysis method.

As of December 1996, the **GPCC analysis** is available over global land areas for the period **from 1986 to 1995**. The **gauge-based analysis of Xie et al. (1996)** is used to complete the period **from 1979 to 1985**. That analysis is constructed by interpolating station observations of monthly precipitation for over 6000 gauges collected in the Climate Anomaly Monitoring system (CAMS) of the NOAA Climate Prediction Center (CPC) (Ropelewski et al. 1984) and in the Global Historical Climatology Network (GHCN) of the DOE Carbon Dioxide Information Analysis Center (CDIAC) (Vose et al. 1992) using the same algorithm as used by the GPCC.

The **quality of the gauge-based analysis** depends primarily on the **gauge network density**. Previous studies (e.g., Rudolf et al. 1994; Xie and Arkin 1995; Xie et al. 1996) showed that the random error of the gauge-based analysis decreases with increasing gauge network density, while significant bias exists over grid boxes without gauges, where values are determined by interpolating observations over the surrounding areas.

At present, **nearly half of the 2.5¹at-long grid boxes** over the global land areas have **no gauge coverage**, while **fewer than 20% of them contain 5 or more gauges in the GPCC and Xie et al. (1996) gauge datasets**. Intensive efforts are being made by the GPCC to collect and use gauge observations from over 35 000 stations worldwide, and improvements are expected in the quality of the gaugebased analysis.

GPCC Global Rain Gauge Analysis Data

For more information, check:

- GPCCdescr.pdf
- <http://www.dwd.de/en/FundE/Klima/KLIS/int/GPCC/GPCC.htm>
- http://orias.dwd.de/GPCC/GPCC_Visualizer

Characteristics of the gridded analysis products being available from the GPCC
(from: GPCCdescr.pdf)

(...)

The **Monitoring Product** of monthly precipitation for global climate monitoring is based on SYNOP (after high level QC) and monthly CLIMAT reports from totally 7,000 stations and is available within about 2 months after observation month. The operational production started with the year 1996 and is going on to near-present. An Interim Version of the Monitoring Product covering the period 1986-1995 has been derived from similar input data in 1994/1995 after GPCC's development phase. The series has been complemented backwards to 1979 by another preliminary gauge product using the same analysis method but a reduced input data set (Xie, Rudolf, Schneider and Arkin, 1996). The Monitoring Product supplies the in situ component to the satellite-gauge combinations of GPCP (Huffman et al. 1995, Adler et al. 2003) and of **CMAP (Xie and Arkin 1997) (=> SCENGEN)**. Figures 1 and 2 illustrate exemplarily GPCC gauge-based products in map format.

(...)

The **Full Data Product** is of much higher accuracy and recommended to be preferred for hydrometeorological studies and verification. The analysis includes all stations supplying data for the individual month. The data coverage varies from less than 10,000 and to more than 40,000 stations. A new full data re-analysis is performed in irregular time intervals, which are set with respect of data base improvements. The current Full Data Product is Version 3 covering the period from 1951 to 2004 (Figure 3).

(...)

At first, a comment on the data requirements: The **accuracy of gauge analyses** mainly depends on the number of stations being used. In order to calculate monthly area mean precipitation on 2.5° gridboxes with an **error of not more than 10%, between 8 and 16 stations per gridbox are needed** (WMO 1985, Rudolf et al. 1994). To cover the global land-surface by gridded data of this accuracy, as requested by the GPCP plan (WMO 1990), this requirement adds up to 40,000 stations world-wide.

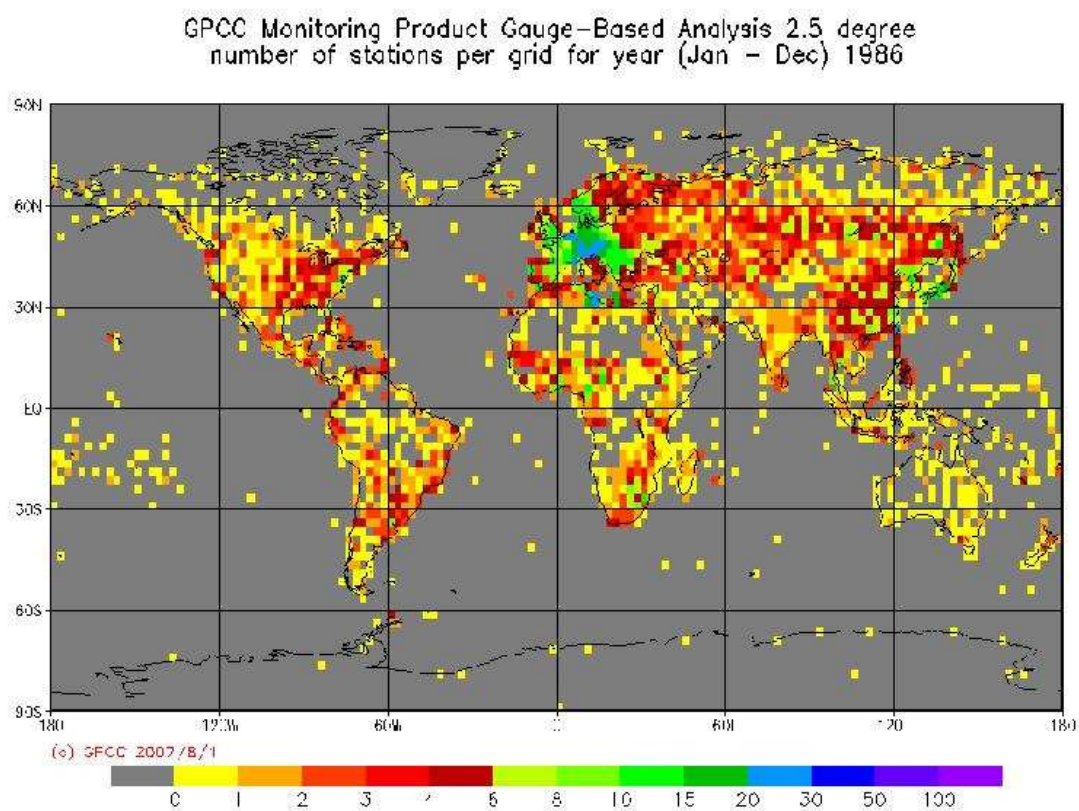
The sampling error of gridded monthly precipitation data has been quantified by the GPCC for various regions of the world. Based on statistical experiments using data from very dense networks, the relative sampling error of gridded monthly precipitation is between +/- 7% and 40% of the true area-mean, if 5 raingauges are used, and with 10 stations the error can be expected within the range of +/- 5% and 20% (Rudolf et al. 1994). The error range for a given number of stations represents the spatial variability of precipitation in the considered region.

Figures shown below:

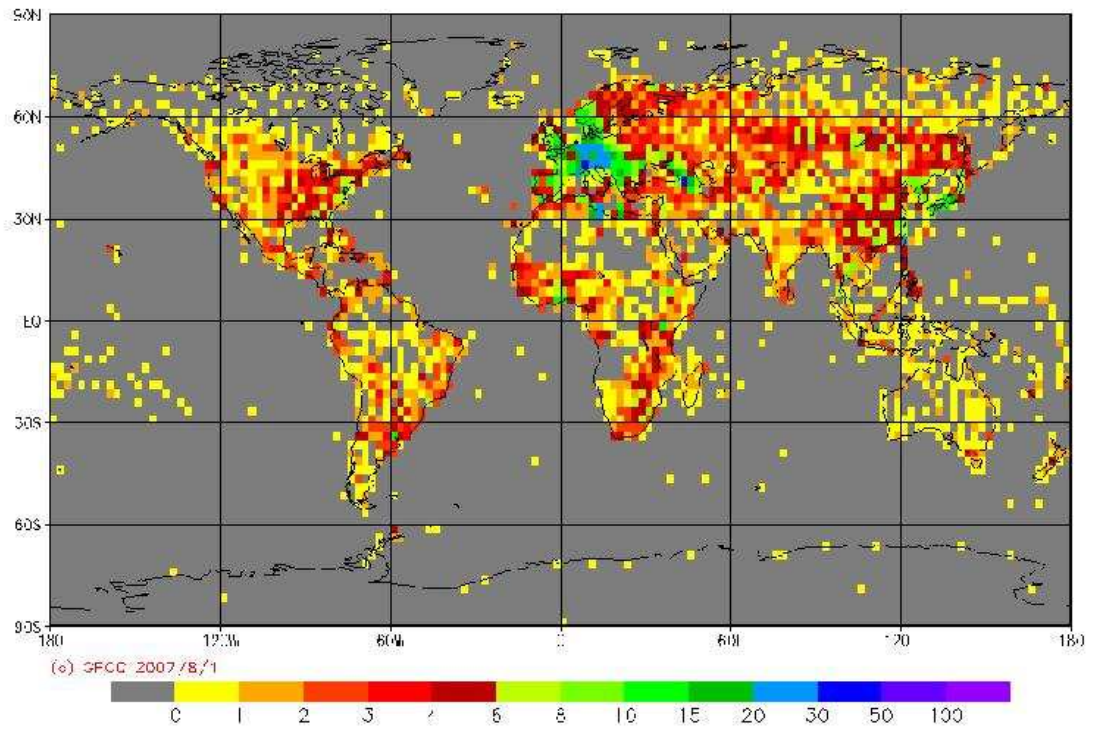
1-3: GPCC Monitoring Product (*i.e. used in the construction of the baseline climatology included in SCENGEN*) gauge-based analysis: number of used meteorological stations per $2.5^\circ \times 2.5^\circ$ grid cell for 1986, 1990 and 1995, respectively

4-6: GPCC Full Product (*i.e. extended data set available from GPCC but NOT used for construction of baseline climatology in SCENGEN*) gauge-based analysis: : number of used meteorological stations per $2.5^\circ \times 2.5^\circ$ grid cell for 1986, 1990 and 1995, respectively

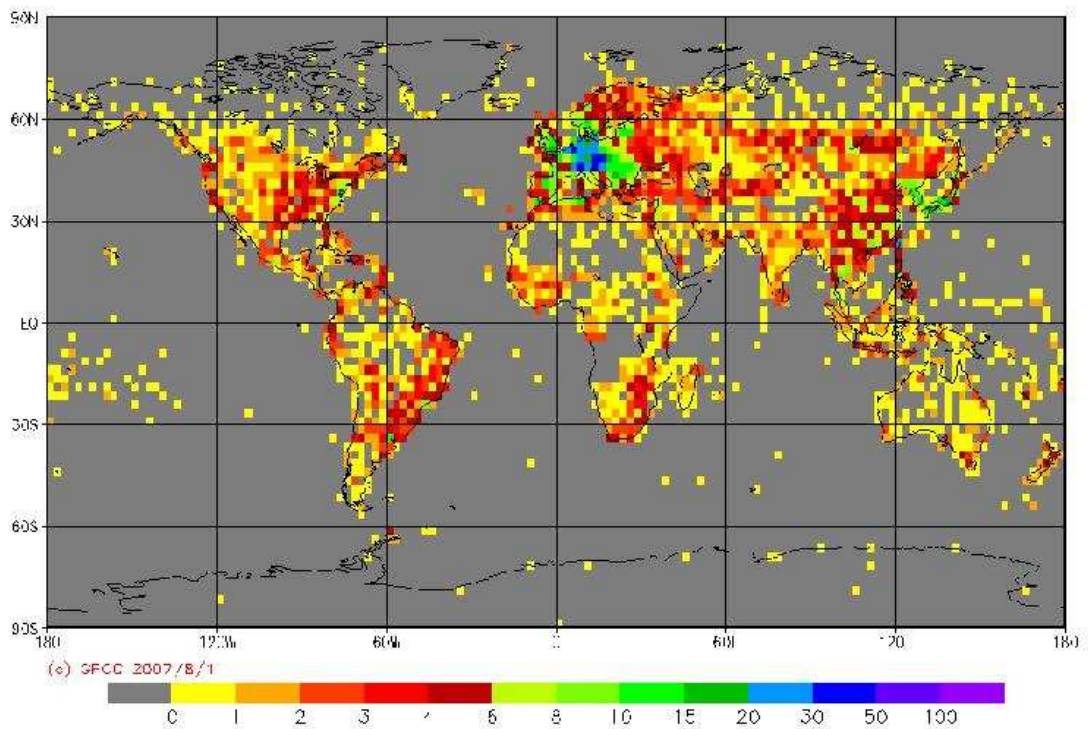
7-9: GPCC Monitoring Product (*i.e. used in the construction of the baseline climatology included in SCENGEN*) gauge-based annual precipitation per $2.5^\circ \times 2.5^\circ$ grid cell for 1986, 1990 and 1995, respectively.



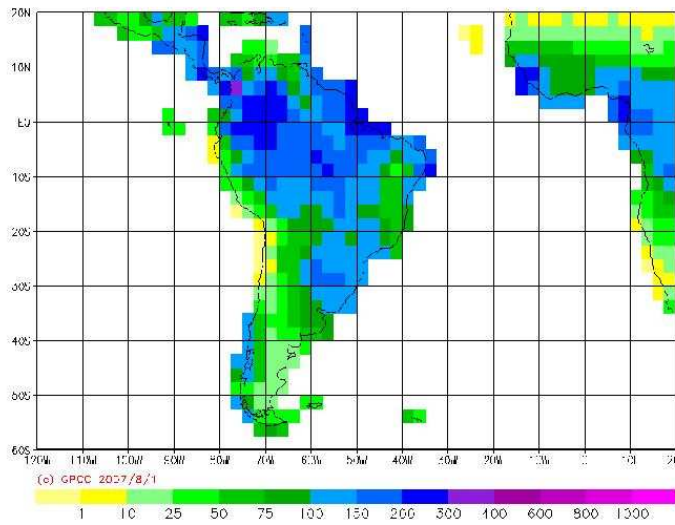
GPCC Monitoring Product Gauge-Based Analysis 2.5 degree number of stations per grid for year (Jan - Dec) 1990



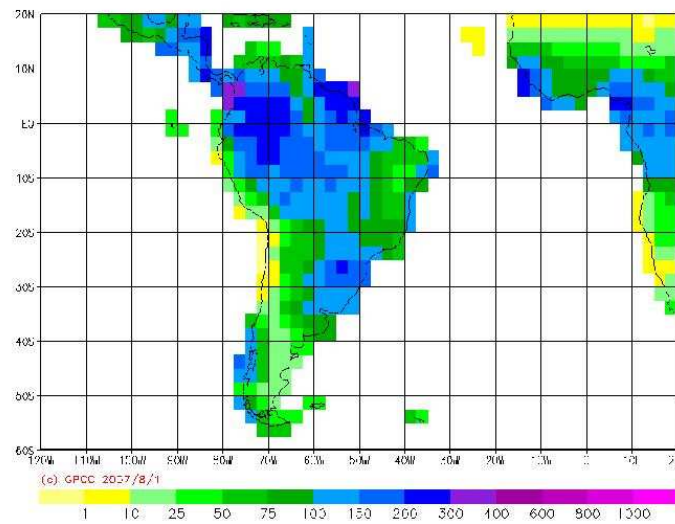
GPCC Monitoring Product Gauge-Based Analysis 2.5 degree number of stations per grid for year (Jan - Dec) 1995



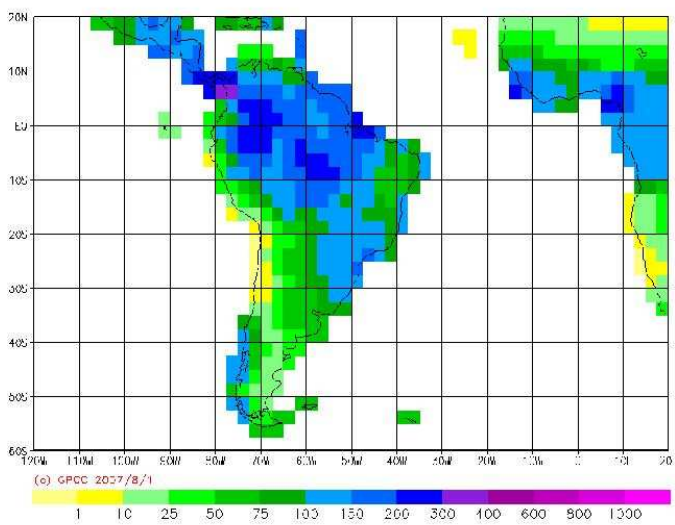
GPCC Monitoring Product Gauge-Based Analysis 2.5 degree precipitation for year (Jan - Dec) 1986 in mm/month



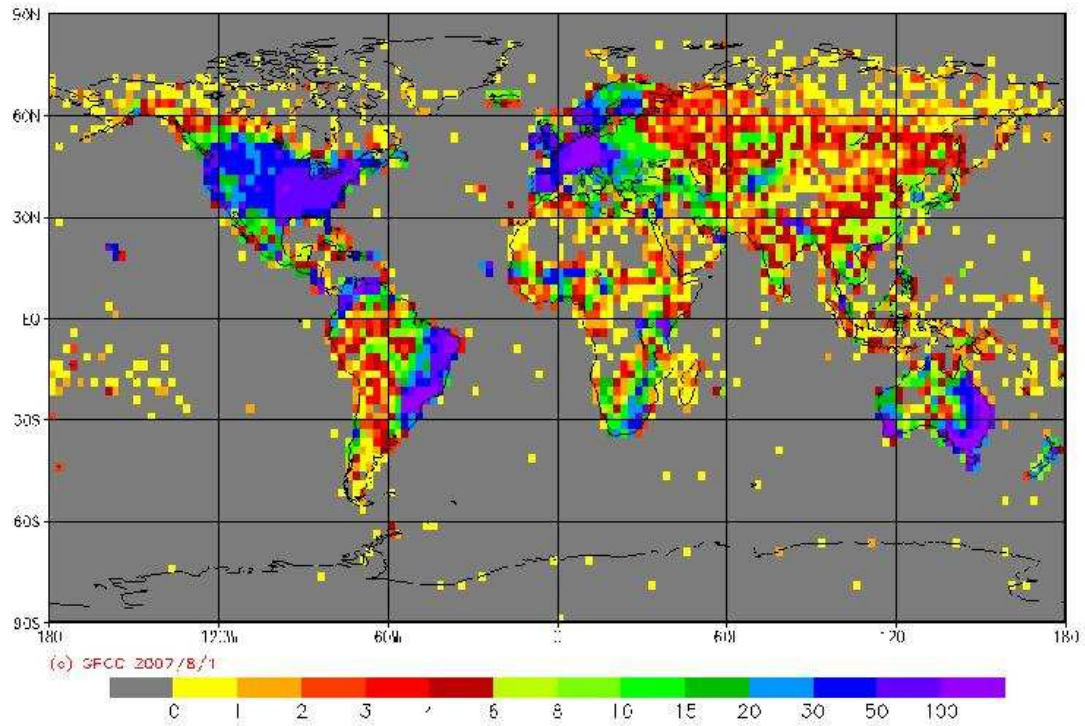
GPCC Monitoring Product Gauge-Based Analysis 2.5 degree precipitation for year (Jan - Dec) 1990 in mm/month



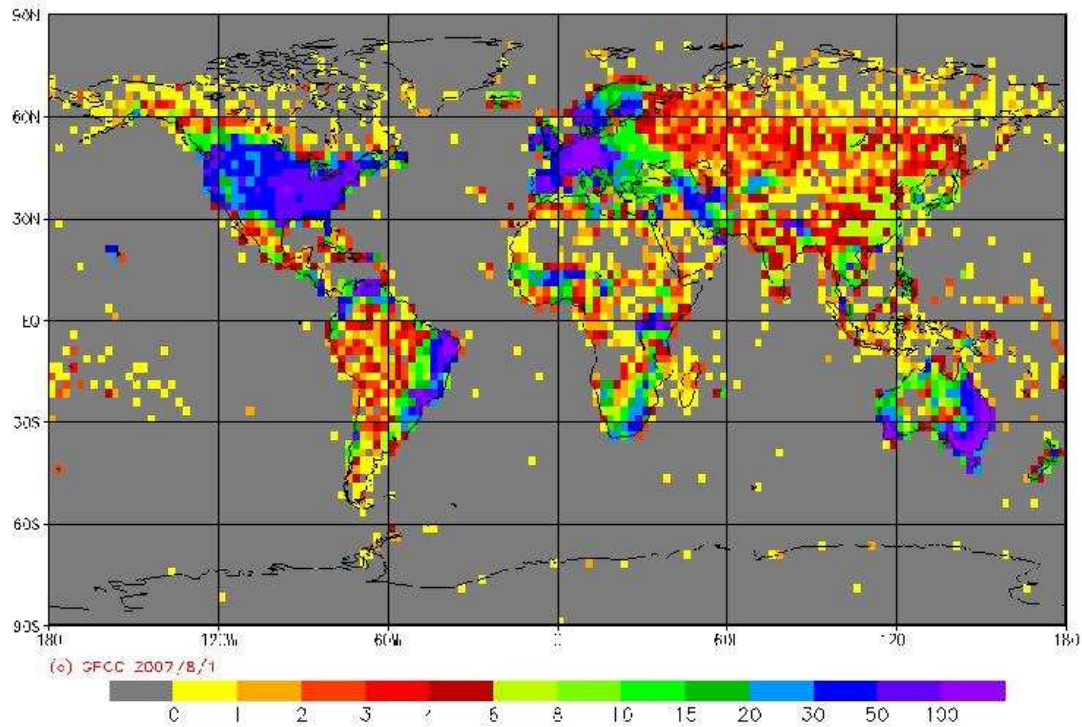
GPCC Monitoring Product Gauge-Based Analysis 2.5 degree precipitation for year (Jan - Dec) 1995 in mm/month



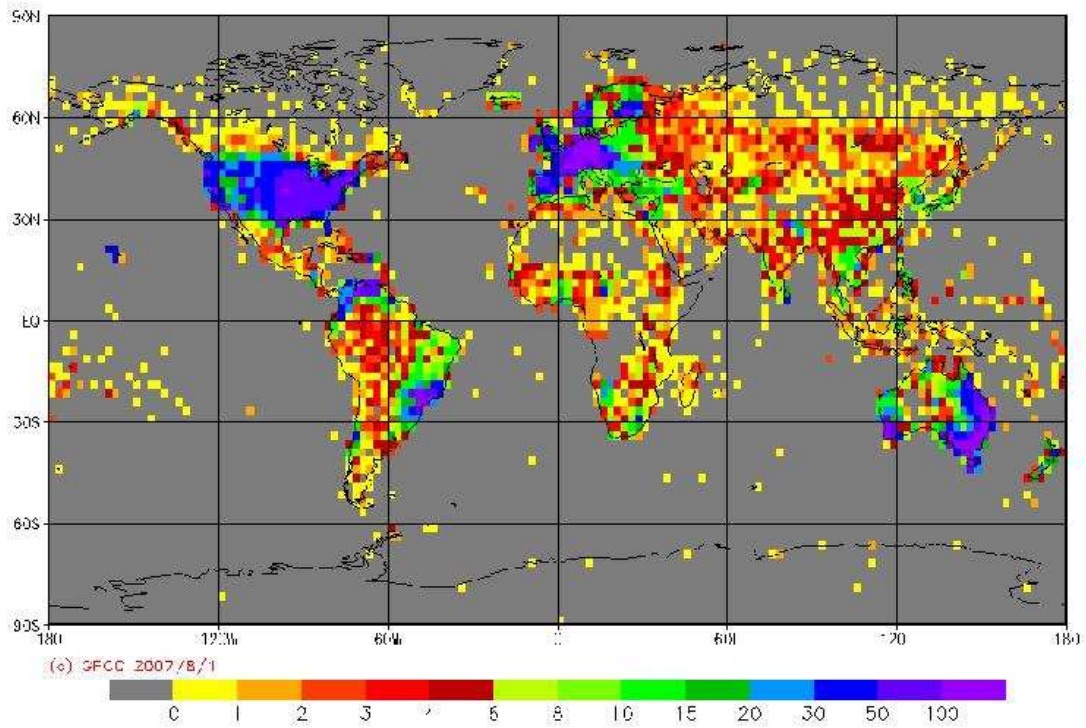
GPCC Full Data Product Version 3 Gauge-Based Analysis 2.5 degree
number of stations per grid for year (Jan - Dec) 1986



GPCC Full Data Product Version 3 Gauge-Based Analysis 2.5 degree
number of stations per grid for year (Jan - Dec) 1990



GPCC Full Data Product Version 3 Gauge-Based Analysis 2.5 degree
number of stations per grid for year (Jan - Dec) 1995



ANNEX 2

Questionnaires: land use change scenario creation and modelling (April, 2007)

	Baker	Catamayo-Chira	Cauca	Lago de Nicaragua	Quaraí/Cuareim
¿Área de interés?	Áreas que serán inundadas por las represas hidroeléctricas planificadas; mapeo de potenciales nuevas redes de infraestructura; quizás: proyecciones para extensión del área forestal productivo	Dos subcuencas en donde se dispone mayor información y que han sufrido mayores transformaciones en los últimos años: Quiroz, Catamayo	Analizar información existente, seleccionar un tramo de la cuena alta donde el transporte de sedimentos sea más significativo	Principalmente se interesa para cambios en el uso de la tierra en el Norte y Este de la cuenca del Lago Cocibolca: representan áreas de mayor extensión y donde existe la principal actividad agrícola y ganadera.	Cuenca del Quaraí, tal vez en primer paso en sitios específicos donde cambios de uso pueden causar impactos más grandes
¿Objetivos?	Caracterizar qué tipo de cuerpo de agua estará afectada por las inundaciones y cual es su representatividad en la cuenca, caracterizar tipos de uso/cobertura se verán afectados; ver como la accesibilidad en la cuenca pueda cambiar por potenciales nuevas redes de infraestructura, y evaluar el efecto que esto pueda traer para (i) nuevas presiones sobre áreas anteriormente de difícil acceso, y (ii) nuevas potencialidades para el (eco)turismo en la región		Cuál es la carga de sedimentos del río? Correlacionar estos datos con la información de cobertura y tipo de suelo con el fin de evaluar la pérdida de suelo. Estos resultados permiten definir escenarios y en consecuencia planificar el manejo y la gestión en las cuencas.	Se realizó todo el cambio que se podía realizar? (áreas que quedan sin cambio de uso permanecerán así por sus características topográficas o por estar protegidas por ley?)	¿Qué es el impacto del cultivo de arroz? ¿Hay suficiente agua para todos los usuarios?
¿Estudios previos sobre cambios de uso de suelo?	TWINBAS: análisis de los cambios en el uso del suelo entre 1979-2000 y proyecciones hacia el futuro (regresión logística) en la cuenca del Vergara; Cuenca del Aysen?	Catamayo: Estudio multitemporal de la cobertura vegetal: 1984-1992 y 1992-2002			Ningún estudio sobre cambios de uso
¿Mapas de uso histórico?	Antecedentes sobre las quemadas forestales (crónicas existentes): descripciones, no son mapas; Mapa de áreas que han sido afectadas por incendios forestales (falta aclarar el proceso bajo el cual dicha información ha sido generada); Inventario de los recursos	Quiroz (Perú): Mapa de usos de suelo (1972, Instituto Nacional de Recursos Naturales, 1:250.000), Mapa de usos de suelo (1994, INADE, 1:100.000), Mapa en formato análogo (1966-1968, IMICHIRA), Mapa en formato análogo (1952, MORRINSON);	Existe información de la década de los años noventa y de la actual. También existe de años anteriores, pero no digital	Mapa de uso de suelo (cobertura forestal) en los años '80; Mapa de uso de suelo (cobertura forestal) en el año 2000; Imágenes satelitales; Censo Agropecuario 2003	CBERS imágenes satelitales de 2007 (20m); LANDSAT MSS y otros desde 1970; Estudios sobre futuros escenarios del cultivo de arroz en Río Grande do Sul

	Baker	Catamayo-Chira	Cauca	Lago de Nicaragua	Quaraí/Cuareim
	vegetacionales, forestales y naturales a nivel nacional (Corporación Nacional Forestal)	Catamayo: Mapa de usos de suelo (finales 1980, inicios 1990, Plan hidráulico de Loja)			
¿Factores determinantes para cambios?	Desarrollo hidroeléctrico y cambios en infraestructura, poblacionales, asociados a lo anterior; probablemente, a largo plazo, el cambio climático	Fenómenos naturales (El niño); Cambios antropogénicos (puesta en cultivo y otros); Migración por fenómenos de sequía; Construcción y puesta en marcha de sistemas regulados San Lorenzo y Chira-Piura (fuera de la zona SWAT); Sistemas de riego (menos impacto)	Económicos, sociales, culturales, tecnológicos y ambientales.	Expansión de la frontera agrícola y ganadera	No se espera grandes cambios en el futuro cercano. Se puede esperar un cambio del cultivo de arroz a soya. No se espera forestaciones
¿Tipo de futuros escenarios para modelar?	Limitado; escenarios de implementación de los planes de desarrollo hidroeléctrico.	Minería puede resultar de gran impacto; Declaraciones de zonas intangibles pueden incidir en el (cambio de) uso	La condición ideal de ordenamiento y manejo desacuerdo con la potencialidad de los suelos según su aptitud.	Habría pocos cambios, identificar zonas sensibles a erosión, qué pasaría si se reforestan esas zonas o microcuencas sensibles	Cultivo de arroz y bovinos no ha cambiado mucho, puede ser interesante revisar los estudios sobre futuros escenarios del cultivo de arroz en Río Grande do Sul. Ovinos ha disminuido en los últimos 15 años, pero parece estabilizarse. Se podría esperar un establecimiento de la industria maderera, pero todavía es una especulación
¿Modelo para simular escenarios?	un mapeo de áreas inundadas y otros cambios a grandes rasgos, basado en 'expert judgment' y un DEM y cotas proyectadas	crear diferentes escenarios con ayuda de organizaciones locales conocedoras del terreno, que ya trabajan con el proyecto y pueden ayudar a consensuar los escenarios			
¿Parámetro a modelar?	qué tipos de cobertura/uso se verán afectados y en qué grado, por el desarrollo hidroeléctrico	Producción de agua y sedimentos, necesidad/relevancia de obras de protección y medidas de mitigación para futuros FEN y la conveniencia de declarar zonas intangibles y propuestas de (nuevas) actividades económicas (turismo, agroexportación, forestería,...)	Crear directrices en el manejo adecuado de las cuencas, igualmente para priorizar la mitigación de los problemas ambientales que más afectan a la comunidad y así destinar eficazmente los recursos económicos para ejecutar los procesos de reconversión.	Erosión y transporte de sedimentos hacia el lago, calidad de agua del lago	Impactos sobre calidad del agua en el Río Quaraí y cambios en el ciclo hidrológico por cambios en las características naturales del balance hidrológico vertical en la cuenca; disponibilidad de agua
¿Modelo para simular efectos?		SWAT, WaTEM/SEDEM	SWAT	¿Watshman?	IPH-MGB, MODSIM
¿Cronograma preliminar?	Depende del anuncio de planes más concretos para el desarrollo hidroeléctrico; ya se	07-08/2007: desarrollar metodología, planificar talleres participativos para la creación	inicio planeado para el mes de agosto 2007		Junio/julio 2007: definición de escenarios de cambios de uso; Agosto-Diciembre 2007:

	Baker	Catamayo-Chira	Cauca	Lago de Nicaragua	Quaraí/Cuareim
	tiene un mapeo preliminar de áreas que resultarían potencialmente inundadas, se irán actualizando en la medida que nueva información es proporcionada	de escenarios consensuados con agentes locales; el análisis multitemporal de la cobertura para 3 periodos en los últimos 50 años (dependiente de la información); 08-11/2007: creación de escenarios; 11-12/2007: aplicación de escenarios al WaTEM/SEDEM y SWAT; 01/2008: análisis de resultados, conclusiones y recomendaciones			simulaciones y discusión de resultados; Enero 2008: informe con escenarios y pautas para el desarrollo de la cuenca del Quaraí
¿Asistencia?	No requiere mayor asistencia. EULA podría contribuir al compartir las experiencias de la aplicación de regresión logística realizada en el contexto de TWINBAS	sí	Es oportuno contar con otras experiencias y con la asistencia de personas expertas en estos temas.	Conocer pasos y enfoque de otros partners	Se considera que los conocimientos y experiencia es suficiente para desarrollar el paquete. Se podría dar soporte a partners en asuntos relacionados, como modelaciones y geoprocessing. DNH necesitará soporte de IPH.